The Many Faces of Biodiversity: Climate-Driven Forest Reassembly Across Ecological Scales

By Ilya Shabanov

Thesis submitted to Victoria University of Wellington in fulfilment of the requirements for the degree of Doctor of Philosophy in Computational Ecology

2026

Abstract

Climate change is rapidly reshaping ecosystems worldwide, forcing species to shift their distributions and driving profound compositional and functional changes in ecological communities. These changes are neither uniform nor monotonous across biomes, spatial scales, taxa, time frames, and methodological approaches, resulting in contradictory biodiversity projections and uncertainty about the vulnerability of affected species. Given the accelerating pace of climate change, understanding these dynamics in a spatially, temporally, and taxonomically explicit manner is crucial for guiding conservation policy and anticipating impacts on ecosystem functioning and services.

Using the New Zealand National Vegetation Survey (NVS), this thesis develops new approaches to diagnose ecological change, understand the mechanisms underlying forest reassembly, and forecast future biodiversity trajectories. The primary contributions are (i) the development of a hierarchical biome-based modelling framework that links climate-driven habitat redistribution with species niche matching to project biodiversity trajectories, (ii) the integration of functional trait and isotope data with long-term forest inventories to identify community assembly mechanisms underlying forest reorganisation, and (iii) the development of a machine-learning framework that detects early signals of climate-driven abundance change within species' existing ranges. Collectively, these contributions show that biodiversity change emerges from processes operating at three nested ecological levels: species, communities, and biomes.

Paper 1 addresses contradictions among biodiversity observations and projections, introducing a hierarchical biome–affinity modelling framework that combines projections of climate-driven biome area changes with species' environmental preferences and

abundances to estimate landscape-scale biodiversity potential. Applied to New Zealand forests across multiple climate scenarios, the framework reveals a potential non-linear biodiversity trajectory driven by two opposing processes: the expansion of warm-adapted forests, which lose species due to tighter upper thermal limits, and the contraction of cold-adapted biomes, where relaxed lower thermal limits allow colonisation by additional species. Depending on the socioeconomic scenario, this trend either saturates or peaks around mid-century.

Paper 2 investigates the community assembly mechanisms underlying forest reorganisation. Using long-term forest inventory data combined with newly compiled functional trait and isotope datasets, the study analyses trends in community-weighted trait moments and multi-trait functional diversity indices across New Zealand's major forest types. Despite shared trends toward warm-adapted species and poleward migrations, the mechanisms affecting these trends differ among biomes. Cold-adapted forests experience strong functional restructuring and environmental filtering, whereas warm-adapted forests shift toward drought-avoidance strategies and increasing functional redundancy. The results also suggest that rising CO_2 concentrations influence these trajectories by promoting ectomycorrhizal associations in beech forests and enabling drought-avoidant strategies in warm-adapted podocarp forests.

Paper 3 develops the Abundance Trend Indicator (ATI), a machine-learning framework that infers environmental drivers of within-range abundance shifts from resurveyed forest inventory plots. Because such shifts can precede detectable range-margin movements by decades to centuries in long-lived trees, ATI provides an early indicator of climate-driven biodiversity change. Applied to widespread New Zealand species, the

method reveals highly individualistic responses to environmental change, helping explain why many species do not track climate shifts directly.

Together, these studies demonstrate that biodiversity trajectories emerge from interactions among species-level responses, community assembly processes, and biome-scale dynamics. Although these processes often share broad global trends, such as thermophilisation and poleward migration, they frequently arise through contrasting mechanisms. By integrating these perspectives and introducing methodological advances, this thesis contributes to a more predictive understanding of forest responses to climate change and provides new tools for anticipating biodiversity change.

Acknowledgements

I would like to thank my wife Marina, who helped me navigate the ups and downs of this arduous, sometimes pointless, sometimes elating process. She always stood by with infinite patience, relentless loyalty, heartfelt camaraderie and of course a good dose of cynical humour.

A bout of gratitude to my peers Colan, Su Min, Katrijn, Zoe, Jim, Lisa & Carla for shared meals and open ears. You made the journey about more than its destination.

A tip of my hat to my supervisors Julie, Jono & Andrew, for accepting my rough edges, impatience and directness, and yet sticking through to the end. It is a great lesson in humility to see how we can align, even when we don't always agree. Thank you.

Thank you to those whose numerous conversations, helped me along the way from various Iwi, institutions and government bodies across New Zealand.

My sincere reverence to Captain Pipi Spielhand, for reminding me that everything is possible & that the pirate can never be conquered by the world and to Dr Ross Buchan, for supporting my early academic endeavours with his time and friendship.

All paths are my path.

Table of Contents

The Many Faces of Biodiversity: Climate-Driven Forest Reassembly Across Ecological Scales **0**
Abstract 1
Acknowledgements 4
Table of Contents **5**
1. Introduction 9
2. Background 13
2.1. Species Distribution Models 13
2.1.1. Challenges of SDMs 14
2.1.2. Future Projections using SDMs 18
2.1.5. Conclusion 19
2.2. Functional Ecology & Functional Indices 20
2.2.1. Challenges of Functional Ecology 21
2.2.2. Combining Traits into Functional Trait Indices 25
2.2.3. Conclusion 27
2.3. New Zealand based models 28
3. Thesis Aims & Structure 30
4. Approaching Peak Biodiversity: Non-linear Responses of Plant Biodiversity to Climate Warming (BdP) **33**
4.1. Abstract 33
4.2. Introduction 35
4.3. Methods 39
4.3.1. Training Data 40
4.3.1.1. Biome Data 40
4.3.1.2. Present and Future Predictor Variables 41
4.3.2. Model Choice, Training and Uncertainty Estimates 42
4.3.2.1. Choice of Model 42
4.3.2.2. Extrapolation Threshold 42
4.3.3. Range and Niche Shifts 43
4.3.4. Species Climate Affinity Framework 43
4.3.4.1. Species-Biome Affinity 45
4.3.4.2. Landscape Affinity 47
4.3.4.3. Normalising and Fitting Affinity Trends 48
4.3.4.4. Dominant and subordinate species sets 49
4.4. Results 49
4.4.1. Changes in Biome Area and Transitions 49
4.4.2. Range and Niche Shifts 51

4.4.3. Changes in Species Richness Potential 52
4.5. Discussion 55
4.5.1. Ecological Interpretation 56
4.5.2. Framework Interpretation and Limitations 61
4.6. Conclusion 62
4.7. Data Availability Statement 63
4.8. References 63
5. Climate-Driven Forest Reassembly Follows Divergent Functional Pathways in Cold- and Warm-Adapted Communities (TrP) 81
5.1. Abstract 81
5.2. Introduction 83
5.3. Methods 87
5.3.1. Species Occurrence, Abundance Data, and Forest Types 87
5.3.2. Trait Data and Species Selection 88
5.3.3. Environmental Variables 90
5.3.4. Community Weighted Trait Moments 91
5.3.5. Community Environmental Index 91
5.3.6. Functional and Taxonomic Diversity Indices 92
5.3.7. Standardised Effect Sizes (SES) and Null Models 93
5.3.8. Linear regressions and statistical testing 94
5.3.9. Influence of species groups on metric trends 95
5.4. Results 97
5.4.1. Widespread shifts towards warm-adapted, low-elevation species 97
5.4.2. Niche packing and differential traits in functional divergence 98
5.4.3. Some Species Groups Contribute more strongly to functional change 101
5.4.4. Functional change differs among forest types 102
5.5. Discussion 105
5.6. Conclusion 111
5.7. References 112
6. A Machine Learning Framework for Mapping Shifts in Species' Abundance from Long-term Monitoring Data (AtiP) 131
6.1. Abstract 131
6.2. Introduction 132
6.3. Materials and Methods 136
6.3.1. Occurrence dataset and training labels (Step 1) 138
6.3.2. Predictor Variables and Training Data (Step 2) 140
6.3.3. Data cleaning (Step 3) 142
6.3.4. Model training (Step 4) 143
6.3.5. Unmasked ATI maps (Step 5) 144
6.3.6. Similarity maps (Step 6) 144

6.3.7. Final ATI map (Step 7) 145
6.3.8. Abundance gradients (Step 8) 146
6.3.9. Climate vulnerability assessment (Step 9) 147
6.3.10. Feature importance (Step 10) 148
6.3.11. Synthetic species 148
6.4. Results 149
6.4.1. Assessing species' climate vulnerability 149
6.4.2. Abundance shifts polewards and upwards towards steeper, wetter, cooler areas with lower isothermality 151
6.4.3. Species respond individually and are far from the mean 152
6.4.4. Elevation and temperature insufficiently explain abundance shifts 154
6.5. Discussion 156
6.5.1. Method interpretation 157
6.5.2. Ecological results 160
6.6. Conclusion 163
6.7. References 163
7. Summary of Results 177
7.1 Biodiversity paper (BdP) 178
7.2 Traits paper (TrP) 180
7.3 ATI Paper (AtiP) 182
8. General Discussion 184
8.1 Mechanisms of forest reassembly across ecological scales 186
8.2 The role of Functional Traits in Biodiversity Projections 191
8.3 Opportunities for Conservation 193
8.3.1 Implications for New Zealand 196
8.4 Methodological and conceptual advances 197
8.5 Limitations and future research 201
8.6 Conclusion 204
9. Acknowledgements 206
10. References 207
Appendix A: Supplementary Materials for BdP 253
A1. Variable Choice 253
A2. Available Biomes 254
A3. Model Scores 255
A4. Prediction Probability Uncertainty 258
A5. Affinity Trends 261
A5.1 Affinity Regression 263
A6. Uncertainty Partitioning 265
A6.1 Agreement between Climate Models 266
A7. Forecast Horizon 269

A8. Range and Niche Shifts supplement 272
A9. Species Abundances 273
A10. References 277
Appendix B: Supplementary Materials for TrP 281
B1. Data 281
B2. Imputation 284
B2.1 Taxonomic Eigenvectors 285
B2.2. Imputation Error 285
B2.3. Error and Hyperparameter Choice 287
B3. Supplementary Methods 287
B3.1 Formulae for computing trait moments 287
B3.2. Rate of Directional Change: plot occupancy over time 288
B3.3. Rate of Turnover: Index of Dissimilarity change per Year 289
B3.4. Null Models 290
B4. Supplementary Results 292
B4.1 Changes in climate 292
B4.2. Community environmental preferences 293
B4.3. Temporal Trends of Trait Moments 294
B4.4. The rate and identity of species change and turnover differ by forest 295
B4.5. Trend Contribution by Species Group 296
B4.6. Impact of tree ferns on trends 299
B5. References 301
Appendix C: Supplementary materials for AtiP 304
C1. Supplementary Methods 304
C1. Dataset Statistics 304
CC2. Variable Sets 307
CC3. Noise filtering 313
C1.4. Model training 317
C1.5. Similarity masking 319
C1.6. Difficulty score 320
C1.7. Regression To The Mean 323
C1.8. Binarisation of data and regression 326
C2. Evidence for Data Errors 328
C2.1. Rapid shifts in community composition 329
C2.2. Measurement goals impact plot surveys 331
C2.3. Misidentification of species of the same genus 332
C2.4. Conclusion 336
C3. Supplementary Results 337
C3.1. Training performance on subsets of data 337
C3.2. An optimal noise removal rate is 12-15% 338

C3.3. Noise removal is necessary for accurate predictions 342
C3.4. Synthetic Species Experiment 344
C3.5. Statistical Significance Testing for the Abundance Gradient 348
C4. References 349

1. Introduction

Earth is changing. Human activities, climate change, biodiversity loss, and the introduction of new colonists are reshaping the Earth's systems at an unprecedented rate (Cardinale et al. 2012; Chapin et al. 2000). These effects are interconnected, nonlinear, and compounding, and they propagate through ecological systems in cascades that remain poorly understood (Wookey et al. 2009; Lenton et al. 2023). Disturbances like wildfires or floods, which have traditionally been quantified along frequency and severity axes, have now departed so far from historical baselines that "novelty" has emerged as a third metric capturing their dissimilarity from past conditions (Turner and Seidl 2023). Similarly, the biotic composition of natural ecosystems has shifted into no-analogue states under rapid climate and land-use change, exceeding rates of species turnover observed during the last glacial transition (Staples et al. 2022; Kerr et al. 2025). In this rapidly changing environment, worldwide species rarely persist by remaining stationary, which accelerates large-scale biodiversity rearrangements and geographic redistributions (Lawlor et al. 2024). The biggest challenge of Ecology in the 21st century, therefore, is to develop robust frameworks that understand and predict the ecosystem responses to these interacting drivers so that policy and management interventions can effectively mitigate climate-driven impacts.

An abundance of studies document that, as a response to climate change, the majority of species (~50-80%) track their thermal niches by shifting their ranges along elevational and latitudinal gradients towards cooler temperatures (Lawlor et al. 2024; Rubenstein et al. 2023). But only about 20% of studies explicitly incorporate additional factors, such as precipitation (Taheri et al. 2021), which, in some cases, can be the major driver (Crimmins

et al. 2011; Fei et al. 2017) and interact with additional factors, such as topography or soil properties (Stephenson 1998). Consequently, the rate and magnitude of range shifts are below expected values based on temperature alone and vary heterogeneously across taxa and regions (Chen et al. 2011). Niche tracking therefore represents only a partial and often delayed component of species' responses, limiting the reliability of predictions based solely on climate–range shift relationships

A significant fraction of species (around one third (Lawlor et al. 2024)) deviates from expectations of thermal niche tracking, shifting downslope or toward the equator, or showing no detectable movement despite rapid climatic change (Lenoir et al. 2010). In shorter-lived and more easily dispersed plant species, biotic interactions may mediate these responses, as competitive release enables colonisation of newly suitable environments (Lenoir et al. 2010), especially within milder, downslope habitats, where, consistent with the stress-gradient hypothesis, competitive pressure increases (Bertness and Callaway 1994; Vetaas 2002). Long-lived trees, by contrast, typically respond far more slowly, with demographic adjustments lagging climate change by centuries to millennia (Beckage et al. 2008; Staples et al. 2022), resulting in locally novel, transient species assemblages (Jump et al. 2012). For instance, in New Zealand, despite being unable to reproduce, a cohort of adult red beeches (*Fuscospora fusca*) persists above today's timberline because of a brief warming event in the 17th century (Wardle and Coleman 1992). However, even slow-growing trees often exhibit changes in abundance within their current ranges before detectable range movement (Breshears et al. 2008), providing early and sensitive indicators of impending range shifts.

Biotic rearrangement often happens abruptly. As thermal limits are shared among coexisting species (Trisos et al. 2020), crossing them can lead to an abrupt, often irreversible tipping point and species' extinctions (Lenton et al. 2023; Urban 2024). For instance, mangrove expansion in Florida happens at a constant rate but decreases sharply when winter temperatures drop below -4°C (Cavanaugh et al. 2014). Demographic buffering further obscures observations of fitness because many species exhibit demographic compensation, in which declines in one vital rate (e.g. reproduction) are counterbalanced by increases in another (e.g. growth), producing stable population growth until a threshold is crossed and both rates decline (Doak and Morris 2010; Bohner and Diez 2020; Villellas et al. 2015). Land-use change can compound these dynamics, as interactions among deforestation, warming, and fire risk push forests toward savanna transitions (Nepstad et al. 2008). Such threshold behaviour also governs phenological interactions, as, for instance, in the spruce bark beetle, where warming allows for an additional generation per year and increased infestation risk (Jakoby et al. 2019) or mismatched plant-pollinator phenology leading to reduced reproduction rates (Forrest 2015). Collectively, these dynamics, therefore, call for approaches that move beyond simple correlations and explicitly capture the non-linear conditions under which ecological change accelerates and communities reorganise.

At the community scale, species' range shifts lead to broader changes in biodiversity, which have profound effects on ecosystems and are best examined collectively rather than as isolated species-level responses (Pereira et al. 2024). In most cases higher biodiversity ensures consistent ecosystem resilience and functioning, through the insurance effect of niche-complementary species that can compensate when others decline (Yachi and Loreau 1999; Turnbull et al. 2016). This enables ecosystems to maintain

functions such as production, resilience, and the ability to mitigate the effects of climate change (Hisano et al. 2018; Liang et al. 2016; Carnicer et al. 2019). Productive ecosystems, in turn, provide essential services to humans, such as biomass production, carbon sequestration, pollination, water purification, and other contributions to human well-being (Brockerhoff et al. 2017). The biodiversity lens, therefore, links range-shift dynamics to their broader ecological and societal consequences and clarifies how community-level responses shape the future functioning of forests.

While global extinction rates undeniably exceed historical rates (Proença and Pereira 2017; Pereira et al. 2024), local trends are often inconclusive, contradictory across space and scale and non-linear (Boënnec et al. 2024; Wilkes et al. 2025). For instance, in Great Britain, plant communities became species richer (Montràs-Janer et al. 2024), and plant richness on European summits increased (Steinbauer et al. 2018). These increases may mask declines or extinctions of rarer native species in favour of widespread generalists (Finderup Nielsen et al. 2019). However, contrary to expectations, in the Arctic, which experiences stronger warming, over the last 50 years, plant species richness did not change, and homogenisation did not occur (García Criado et al. 2025). Similarly, strong species turnover occurs at the global scale, but no clear richness trend can be derived (Dornelas et al. 2014). Collectively, these trends point towards a longer, more complex and non-linear trajectory for biodiversity, which starts with increased species richness due to expansion of warm-adapted generalists (Gottfried et al. 2012), but a delayed extinction of increasingly mal-adapted species lagging behind climate forcing (Cotto et al. 2017) and prompts conservationists to shift the attention to compositional changes rather than cumulative biodiversity metrics (Li et al. 2025). Forecasting these trends, therefore, will likely require novel, mechanistic and non-linear approaches (Lalechère et al. 2025).

2. Background

2.1. Species Distribution Models

Species distribution models (SDMs) offer a well-established framework for studying range shifts and biodiversity rearrangement (Franklin 2023). An SDM is a parametric function of environmental predictor variables, which typically yields a single ecologically meaningful quantity related to abundance, habitat suitability, or presence at the given location. Correlative SDMs use species' observations to parametrise this function (Guisan and Thuiller 2005). Their success is owed to easily accessible packages such as MaxEnt (Phillips et al. 2006) and to simple data requirements (e.g., presence records of a species). The second class of SDMs, mechanistic SDMs, estimate a species' fitness in a given environment by incorporating physiological and mechanistic data, rather than presence and absence alone (Buckley et al. 2018). This approach is typically data-limited but promises to provide better forecasts, especially for quickly evolving or invasive species (Lu et al. 2024; Fenollosa et al. 2025). Correlative models often underestimate a species' range as occurrence data is drawn from its realised niche after limitation through biotic and dispersion filters, while mechanistic models tend to overestimate these ranges, as they typically don't account for these filters (Sillero et al. 2021). Here, I focus on correlative SDMs, as current data constraints in New Zealand render them presently the only option for large-scale biodiversity analysis.

2.1.1. Challenges of SDMs

Correlative SDMs assume that species are at equilibrium with their climate (i.e., that the realised niche remains static under current environmental conditions), which is often not true (Sandel et al. 2025) and worsens with increasing climate change (Alexander et al. 2018). The reasons are dispersal and extinction lags, interactions with other species, and anthropogenic land-use change, which can result in disequilibrium for millennia after changes have occurred (Staples et al. 2022). This disequilibrium leads SDMs to inferring a distorted version of the fundamental niche (Thuiller et al. 2013) and can result in poor performance (Lee-Yaw et al. 2022), overprediction of species distributions (Velazco et al. 2020), or an inability to predict range shift directions (Sofaer et al. 2018). Despite this fundamental shortcoming, SDMs have proven to be powerful tools to help identify endangered species, invasion risks and other conservation-relevant factors (Guisan et al. 2013; Frans et al. 2022; Ferrier et al. 2002), as well as serve as a starting point for more complex models (Guisan et al. 2025).

The performance and fidelity of SDMs are sensitive to the choice of data. Particularly, presence-only data, which is widely used because herbaria and citizen-science platforms such as iNaturalist rarely provide absence records (Elith et al. 2020). Moreover, presence-only data often contain strong sampling and taxonomic biases, as well as positional and taxonomic inaccuracies (Graham et al. 2008; Wilkes et al. 2025). Presence–absence datasets or a combination of both offer a more robust alternative (Simmonds et al. 2020). Forest inventories that supply such data, however, can be affected by species misidentification (≈5.9%) (Scott and Hallam 2003), observer detection errors, and plot relocation mistakes (if resurveying plots) that result in species richness

estimates fluctuating by 15% - 21% depending on observer and location (Verheyen et al. 2018). Although rarely employed, automated outlier-detection algorithms can mitigate these issues and improve model performance (Liu et al. 2018; Halladin-Dąbrowska et al. 2019). Not accounting for errors and biases in the data can result in conflicting conclusions drawn from the same data (Wilkes et al. 2025), and addressing this is therefore essential to leverage large sets of ecological data for reliable conservation guidance (McCrea et al. 2023).

Covariate selection is a central determinant of reliability in SDMs, as the predictors included dictate which processes the model can capture. Mechanistically relevant covariates such as soil properties and topography often explain substantial variation in species distributions (Chauvier et al. 2021) and, for some taxa, can outweigh climatic variables (Lima et al. 2024). Yet adding predictors indiscriminately increases redundancy and collinearity, which can distort inference and undermine transferability when environmental correlation structures differ between training and prediction regions (Dormann et al. 2013). Including spatial covariates can improve model fit, but often reduces the ability to forecast into new areas because they capture patterns that are not mechanistically transferable (Brodie et al. 2020). Although automated procedures can make the choice of covariates more objective (Adde et al. 2023), they frequently yield divergent outcomes and therefore should not replace domain expertise (van Steenderen and Sutton 2024). Model performance further depends on covariate resolution (Chauvier et al. 2022) because key ecological processes, such as tree water balance, emerge from fine-scale interactions among climatic, topographic and edaphic variables (Stephenson 1998; Rapacciuolo et al. 2014). Covariates should therefore be mechanistically grounded,

minimally redundant, matched to ecologically relevant scales, and applied consistently across the species' range.

All spatial datasets are subject to spatial autocorrelation (SAC), which implies that geographically close observations are more alike than expected by chance. If unaccounted for, this leads to degraded SDM performance and to misleading significance tests for explanatory variables (Dormann 2007; Segurado et al. 2006). When used for range-shift prediction rather than inference, SAC leads to overestimates of range limits (Crase et al. 2014). Data thinning can reduce these artefacts by removing spatially redundant observations, although doing so reduces sample size and sometimes worsens predictive performance (Gaul et al. 2020; Ten Caten and Dallas 2023). A wide array of statistical approaches has been developed that explicitly model and incorporate measurement errors and biases to allow for better inference under spatial autocorrelation (Guélat and Kéry 2018; Raiter and Hawlena 2024; F. Dormann et al. 2007). If prediction, rather than inference, is the goal, non-parametric machine learning models can achieve comparable or better performance on SAC data if hyperparameters are optimised (Schratz et al. 2019). For effective conservation planning and spatially autocorrelated data, addressing SAC is therefore beneficial (Domisch et al. 2019; Crase et al. 2014).

The underlying mathematical function of an SDM can be modelled through numerous approaches, such as generalised linear models (e.g.MaxEnt, (Phillips et al. 2006)), probabilistic frameworks (Martínez-Minaya et al. 2018) or non-parametric machine learning methods, such as random forests (Breiman 2001; Valavi et al. 2021). The choice of modelling algorithm influences the predictive accuracy of SDMs (Norberg et al. 2019;

Buisson et al. 2010; Valavi et al. 2022), the extent to which they can reliably extrapolate beyond their environmental training domain (Charney et al. 2021) and consequently the projections of climate change-induced range shifts (Beaumont et al. 2016). Uncertainty arising from these differences is often addressed through ensemble methods, which combine predictions across models (Marmion et al. 2009). However, such ensembles do not always improve accuracy (Valavi et al. 2022; Hao et al. 2020), and the alleged performance gains might be artefacts of poorly tuned underlying algorithms (Soley-Guardia et al. 2024). Extrapolation problems can be constrained by measuring the similarity between training and predicted data, and by limiting predictions to a geographic area and time frame that resemble the training data (Elith et al. 2010; Owens et al. 2013; Velazco et al. 2024). Selecting and validating modelling algorithms remains essential for producing reliable biodiversity forecasts.

At the same time, SDM methodology is rapidly diversifying. Recent advances incorporate biotic interactions (Ovaskainen 2020), improving predictions, particularly for rare species (Thompson et al. 2020). In parallel, the integration of species' functional traits(Green et al. 2022) into process-based or mechanistic models (Connolly et al. 2017; Evans et al. 2016; Laughlin et al. 2012), offers the potential to capture evolutionary responses occurring alongside range shifts, such as increased voltinism under longer growing seasons (Thuiller et al. 2013). Interpretability and trust of these models can be improved by combining the algorithmic outputs with human judgment (Frans et al. 2022). New methods leverage the complexity of high-resolution satellite imagery and use deep learning, resulting in higher prediction accuracy (Dollinger et al. 2024; Bourel et al. 2025). However, given the expanding methodological landscape and the absence of consensus on a single best approach (Urban 2024), ensuring that statistical model assumptions are met may be

more critical than adopting increasingly novel methods, as mismatches between data and method can compromise inference (Sillero et al. 2021; Dormann et al. 2013).

2.1.2. Future Projections using SDMs

When SDMs are used to project biodiversity, they rely on climate data projections from global circulation models (GCMs) (Eyring et al. 2016), which assume specific scenarios of future human emissions and politics (Schipper et al. 2020). A widely used framework describing these scenarios is the shared socio-economic pathway (SSP), which combines political development, land-use change, and greenhouse gas emissions into scenarios ranging from sustainable low-emission futures (e.g., SSP1-2.6) to high-emission, fossil-fuel-dominated futures (e.g., SSP5-8.5) (Kim et al. 2018). There is currently no consensus on which scenario is most probable (Huard et al. 2022), and biodiversity forecasts should therefore base predictions on a consensus of different models (Rose et al. 2024; Dyderski et al. 2018), an average of their inputs (Knutti et al. 2010), or present the alternative predictions explicitly.

Combined GCMs, SSP scenarios, and the choice of underlying SDM constitute the primary sources of uncertainty for biodiversity projections (Thuiller et al. 2019; Morley et al. 2020; Brodie et al. 2022). Similar to SDM ensembles, combining multiple GCMs and SSPs improves prediction robustness (Goberville et al. 2015). However, prediction variance remains substantial, with extinction-risk estimates varying tenfold (Urban 2024), fueling ongoing debates over the applicability of ecological models (Lubiana Botelho et al. 2025; Woodstock and Harris 2025; Guisan et al. 2013). A comprehensive framework for managing these uncertainties remains underdeveloped, and current practice focuses on their

explicit quantification and transparent communication (Davies et al. 2023; Brodie et al. 2022). However, in a recent meta-review, only 19% of studies analysed reported uncertainty (Qazi et al. 2022). As model assumptions can have significant impacts on conservation decisions (Muscatello et al. 2021), acknowledging both the magnitude and origin of uncertainty is essential, allowing researchers to frame uncertainty as a tool for building trust with decision-makers rather than as a modelling limitation.

2.1.5. Conclusion

Despite the mathematically straightforward task of fitting a single-valued function, SDMs encompass a wide array of modelling approaches that differ in their assumptions and trade-offs (Valavi et al. 2022). This diversity reflects the numerous interacting sources of error and uncertainty arising from the quality and resolution of occurrence data, covariate selection, model structure, and future climate projections, which compound as spatial and temporal prediction scales increase and need to be addressed by the SDM. However, recent methodological syntheses have clarified these pitfalls and provided practical guidelines for avoiding them (Sillero et al. 2021; Soley-Guardia et al. 2024). Practitioners who follow these guidelines, applying rigorous data filtering, mechanistically grounded covariate selection, and explicit treatment of covariance structures, can generate SDMs that provide robust insights for studying and preserving biodiversity (Thuiller et al. 2013; Woodstock and Harris 2025; Frans and Liu 2024). SDMs therefore represent an increasingly capable modelling framework, with ongoing advances steadily reducing remaining limitations and broadening the ecological questions they can address (Maréchaux et al. 2021; Urban 2024).

2.2. Functional Ecology & Functional Indices

To gain a better mechanistic understanding of plant responses to climatic shifts, ecologists group species based on morphology, anatomy and strategy (Laughlin 2023; Grime 1977). These groups delineate species which share similar traits, which collectively modulate their responses to biotic and abiotic conditions, laying the foundation for modern functional ecology (Violle et al. 2007). Here, I adopt Violle et al.'s definition of a functional trait as a "morpho-physio-phenological trait which has an impact on fitness" and "is measurable at the level of the individual, without additional information from the environment". Combinations of such functional traits into trait syndromes reflect ecological strategies that allow species to succeed in a given environment (Laughlin 2023), modulating long-term shifts in species composition (Henn et al. 2024) and ecosystem services (Bu et al. 2018). Functional traits, therefore, offer a mechanistic link between plants and their environment, which is critical to understand plant responses under novel climatic conditions (Funk et al. 2017).

Functional traits across species are not arranged in groups, but spread along a continuum within a multi-dimensional space of continuous strategies, characterised by trade-offs and linkages between traits and functions (Laughlin 2023). Based on six leaf traits, the Leaf Economic Spectrum, for example, describes a global trade-off from conservative resource use to fast resource acquisition (Wright et al. 2004), corresponding to Grime's stress-tolerant and ruderal strategies (Grime 1977) or the r-K selection spectrum (Pianka 1970). However, while plant strategies are often qualitative and derived from long observational studies, trait spectra can be constructed by computationally identifying meaningful directions in multi-dimensional trait space. This includes the wood

economics spectrum (Chave et al. 2009) (trade-off between density and growth), a root economics spectrum (Kong et al. 2019) (acquisitive to recalcitrant roots), or a fast-slow continuum (Salguero-Gómez et al. 2016) (fast to slow growing species). These spectra, however, are simplifications with limited predictive power, typically explaining less than 75% of variation (Díaz et al. 2016). More fundamentally, they remain imperfect proxies for ecological functions. Phenotypic plasticity can decouple trait values from resource use (Anderegg et al. 2018), and species' fitness may depend on trait distinctiveness within communities rather than absolute trait values (Mahaut et al. 2023). Together, these factors weaken the trait–function relationship and highlight the ongoing challenge of predicting ecosystem functioning from traits (Funk et al. 2017; Lavorel and Garnier 2002).

2.2.1. Challenges of Functional Ecology

Linking functional traits to ecosystem functioning or fitness has proven challenging for multiple reasons. First, despite being well-studied and correlated with the environment (Wieczynski et al. 2019), single traits lack explanatory power (Martínez-Vilalta et al. 2023) because evolution operates on coordinated trait syndromes, where multiple traits interact under trade-offs within specific environmental contexts (Díaz 2025). Second, relationships between traits and fitness depend on the combination of the individual's other traits (Swenson et al. 2020; Mueller et al. 2024) and the local-scale environment shaped by microclimates and disturbances, rather than climate, making insights difficult to transfer (Bruelheide et al. 2018). Third, in addition to strong environmental filtering (Caruso et al. 2020), trait combinations are constrained by evolutionary history, leading to different trait combinations in similar environments (Medeiros et al. 2020; Lamouroux et al. 2002). Finally, trait values can vary strongly across individuals of the same species

(intraspecific variation or ITV), obscuring clear trait environment relationships, especially if traits are measured on only a few individuals (Albert et al. 2011; Chacón-Labella et al. 2023). Although our understanding of how environment, evolution and traits interact is imperfect, it remains the most promising mechanistic approach to improve predictions of future climate and biodiversity rearrangement under no-analogue climate (Van Bodegom et al. 2012; Chacón-Labella et al. 2023; Hagan et al. 2023).

The first major challenge in trait-based ecology is the selection of informative traits to answer the respective research question (Funk et al. 2017) because traits must align with the mechanisms, environments, and functions under study (Chacón-Labella et al. 2023). Globally defined "keystone" traits, such as the leaf economic spectrum (Wright et al. 2004), capture broad r–K strategies but can be locally irrelevant. Wetland plants, for instance, exhibit specialised traits that enable persistence under waterlogged, anoxic conditions (e.g., aerenchyma formation or root porosity), and are largely decoupled from the LES (Pan et al. 2019). Although databases such as TRY (Kattge et al. 2020) provide extensive trait coverage, they typically don't cover specialist or expensive-to-measure traits. For instance, we found nitrogen-15 ($\Delta^{15}N$) and carbon-13 ($\Delta^{13}C$) isotopes, which offer mechanistic insight into nutrient acquisition, nutrient limitation, water-use efficiency, and plant–microbe associations (Dawson et al. 2002; Song and Zhou 2021; McLauchlan et al. 2010), largely missing for the New Zealand flora. This limited understanding and availability of context-dependent traits result in overreliance on one to three easily measured, mainly foliar traits, thereby constraining predictive applications (Green et al. 2022). Enhancing trait-based predictions, therefore, requires the employment of a broader suite of functionally explicit interacting traits across multiple organs, directly relating to species fitness (Laughlin 2014).

For the selected traits to be used in a predictive fashion, the trait-environment relationships must be assumed transferable across species and locations (Shipley et al. 2016). There is currently no consensus on how well this assumption holds. For example, Tundra plant communities across four global sites showed consistent trait-environment relationships (Kemppinen et al. 2021), and traits successfully predicted relative growth rates of trees along large environmental gradients in Hawaii (Medeiros et al. 2019). In contrast, attempts to use data from one Australian site to predict patterns in another failed (Thomas and Vesk 2017), and traits of trees globally only poorly predict growth rates (Paine et al. 2015). The lack of consensus can be explained by scale (local factors filter traits stronger than global) (Bruelheide et al. 2018), the choice of traits irrelevant to fitness at the given location (Yang et al. 2018; Anderegg 2023), our lack of understanding how integrated phenotypes (i.e. the coordinated combination of multiple traits) influence performance (Díaz 2025), or the differential importance of traits on different life and successional stages (Visser et al. 2016; González-Melo et al. 2024; Sun et al. 2025). This discourse indicates a rapidly maturing field rather than a theoretical impasse, as new frameworks, experiments, and databases explicitly synthesise scale, trait coordination, and life-history context to advance a more robust and mechanistic understanding of ecological function (Laughlin 2024).

This understanding can benefit from integrating evolutionary theory, which connects traits to their impact on fitness (Ackerly and Monson 2003; Caruso et al. 2020) and can help explain the limited predictive power of individual traits (Green et al. 2022). For example, drought stress can be avoided (e.g., succulence), tolerated (e.g., hydraulic safety), or escaped (e.g., tap roots) (Laughlin 2023). While each strategy confers survival at a given

location, the species will differ in their traits, precluding the identification of a trait-environment relationship. Evolution will also constrain trait–environment relationships, as plant biomass responses to nitrogen availability, for example, vary widely yet remain phylogenetically structured, with closely related species responding more similarly than expected by chance (Wooliver et al. 2016). At the community level, these constraints can lead to different trait combinations in similar environments (Anderegg 2023). Moreover, evolutionarily conserved traits serve multiple functions (e.g. thicker leaves confer resistance to herbivory and drought), making their impacts on fitness context-dependent (Sack and Buckley 2020). In evolutionary terms, a central mistake in functional ecology, therefore, has been the assumption of a universal trait–environment convergence, which is common for some traits (Carta et al. 2022) but not universal. Because selection acts on phenotypes expressed in particular environments (Díaz 2025), trait-based models must jointly incorporate traits and environment to identify multiple viable phenotypes, rather than assume continuous trait–environment gradients.

Plant traits exhibit significant trait variability not only at the species level but also at the individual level. Intraspecific trait variation (ITV) is globally widespread, explaining 25-32% of the variation among 629 communities and 36 functional traits (Siefert et al. 2015). This variation is particularly pronounced in species-poor communities and at local spatial scales (Jung et al. 2010). As the spatial scale increases, however, the importance of ITV is overtaken by between-species variation (Albert et al. 2011; Da et al. 2022). Quantifying ITV is methodically challenging (Yang et al. 2020) and likely not generalisable because it depends on the trait choice, as leaf nutrient traits and whole-plant traits exhibit higher ITV than other functional dimensions (Westerband et al. 2021). Consequently,

the importance of ITV motivates a shift toward individual-based approaches (Violle et al. 2012), which remain data-intensive but are essential when ITV is relevant to the research question (Chacón-Labella et al. 2023). Recognising patterns of intraspecific trait variation that meaningfully affect ecological processes and incorporating them in the respective analyses is therefore essential for improving trait-based predictions.

2.2.2. Combining Traits into Functional Trait Indices

Biodiversity often refers to species richness, which treats species equally, and neglects their differences in abundance and function. However, dominant species influence ecosystems disproportionately (Mass Ratio Hypothesis) (Grime 1998). Consequently, their traits and trait diversity exert a larger effect on ecosystem functions (Díaz and Cabido 2001). Community-weighted mean trait values (CWM), for instance, globally have strong relationships with biomass accumulation, nutrient cycling, and regeneration dynamics (Rosenfield and Müller 2020). However, mean trait values alone incompletely characterise communities, because even when mean values remain equal, trait distributions can vary in variance or skew, which capture additional aspects such as adaptability or ongoing migration (Enquist et al. 2015). Such higher-order moments, too, differ substantially across biogeographic gradients and can be used to assess the impacts of climate change (Wieczynski et al. 2019). Recently, research has focused on combining multiple traits into multi-trait functional diversity indices, enabling more comprehensive quantification of ecosystem functioning (Villéger et al. 2008). Trait indices link functional strategies to ecosystem function (Funk et al. 2017; Kühn et al. 2021) more reliably predict biomass (Clark et al. 2012),(Clark et al. 2012), productivity (Yan et al. 2023),(Yan et al. 2023), and multifunctionality (Mouillot et al. 2011),(Mouillot et al. 2011) than single traits. Moreover,

they can be used to infer community assembly mechanisms (Mouchet et al. 2010) and thus offer a straightforward method to generate additional insights from trait data.

Currently there is an abundance of functional diversity indices and libraries (Mammola et al. 2021). The current consensus, however, is that functional diversity is multi-dimensional. The most widely adopted approach is based on: Functional Richness (FRic), Evenness/Regularity(FEve) and Divergence(FDiv) (Villéger et al. 2008) and dispersion (FDis) (Laliberté and Legendre 2010), with ongoing debate on how these are best calculated (Schmera et al. 2023) and the inclusion of additional dimensions such as redundancy or rarity (Ricotta and Pavoine 2024). FRic captures the range of plant strategies and can be calculated as the volume of trait space occupied by species (Cornwell et al. 2006). FDiv captures the abundance distribution in trait space and is low when species are functionally similar. It is calculated from the species' distance to the centre of the trait volume. FEve measures how evenly spaced the between-species trait differences are and is calculated by averaging the smallest between-species differences using a minimum spanning tree (Pla et al. 2012). Evenness peaks when abundance is spread evenly across the trait spectrum. FDis captures trait dispersion in a way that is largely independent of species richness and is measured in the multi-dimensional trait space as the species' abundance-weighted average distance from the centroid (Laliberté and Legendre 2010). While alternatives to these definitions have recently been proposed (Schmera et al. 2023), this thesis will focus on the original definitions, due to their widespread acceptance and maturity.

Aspects of functional diversity correlate with ecological processes and community assembly mechanisms (Guillerme et al. 2025). Low functional richness or evenness

suggests that a community may lack or underrepresent key functional strategies for exploiting available resources, thereby reducing productivity and increasing vulnerability to invasion by species with complementary traits (Mason et al. 2005). Indeed, FRic and FDis are lowered in invaded communities (Castro-Díez et al. 2016; Kuebbing et al. 2018). High functional richness, on the other hand, corresponds to communities in which abiotic filters are relaxed, allowing multiple competing functional strategies to coexist, thus increasing their functional differences due to the principle of limiting similarity (Weiher and Keddy 1995). However, multiple assembly mechanisms can operate simultaneously along different niche axes (e.g., aboveground and belowground), revealing distinct patterns depending on the traits selected (Spasojevic and Suding 2012). Finally, diversity indices change predictably during succession, with FRic increasing and FEve decreasing, although these trajectories vary with environmental resource availability (van der Sande et al. 2024). Functional diversity patterns should therefore complement trait analysis to answer additional questions related to community assembly and ecosystem processes (Mason and de Bello 2013).

2.2.3. Conclusion

Despite its numerous challenges, trait-based ecology is a rapidly evolving approach that combines physiology, evolution, and environment to develop a mechanistic understanding of plant responses to climate change, which is necessary for predicting biodiversity rearrangement in the future (Thuiller et al. 2013). As climate and biotic composition shift into no-analogue states, communities will need to adapt, as mediated by trait composition and plasticity, and thereby determine how effectively ecosystem functioning can be maintained. Predicting these changes at larger scales is necessary but remains out of

reach, due to the complexities of species' range dynamics, limited data availability and a lack of conceptual understanding (Martínez-Vilalta et al. 2023; Verberk et al. 2013). However, recent work outlines a clear methodological roadmap, which combines theory-driven trait selection, improved trait coverage, and careful treatment of range-shift estimation biases. Together these advances enhance the feasibility of predicting biodiversity rearrangement at macroecological scales (Comte et al. 2024).

2.3. New Zealand based models

Three properties make New Zealand potentially distinct with regard to modelling climate-change responses. First, palaeoecological evidence suggests an over-representation of warm-adapted species, resulting from repeated glacial cycles in the absence of a continuous cold environment, whereby cold-adapted species found fewer refugia, retreated farther, and did not recover their climatically suitable ranges (McGlone et al. 2016). This applies particularly to beeches, which dominate New Zealand's cold-adapted forests yet remain out of equilibrium with climate (Leathwick 1998), making them harder to model from climate data (Leathwick et al. 1996). However, refugia dynamics are documented globally (Parducci et al. 2012; Zeng et al. 2015), and similarly result in underfilling of the species' potential ranges (Seliger et al. 2021; Svenning and Skov 2004). Second, introduced browsers restructure forests by palatability (Hawcroft et al. 2024) and because many of New Zealand's trees are bird-dispersed (McGlone et al. 2016), the depletion of its avifauna may constrain climate-tracking more severely here than elsewhere (Fricke et al. 2022). Third, Polynesian and subsequent European burning from AD 1280 dramatically reduced forest cover and expanded grasslands that had

previously been largely confined above treeline (Perry et al. 2014). Collectively, these observations have led to the view that in New Zealand indirect effects of climate change such as invasive species outweigh direct ones (Macinnis-Ng et al. 2021; Keegan et al. 2022).

Potentially due to the prevalence of this assumption only very few studies in New Zealand have tested or modelled direct climate-change responses. Moreover, existing studies exhibit limitations either in spatial extent, climatic resolution, or taxonomic coverage. For instance, the presently most cited study in New Zealand found no evidence for treeline shifts of four beech species, but was conducted decades ago at a single South Island location (Cullen et al. 2001). Similarly, early work projected broad changes in tree distributions but used a coarse 5-km grid and now-outdated climate projections (Leathwick et al. 1996). More recently, using SDMs, the area suitable for *Nothofagus* species was projected to decline by 12.1% in 2070 (Mathias et al. 2023), while 52% of current fern habitat may become unsuitable by 2100 (Watts and Watkins 2022). Only one recent study made use of the entire NVS dataset across a wide range of 48 tree species, and while not focused on climate change, found the importance of both climate and biotic competition on demographic rates (Jo et al. 2025). This leaves a substantial gap between the availability of decades of nationwide vegetation records (NVS, (Wiser et al. 2001)), and their use for detecting direct climate change effects of New Zealand's flora. It is therefore timely to challenge the assumption of the predominance of indirect climate change impacts and attempt to model them into the near future.

3. Thesis Aims & Structure

Based on New Zealand's vast forest inventory data (NVS, (Wiser et al. 2001)) I want to understand the collective changes forests in New Zealand experience in the 21st century and the impacts this has on their biodiversity, composition, and resilience. The first lens through which this problem is explored is to forecast the trajectory of taxonomic biodiversity as species continue shifting their ranges. The second lens is to investigate which functional and compositional changes underlie shifts in biodiversity and which assembly mechanisms cause them. This task requires the collection of functional traits of native woody plants to supplement existing collections (e.g. TRY (Kattge et al. 2020) or EcoTraits Landcare Research 2005). Finally, I will assess range shifts that have already occurred, understand their drivers and make predictions about which species are at risk in the coming decades. Collectively these three chapters cover different dimensions of change from total biodiversity to the fate of single species and provide explanations from abiotic drivers to community assembly mechanisms and thus contribute to our understanding of climate change-related shifts in plant biodiversity under no-analogue climates.

The biodiversity paper (BdP) addresses the question of why biodiversity projections are globally inconclusive (Rubenstein et al. 2023). It starts from the observation that most existing forecasts implicitly assume linear biodiversity responses to warming (Boënnec et al. 2024), rely on species-level distribution models with limited ecological realism (Lee-Yaw et al. 2022), and inadequately account for interacting drivers, scenario uncertainty, and data bias, leading to substantial uncertainty and contradictory empirical results (Johnson et al. 2024). To address these limitations, the paper uses a biome-based SDM and argues

that this approach can better capture joint species responses to abiotic constraints while implicitly reflecting biotic interactions. Based on climate projections and biome composition, it develops a novel thermal affinity metric that links species' realised temperature niches to projected biome distributions under alternative SSP–RCP scenarios. Thermal affinity can then be used as a spatially explicit estimate of the number of species passing through the abiotic filter and thus as an estimate of future species richness.

The traits paper (TrP) addresses how climate-driven shifts in forest composition stem from divergent community assembly mechanisms and functional reorganisation across biomes. While forest communities globally exhibit broad trends such as thermophilisation (Gottfried et al. 2012), increasing local species richness (Montràs-Janer et al. 2024; Steinbauer et al. 2018), and homogenisation (Li et al. 2025), these aggregate patterns obscure differential and context-dependent mechanisms. Moreover, research on the development of these trends in New Zealand is scarce and the direct impacts of climate change are debated (Keegan et al. 2022). The paper adopts a functional trait–based framework to infer the ecological strategies and assembly processes underlying forest reassembly. Using long-term NVS data supplemented with newly compiled and collected functional trait and isotope data, the study partitions forest communities into cold-adapted, warm-adapted, and ecotonal types. It then contrasts their community-weighted mean traits, multi-trait functional diversity indices, and a novel abundance-based turnover metric to identify the differences in their functional strategies, assembly mechanisms, and turnover rates. In doing so, this paper adds detail to the biodiversity patterns identified in the first paper by revealing the functional and assembly-level processes that drive forest reorganisation under ongoing climate change.

The abundance trend indicator paper (AtiP) shifts the focus from community- and biome-level changes to the fate of individual species, asking how climate change is already reshaping species' distributions within their current ranges and which taxa show signs of decline. It proposes the Abundance Trend Indicator (ATI), an SDM-like machine-learning approach that learns the conditions under which changes in species' abundance have occurred. Rather than species presences and absences ATI is based on abundance differences in repeated measurements of NVS plots and various climatic, edaphic and topographic variables. This reveals subtle within range abundance shifts, which precede range-shifts by decades or centuries in long-lived trees (Breshears et al. 2008; Beckage et al. 2008) and can identify species-specific and global drivers. Based on how much of a species' extent is projected to experience abundance declines, ATI can reveal the identity of vulnerable species and explain what drives their vulnerabilities. This study highlights how existing forest inventory data can be used in novel ways to aid conservation decisions and deepen understanding of range and niche shifts.

The window for effective climate action is open, but closing (Díaz et al. 2019; Pörtner et al. 2023), which demands science-based strategies that can guide the rapid, integrated transformations required to secure a resilient future. Chief among them is resolving how species respond to accelerating environmental pressures, because maintaining local diversity and the interactions it supports is fundamental for ecosystem health (Valiente-Banuet et al. 2015). At the same time, attention to broader-scale biodiversity assembly processes is needed, as community restructuring, turnover, and non-linear thresholds collectively determine ecosystem functioning (Turnbull et al. 2016). These two perspectives operate with distinct temporal and spatial dynamics and require different

methodological approaches. However, they can be derived from the same forest inventory data, and advances in field data collection protocols continue to improve in this direction (Chirici et al. 2012). This data enables spatially and temporally explicit predictions to identify where, when, and how ecosystems are most vulnerable, thereby surpassing expert opinion, which is commonly employed in conservation policy decisions (Di Febbraro et al. 2018). By integrating these complementary perspectives, this thesis advances that goal by developing novel methods to diagnose present biogeographic change, quantify emerging ecological signals, and forecast plausible futures for New Zealand's forests.

4. Approaching Peak Biodiversity: Non-linear Responses of Plant Biodiversity to Climate Warming (BdP)

4.1. Abstract

1. Climate change is shifting species distributions, producing widespread changes in species richness. However, these changes differ across biomes, climate trajectories, and species sensitivities, hampering our understanding of biodiversity change and obstructing future projections.
2. Here, we assess how different climatic variables affect trajectories of species richness across six distinct biomes individually and collectively, under four SSP-RCP scenarios from present day to 2100. Using satellite data for biome classification and 13159 vegetation surveys from

New Zealand spanning subtropical to alpine environments, we develop a novel hierarchical modelling approach: the landscape affinity framework. It combines a spatially explicit projection of biome area with the climatic niches of 1028 plant species within those biomes, into a single value, which we interpret as a proxy estimate for the overall local species richness across the entire landscape at a given time and SSP scenario.

3. Our projections suggest a loss of area for cold-adapted biomes but increases in their species richness, while warm-adapted biomes expand, losing species. At the landscape scale, these opposing trends combine to produce climatic conditions initially conducive to increased species richness, followed around mid-century, by either saturation or decline, depending on the emission pathway.
4. Synthesis: Our results reveal how non-linear and diverse species richness trends can arise from regionally monotonous trajectories, thereby reconciling previous contradictions in biodiversity studies, and highlight that the future of plant diversity in New Zealand depends on socioeconomic choices, geographic scale, and the biome under study.

4.2. Introduction

Rapid, climate-driven reorganisation of biodiversity is transforming ecosystems globally (Lawlor et al., 2024), pushing species in the mid-21st century towards thermal regimes and ecosystem states without historical precedent (Kerr et al., 2025; Mora et al., 2013). These environmental changes collectively impact ecosystem productivity (Mao et al., 2022; Yachi & Loreau, 1999), carbon sequestration capacity (Carnicer et al., 2019; Sakschewski et al., 2016), resilience (Oliver et al., 2015), and critically, the ecosystems' ability to buffer further climate change (Hisano et al., 2018). As climatic

thresholds are crossed and tolerance limits exceeded, changes can occur abruptly, affecting whole communities simultaneously (Trisos et al., 2020), progress rapidly (Urban, 2024) and driving potentially irreversible biome shifts (Brandt et al., 2013). Despite the severity of these risks, there remains optimism that targeted interventions can slow or avert biodiversity decline (Bergstrom et al., 2021; Langhammer et al., 2024). However, for these interventions to be effective, they must be based on accurate biodiversity projections, which account for the spatially heterogeneous and non-linear nature of natural systems (Boënnec et al., 2024; Pressey et al., 2007) and span large spatial scales and diverse taxonomic groups (Pilotto et al., 2020).

Projections of biodiversity cannot be based solely on observations, as they yield conflicting and often misleading signals given the complexity of ecological datasets (Rubenstein et al., 2023). Observed species richness trends have demonstrated increases (Montràs-Janer et al., 2024; Steinbauer et al., 2018), declines (Pereira et al., 2024) and apparent stability (Dornelas et al., 2014; García Criado et al., 2025; Vellend et al., 2013), as well as a decoupling of local trends and global trajectories (Pilotto et al., 2020) These contradictory observations can stem from a lag between climate forcing and biodiversity responses (Cotto et al., 2017), invasions by non-native generalists that co-exist with natives (Sax & Gaines, 2008), persistent seed-banks (Plue et al., 2017), life-history traits of individuals and populations facilitating survival under deteriorating conditions (Figueiredo et al., 2019), collectively compounding to a difficult-to-predict non-equilibrium state (Lalechère et al., 2025). These trends are often falsely assumed to be linear (Boënnec et al., 2024), despite, for instance, that the health and density of vegetation shows predominantly unimodal trajectories globally (Higgins et al., 2023). Moreover, trends in biodiversity may weaken, vanish, or reverse once spatial, temporal and phylogenetic autocorrelation is accounted for (Johnson et al., 2024), calling into question whether

local species richness forecasts are useful for inferring landscape or global changes (Valdez et al., 2023).

The disconnect between local and landscape species richness projections can also result from collectively modelling biomes that have heterogeneous abiotic characteristics and extinction dynamics (Figueiredo et al., 2019). For instance, warming increases species richness in alpine communities at the lower thermal limit (Steinbauer et al., 2018) and decreases it in tropical communities at the upper thermal limit (Fortier et al., 2024). These differential climate responses are also observed across taxa with similar traits and phenology (Martén-Rodríguez et al., 2025), indicating that biomes with similar environmental filters and adaptations may respond similarly to climate change. Moreover, biome states are stabilised by feedbacks that maintain distinct species assemblages under similar climates (e.g. grasslands and forests; (Pausas & Bond, 2021). Incorporating the collective responses of biomes, in addition to the individual responses of their constituent species, may therefore enable species richness projections to be scaled more effectively from local to landscape scales.

Biodiversity projections often rely on species distribution models (SDMs) that correlatively estimate species occurrences (D'Amen et al., 2017; Pereira et al., 2010) or biodiversity patterns (Midolo et al., 2025) from climate data. However, combining responses of individual species into a biodiversity estimate ignores their interactions and may overestimate overall species richness (Calabrese et al., 2014; Grenié et al., 2020). Although joint SDMs attempt to relax this assumption by modelling multiple species simultaneously, they require more and often sparse co-occurrence data (Ovaskainen, 2020; Pichler & Hartig, 2021), which may increase spatial biases and, if not accounted for, adversely affect model performance (Sandel et al., 2025). More fundamentally, the

species-centred SDM framework struggles to capture biome-specific feedbacks (e.g., fire in grasslands) that maintain distinct species pools under otherwise similar abiotic conditions (Pausas & Bond, 2021). Incorporating community-level environmental constraints can therefore improve predictive performance (Caradima et al., 2019). Moreover, biomes are more strongly climatically constrained than the species within them (Prentice et al., 1992). This can however be methodologically challenging, requiring multiple models operating at different scales (D'Amen et al., 2017). For example, paired models of α and β-diversity can be combined with sparse survey data to reconstruct spatially explicit community composition (Mokany et al., 2011). Models that integrate community-level structure are therefore likely to be better suited to predicting biodiversity outcomes, particularly when a large species pool containing rare species is modelled.

To obtain future projections, biodiversity models are coupled with a wide array of climate models (Eyring et al., 2016), which rely on assumptions about human greenhouse gas emissions and land-use change scenarios (Jaureguiberry et al., 2022; Schipper et al., 2020). These scenarios are embodied in the shared socioeconomic pathways (SSPs), quantifying scenarios from sustainable, low-emission worlds (SSP1–2.6) with potentially positive impacts on biodiversity by the end of the century (Pang et al., 2024), to fragmented or fossil-fuel–driven, high-emission futures (SSP3-7.0 and above) with detrimental effects (Kim et al., 2018). Biodiversity and extinction projections can fluctuate more than 10-fold based on scenario and model choice (Urban, 2024; Wiens & Zelinka, 2024) or become entirely unreliable when extrapolated beyond the set of currently known conditions, which imposes both temporal and spatial limits on projections (Charney et al., 2021; Velazco et al., 2024). Finally, "hidden uncertainty", including taxonomic, sampling and collection biases, can undermine the quality of the underlying species occurrence data (Wilkes et al., 2025). Because these uncertainties are unavoidable, modelling approaches must explicitly quantify

extrapolation thresholds and sources of uncertainty, information that is itself essential for guiding effective conservation decisions (Brodie et al., 2022), but which is often neglected (Qazi et al., 2022).

Here, we aim to model plant species richness across New Zealand's terrestrial biomes and identify their collective trajectory using a novel hierarchical modelling approach that combines biome-level dynamics with individual species preferences. New Zealand combines broad subtropical-to-sub-Antarctic and coastal-to-alpine climatic and elevational gradients, diverse flora, high endemism, extensive conserved lands, and almost 70 years of forest inventory data (Wiser et al., 2001), making it an ideal system for understanding landscape-scale biodiversity dynamics. Although its glacial and recent land-use history has left parts of the landscape with a flora that is in climatic disequilibrium (McGlone et al., 2016; Perry et al., 2014), this legacy varies among species and regions (Leathwick et al., 1996; Marske & Boyer, 2024), while biomes, modelled here, remain more strongly climatically constrained than individual species (Prentice et al., 1992). Our study encompasses six major natural ecosystems under four SSP-RCP scenarios through 2100. We aimed to (1) quantify the spatial and temporal reorganisation of major terrestrial biomes, and (2) estimate the impacts of these changes on plant biodiversity trajectories. Using satellite imagery and machine learning, we first model how biome distributions shift through time, then combine these projections with changes in the climatic suitability of each biome for its constituent species to estimate trajectories of species richness. This novel approach captures 1,028 species, avoids sampling and taxonomic biases, and readily identifies non-linear, long-term biodiversity trajectories. This enables a clearer, spatially and temporally explicit picture of the future of New Zealand's terrestrial biomes, providing a framework for large-scale, hierarchical studies of species richness worldwide.

4.3. Methods

We used three spatially-explicit pixel-based datasets: time-varying climatic variables, static environmental variables, and satellite-derived biome classifications. We trained a machine learning model to predict biome identity from climate and environmental data, then applied it to future climate scenarios to map projected biome distributions. We limited spatial and temporal extrapolation using a threshold based on the similarity between future and present-day data. Uncertainty was partitioned to understand how the choice of climate model or SSP influences the outputs. Based on species' abundance from plots within biomes, we developed a species-biome affinity method to estimate biodiversity trends for 1028 species (**Fig. 4.1**).

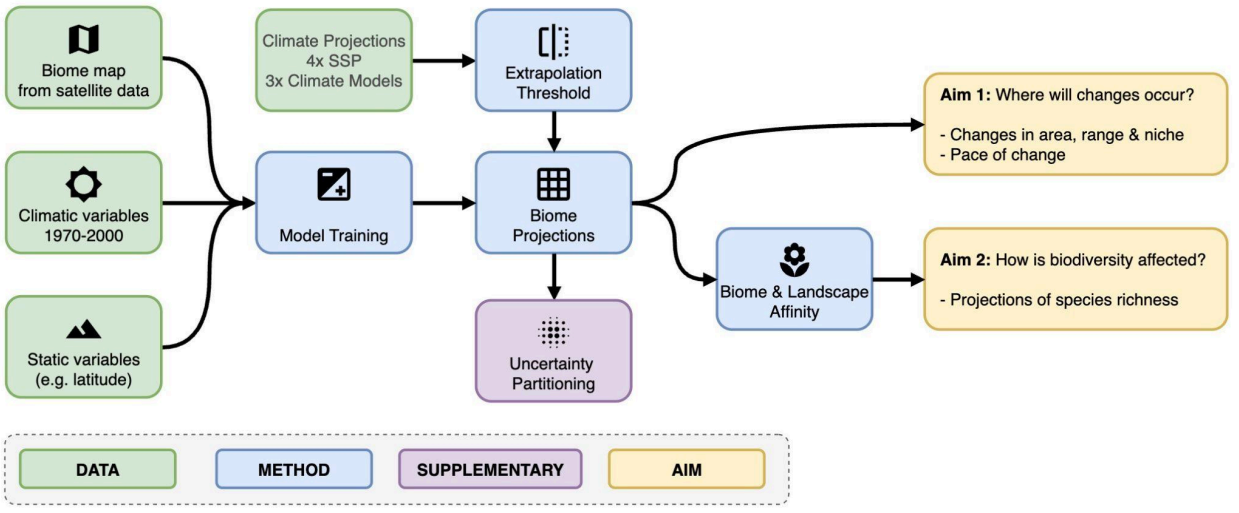


Figure 4.1: Schematic overview of data, methods and goals used in this study.

4.3.1. Training Data

4.3.1.1. Biome Data

Using the Basic Ecosystem layer from New Zealand's Landcare Research database (Landcare Research, 2024), we determined the biome of each pixel, focusing on six biomes (Beech forests, Podocarp (which also included broadleaved species) forests, Mixed forests, Shrublands, Alpine ecosystems and Tussock grasslands) (***Fig. A12***). This excluded all agricultural, silvicultural, urban or barren land and included 94% of all natural ecosystems, with the remaining 6% containing data-deficient or unspecified classes (***Fig. A2***). The data were rescaled to 1 km^2 resolution to match the climate data. Since biomes partly reflect temperature and elevation gradients (***Fig. A13***), we use the terms "warm-adapted" for podocarp forests, mixed forests and shrublands, and "cold-adapted" for beech forests, alpine vegetation and tussock grasslands when discussing broad cross-biome responses, noting latitudinal overlap of the six biomes.

4.3.1.2. Present and Future Predictor Variables

We used 28 static topographic and edaphic variables (e.g. elevation) from the NZEnvDS dataset (McCarthy et al., 2021), and 19 Bioclim variables from WorldClim 2.1 (average of the years 1970 - 2000) (Fick & Hijmans, 2017) scaled to a 1 km^2 per pixel resolution (referred to as present-day baseline). To facilitate interpretation, we eliminated 22 variables by stepwise exclusion of pairs with correlations above 0.7 (Section S1, ***Fig. A1***). Climate data projections 2020-40 (abbreviated by the mid-point year e.g. "2030" in some figures), 2040-60, 2060-80 and 2080-2100 were obtained from Worldclim for Phase 6 of the Coupled Model Intercomparison Project (CMIP6) under four scenarios from shared economic pathways (SSPs) combined with representative concentration pathways (SSP1-2.6, SSP2-4.5, SSP3-7.0 and SSP5-8.5) (Kim et al., 2018). To capture coupled carbon–climate

and biosphere–atmosphere feedbacks in future climate projections, we selected Global Circulation Models (GCMs) with an Earth System Model (ESM) (Table A1) and averaged their projections. While averaging GCMs can obscure divergent spatial responses (Goberville et al., 2015; Knutti et al., 2010), in our case the biome predictions based on the different GCMs showed total disagreement in only ~1.7% of forest area (***Fig. A5***). The GCM choice did not substantially affect the landscape affinities trends (***Fig. A8***) or the biome area trends underlying them (***Fig. A9***). This consistency is expected because biome distributions are predominantly constrained by long-term climatic regimes rather than short-term climatic fluctuations (Prentice et al., 1992; Sato, 2026) and supports the use of the ensemble mean, allowing the analyses to be focused on isolating the consequences of SSP scenarios, which are more directly relevant to climate mitigation decisions.

4.3.2. Model Choice, Training and Uncertainty Estimates

4.3.2.1. Choice of Model

We framed biome prediction as a multi-class classification task and selected oblique random forests (ORFs), which combine the interpolation strengths of random forests with the extrapolation capabilities of linear models (Charney et al., 2021), yielding smoother, more ecologically realistic decision surfaces (Katuwal et al., 2020; Menze et al., 2011). The model was trained on 35,000 randomly selected pixels, as adding more pixels to the training did not improve performance. Performance was assessed via 5-fold spatial cross-validation with the block size automatically determined to be 76 km using the semivariogram method in the `cv_spatial_autocor` function of the blockCV package (Valavi et al., 2019). The average performance exceeded the established threshold for reliable predictions in ecology using the true skill statistic (Yoon & Lee, 2023) (see Section S3 for

details and ***Fig. A3***). Model confidence was high, as the probability of the predicted class was 3-4x higher than that of the second most probable class (see Section S4 and ***Fig. A4***).

4.3.2.2. Extrapolation Threshold

Extrapolating predictions to environmental conditions dissimilar from the training data can lead to degraded and unpredictable model performance. We quantified this dissimilarity using the Shape method(Velazco et al., 2024). For any datapoint (i.e. a vector of environmental variables), the Shape distance is 0 for observed data points, and 1 if the point is as distant from the nearest training point as the existing points are to the centroid of the training data. Because this value depends on the predictor variables, climate projections, and quantifies novel and unobserved climate, no objective or universally valid threshold exists for distinguishing reliable from unreliable extrapolation. We selected a conservative threshold by comparing alternative variable sets, dissimilarity methods, and threshold values, and by evaluating the resulting forecast horizons against previous studies (see discussion in section S7, **Fig. S9**). This resulted in a Shape threshold of ~1, corresponding to a forecast horizon of approximately 2070 under SSP3-7.0, typical for landscape-scale forest analyses (e.g., (Ali et al., 2023; Dyderski et al., 2018; Noce et al., 2017). It is important to note that this threshold can't be easily validated, as a space-for-time substitution or spatial cross-validation method tests the ability of the predictive model to generalise spatially, rather than the validity of the climate novelty threshold.

4.3.3. Range and Niche Shifts

To identify which environmental conditions change strongly (niche shifts) within individual biomes, we compared their present-day distributions to the future projections using Cohen's d (Cohen,

2013). Cohen's d measures the difference of two samples (e.g. present-day precipitation at each pixel of a biome *vs*. projected precipitation at the biome's projected pixels) relative to their standard deviation (small: 0.2–0.5; medium: 0.5–0.8; large: >0.8). To quantify the rates of change in environmental conditions in absolute terms rather than in standard deviations (e.g. latitude change in km per decade) we used the slope of a linear regression over the mean value of that variable in the respective biome over time.

4.3.4. Species Climate Affinity Framework

Inspired by the community temperature index(Devictor et al., 2008), we developed a species–biome affinity metric describing how closely the realised climatic distribution of a species corresponds to the climatic conditions found within a biome (examples in ***Fig. A13***). We calculate it separately for each climatic variable, such as mean annual temperature (MAT), which reduces data requirements and allows us to calculate affinities at scale for 1028 species. As climate and biome distributions change over time, climatic conditions within a biome may become more or less closely aligned with those associated with a species' realised distribution (**Fig. 4.2**A). Decreasing species–biome affinity therefore indicates increasing climatic mismatch, which will generally reduce plant performance as conditions diverge from those to which populations are climatically adapted (Townsend Peterson et al., 2011). A single species affinity does not directly predict a species' realised demographic performance, as this depends on a variety of factors such as dispersal, habitat availability, priority effects, and biotic interactions. However, because, on average, most species shift their distributions in response to temperature change(Lawlor et al., 2024), altered temperature affinity across large parts of the species pool can indicate trends in biomes' overall species richness, which can manifest as changes in beta or alpha diversity.

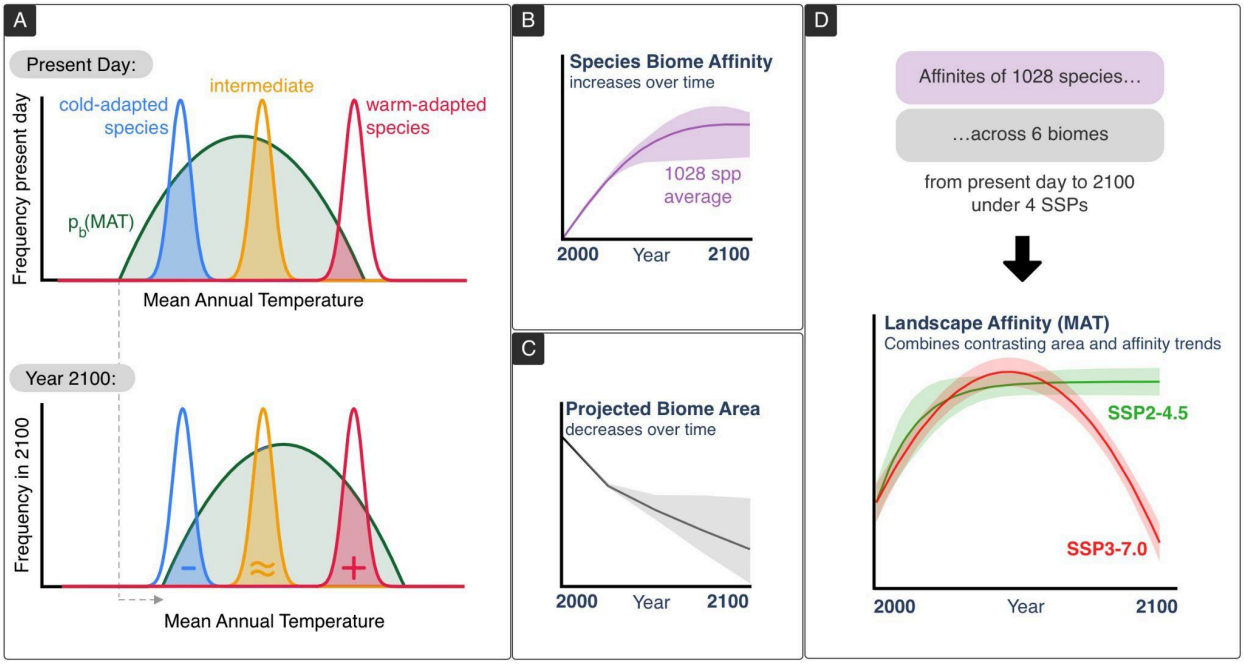


***Figure 4.2**: Schematic overview of the affinity framework for mean annual temperature (MAT). (A) Mean annual temperature distribution of all biome pixels (green line), with realised niches of three example species (blue, yellow and red lines) superimposed. As climate change shifts biome distributions, biomes become more or less suitable for individual species. The shaded area is proportional to the species-biome affinity. (B) Average species-biome affinity for 1028 species over time, with variation interval due to SSP uncertainty. (C) Projected biome area over time. (D) Areas and affinities across six biomes are combined into a single landscape affinity index, yielding trajectories that depend on the interplay among biome area, species abundances and affinities in the biomes, and SSP.*

Species' biome-affinities can be further combined into a single landscape-affinity metric by averaging them weighted by the species' cover within each biome and the biome area (**Fig. 4.2** B-D). This yields a single trajectory for each SSP and estimates how well environmental conditions across all biomes (i.e., the landscape) match the climatic preferences of the species present in the pool. Because landscape affinity combines all biomes, it will only increase or decrease if the species pool across all

biomes collectively experiences stronger levels of altered temperature match, taking into account a strongly overlapping species pool in New Zealand's terrestrial biomes (***Fig. A14***).

4.3.4.1. Species-Biome Affinity

For each biome b, we estimated the availability of the focal environmental variable V (for example, mean annual temperature, MAT) across all raster pixels classified to that biome. We fitted a kernel density estimate to these pixel values, yielding the biome-specific probability-density function $p_b(V)$ (Examples for present day in ***Fig. A13***). This function quantifies how common each environmental value is within biome b.

We then used 10,128 New Zealand Vegetation Survey plots (Wiser et al., 2001) to quantify each species' association with these available conditions. For every plot i, let r_{si} denote the relative cover of species s, and let V_i denote the value of V in the raster pixel containing that plot. We defined the environmental affinity of species s within biome b as the cover-weighted probability of the environmental conditions the species occupies:

$$a(s,b) = N \cdot \sum_{i \in b} r_{si} \cdot p_b(V_i)$$

With the normalisation factor:

$$N = \left(\sum_{i \in b} r_{si} \right)^{-1}$$

Thus, plots in which a species is more abundant contribute more strongly to its affinity. Affinity is high when a species is concentrated at climatic values common within the biome and low when it is concentrated toward less common parts of the biome's climatic distribution (**Fig. 4.2** A). The

normalisation factor ensures that the number of occupied plots or species' total abundance does not influence affinity, as it strictly captures only the climatic match between species and biome. This property makes affinity comparable across species and biomes, even as the number of occupied plots and baseline abundances differ.

Importantly, $p_b(V)$ and thus affinity itself are not constant over time periods or SSPs. As projected biome areas shift in response to climate and the climate within the biomes depends on the SSP, the probability-density function also shifts (the green line shifts rightwards in **Fig. 4.2** A). For simplicity, we omit the time and SSP index in the formulae, noting that every affinity value can be calculated for any timeframe or SSP combination, yielding affinity trajectories (**Fig. 4.2** B). However, to make these trajectories more informative, they can be normalised in various ways (see section below).

4.3.4.2. Landscape Affinity

Next, we combined species' affinities $a(s,b)$ across the six biomes b into a single landscape-affinity metric to describe climatic correspondence at the landscape scale (**Fig. 4.2** B - D). Landscape-affinity is the average affinity of a species across biomes weighted by the (projected) area of the biome $Ar(b)$ and the species' relative cover within that biome $c(s,b)$:

$$la(s) = N \cdot \sum_b a(s,b) \cdot Ar(b) \cdot c(s,b)$$

Where the normalisation factor is:

$$N = \left(\sum_b Ar(b)\right)^{-1} \left(\sum_b c(s,b)\right)^{-1}$$

Landscape affinity is higher for a species present in larger biomes (large $Ar(b)$), where it is abundant (large $c(s,b)$) and where it is well matched with respect to the variable (e.g. temperature;large $a(s,b)$). Landscape affinity therefore quantifies how closely a species' realised niche matches

environmental conditions across the landscape, conditional on its current distribution and the spatial extent of suitable biomes. Since changes in biome area and climatic affinity need not coincide, landscape affinity can result in a non-linear trajectory. By incorporating species prevalence within biomes, the metric also indirectly captures constraints on species' realised distributions: increasing climatic suitability within a biome does not increase a species' landscape affinity if the species is absent from that biome because of biotic interactions, dispersal limitation, or other non-climatic constraints. Thus, landscape affinity provides an indicator of how environmental change may alter the species richness a landscape can support, though it is limited by considering climatic variables independently rather than accounting for their interactions. Similar to the species-biome affinity, landscape affinity is not constant over time and SSP, as the constituent affinity and biome area are not constant, yielding landscape affinity trajectories (**Fig. 4.2** D)

4.3.4.3. Normalising and Fitting Affinity Trends

To better compare landscape affinity trajectories over time t among environmental variables and species, we expressed each trajectory $la(s,t)$ relative to the historical baseline period 1970–2000 ($t = 0$) through a two-step procedure (Section S5). First, trajectories are standardised so that the present-day distribution of landscape affinities has a mean of zero and a variance of one across species. This is done by calculating the baseline mean μ_0 and standard deviation across species σ_0 of the present-day landscape affinity $la(s, t = 0)$ and transforming $laV(s,t) = \frac{la(s,t)-\mu_0}{\sigma_0}$. This expresses landscape affinity in standard deviation units, making it comparable across variables. Second, landscape affinities for individual species are offset by the affinity at baseline $laF(s,t) = laV(s,t) - laV(s,0)$.

After full normalisation, every species' normalised landscape affinity is zero at the present-day baseline, and subsequent values represent changes from the initial affinity in units of the among-species baseline variation. This transformation removes species-specific baseline offsets and variable-specific scale differences, enabling comparison of temporal trajectories. However, it does not imply physiological equivalence among environmental variables. Therefore, we interpret normalised affinities by their direction and temporal trajectory rather than by absolute magnitude across variables.

To quantify these temporal trajectories, trends were fitted with a bent-cable model (Chiu et al., 2006), which consists of two linear segments joined by a smooth quadratic transition, forming a continuous function that is particularly well suited for identifying ecological thresholds. The quadratic transition was constrained to span ≥20 years, and 95% confidence intervals were derived by bootstrap (n = 100). Importantly, the model fit can yield a purely linear or quadratic function. See Table A2 for goodness of fit.

4.3.4.4. Dominant and subordinate species sets

To assess biome homogenisation, species were split into two disjunct sets: dominant (collectively ≥50% of total canopy cover and 7–39 species per biome) and subordinate (689–906 species per biome). Increasing affinity within the dominant set and/or decreasing affinity within the subordinate set indicates potentially diminishing species richness and increasing homogenisation within biomes, as the focal variable becomes increasingly mismatched with the species' current realised niche.

4.4. Results

4.4.1. Changes in Biome Area and Transitions

Biome distributions under future climates show a transition trajectory from alpine biomes to tussock grasslands to beech forests and to mixed forests (**Fig. 4.3**A), resulting in a strong area gain of mixed forest of about 4% per decade under SSP3-7.0 (**Fig. 4.3**B). Lower-emission scenarios yield similar but less pronounced trajectories. These gains led to a shrinkage of cold-adapted biomes at a rate of 2-4% per decade, while the extent of podocarp forests remained largely unchanged (**Fig. 4.3** B). Shrublands exhibited the strongest growth, predominantly through transitions from podocarp forests and tussock grasslands. The magnitude of the projected change in biome area varies strongly by SSP, but the direction of change remains consistent among scenarios (***Fig. A7***).

Model predictions remained largely within the extrapolation threshold until 2061–2080. Beyond this time frame, podocarp forests were associated with the largest portion of novel climate (~25% of grid cells under SSP3-7.0 by 2061–2080). Cold-adapted biomes (alpine, tussock, beech) remained largely within the training domain (~5% extrapolation by 2070). However, by century's end, unreliable predictions expand sharply, encompassing ~90% of biomes under SSP5-8.5 and >50% under SSP3-7.0 (**Fig. 4.3**C).

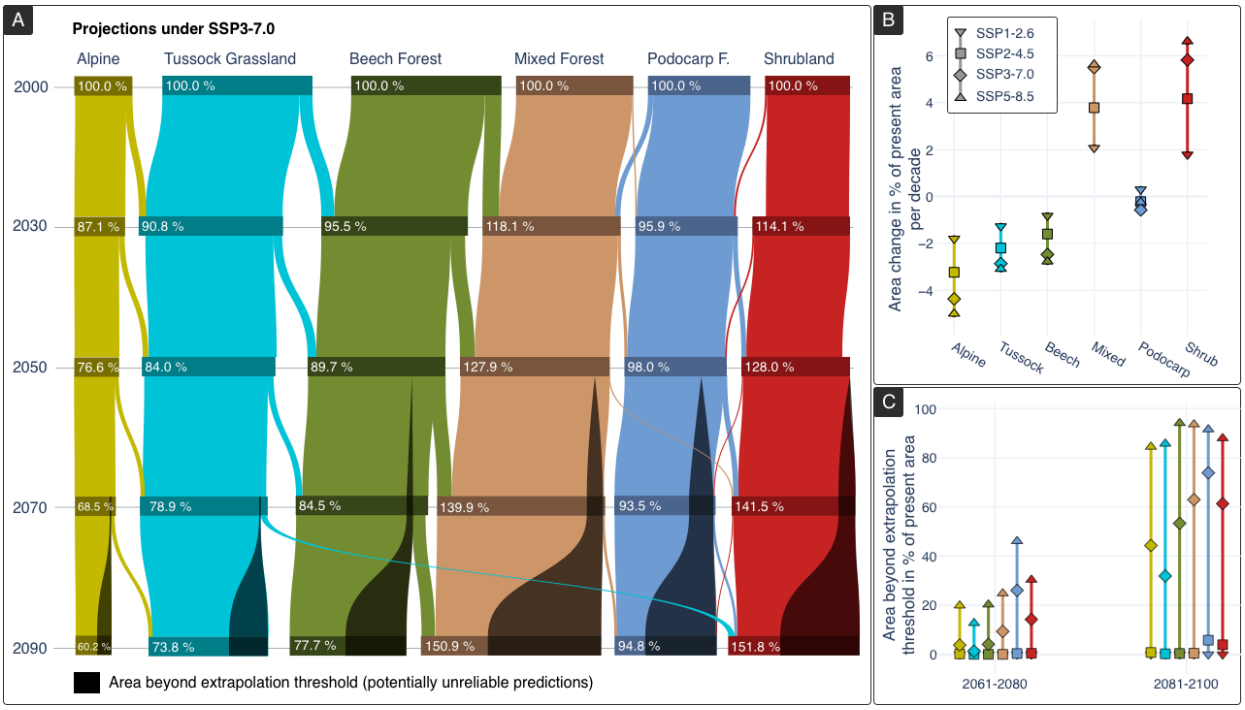


***Figure 4.3**: Changes in biome area. **(A)** Biome transitions from present day (top) to 2090 (bottom) under SSP3-7.0; percentages show area relative to present day; only the two largest transitions per biome are shown. Black colour marks areas beyond the extrapolation threshold. **(B)** Area change per decade as % of current expanse. **(C)** Proportion of pixels/area within each biome strongly differing in climate from present-day and exceeding the defined extrapolation threshold for 2060-2080 and 2080-2100. In (B) and (C), each dot represents an SSP scenario, with SSP3-7.0 highlighted by a larger marker.*

4.4.2. Range and Niche Shifts

Mean temperature showed the greatest and most uniform change across biomes (~0.25°C per decade; **Fig. 4.4**A). Decreases in isothermality likely reflect annual temperature ranges changing at roughly twice the rate of diurnal ranges (***Fig. A11***). Precipitation effects were biome-specific: alpine

biomes became wetter and less seasonal at ~30–50 mm per decade, reaching a medium effect size by century's end (***Fig. A11***, Fig. 4.4 B). All biomes shifted upward at 4–10 m per decade, fastest in mixed forests and slowest in shrublands, while beech forests showed the strongest geographic displacement at ~6 km per decade (Fig. 4.4 B).



Figure 4.4*: Differences in climatic, geographic and topographic variables from present-day distribution to projected future distributions. Marker shape indicates SSP; colour indicates biome.* ***(A)*** *Cohen's d for temperature, precipitation, and isothermality; background colour shows absolute effect size.* ***(B)*** *Rate of change per decade for the four most biome-divergent variables (units in axis titles).*

4.4.3. Changes in Species Richness Potential

We estimated species affinities across all SSPs within each biome (**Fig. 4.5**C, ***Fig. A6***) and collectively as landscape affinity (**Fig. 4.5**A and B). Affinity trajectories differed among climatic variables, SSPs, and biomes, but dominant (~25 species) and subordinate (~750 species) species generally responded similarly (***Fig. A6***). Mean annual temperature was the principal exception: In warm-adapted podocarp forests and shrublands, subordinate species affinity declined while dominant species affinity increased, consistent with thermal homogenisation and potential richness loss. In cold-adapted biomes, subordinate affinity increased, suggesting potential richness gains. Yet because cold-adapted biomes contracted while warm-adapted ones expanded, these opposing signals combined into a non-linear landscape affinity trajectory: a "peak affinity" around mid-century (**Fig. 4.5** A) where temperature and biome expanse together may enable larger species pools at the landscape (but not biome) level. Whether this state persisted beyond the peak depended on the emission pathway.

Individual species responses varied substantially around this aggregate trajectory. Even under lower-emission scenarios, approximately one-third of species experienced a decline in temperature landscape affinity (**Fig. 4.5** B). Under high-emission scenarios, negatively affected species included five of the seven most widespread beech-forest species: *Lophozonia menziesii*, *Fuscospora*

cliffortioides (beech trees), *Blechnum discolor* (ground fern), and *Pseudowintera colorata, Griselinia littoralis* (shrubs). Under lower-emission scenarios, only *F. cliffortioides* showed a negative response, indicating that higher warming disproportionately reduced thermal affinity among species characteristic of beech forests. Moreover, early-successional disturbance-specialist species such as *K. ericoides*, *C. dealbata*, and *M. ramiflorus* showed consistently strong increases in affinity under both low- and high-emission scenarios.

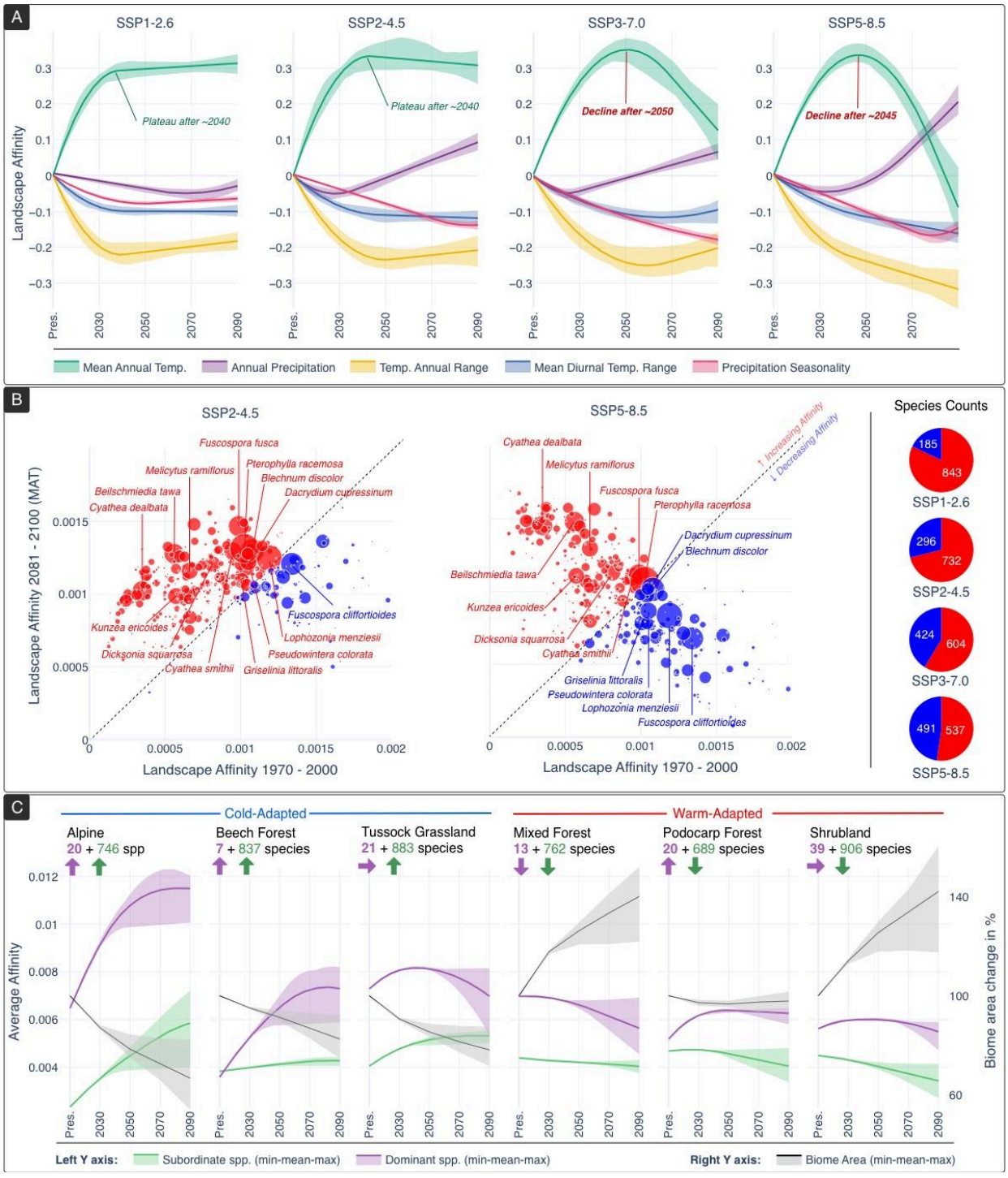

A
SSP1-2.6
SSP2-4.5
SSP3-7.0
SSP5-8.5
Landscape Affinity
Plateau after ~2040
Plateau after ~2040
Decline after ~2050
Decline after ~2045
Pres.
2030
2050
2070
2090
Mean Annual Temp.
Annual Precipitation
Temp. Annual Range
Mean Diurnal Temp. Range
Precipitation Seasonality
B
SSP2-4.5
SSP5-8.5
Landscape Affinity 2081 - 2100 (MAT)
Landscape Affinity 1970 - 2000
↑ Increasing Affinity
↓ Decreasing Affinity
Fuscospora fusca
Melicytus ramiflorus
Pterophylla racemosa
Blechnum discolor
Dacrydium cupressinum
Beilschmiedia tawa
Cyathea dealbata
Fuscospora cliffortioides
Kunzea ericoides
Lophozonia menziesii
Dicksonia squarrosa
Pseudowintera colorata
Cyathea smithii
Griselinia littoralis
Species Counts
185
843
SSP1-2.6
296
732
SSP2-4.5
424
604
SSP3-7.0
491
537
SSP5-8.5
C
Cold-Adapted
Warm-Adapted
Alpine
20 + 746 spp
Beech Forest
7 + 837 species
Tussock Grassland
21 + 883 species
Mixed Forest
13 + 762 species
Podocarp Forest
20 + 689 species
Shrubland
39 + 906 species
Average Affinity
Biome area change in %
Left Y axis:
Subordinate spp. (min-mean-max)
Dominant spp. (min-mean-max)
Right Y axis:
Biome Area (min-mean-max)

***Figure 4.5**: Affinity trends. **(A)** Fully normalised landscape affinity for environmental variables (colour) with 95% confidence intervals, by SSP (columns). **(B)** Comparison of mean annual temperature landscape affinity for the 1028 species in present-day (x-axis) vs end of century (y-axis) for two SSPs. Marker size corresponds to species cover. The 15 most widespread species are annotated. Species below the diagonal decrease in affinity over time and are highlighted in blue. The pie charts on the right summarise the number of species with increasing (red) and decreasing (blue) landscape affinity. **(C)** Mean annual temperature affinity by biome, split into dominant (collectively ≥50% of cover) and subordinate species. Shading spans the min–max across SSPs; species counts appear below each title; arrows indicate the direction of change from present day to 2100. Affinity is not normalised to explicitly show between-group differences. The secondary y-axis shows mean projected biome area (min–max across SSPs shaded).*

4.5. Discussion

Our study modelled changes in terrestrial biome shifts in response to climate change in New Zealand (Aim 1) and quantified how shifting temperature regimes align with species' realised thermal niches via climatic affinity, providing an indicator of potential changes in future species richness (Aim 2). Combining species' climatic affinities with projected biome-area shifts revealed two central patterns: (1) mean annual temperature shifted more consistently and strongly across biomes than other environmental variables, such as precipitation, and (2) its potential effects on biodiversity became strongly non-linear when integrated across the landscape. This pattern suggests an initial increase in potential species richness, followed by saturation under lower-emission scenarios but eventual decline under high-emission scenarios, creating a potential "peak-biodiversity" window around mid-century, especially if the ca. 30-50% negatively affected species persist in place for some

time (**Fig. 4.5** B). Importantly, this modelled peak emerged only when considering the collective trajectories of all six biomes, whereas individual biomes showed more monotonic and contrasting responses, with increasing and decreasing thermal affinity in cold-adapted and warm-adapted biomes, respectively. Thus, biodiversity responses that appear contradictory across individual biomes may represent different components of a collective, but non-linear trajectory at the landscape-scale(García Criado et al., 2025; Pereira et al., 2024; Steinbauer et al., 2018).

4.5.1. Ecological Interpretation

Biomes were projected to move upwards at ~4-10m per decade and polewards at 4-5km/per decade, largely matching global elevational range shift estimates of 6–15 m per decade, but slightly lagging behind latitudinal shifts (Fei et al., 2017; Lawlor et al., 2024; Parmesan, 2006). The model correctly identified shrublands as the strongest expanding vegetation type (**Fig. 4.3**), matching their global expansion (Myers-Smith et al., 2011), albeit at a slightly lower rate than global observations from 1960-2020 (0.2 - 0.6% instead of 0.89% (Wu et al., 2024)). Our models projected a shrinkage of temperature-limited ecosystems by about 1- 5% per decade (alpine, tussock grasslands, and beech forest biomes), which was also slightly below the 16% global shrinkage observed over three decades from 1982-2012 in satellite observations (Keenan & Riley, 2018). This slower pace may be caused by higher data resolution (1km) in our study. Global climate data studies are typically obtained at coarser resolutions of over 10km, which can fail to capture microrefugia and overestimate range shifts (Maclean & Early, 2023), explaining the slower pace of change in this study. Collectively, these results highlight that New Zealand may be experiencing climate-driven biome shifts largely in line

with global observations, albeit at a slower pace, suggesting that direct climatic effects on biome distributions may be more important under future warming than previously anticipated (Macinnis-Ng et al., 2021).

Biome transition forecasts followed a trajectory towards warm-adapted biomes, transforming alpine biomes from tussock grasslands to beech forests and mixed forests (**Fig. 4.3**), matching the trend of thermophilisation in European mountains (Gottfried et al., 2012). Until 2100, the predicted area losses are highly dependent on SSP (**Fig. 4.3**D) and range from 25% to 65% in alpine ecosystems, aligning with previous predictions of up to 55% habitat loss (Engler et al., 2011). Given the substantial expansion of shrublands and the transition of ~11% of the tussock grassland area to shrublands by 2080 under SSP3-7.0, warming might lead to a sudden, irreversible transition of montane biomes to alpine shrublands (Brandt et al., 2013), decreasing their species richness and lowering their resilience (Boscutti et al., 2018). In particular, New Zealand's tussock grassland biodiversity may be disproportionately affected, as it shares the fewest species with neighbouring biomes (***Fig. A14***), requiring more species migration, whereas other biomes may adjust through changes in the abundance of already shared species. However, projected shifts vary up to five-fold by 2100 depending on SSP (***Fig. A9***) and plateau under lower-emission scenarios.

Despite shrinking extent, the cold-adapted biomes showed a temperature profile conducive to an increasing number of species in the next century (**Fig. 4.5**C), also matching European observations since the 1990s (Lamprecht et al., 2018), and across tree species in New Zealand (Shabanov et al., 2026). Montane biomes are strongly temperature-limited, and this filter intensifies with elevation (Schroeder et al., 2024) but is being relaxed by ongoing warming, which is occurring more rapidly at higher elevations (Ohmura, 2012), expanding potential species pools and signalling a shift in

community assembly away from strict abiotic control (Bektaş et al., 2023). However, warming may not always increase species richness, as alpine biodiversity strongly depends on historical patterns of biodiversity and is subject to geographic dispersal limitation (Testolin et al., 2021). Increased shrub presence, for instance, can suppress biodiversity (Boscutti et al., 2018; Walker et al., 2006), especially when involving invasive species that disrupt soil mutualisms (Moyle & Deslippe, 2024). The ecological consequences of continued warming are thus likely to remain context-dependent (Midolo et al., 2025), underscoring the need for long-term monitoring and adaptive management interventions, such as the removal of shrubs or invasive species (Kudo et al., 2017; Leon-Garcia et al., 2025; Losapio et al., 2024), to sustain biodiversity in these vulnerable ecosystems.

Over the course of the 21st century our models projected that shrublands and mixed forests will expand by ~20-40% (**Fig. 4.3**D), with mixed forests dominating at higher elevation and shrublands remaining restricted to lowland areas (**Fig. 4.4** B). Simultaneously, the thermal mismatch of the species in these two biomes and podocarp forests increases indicating a potential species loss (**Fig. 4.5**C). Homogenisation is widespread globally and characterised by increasing local species richness (alpha diversity), but declining species turn-over at regional scales (beta diversity) (Steinbauer et al., 2018; Zwiener et al., 2018) globally widespread pattern, also common to vertebrates (Rolls et al., 2023) and invertebrates (Mouton et al., 2020) is projected to persist into the future, particularly under continued deforestation (Pereira et al., 2024). One feasible mechanism may be the expansion of generalist species with wide climatic tolerances, displacing less adaptable habitat specialists (Shabanov et al., 2025), which may coexist for some time, but ultimately face local extinction when recruitment fails due to a strong climatic mismatch (Tilman et al., 1994). This loss of biodiversity is also consistent with the hump-backed model of productivity, which predicts increased

species richness at higher productivity levels due to reduced abiotic stress and increased resource availability (Fraser et al., 2015).

Our projected ~16.5% contraction of beech forests (***Fig. A9***) and their transition towards mixed broadleaf forest is supported by previous New Zealand-based modelling studies. A previous study of 41 tree species predicted general upslope migrations and increasing establishment of broadleaved species within *Nothofagus*-dominated beech forests (Leathwick et al., 1996), while more recent projections estimate a 12.1% decline in climatically suitable area for *Nothofagus* species by 2070 under high emissions (Mathias et al., 2023). Moreover, under high emissions, our projections indicate substantial climate-driven reorganisation where five of the seven most widespread species showed reduced thermal affinity, consistent with major community shifts (**Fig. 4.5** B). This result contrasts with the inference that relatively static, disturbance-mediated beech treelines imply limited direct climate responses (Cullen et al., 2001), but is plausible due to the broad elevational distribution of beech forests spanning more than 1,000 m (***Fig. A13***). Long-term resurveys are now needed to determine whether, and how rapidly, this predicted reorganisation is occurring in contemporary beech forests.

More broadly, New Zealand's glacial history has produced a flora containing many species associated with warmer conditions (McGlone et al., 2016), and a higher species richness in warmer regions (Leathwick et al., 1998), which aligns with the initial increase in thermal affinity under moderate warming we show in this study. However, disturbance history complicates climate-based projections, and New Zealand's extensive grasslands and

shrublands partly reflect a history of anthropogenic disturbance rather than climatic equilibrium (Perry et al., 2014), potentially contributing to the relatively poor predictability of shrublands in this study (***Fig. A3***). Nevertheless, observed succession from tussock through Mānuka (*L. scoparium*) shrubland (Ropars et al., 2018) to beech forest (Wyse et al., 2018) supports the direction of our projected tussock-to-beech transition, while suggesting that climate-based projections simplify its intermediate successional stages. Together, this agreement across scales supports a broader climate-driven reorganisation of New Zealand's vegetation, substantially expanding the modelled species pool to 1,028 species.

Contrasting responses among biomes suggest that New Zealand may experience substantial compositional instability over the near to mid-century, with warming relaxing abiotic constraints in cold-adapted biomes and allowing additional species to establish, but contraction of these biomes simultaneously reducing the habitable area available to their associated species (**Fig. 4.3**D and **Fig. 4.5**C). In warm-adapted forests, rising temperatures increasingly exceed the climatic niches of resident species, reducing climatic matching (**Fig. 4.5**A). These opposing temperature responses produce uncertain responses that strongly differ in their trajectory ranging from saturation to strong decline at the landscape level. Importantly, our models project that even under low-emission scenarios, many species' loss of thermal affinity is locked in (**Fig. 4.5**B). Realised gains or losses in species richness depend on species' ability to track shifting climatic conditions and are constrained by dispersal limitation, habitat fragmentation, and other non-climatic processes (Jo et al., 2025). Nevertheless, opposing richness trajectories among biomes provide a mechanism for reconciling apparently conflicting biodiversity projections.

4.5.2. Framework Interpretation and Limitations

The biome–affinity framework trades precision for coverage by coupling two hierarchical signals. First, biome-area projections describe the shifting community "envelope" and its changing extent. These projections capture the stabilising feedbacks and shared responses of species subject to similar abiotic filters (Pausas & Bond, 2021). Second, affinities quantify how closely each species' realised niche aligns with the evolving environmental profile of its biome. Potential species richness then follows from combining these responses across 1,028 species at the landscape scale. Individual species react to different abiotic drivers, but biomes remain more strongly climatically constrained than the species within them (Prentice et al., 1992), and the majority of species follow temperature gradients (Lawlor et al., 2024). Aggregating across a species pool of this size therefore informs on potential species richness, while requiring far less data than stacked or joint SDMs (Caradima et al., 2019; Grenié et al., 2020), which are typically restricted to common, well-sampled species. Affinity nevertheless measures only the match between climate and a species' niche, and that match may shift faster than the distribution itself (Alexander et al., 2018; Bertrand et al., 2011). We therefore interpret landscape affinity as a measure of the pressures and trajectories acting on overall species richness across a wide area, rather than a deterministic forecast of it.

Future projections involve inherent uncertainties, which we validate where possible. Biome predictions generalised well spatially (***Fig. A3***), with high model confidence across classes (***Fig. A4***), climate models largely agreed on biome area (***Fig. A5***) and thermal affinity trajectories (***Fig. A8***), leaving the SSP scenario as the dominant source of divergence by the end of the century (***Fig. A9***). The climate data themselves are the least tractable source of uncertainty, because coarse global models incompletely resolve New Zealand's complex topography, orographic precipitation and

climatic extremes (Gibson et al., 2024). These limitations most strongly affect mountainous regions and species-level responses to extreme events, whereas our analysis targets long-term biome shifts, a large portion of which occur at lower elevations (***Fig. A13***). Regional climate models could therefore refine the spatial detail of these trajectories. Further predictive gains may come from resolving species-specific physiological and community-level ecological responses, which determine how climatic change translates into realised biodiversity change (Conradi et al., 2024).

Two processes could be added to the framework as ecological data improve. First, the model does not constrain dispersal and therefore likely overestimates range shifts (Hellegers et al., 2025). This limitation may be modest, because many New Zealand species already occur across several biomes (***Fig. A14***). Such species can respond through changes in local abundance before range boundaries move (Breshears et al., 2008). Second, climate-driven change in abundance will interact with other global change drivers, particularly biological invasions, which are pronounced in New Zealand (Keegan et al., 2022; Macinnis-Ng et al., 2021). These outcomes differ strongly among species (Shabanov et al., 2026) and ecological contexts (Deslippe & Veenendaal, 2025). Resolving either process across 1,028 species would require substantially more trait, demographic and compositional data, and more mechanistic models (Hulme, 2020; Urban et al., 2016), but highlight a direction for future research.

4.6. Conclusion

New Zealand's terrestrial biomes are projected to reorganise substantially this century. Cold-adapted alpine, tussock and beech systems retreat, while shrublands and mixed forests expand upward and southward, with species pools potentially increasing in retreating biomes and

vice versa. The combined trajectory of biome area and climatic match yields a turning point near mid-century, when the largest number of species are favourably matched to temperature, and beyond which this match saturates or declines according to the emissions pathway. This offers a mechanism to reconcile inconsistent worldwide observations of increasing, declining, and stable species richness by framing them as part of a larger, slower, non-linear ecosystem response to progressing climate change. Compositional change nevertheless appears unavoidable, because affinities shift even under low-emission scenarios. This is particularly relevant for New Zealand's ecology, which often assumes climate change's direct impacts are a minimal threat (Keegan et al., 2022). Lastly, we show that different emission pathways may produce fundamentally different responses (saturation or collapse), leaving us with the possibility and responsibility to act.

4.7. Data Availability Statement

Biome predictions with associated uncertainties, raw species and landscape affinities, as well as their fits, are available at https://doi.org/10.5281/zenodo.18929925 (peer review link).

4.8. References

Alexander, J. M., Chalmandrier, L., Lenoir, J., Burgess, T. I., Essl, F., Haider, S., Kueffer, C., McDougall, K., Milbau, A., Nuñez, M. A., Pauchard, A., Rabitsch, W., Rew, L. J., Sanders, N. J., & Pellissier, L. (2018). Lags in the response of mountain plant communities to climate change. *Global Change Biology*, *24*(2), 563–579.

Ali, F., Khan, N., Khan, A. M., Ali, K., & Abbas, F. (2023). Species distribution modelling of Monotheca buxifolia (Falc.) A. DC.: Present distribution and impacts of potential climate change. *Heliyon*, *9*(2), e13417.

Bektaş, B., Thuiller, W., Renaud, J., Guéguen, M., Calderón-Sanou, I., Valay, J.-G., Colace, M.-P., & Münkemüller, T. (2023). A spatially explicit trait-based approach uncovers changes in assembly processes under warming. *Ecology Letters*, *26*(7), 1119–1131.

Bergstrom, D. M., Wienecke, B. C., van den Hoff, J., Hughes, L., Lindenmayer, D. B., Ainsworth, T. D., Baker, C. M., Bland, L., Bowman, D. M. J. S., Brooks, S. T., Canadell, J. G., Constable, A. J., Dafforn, K. A., Depledge, M. H., Dickson, C. R., Duke, N. C., Helmstedt, K. J., Holz, A., Johnson, C. R., … Shaw, J. D. (2021). Combating ecosystem collapse from the tropics to the Antarctic. *Global Change Biology*, *27*(9), 1692–1703.

Bertrand, R., Lenoir, J., Piedallu, C., Riofrío-Dillon, G., de Ruffray, P., Vidal, C., Pierrat, J.-C., & Gégout, J.-C. (2011). Changes in plant community composition lag behind climate warming in lowland forests. *Nature*, *479*(7374), 517–520.

Boënnec, M., Dakos, V., & Devictor, V. (2024). Sources of confusion in global biodiversity trends. *Oikos (Copenhagen, Denmark)*, *2024*(6), e10732.

Boscutti, F., Casolo, V., Beraldo, P., Braidot, E., Zancani, M., & Rixen, C. (2018). Shrub growth and plant diversity along an elevation gradient: Evidence of indirect effects of climate on alpine ecosystems. *PloS One*, *13*(4), e0196653.

Brandt, J. S., Haynes, M. A., Kuemmerle, T., Waller, D. M., & Radeloff, V. C. (2013). Regime shift on the roof of the world: Alpine meadows converting to shrublands in the southern Himalayas. *Biological Conservation*, *158*, 116–127.

Breshears, D. D., Huxman, T. E., Adams, H. D., Zou, C. B., & Davison, J. E. (2008). Vegetation synchronously leans upslope as climate warms. *Proceedings of the National Academy of Sciences of the United States of America*, *105*(33), 11591–11592.

Brodie, S., Smith, J. A., Muhling, B. A., Barnett, L. A. K., Carroll, G., Fiedler, P., Bograd, S. J., Hazen, E. L., Jacox, M. G., Andrews, K. S., Barnes, C. L., Crozier, L. G., Fiechter, J., Fredston, A., Haltuch, M. A., Harvey, C. J., Holmes, E., Karp, M. A., Liu, O. R., … Kaplan, I. C. (2022). Recommendations for quantifying and reducing uncertainty in climate projections of species distributions. *Global Change Biology*, *28*(22), 6586–6601.

Calabrese, J. M., Certain, G., Kraan, C., & Dormann, C. F. (2014). Stacking species distribution models and adjusting bias by linking them to macroecological models. *Global Ecology and Biogeography: A Journal of Macroecology*, *23*(1), 99–112.

Caradima, B., Schuwirth, N., & Reichert, P. (2019). From individual to joint species distribution models: A comparison of model complexity and predictive performance. *Journal of Biogeography*, *46*(10), 2260–2274.

Carnicer, J., Domingo-Marimon, C., Ninyerola, M., Camarero, J. J., Bastos, A., López-Parages, J., Blanquer, L., Rodríguez-Fonseca, B., Lenton, T. M., Dakos, V., Ribas, M., Gutiérrez, E., Peñuelas, J., & Pons, X. (2019). Regime shifts of Mediterranean forest carbon uptake and reduced resilience driven by multidecadal ocean surface temperatures. *Global Change Biology*, *25*(8), 2825–2840.

Charney, N. D., Record, S., Gerstner, B. E., Merow, C., Zarnetske, P. L., & Enquist, B. J. (2021). A test of species distribution model transferability across environmental and geographic space for 108 western north American tree species. *Frontiers in Ecology and Evolution*, *9*(689295). https://doi.org/10.3389/fevo.2021.689295

Chiu, G., Lockhart, R., & Routledge, R. (2006). Bent-cable regression theory and applications. *Journal of the American Statistical Association*, *101*(474), 542–553.

Cohen, J. (2013). *Statistical power analysis for the behavioral sciences* (2nd ed.). Routledge. https://doi.org/10.4324/9780203771587

Conradi, T., Eggli, U., Kreft, H., Schweiger, A. H., Weigelt, P., & Higgins, S. I. (2024). Reassessment of the risks of climate change for terrestrial ecosystems. *Nature Ecology & Evolution*, *8*(5), 888–900.

Cotto, O., Wessely, J., Georges, D., Klonner, G., Schmid, M., Dullinger, S., Thuiller, W., & Guillaume, F. (2017). A dynamic eco-evolutionary model predicts slow response of alpine plants to climate warming. *Nature Communications*, *8*(1), 15399.

Cullen, L. E., Stewart, G. H., Duncan, R. P., & Palmer, J. G. (2001). Disturbance and climate warming influences on New Zealand Nothofagus tree-line population dynamics: *Disturbance and climate warming at tree line*. *The Journal of Ecology*, *89*(6), 1061–1071.

D'Amen, M., Rahbek, C., Zimmermann, N. E., & Guisan, A. (2017). Spatial predictions at the community level: from current approaches to future frameworks: Methods for community-level spatial predictions. *Biological Reviews of the Cambridge Philosophical Society*, *92*(1), 169–187.

Deslippe, J. R., & Veenendaal, J. A. (2025). Plant invasions in a changing climate: Reshaping communities, ecosystem functions, and services. *Annual Review of Ecology, Evolution, and Systematics*, *56*(1), 571–596.

Devictor, V., Julliard, R., Couvet, D., & Jiguet, F. (2008). Birds are tracking climate warming, but not fast enough. *Proceedings. Biological Sciences*, *275*(1652), 2743–2748.

Dornelas, M., Gotelli, N. J., McGill, B., Shimadzu, H., Moyes, F., Sievers, C., & Magurran, A. E. (2014). Assemblage time series reveal biodiversity change but not systematic loss. *Science*, *344*(6181), 296–299.

Dyderski, M. K., Paź, S., Frelich, L. E., & Jagodziński, A. M. (2018). How much does climate change threaten European forest tree species distributions? *Global Change Biology*, *24*(3), 1150–1163.

Engler, R., Randin, C. F., Thuiller, W., Dullinger, S., Zimmermann, N. E., Araújo, M. B., Pearman, P. B., Le Lay, G., Piedallu, C., Albert, C. H., Choler, P., Coldea, G., De LAMO, X., Dirnböck, T., Gégout, J.-C., Gómez-García, D., Grytnes, J.-A., Heegaard, E., Høistad, F., … Guisan, A. (2011). 21st century climate change threatens mountain flora unequally across Europe: CLIMATE CHANGE IMPACTS ON MOUNTAIN FLORAE. *Global Change Biology*, *17*(7), 2330–2341.

Eyring, V., Bony, S., Meehl, G. A., Senior, C. A., Stevens, B., Stouffer, R. J., & Taylor, K. E. (2016). Overview of the Coupled Model Intercomparison Project Phase 6 (CMIP6) experimental design and organization. *Geoscientific Model Development*, *9*(5), 1937–1958.

Fei, S., Desprez, J. M., Potter, K. M., Jo, I., Knott, J. A., & Oswalt, C. M. (2017). Divergence of species responses to climate change. *Science Advances*, *3*(5), e1603055.

Fick, S. E., & Hijmans, R. J. (2017). WorldClim 2: new 1-km spatial resolution climate surfaces for global land areas: NEW CLIMATE SURFACES FOR GLOBAL LAND AREAS. *International Journal of Climatology: A Journal of the Royal Meteorological Society*, *37*(12), 4302–4315.

Figueiredo, L., Krauss, J., Steffan-Dewenter, I., & Sarmento Cabral, J. (2019). Understanding extinction debts: spatio–temporal scales, mechanisms and a roadmap for future research. *Ecography*, *42*(12), 1973–1990.

Fortier, R. P., Kullberg, A. T., Soria Ahuanari, R. D., Coombs, L., Ruzo, A., & Feeley, K. J. (2024). Hotter temperatures reduce the diversity and alter the composition of woody plants in an amazonian forest. *Global Change Biology*, *30*(11), e17555.

Fraser, L. H., Pither, J., Jentsch, A., Sternberg, M., Zobel, M., Askarizadeh, D., Bartha, S., Beierkuhnlein, C., Bennett, J. A., Bittel, A., Boldgiv, B., Boldrini, I. I., Bork, E., Brown, L., Cabido, M., Cahill, J., Carlyle, C. N., Campetella, G., Chelli, S., … Zupo, T. (2015). Plant ecology. Worldwide evidence of

a unimodal relationship between productivity and plant species richness. *Science (New York, N.Y.)*, *349*(6245), 302–305.

García Criado, M., Myers-Smith, I. H., Bjorkman, A. D., Elmendorf, S. C., Normand, S., Aastrup, P., Aerts, R., Alatalo, J. M., Baeten, L., Björk, R. G., Björkman, M. P., Boulanger-Lapointe, N., Butler, E. E., Cooper, E. J., Cornelissen, J. H. C., Daskalova, G. N., Fadrique, B., Forbes, B. C., Henry, G. H. R., … Vellend, M. (2025). Plant diversity dynamics over space and time in a warming Arctic. *Nature*, 1–9.

Gibson, P. B., Stuart, S., Sood, A., Stone, D., Rampal, N., Lewis, H., Broadbent, A., Thatcher, M., & Morgenstern, O. (2024). Dynamical downscaling CMIP6 models over New Zealand: added value of climatology and extremes. *Climate Dynamics*, *62*(8), 8255–8281.

Goberville, E., Beaugrand, G., Hautekèete, N.-C., Piquot, Y., & Luczak, C. (2015). Uncertainties in the projection of species distributions related to general circulation models. *Ecology and Evolution*, *5*(5), 1100–1116.

Gottfried, M., Pauli, H., Futschik, A., Akhalkatsi, M., Barančok, P., Benito Alonso, J. L., Coldea, G., Dick, J., Erschbamer, B., Fernández Calzado, M. R., Kazakis, G., Krajči, J., Larsson, P., Mallaun, M., Michelsen, O., Moiseev, D., Moiseev, P., Molau, U., Merzouki, A., … Grabherr, G. (2012). Continent-wide response of mountain vegetation to climate change. *Nature Climate Change*, *2*(2), 111–115.

Grenié, M., Violle, C., & Munoz, F. (2020). Is prediction of species richness from stacked species distribution models biased by habitat saturation? *Ecological Indicators*, *111*(105970), 105970.

Hellegers, M., Krist, D. H., & Schipper, A. M. (2025). Many plant species in Europe have limited capacity to track climate change. *Diversity & Distributions*, *31*(11), e70115.

Higgins, S. I., Conradi, T., & Muhoko, E. (2023). Shifts in vegetation activity of terrestrial ecosystems attributable to climate trends. *Nature Geoscience*, *16*(2), 147–153.

Hisano, M., Searle, E. B., & Chen, H. Y. H. (2018). Biodiversity as a solution to mitigate climate change impacts on the functioning of forest ecosystems: Biodiversity to mitigate climate change impacts. *Biological Reviews of the Cambridge Philosophical Society*, *93*(1), 439–456.

Hulme, P. E. (2020). Plant invasions in New Zealand: global lessons in prevention, eradication and control. *Biological Invasions*, *22*(5), 1539–1562.

Jaureguiberry, P., Titeux, N., Wiemers, M., Bowler, D. E., Coscieme, L., Golden, A. S., Guerra, C. A., Jacob, U., Takahashi, Y., Settele, J., Díaz, S., Molnár, Z., & Purvis, A. (2022). The direct drivers of recent global anthropogenic biodiversity loss. *Science Advances*, *8*(45), eabm9982.

Jo, I., Bellingham, P. J., Richardson, S. J., Hawcroft, A., & Wright, E. F. (2025). Tree demographic drivers across temperate rain forests, after accounting for site-, species-, and stem-level attributes. *Ecology*, *106*(1), e4471.

Johnson, T. F., Beckerman, A. P., Childs, D. Z., Webb, T. J., Evans, K. L., Griffiths, C. A., Capdevila, P., Clements, C. F., Besson, M., Gregory, R. D., Thomas, G. H., Delmas, E., & Freckleton, R. P. (2024). Revealing uncertainty in the status of biodiversity change. *Nature*, *628*(8009), 788–794.

Katuwal, R., Suganthan, P. N., & Zhang, L. (2020). Heterogeneous oblique random forest. *Pattern Recognition*, *99*(107078), 107078.

Keegan, L., School of Biological Sciences, University of Auckland, Private Bag 92019, Auckland 1142, New Zealand, White, R., & Macinnis-Ng, C. (2022). Current knowledge and potential impacts of climate change on New Zealand's biological heritage. *New Zealand Journal of Ecology*. https://doi.org/10.20417/nzjecol.46.10

Keenan, T. F., & Riley, W. J. (2018). Greening of the land surface in the world's cold regions consistent with recent warming. *Nature Climate Change*, *8*(9), 825–828.

Kerr, M. R., Ordonez, A., Riede, F., Atkinson, J., Pearce, E. A., Sykut, M., Trepel, J., & Svenning, J.-C. (2025). Widespread ecological novelty across the terrestrial biosphere. *Nature Ecology & Evolution*, *9*(4), 589–598.

Kim, H., Rosa, I. M. D., Alkemade, R., Leadley, P., Hurtt, G., Popp, A., van Vuuren, D. P., Anthoni, P., Arneth, A., Baisero, D., Caton, E., Chaplin-Kramer, R., Chini, L., De Palma, A., Di Fulvio, F., Di Marco, M., Espinoza, F., Ferrier, S., Fujimori, S., … Pereira, H. M. (2018). A protocol for an intercomparison of biodiversity and ecosystem services models using harmonized land-use and climate scenarios. *Geoscientific Model Development*, *11*(11), 4537–4562.

Knutti, R., Furrer, R., Tebaldi, C., Cermak, J., & Meehl, G. A. (2010). Challenges in combining projections from multiple climate models. *Journal of Climate*, *23*(10), 2739–2758.

Kudo, G., Kawai, Y., Amagai, Y., & Winkler, D. E. (2017). Degradation and recovery of an alpine plant community: experimental removal of an encroaching dwarf bamboo. *Alpine Botany*, *127*(1), 75–83.

Lalechère, E., Lenoir, J., Marrec, R., Essl, F., Kühn, I., & Ergon, T. (2025). Assessing biodiversity trends in a quasi-permanent non-equilibrium state. *Trends in Ecology & Evolution*, *40*(10), 949–959.

Lamprecht, A., Semenchuk, P. R., Steinbauer, K., Winkler, M., & Pauli, H. (2018). Climate change leads to accelerated transformation of high-elevation vegetation in the central Alps. *The New Phytologist*, *220*(2), 447–459.

Landcare Research. (2024). *Basic Ecosystems* [Dataset]. https://doi.org/10.7931/L1HM1

Langhammer, P. F., Bull, J. W., Bicknell, J. E., Oakley, J. L., Brown, M. H., Bruford, M. W., Butchart, S. H. M., Carr, J. A., Church, D., Cooney, R., Cutajar, S., Foden, W., Foster, M. N., Gascon, C., Geldmann, J., Genovesi, P., Hoffmann, M., Howard-McCombe, J., Lewis, T., … Brooks, T. M. (2024). The positive impact of conservation action. *Science (New York, N.Y.)*, *384*(6694), 453–458.

Lawlor, J. A., Comte, L., Grenouillet, G., Lenoir, J., Baecher, J. A., Bandara, R. M. W. J., Bertrand, R., Chen, I.-C., Diamond, S. E., Lancaster, L. T., Moore, N., Murienne, J., Oliveira, B. F., Pecl, G. T., Pinsky, M. L., Rolland, J., Rubenstein, M., Scheffers, B. R., Thompson, L. M., … Sunday, J. (2024). Mechanisms, detection and impacts of species redistributions under climate change. *Nature Reviews. Earth & Environment*, *5*(5), 351–368.

Leathwick, J. R., Burns, B. R., & Clarkson, B. D. (1998). Environmental correlates of tree alpha-diversity in New Zealand primary forests. *Ecography*, *21*(3), 235–246.

Leathwick, J. R., Whitehead, D., & McLeod, M. (1996). Predicting changes in the composition of New Zealand's indigenous forests in response to global warming: a modelling approach. *Environmental Software*, *11*(1–3), 81–90.

Leon-Garcia, I. V., Classen, A. T., Giejsztowt, J., & Deslippe, J. R. (2025). Long-term warming and dominant species removal alter plant community composition in invaded alpine tussock grasslands in New Zealand. *Journal of Vegetation Science: Official Organ of the International Association for Vegetation Science*, *36*(6), e70090.

Losapio, G., De Moraes, C. M., Dirzo, R., Tscheulin, T., Zouros, N., & Mescher, M. C. (2024). Habitat protection and removal of encroaching shrubs support the recovery of biodiversity and ecosystem functioning. *Conservation Science and Practice*, *6*(4), e13111.

Macinnis-Ng, C., Mcintosh, A. R., Monks, J. M., Waipara, N., White, R. S. A., Boudjelas, S., Clark, C. D., Clearwater, M. J., Curran, T. J., Dickinson, K. J. M., Nelson, N., Perry, G. L. W., Richardson, S. J., Stanley, M. C., & Peltzer, D. A. (2021). Climate-change impacts exacerbate conservation threats in island systems: New Zealand as a case study. *Frontiers in Ecology and the Environment*, *19*(fee.2285), 216–224.

Maclean, I. M. D., & Early, R. (2023). Macroclimate data overestimate range shifts of plants in response to climate change. *Nature Climate Change*, *13*(5), 484–490.

Mao, F., Du, H., Zhou, G., Zheng, J., Li, X., Xu, Y., Huang, Z., & Yin, S. (2022). Simulated net ecosystem productivity of subtropical forests and its response to climate change in Zhejiang Province, China. *The Science of the Total Environment*, *838*(Pt 1), 155993.

Marske, K. A., & Boyer, S. L. (2024). Phylogeography reveals the complex impact of the Last Glacial Maximum on New Zealand's terrestrial biota. *Journal of the Royal Society of New Zealand*, *54*(1), 8–29.

Martén-Rodríguez, S., Cristobal-Pérez, E. J., de Santiago-Hernández, M. H., Huerta-Ramos, G., Clemente-Martínez, L., Krupnick, G., Taylor, O., Lopezaraiza-Mikel, M., Balvino-Olvera, F. J., Sentíes-Aguilar, E. M., Díaz-Infante, S., Aguirre Jaimes, A., Novais, S., Cortés-Flores, J., Lobo-Segura, J., Fuchs, E. J., Delgado-Carrillo, O., Ruiz-Mercado, I., Sáyago-Lorenzana, R., … Quesada, M. (2025). Untangling the complexity of climate change effects on plant reproductive traits and pollinators: A systematic global synthesis. *Global Change Biology*, *31*(2), e70081.

Mathias, S., van Galen, L. G., Jarvie, S., & Larcombe, M. J. (2023). Range reshuffling: Climate change, invasive species, and the case of *Nothofagus* forests in Aotearoa New Zealand. *Diversity & Distributions*, *29*(11), 1402–1419.

McCarthy, J., Leathwick, J., Roudier, P., Barringer, J., Etherington, T., Morgan, F., Odgers, N., Price, R., Wiser, S., & Richardson, S. (2021). New Zealand Environmental Data Stack (NZEnvDS): A standardised collection of spatial layers for environmental modelling and site characterisation. *New Zealand Journal of Ecology*, *45*, 3440.

McGlone, M. S., Buitenwerf, R., & Richardson, S. J. (2016). The formation of the oceanic temperate forests of New Zealand. *New Zealand Journal of Botany*, *54*(2), 128–155.

Menze, B. H., Kelm, B. M., Splitthoff, D. N., Koethe, U., & Hamprecht, F. A. (2011). On Oblique Random Forests. In *Lecture Notes in Computer Science* (pp. 453–469). Springer Berlin Heidelberg.

Midolo, G., Clark, A. T., Chytrý, M., Essl, F., Dullinger, S., Jandt, U., Bruelheide, H., Argagnon, O., Biurrun, I., Chiarucci, A., Ćušterevska, R., De Frenne, P., De Sanctis, M., Dengler, J., Divíšek, J., Dziuba, T., Ejrnæs, R., Garbolino, E., Illa, E., … Keil, P. (2025). Six decades of losses and gains in alpha diversity of European plant communities. *Ecology Letters*, *28*(11), e70248.

Mokany, K., Harwood, T. D., Overton, J. M., Barker, G. M., & Ferrier, S. (2011). Combining α - and β -diversity models to fill gaps in our knowledge of biodiversity: Filling gaps in biodiversity knowledge. *Ecology Letters*, *14*(10), 1043–1051.

Montràs-Janer, T., Suggitt, A. J., Fox, R., Jönsson, M., Martay, B., Roy, D. B., Walker, K. J., & Auffret, A. G. (2024). Anthropogenic climate and land-use change drive short- and long-term biodiversity shifts across taxa. *Nature Ecology & Evolution*, *8*(4), 739–751.

Mora, C., Frazier, A. G., Longman, R. J., Dacks, R. S., Walton, M. M., Tong, E. J., Sanchez, J. J., Kaiser, L. R., Stender, Y. O., Anderson, J. M., Ambrosino, C. M., Fernandez-Silva, I., Giuseffi, L. M., & Giambelluca, T. W. (2013). The projected timing of climate departure from recent variability. *Nature*, *502*(7470), 183–187.

Mouton, T. L., Tonkin, J. D., Stephenson, F., Verburg, P., & Floury, M. (2020). Increasing climate-driven taxonomic homogenization but functional differentiation among river macroinvertebrate assemblages. *Global Change Biology*, *26*(12), 6904–6915.

Moyle, D. M., & Deslippe, J. R. (2024). Invasion alters plant and mycorrhizal communities in an alpine tussock grassland. *Oecologia*, *206*(3–4), 317–333.

Myers-Smith, I. H., Forbes, B. C., Wilmking, M., Hallinger, M., Lantz, T., Blok, D., Tape, K. D., Macias-Fauria, M., Sass-Klaassen, U., Lévesque, E., Boudreau, S., Ropars, P., Hermanutz, L., Trant, A., Collier, L. S., Weijers, S., Rozema, J., Rayback, S. A., Schmidt, N. M., … Hik, D. S. (2011). Shrub expansion in tundra ecosystems: dynamics, impacts and research priorities. *Environmental Research Letters*, *6*(4), 045509.

Noce, S., Collalti, A., & Santini, M. (2017). Likelihood of changes in forest species suitability, distribution, and diversity under future climate: The case of Southern Europe. *Ecology and Evolution*, *7*(22), 9358–9375.

Ohmura, A. (2012). Enhanced temperature variability in high-altitude climate change. *Theoretical and Applied Climatology*, *110*(4), 499–508.

Oliver, T. H., Heard, M. S., Isaac, N. J. B., Roy, D. B., Procter, D., Eigenbrod, F., Freckleton, R., Hector, A., Orme, C. D. L., Petchey, O. L., Proença, V., Raffaelli, D., Suttle, K. B., Mace, G. M., Martín-López, B., Woodcock, B. A., & Bullock, J. M. (2015). Biodiversity and resilience of ecosystem functions. *Trends in Ecology & Evolution*, *30*(11), 673–684.

Ovaskainen, O. (2020). *Joint Species Distribution Modelling: With Applications in R*. Cambridge University Press.

Pang, S. E. H., Slik, J. W. F., Chisholm, R. A., & Webb, E. L. (2024). Conserving Southeast Asian trees requires mitigating both climate and land-use change. *Nature Sustainability*, *7*(10), 1313–1323.

Parmesan, C. (2006). Ecological and Evolutionary Responses to Recent Climate Change. *Annual Review of Ecology, Evolution, and Systematics*, *37*(Volume 37, 2006), 637–669.

Pausas, J. G., & Bond, W. J. (2021). Alternative biome states challenge the modelling of species' niche shifts under climate change. *The Journal of Ecology*, *109*(12), 3962–3971.

Pereira, H. M., Leadley, P. W., Proença, V., Alkemade, R., Scharlemann, J. P. W., Fernandez-Manjarrés, J. F., Araújo, M. B., Balvanera, P., Biggs, R., Cheung, W. W. L., Chini, L., Cooper, H. D., Gilman, E. L., Guénette, S., Hurtt, G. C., Huntington, H. P., Mace, G. M., Oberdorff, T., Revenga, C., … Walpole, M. (2010). Scenarios for global biodiversity in the 21st century. *Science (New York, N.Y.)*, *330*(6010), 1496–1501.

Pereira, H. M., Martins, I. S., Rosa, I. M. D., Kim, H., Leadley, P., Popp, A., van Vuuren, D. P., Hurtt, G., Quoss, L., Arneth, A., Baisero, D., Bakkenes, M., Chaplin-Kramer, R., Chini, L., Di Marco, M.,

Ferrier, S., Fujimori, S., Guerra, C. A., Harfoot, M., … Alkemade, R. (2024). Global trends and scenarios for terrestrial biodiversity and ecosystem services from 1900 to 2050. *Science*, *384*(6694), 458–465.

Perry, G., Wilmshurst, J., & McGlone, M. (2014). Ecology and long-term history of fire in New Zealand. *New Zealand Journal of Ecology*, *38*, 157–176.

Pichler, M., & Hartig, F. (2021). A new joint species distribution model for faster and more accurate inference of species associations from big community data. *Methods in Ecology and Evolution*, *12*(11), 2159–2173.

Pilotto, F., Kühn, I., Adrian, R., Alber, R., Alignier, A., Andrews, C., Bäck, J., Barbaro, L., Beaumont, D., Beenaerts, N., Benham, S., Boukal, D. S., Bretagnolle, V., Camatti, E., Canullo, R., Cardoso, P. G., Ens, B. J., Everaert, G., Evtimova, V., … Haase, P. (2020). Meta-analysis of multidecadal biodiversity trends in Europe. *Nature Communications*, *11*(1), 3486.

Plue, J., Vandepitte, K., Honnay, O., & Cousins, S. A. O. (2017). Does the seed bank contribute to the build-up of a genetic extinction debt in the grassland perennial Campanula rotundifolia? *Annals of Botany*, *120*(3), 373–385.

Prentice, I. C., Cramer, W., Harrison, S. P., Leemans, R., Monserud, R. A., & Solomon, A. M. (1992). A global biome model based on plant physiology and dominance, soil properties and climate. *Journal of Biogeography*, *19*(2), 117–134.

Pressey, R. L., Cabeza, M., Watts, M. E., Cowling, R. M., & Wilson, K. A. (2007). Conservation planning in a changing world. *Trends in Ecology & Evolution*, *22*(11), 583–592.

Qazi, A. W., Saqib, Z., & Zaman-ul-Haq, M. (2022). Trends in species distribution modelling in context of rare and endemic plants: a systematic review. *Ecological Processes*, *11*(1), 40.

Rolls, R. J., Deane, D. C., Johnson, S. E., Heino, J., Anderson, M. J., & Ellingsen, K. E. (2023). Biotic homogenisation and differentiation as directional change in beta diversity: synthesising

driver-response relationships to develop conceptual models across ecosystems. *Biological Reviews of the Cambridge Philosophical Society*, *98*(4), 1388–1423.

Ropars, P., Département de biologie, chimie et géographie, Université du Québec à Rimouski, 300 allée des Ursulines, Rimouski, QC, Canada, G5L 3A1, Comeau, É., Lee, W., & Boudreau, S. (2018). Biome transition in a changing world: from indigenous grasslands to shrub-dominated communities. *New Zealand Journal of Ecology*, *42*(2), 229–239.

Rubenstein, M. A., Weiskopf, S. R., Bertrand, R., Carter, S. L., Comte, L., Eaton, M. J., Johnson, C. G., Lenoir, J., Lynch, A. J., Miller, B. W., Morelli, T. L., Rodriguez, M. A., Terando, A., & Thompson, L. M. (2023). Climate change and the global redistribution of biodiversity: substantial variation in empirical support for expected range shifts. *Environmental Evidence*, *12*(1), 1–21.

Sakschewski, B., von Bloh, W., Boit, A., Poorter, L., Peña-Claros, M., Heinke, J., Joshi, J., & Thonicke, K. (2016). Resilience of Amazon forests emerges from plant trait diversity. *Nature Climate Change*, *6*(11), 1032–1036.

Sandel, B., Merow, C., Serra-Diaz, J. M., & Svenning, J.-C. (2025). Disequilibrium in plant distributions: Challenges and approaches for species distribution models. *The Journal of Ecology*, *113*(4), 782–794.

Sato, H. (2026). Predicting dominant terrestrial biomes at a global scale using machine learning algorithms, climate variable indices, and extreme event indices. *PloS One*, *21*(2), e0324107.

Sax, D. F., & Gaines, S. D. (2008). Colloquium paper: species invasions and extinction: the future of native biodiversity on islands. *Proceedings of the National Academy of Sciences of the United States of America*, *105 Suppl 1*(supplement_1), 11490–11497.

Schipper, A. M., Hilbers, J. P., Meijer, J. R., Antão, L. H., Benítez-López, A., de Jonge, M. M. J., Leemans, L. H., Scheper, E., Alkemade, R., Doelman, J. C., Mylius, S., Stehfest, E., van Vuuren, D. P., van

Zeist, W.-J., & Huijbregts, M. A. J. (2020). Projecting terrestrial biodiversity intactness with GLOBIO 4. *Global Change Biology*, *26*(2), 760–771.

Schroeder, L., Robles, V., Jara-Arancio, P., Lapadat, C., Hobbie, S. E., Arroyo, M. T. K., & Cavender-Bares, J. (2024). Drivers of plant diversity, community composition, functional traits, and soil processes along an alpine gradient in the central Chilean Andes. *Ecology and Evolution*, *14*(2), e10888.

Shabanov, I., Lensen, A., Tonkin, J., & Deslippe, J. R. (2026). A machine learning framework for mapping shifts in species' abundance from long-term monitoring data. *The Journal of Ecology*, *114*(5), e70344.

Shabanov, I., Tonkin, J. D., Lensen, A., & Deslippe, J. R. (2025). Climate-driven forest reassembly follows divergent functional pathways in cold- and warm-adapted communities. In *bioRxiv* (p. 2025.11.18.689113). https://doi.org/10.1101/2025.11.18.689113

Steinbauer, M. J., Grytnes, J.-A., Jurasinski, G., Kulonen, A., Lenoir, J., Pauli, H., Rixen, C., Winkler, M., Bardy-Durchhalter, M., Barni, E., Bjorkman, A. D., Breiner, F. T., Burg, S., Czortek, P., Dawes, M. A., Delimat, A., Dullinger, S., Erschbamer, B., Felde, V. A., … Wipf, S. (2018). Accelerated increase in plant species richness on mountain summits is linked to warming. *Nature*, *556*(7700), 231–234.

Testolin, R., Attorre, F., Borchardt, P., Brand, R. F., Bruelheide, H., Chytrý, M., De Sanctis, M., Dolezal, J., Finckh, M., Haider, S., Hemp, A., Jandt, U., Kessler, M., Korolyuk, A. Y., Lenoir, J., Makunina, N., Malanson, G. P., Montesinos-Tubée, D. B., Noroozi, J., … Jiménez-Alfaro, B. (2021). Global patterns and drivers of alpine plant species richness. *Global Ecology and Biogeography: A Journal of Macroecology*, *30*(6), 1218–1231.

Tilman, D., May, R. M., Lehman, C. L., & Nowak, M. A. (1994). Habitat destruction and the extinction debt. *Nature*, *371*(6492), 65–66.

Townsend Peterson, A., Soberon, J., Pearson, R. G., Anderson, R. P., Martinez-Meyer, E., Nakamura, M., & Araujo, M. B. (2011). *Ecological niches and geographic distributions (MPB-49)*. Princeton University Press.

Trisos, C. H., Merow, C., & Pigot, A. L. (2020). The projected timing of abrupt ecological disruption from climate change. *Nature*, *580*(7804), 496–501.

Urban, M. C. (2024). Climate change extinctions. *Science (New York, N.Y.)*, *386*(6726), 1123–1128.

Urban, M. C., Bocedi, G., Hendry, A. P., Mihoub, J.-B., Pe'er, G., Singer, A., Bridle, J. R., Crozier, L. G., De Meester, L., Godsoe, W., Gonzalez, A., Hellmann, J. J., Holt, R. D., Huth, A., Johst, K., Krug, C. B., Leadley, P. W., Palmer, S. C. F., Pantel, J. H., … Travis, J. M. J. (2016). Improving the forecast for biodiversity under climate change. *Science (New York, N.Y.)*, *353*(6304), aad8466–aad8466.

Valavi, R., Elith, J., Lahoz-Monfort, J. J., & Guillera-Arroita, G. (2019). block CV : An r package for generating spatially or environmentally separated folds for *k* -fold cross-validation of species distribution models. *Methods in Ecology and Evolution*, *10*(2), 225–232.

Valdez, J. W., Callaghan, C. T., Junker, J., Purvis, A., Hill, S. L. L., & Pereira, H. M. (2023). The undetectability of global biodiversity trends using local species richness. *Ecography*, *2023*(3), e06604.

Velazco, S. J. E., Rose, M. B., De Marco, P., Jr, Regan, H. M., & Franklin, J. (2024). How far can I extrapolate my species distribution model? Exploring shape, a novel method. *Ecography*, *2024*(3). https://doi.org/10.1111/ecog.06992

Vellend, M., Baeten, L., Myers-Smith, I. H., Elmendorf, S. C., Beauséjour, R., Brown, C. D., De Frenne, P., Verheyen, K., & Wipf, S. (2013). Global meta-analysis reveals no net change in local-scale plant biodiversity over time. *Proceedings of the National Academy of Sciences of the United States of America*, *110*(48), 19456–19459.

Walker, M. D., Wahren, C. H., Hollister, R. D., Henry, G. H. R., Ahlquist, L. E., Alatalo, J. M., Bret-Harte, M. S., Calef, M. P., Callaghan, T. V., Carroll, A. B., Epstein, H. E., Jónsdóttir, I. S., Klein, J. A., Magnússon, B., Molau, U., Oberbauer, S. F., Rewa, S. P., Robinson, C. H., Shaver, G. R., … Wookey, P. A. (2006). Plant community responses to experimental warming across the tundra biome. *Proceedings of the National Academy of Sciences of the United States of America*, *103*(5), 1342–1346.

Wiens, J. J., & Zelinka, J. (2024). How many species will Earth lose to climate change? *Global Change Biology*, *30*(1), e17125.

Wilkes, M. A., Mckenzie, M., Johnson, A., Hassall, C., Kelly, M., Willby, N., & Brown, L. E. (2025). Revealing hidden sources of uncertainty in biodiversity trend assessments. *Ecography*, *2025*(5), e07441.

Wiser, S. K., Bellingham, P. J., & Burrows, L. E. (2001). Managing biodiversity information: development of New Zealand's National Vegetation Survey databank. *New Zealand Journal of Ecology*, *25*(2).

Wu, Z., Wang, W., Zhu, W., Zhang, P., Chang, R., & Wang, G. (2024). Shrub ecosystem structure in response to anthropogenic climate change: A global synthesis. *The Science of the Total Environment*, *953*(176202), 176202.

Wyse, S., School of Environment, University of Auckland, Private Bag 92019, Auckland 1142, New Zealand, Wilmshurst, J., Burns, B., & Perry, G. (2018). New Zealand forest dynamics: a review of past and present vegetation responses to disturbance, and development of conceptual forest models. *New Zealand Journal of Ecology*, *42*(2). https://doi.org/10.20417/nzjecol.42.18

Yachi, S., & Loreau, M. (1999). Biodiversity and ecosystem productivity in a fluctuating environment: the insurance hypothesis. *Proceedings of the National Academy of Sciences of the United States of America*, *96*(4), 1463–1468.

Yoon, S., & Lee, W.-H. (2023). Application of true skill statistics as a practical method for quantitatively assessing CLIMEX performance. *Ecological Indicators*, *146*(109830), 109830.

Zwiener, V. P., Lira-Noriega, A., Grady, C. J., Padial, A. A., & Vitule, J. R. S. (2018). Climate change as a driver of biotic homogenization of woody plants in the Atlantic Forest. *Global Ecology and Biogeography: A Journal of Macroecology*, *27*(3), 298–309.

5. Climate-Driven Forest Reassembly Follows Divergent Functional Pathways in Cold- and Warm-Adapted Communities (TrP)

5.1. Abstract

1. Climate change can reorganise forests, predominantly towards warm-adapted, lower-elevation species. However, these similar compositional trends can arise through different processes, including immigration, replacement of the species pool, or shifts in the relative abundance of existing species, with distinct consequences for forest function. A mechanistic perspective linking species' traits to community composition can help identify these distinct community assembly mechanisms and thereby link biodiversity change to its consequences for forest structure and function.
2. Here, we use seven functional traits and diversity indices to identify distinct responses of warm- and cold-adapted forest communities. Our analysis spans measurements from 120 widespread plant species, including leaf morphology, size, nutrient content, and foliar isotopes, across 2541 sites from 1984 to 2020 in New Zealand. We derived functional strategies from community-weighted mean trait values, assessed assembly mechanisms using five multi-trait functional

diversity indices, and estimated structural change and turnover rates using abundance-based dissimilarity metrics.

3. Rising temperatures (+0.12 °C/decade) and declining precipitation (-0.87%/decade) altered forest composition toward warm-adapted lowland species and increased functional and species richness. Exotic species were predominantly responsible for expanding functional space, while native species increased richness. Warm-adapted forests primarily showed signs of shifts in water-use strategies, which might be altered by CO_2 fertilisation. Cold-adapted forests experienced the strongest functional shifts, driven by disturbances and water limitation, and revealed a potential advantage of ectomycorrhizal fungal associations for species under elevated CO_2. Mixed ecotonal forests had a high turnover rate, but negligible functional shifts.
4. New Zealand forests follow biome-specific trajectories, characterised by distinct assembly mechanisms and context-dependent ecological responses. While uniform mean trends obscure these responses, they can be disentangled using a functional diversity framework that incorporates isotopic traits, offering a practical means to detect and interpret community reassembly under climate change.

5.2. Introduction

Forests provide humans with critical resources and services, and influence climate at the global scale (Trumbore et al. 2015). However, forest species composition is changing unpredictably and faster than at any time in the Holocene (Lawlor et al. 2024). Most of the biosphere now experiences novel ecological conditions, where combinations of altered climate, defaunation, and floristic disruption fall outside the historical range and create community structures that are not predictable from past dynamics (Kerr et al. 2025; Radeloff et al. 2015). Reduced tree longevity (Locosselli et al. 2020), altered reproductive phenology (Flores et al. 2023), heightened vulnerability to pathogens (Wyka et al. 2018), and intensified pressure from insect outbreaks (Pureswaran et al. 2018) collectively diminish productivity (Mao et al. 2022), carbon sequestration capacity (Carnicer et al. 2019), and resilience (Oliver et al. 2015). As ecological novelty intensifies, there is a growing urgency to identify the mechanisms driving biodiversity rearrangement to safeguard forest health and conserve biodiversity.

Observations of biodiversity rearrangement alone, so far, have struggled to predict these accelerating changes at scale (Rubenstein et al. 2023). For instance, in some places, climate warming has induced expansions of warm-adapted species (Gottfried et al. 2012) (thermophilization) and a concomitant decline of cold-adapted species (Rumpf et al. 2019). By contrast, species richness can remain unchanged (Vellend et al. 2013; Dornelas et al. 2014), increase (Montràs-Janer et al. 2024; Steinbauer et al. 2018), or decrease (Pereira et al. 2024), even in strongly affected Arctic ecosystems (García Criado et al. 2025; Cotto et al. 2017). The speed of biodiversity change depends on the climate (Stephenson and Mantgem 2005; Fadrique et al. 2018), but is rarely quantified. Underlying these conflicting patterns in

the rearrangement of forests are context-dependent mechanisms (Lenoir and Svenning 2015; Lawlor et al. 2024) interacting with hitherto novel climatic conditions (Staples et al. 2022). Moreover, forests exhibit response lags due to long generation times (Breshears et al. 2008), which can be overlooked in comparatively small or short-term datasets (Valdez et al. 2023; Komatsu et al. 2019). Reliable predictions of biodiversity rearrangement, therefore, require a mechanistic understanding of plant-environment interactions, inferred from larger and longer datasets.

Leveraging plant functional traits in models to predict plant responses to environmental change offers a mechanistic approach to plant-environment relationships (Funk et al. 2017). However, while relationships between single traits and environmental gradients exist (Wieczynski et al. 2019), they lack explanatory power and fail to capture the complexity of interacting drivers (Green et al. 2022). Trait syndromes, on the other hand, reflect ecological strategies that allow species to succeed in an environment (Laughlin 2023) and enable predictions of which species will thrive there in the future (Henn et al. 2024). For instance, specific leaf area (SLA) and leaf nitrogen content concurrently increase with temperature and decrease with elevation, signalling their role in a strategy adapted to harsher, nutrient-poorer environments (Homeier et al. 2021). Conversely, lower SLA with higher stem density is associated with higher drought tolerance (Greenwood et al. 2017). Capturing the dynamics of trait syndromes at the community scale holds the key to understanding forest responses and to better forecast changing biodiversity patterns under previously unobserved conditions (Kerr et al. 2025).

The ecological insights derived from trait data are constrained by the traits selected. Measured traits should therefore align with the trait syndromes and functional strategies

most relevant to the climatic context (Hagan et al. 2023). For instance, much of the research has focused on easily measured leaf, seed, and stature traits (Green et al. 2022), which capture broad plant strategies along the r-K spectrum (Díaz et al. 2022), but are less suitable for explaining water use strategies critical in arid environments (Li et al. 2015). In contrast, underutilised traits such as nitrogen-15 ($\Delta^{15}N$) and carbon-13 ($\Delta^{13}C$) isotope ratios provide more mechanistic insight into nutrient acquisition strategies, water-use efficiency (Dawson et al. 2002), and plant-microbe associations (Song and Zhou 2021), while also informing productivity (Luo et al. 2009) and nutrient limitation (McLauchlan et al. 2010) in ecosystems. Accurately forecasting plant community responses to environmental change, therefore, depends on selecting traits with mechanistic links to the relevant environmental drivers.

The relevance of traits and functional strategies depends on the environmental constraints faced by the community (Lebrija-Trejos et al. 2010). For instance, strategies favouring rapid resource acquisition are disadvantageous in harsh environments that favour slow-growing, stress-tolerant species (e.g. alpine tundra; (Spasojevic and Suding 2012) but advantageous in resource-rich environments where competition shapes community assembly (Grime 1977). These assembly processes can be inferred from relationships between functional richness (FRic), the range of strategies present, and functional dispersion (FDis), the degree of trait differentiation (Lamanna et al. 2014; Laliberté and Legendre 2010). Concurrently decreasing FRic and increasing FDis suggest selection for distinct strategies under strong abiotic filtering. Conversely, increasing FRic and stable FDis suggest differentiation of species into distinct niches. Strong abiotic filtering excludes species with traits unsuited to local stressors, producing communities of functionally similar, stress-tolerant species (Le Bagousse-Pinguet et al. 2017). In

contrast, niche complementarity among diverse traits promotes efficient resource use, multifunctionality, and greater resilience (Searle and Chen 2020; Gross et al. 2017). Interpreting functional diversity patterns alongside trait distributions therefore strengthens inferences about the mechanisms governing community assembly and the stability of resulting community structure.

Here, using 36 years of vegetation data from 2,541 forest plots across New Zealand and seven functional traits within a functional diversity framework, we aim to understand the mechanisms behind biodiversity rearrangement in forest communities. To separate regional climatic effects from biome-specific dynamics, we use satellite data to first partition communities into cold-adapted beech forests, warm-adapted podocarp forests, and mixed ecotonal forest types. We then examine temporal trends in functional diversity and community weighted trait values to identify which community assembly mechanisms shaped these biomes (Aim1), and which functional strategies drove changes (Aim 2). Next, we identify which groups of species influenced these trends disproportionately (Aim 3). Lastly, we aim to quantify the consequences of these assembly processes by estimating the rate of species turnover within communities (Aim 4). Together, these aims provide a basis for understanding multiple pathways of forest reassembly, their constituent species and functional strategies, and for anticipating long-term biodiversity trajectories under accelerating climate change.

5.3. Methods

5.3.1. Species Occurrence, Abundance Data, and Forest Types

We utilised forest plots in New Zealand's national forest inventory data (NVS, (Wiser et al. 2001)), which were measured using the RECCE protocol (Hurst 2022), containing 20x20m plots with categorical cover estimates for every height tier category (1 through 6, for individuals > 25m down to < 60cm). These categories were collapsed into a single cover estimate for each species and plot (Fischer 2015). The sum of these estimates was normalised to 1, yielding relative canopy cover values for each species p_j. Plots where the number of species was too low to calculate trait and community metrics (see following sections) were discarded, resulting in a final set of 2541 sites, surveyed a total of 4677 times from 1984 to 2020, with a median of 12 years between surveys. The geographic extent covered the entirety of New Zealand, including Stewart Island (***Fig. B2***).

We assigned one of three forest types (Beech, Podocarp (which also included broadleaved species), or Mixed) to each plot using the satellite-based 25m Basic Ecosystem layer from New Zealand's Landcare Research database (Barringer 2018), as it is the only nationwide forest vegetation classification dataset for existing rather than historic vegetation. We opted to use satellite data, rather than plot composition, as the current classification system is very fine-grained and not publicly available (Wiser and De Cáceres 2018). For each species, we defined its primary forest type as the forest type in which it reached its highest abundance. Species were then classified as endemic, or not, to that primary forest type (e.g. beech forest endemic species). However, most species occurred across all three forest types, differing only in relative abundance. Shrublands were excluded, as

they are structured by different community assembly mechanisms than forests (Subedi et al. 2019) and often comprise early successional stands regenerating after land-use change or natural disturbance. These communities reflect secondary succession rather than climate-driven change in intact forests.

5.3.2. Trait Data and Species Selection

We collected and compiled trait data on seven traits: Specific Leaf Area including the petiole (SLA), stem specific density (SSD), leaf nitrogen content per unit mass (Nmass, mg/g), leaf $\Delta^{13}C$ carbon isotope (in ‰), leaf $\Delta^{15}N$ nitrogen isotope (in ‰), diaspore mass (in mg) and plant maximum height (in m). We collected trait data on the 78 most abundant and locally available tree, shrub, and vine species in the Wellington (New Zealand) region from September 2024 to February 2025. Collection, handling, and measurement followed the protocols in (Pérez-Harguindeguy et al. 2013). Additionally, we downloaded all available traits of the New Zealand flora from the TRY database (Kattge et al. 2020) and the Ecotraits database ([No author] 2005). Measurements from all three sources were combined by taking the average trait value of all entries. To reduce errors, we discarded species with more than three out of seven trait values missing. This yielded a set of 120 species for which trait and occurrence data were present, which were the species used for our analysis. Values x for diaspore mass and plant height were log1p transformed $x' = log(1 + x)$ to normalise their distributions and facilitate linear regression.

The species dataset contained a diverse range of plant growth forms, including both native (both endemic and non-endemic to New Zealand) and exotic species. (Table 1). We retained six ecologically important native non-woody species (monocotyledonous trees:

Freycinetia banksii and *Cordyline australis,* the palm *Rhopalostylis sapida* and four tree fern species), because they are long-lived, structurally dominant components of New Zealand forests and share functional overlap with woody species (Wyse et al. 2018; Brock et al. 2018). Because tree ferns exhibit markedly different trait values (e.g., tiny diaspores), we repeated all analyses excluding tree ferns and compared the results (Section S4.6 and ***Fig. B12***). Although diaspore size differs substantially in raw units, this contrast is reduced after log transformation.

Table 1*: Classifications of 120 species in this study by growth form and biostatus.*

		Count			Count
Growth Form	Tree	86	**Biostatus**	Native	108
	Shrub	19		Exotic	12
	Liana	8			
	Treefern	4			
	Monocotyledonous Tree	3			

Missing trait values (ca. 22%, ***Fig. B3*** B) were imputed using Multiple Imputation by Chained Equations (MICE) with taxonomic eigenvectors (Debastiani et al. 2021) and the miceForest Python implementation (Wilson et al. 2023). This algorithm exhibits superior performance compared to other contemporary methods (Penone et al. 2014). As MICE is not deterministic, we re-ran the imputation algorithm five times and averaged the imputation results. The trait distributions before and after imputation were minimally different and didn't significantly change the correlations between the traits (***Fig. B3*** A and C), validating the imputation approach. The average imputation error was 10.68% of the

standard deviation of the trait. Details of the process and error metric are described in Section 2 of the supplementary materials.

Community assembly mechanisms can be assessed by analysing functional strategies; competition is indicated by species with acquisitive traits, whereas abiotic filtering leads to conservative traits (Grime 1977). We subdivided the species into two disjunct groups: acquisitive and conservative. This was done by running a principal component analysis on five traits in our dataset (SLA, SSD, leaf nitrogen content, diaspore mass, height), which are part of the global spectrum of plant form and function (Díaz et al. 2016) and dividing it along the PC1 median, yielding two equally sized groups. We defined the group with the lower SLA as conservative (e.g. *Metrosideros excelsa*) and the other as acquisitive (e.g. *Clematis vitalba*). Additionally, we determined the type of mycorrhizal association (see Section S4.5 for details) using the FungalRoot database (Soudzilovskaia et al. 2020).

5.3.3. Environmental Variables

We selected a set of 16 variables from NZEnvDS (McCarthy et al. 2021), which included topographic (e.g., elevation), edaphic (e.g., pH), and climatic variables (e.g., mean annual temperature) at 100-m resolution, and determined their values at the plot locations. To assess the climate trend, we obtained monthly rainfall and minimum and maximum temperatures (at 1-km resolution) from the HOTRUNZ dataset (Etherington et al. 2022) and computed 19 ecologically meaningful BioClim variables (O'Donnel and Ignizio 2012). For each plot, we approximated the time series of each variable over the years (1970-2019) with a linear function and used the slope as a measure of climate change at this location. Positive values indicate an increasing trend of this climatic variable over time.

5.3.4. Community Weighted Trait Moments

Community-weighted moments describe the distribution of traits at a location (Enquist et al. 2015) and were used to assess community-level functional strategies (Aim 2). The community-weighted mean (CWM) represents the dominant trait value in a plot and can be used to predict ecosystem functions, such as primary productivity (Violle et al. 2014). Variation and shape in trait distributions are captured by higher-order moments. For example, strong abiotic filtering reduces community weighted variance (CWV), as environmental constraints favour an increasingly narrow range of trait values (Enquist et al. 2015). When trait distributions shift directionally towards a new optimum, communities may "lean" towards that value, reflected in increasing community-weighted skewness (CWS) (Breshears et al. 2008). Community-weighted kurtosis (CWK) describes how heavy-tailed a distribution is: lower values indicate more even trait distributions, consistent with limiting similarity, whereas higher values suggest the clustering of trait values under environmental filtering (Cornwell and Ackerly 2009). We calculated moments only for plots with five or more species (formulae are described in Section S3.1).

5.3.5. Community Environmental Index

The average thermal preference of all species in a community, weighted by their relative abundance, is referred to as the community temperature index (CTI, (Devictor et al. 2008)). Extending this definition to other plot-level variables (climatic, topographic, and geographic), we defined the community environmental indices (CEI). The CEI represents the average of the species' environmental preference (SEP) weighed by their abundance

in the plot i: a_{si} and is defined as $CEI_i = \frac{\sum_s a_{si} \cdot SEP_s}{\sum_s a_{si}}$. Where $SEP_s = \frac{1}{|P_s|} \sum_i v(i)$ is the mean plot-level environmental variable v (e.g., temperature or elevation) across all plots where the species has been observed P_s. The CEI_i is a plot-level variable that can be interpreted as the environmental preference of the entire community inside a forest plot i defined by its species. The CEI for temperature is thus identical to the CTI. We evaluated CEI trends over time using linear mixed models (see Section 2.9) to probe for effects of thermophilization (increasing CEI for mean annual temperature), invasion by lowland species (decreasing CEI for elevation), and others (***Fig. B6***).

5.3.6. Functional and Taxonomic Diversity Indices

To assess community assembly mechanisms (Aim 1), we computed five functional diversity indices for each plot following (Pla et al. 2012): Functional Richness (FRic), functional divergence (FDiv) and functional evenness (FEve) (Villéger et al. 2008), the mean nearest neighbour distance (MNND) in trait space (Swenson and Weiser 2014), and functional dispersion (FDis) (Laliberté and Legendre 2010). FRic is calculated as the volume of the convex hull of species' T trait values for each plot and therefore requires at least T + 1 species to be present (here, T=7). This limitation reduced the number of usable plots for functional diversity calculation by about 20% (1983 sites in 3841 surveys). MNND is calculated as the average Euclidean distance in trait space between each species and its nearest neighbour. These indices are used to quantify the size and packing of trait space. A large FRic value indicates a community with many diverse trait values and therefore correlates well with species richness (Swenson and Weiser 2014). MNND indicates how

similar or packed these species are in trait space, with low values indicating the clustering of functionally similar species. FEve quantifies how evenly species abundances are distributed along trait axes, while FDiv reflects how far species deviate from the centre of trait space, emphasising the presence of functionally extreme species. FDis captures the mean distance of individual species to the community centroid, weighted by relative abundance, thus representing trait dispersion within the community. We transformed $FRic$ to $FRicLog = log(1 + FRic)$ to normalise its distribution and facilitate linear regression.

To assess the taxonomic structure of the communities, we used three metrics: Species Richness (count of species per plot), taxonomic diversity (using Shannon's Index) and evenness (using Pielou's index) (Pla et al. 2012). The Shannon Index of plot i is defined as

$H_i = -\sum_s a_{si} \cdot log(a_{si})$, where a_{si} is the abundance of species s in that plot. The index is largest when all species within a plot have identical abundances. Pielou's index captures the evenness component by normalising Shannon's index by species richness. It is 1 if all species have equal abundances.

5.3.7. Standardised Effect Sizes (SES) and Null Models

Functional richness, mean nearest neighbour distance and functional dispersion are strongly correlated with species richness (***Fig. B4***). Consequently, observed changes in these three metrics may reflect variation in richness rather than underlying shifts in functional structure. To disentangle the effects of species richness from functional restructuring, we constructed a null model distribution and calculated standardised

effect sizes for each functional diversity metric (Swenson and Weiser 2014). For each plot containing S species, we took 1000 random draws of S species and recalculated the functional diversity metric m, yielding a null-distribution P_0. The standardised effect size for this metric and plot is then defined as $SES(m) = \frac{m - \mu(P_0)}{\sigma(P_0)}$. Values greater than zero indicate that m exceeds expectations under random assembly, effectively decoupling functional diversity from species richness. To avoid artificially inflating the representation of rare species and increasing the variance of the null-distribution, species were sampled with probabilities proportional to their observed frequency within the relevant forest type (Details in Section S 3.4).

5.3.8. Linear regressions and statistical testing

For temporal trend analysis (CEI, functional and taxonomic diversity indices, species richness, and trait moments), we fitted separate linear mixed-effects models for each metric and forest type using the statsmodels Python package (Seabold and Perktold 2010), with plot ID included as a random intercept to account for repeated measurements within the same plot. Fixed effects (e.g., Year) were tested using Wald tests, assuming an asymptotic normal distribution of the test statistic. Parameters were estimated via restricted maximum likelihood. For estimating the rate of change, a regression was run on estimates per year, using ordinary least squares regression with the same significance testing.

Because models included only a single explanatory variable (Year), explained variance (calculated using (Nakagawa and Schielzeth 2013)) was low (marginal R^2<0.2 for all metrics; see ***Fig. B4*** for an example). All R^2 and p-values are provided in a supplementary

table. This was expected given the simplicity of the models and does not undermine inference, as our goal was to estimate the direction of temporal trends rather than to maximise predictive power.

5.3.9. Influence of species groups on metric trends

To understand whether specific subsets of species (e.g. exotics) had disproportionately strong effects on functional or taxonomic richness and diversity (hereafter collectively: "metrics"), we assessed each species' contribution to temporal trends using a sequential (leave-one-out) approach, as follows:

1. Let m be the slope of the linear regression (Section 5.3.8) for a metric.
2. We excluded a species s, re-ran the linear regressions. Species impact was defined as $\delta_s = |m| - |m_s|$, where m is the original slope and m_s is the slope after excluding species s. A value of s=0 indicates no influence of the species on the trend. Positive values indicate that inclusion of the species strengthens the magnitude of the temporal trend, whereas negative values indicate it dampens it.
3. For each metric, the set of all species impacts $\{\delta_s\}$ was transformed to have zero mean and unit variance, making the resulting standardised effect sizes comparable across metrics.
4. The impact of a species group I (e.g. exotic species) was defined as the mean standardised impact of its species: $\Delta_I = \frac{1}{|I|}\sum_{s \in I} \delta_s$

5. We asked the question whether Δ_I had a significantly different impact from a random group of the same size and assessed this using a null model approach.
6. First, we constructed the null distribution $P_0 = \{\Delta^{(i)}\}$ by randomly sampling 1000 species assemblages of size $|I|$ according to their frequencies (see section 5.3.7) and computing their average impact.
7. Next, we computed the standardised effect size using the mean μ_0 and standard deviation σ_0 of the null distribution: $SES(\Delta_I) = \frac{\Delta_I - \mu_0}{\sigma_0}$.
8. Finally, we computed a two-sided p-value $p = \frac{1+\#\{|\Delta^{(i)} - \mu_0| \geq |\Delta_I - \mu_0|\}}{1001}$. The influence score from the i-th draw of the null model is denoted by $\Delta^{(i)}$ and #{…} is the number of times the equation holds true across the 1000 elements of P_0. A 1 was added to avoid a zero p-value.

This framework allowed us to identify species groups whose contributions to temporal trends deviated from random expectations. We analysed multiple groups: acquisitive and conservative strategists (Section 5.3.2), native and exotic species (bio status), primary forest type (Section 5.3.1), and mycorrhizal type (***Fig. B9***). We acknowledge that, when analysing only two disjunct groups (e.g., native vs. exotic species), a simpler comparison of groups using Cohen's d is a viable approach. However, the null-model approach has the advantage of assessing the impact of an arbitrary group of species and provides p-values for significance testing.

5.4. Results

5.4.1. Widespread shifts towards warm-adapted, low-elevation species

Community environmental indices for elevation, latitude, mean annual temperature, slope, and precipitation showed coordinated shifts within forest types (Fig. 5.1, complete list in *Fig. B6*). CEIs of all forest types shifted towards higher mean annual temperatures and lower latitudes (away from the poles), indicating a thermophilization of communities, through inclusion of more warm-adapted higher-latitude species. The CEI of elevation shifted significantly only in mixed forest, indicating an additional proliferation of low elevation species at the expense of montane species. Beech and Podocarp communities shifted towards more drought-adapted species, leading to lower annual precipitation CEI. The pH affinity of communities increased significantly, however, the magnitude of change was small (+ 0.01 - 0.02 over 36 years).



Figure 5.1: Temporal trends of community environmental indices (CEI, reflecting the environmental conditions favoured by the species present in a plot) for six plot-level variables over time for the three studied forest types (indicated by colour). Significant relationships are displayed as solid lines (insignificant ones are dashed); 95% confidence intervals are shaded. Exact R^2 and p-values in supplementary table.

5.4.2. Niche packing and differential traits in functional divergence

The taxonomic composition of all forest types grew more species rich and taxonomically diverse over time (Fig. 5.2, top row). Beech forests showed the weakest trends and decreased in taxonomic evenness, indicating increasing dominance by fewer species,

despite more species overall. Functional richness (FRic) and dispersion (FDis) increased simultaneously, accompanied by a decreasing MNND, indicating broader niches with more tightly packed species, except for FDis in beech forests, which showed a non-significant trend (Fig. 5.2, centre row). The standardised effect sizes (SES) of the functional indices were negative, indicating that functional diversity trends were largely driven by species richness and revealing trait underdispersion. Trait underdispersion increased significantly over time in mixed forests (negative trend in SES(FricLog)). Functional evenness decreased across all forest types, but was significant only in Podocarp forests, suggesting a more clustered functional trait space. In beech forests, a decreasing FDiv trend similarly indicated species traits clustering around the centroid of functional space.

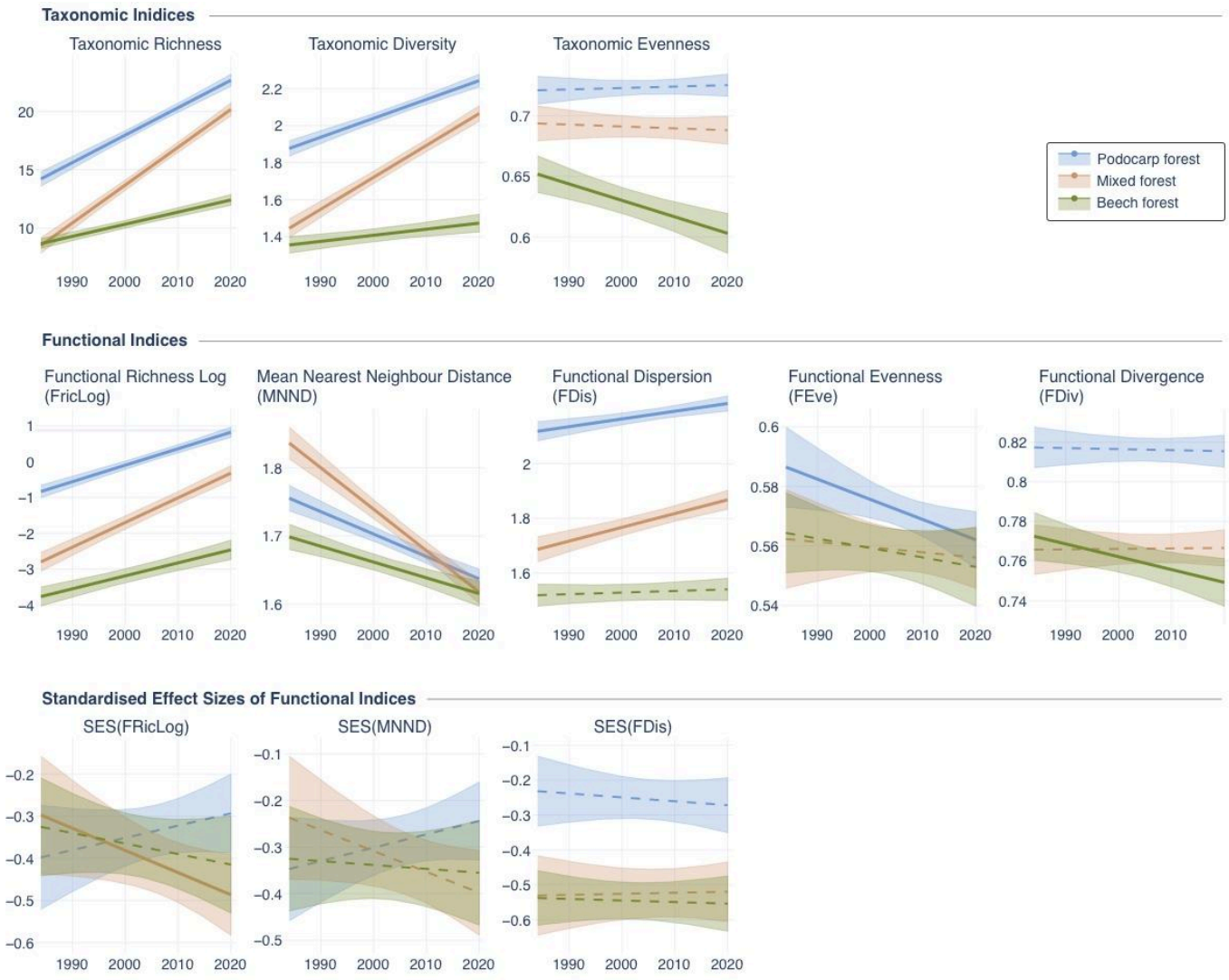


Figure 5.2: Temporal trends of multi-trait functional diversity indices, species richness, taxonomic diversity (Shannon's index) and taxonomic evenness (Peilou's index) for the three studied forest types (indicated by colour). Significant relationships are displayed as solid lines (non-significant ones with $p < 0.05$ are dashed), 95% confidence intervals are shaded. Exact R^2 and p-values in supplementary table.

5.4.3. Some Species Groups Contribute more strongly to functional change

Multiple individual groups of species affected the temporal trends of different metrics (in Fig. 5.2) more than would be expected by chance (from here on simply “influenced”). Species richness was influenced by all species groups, consistent with broadly shared contributions across the community (Fig. 5.3). One exception was the influence of arbuscular mycorrhizal species in beech forests (dominated by beeches with ectomycorrhizal (EcM) associations)(***Fig. B9***). Increasing functional richness trends were influenced by exotic species and podocarp forest endemics (Fig. 5.3). In podocarp forests, EcM species also influenced functional richness (***Fig. B9***). Declining MNND was influenced by different groups in the three forest types. In podocarp forests, no specific group influenced the MNND trend, while in beech forests, acquisitive tree species from podocarp forests influenced it the most. In mixed forests, only podocarp endemic species and tree ferns influenced the MNND trend. Falling taxonomic evenness in the beech forest was influenced by acquisitive species, which were less likely to be trees or AM-associated. Increasing functional dispersion in podocarp forests was influenced by natives, whereas in mixed forests it was dominated by podocarp-endemics with conservative strategies, suggesting a similar set of influential species in both forest types. Declining functional divergence in beech forests was influenced by beech forest endemics, which were less likely to be native, acquisitive, or trees. The decrease in functional evenness in podocarp forests was influenced by acquisitive endemic species.

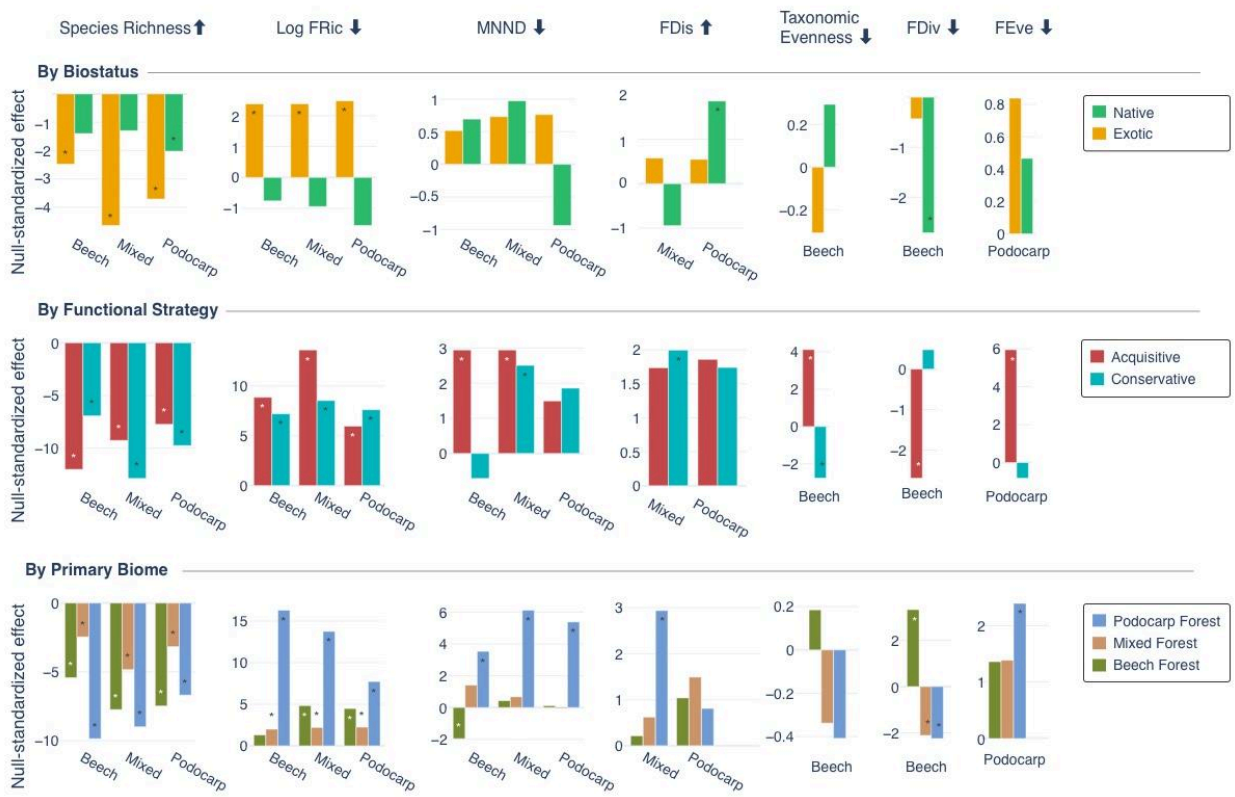


Figure 5.3: Null standardised effect sizes for the impact of different subgroups (biostatus, functional strategy and primary biome) of species on the trends of richness, evenness, FRicLog, FDiv, FDis, FEve and MNND). An arrow next to the trait name indicates the trend direction. Positive values indicate that this group contributes more to the trend than expected by chance of a group the same size. Only metrics with significant trends are shown. An asterisk indicates groups that have a statistically significant deviation from the null distribution ($p < 0.05$).

5.4.4. Functional change differs among forest types

The forest types showed marked differences in CWM trait values over time (Fig. 5.4). Beech forests exhibited the strongest functional change, but in contrasting directions. Traits associated with conservative strategies increased (increasing diaspore mass,

decreasing leaf nitrogen content), while traits linked to ruderal strategies (shorter maximum height and lower stem specific density) also shifted, emphasised by changes in skewness. The variance of leaf $\Delta^{13}C$ increased, indicating a wider range of water-use strategies, while the variance of leaf $\Delta^{15}N$ declined. Podocarp forests only showed significant reductions in CWM leaf $\Delta^{13}C$ and reduced skew in stem specific density, indicating shifting water-use strategies. Mixed forests showed minimal functional change but increased skewness and kurtosis for diaspore mass and increased skewness for leaf nitrogen content. For diaspore mass, this may indicate an increase in species with large values, which is supported by a positive, albeit non-significant, trend in CWM mirroring beech forests. While we did not find significant temporal trends in specific leaf area CWM, it was the trait with the largest positive value across all traits (*Fig. B7*), indicating a community shifting towards lower values, corresponding to a more conservative strategy.

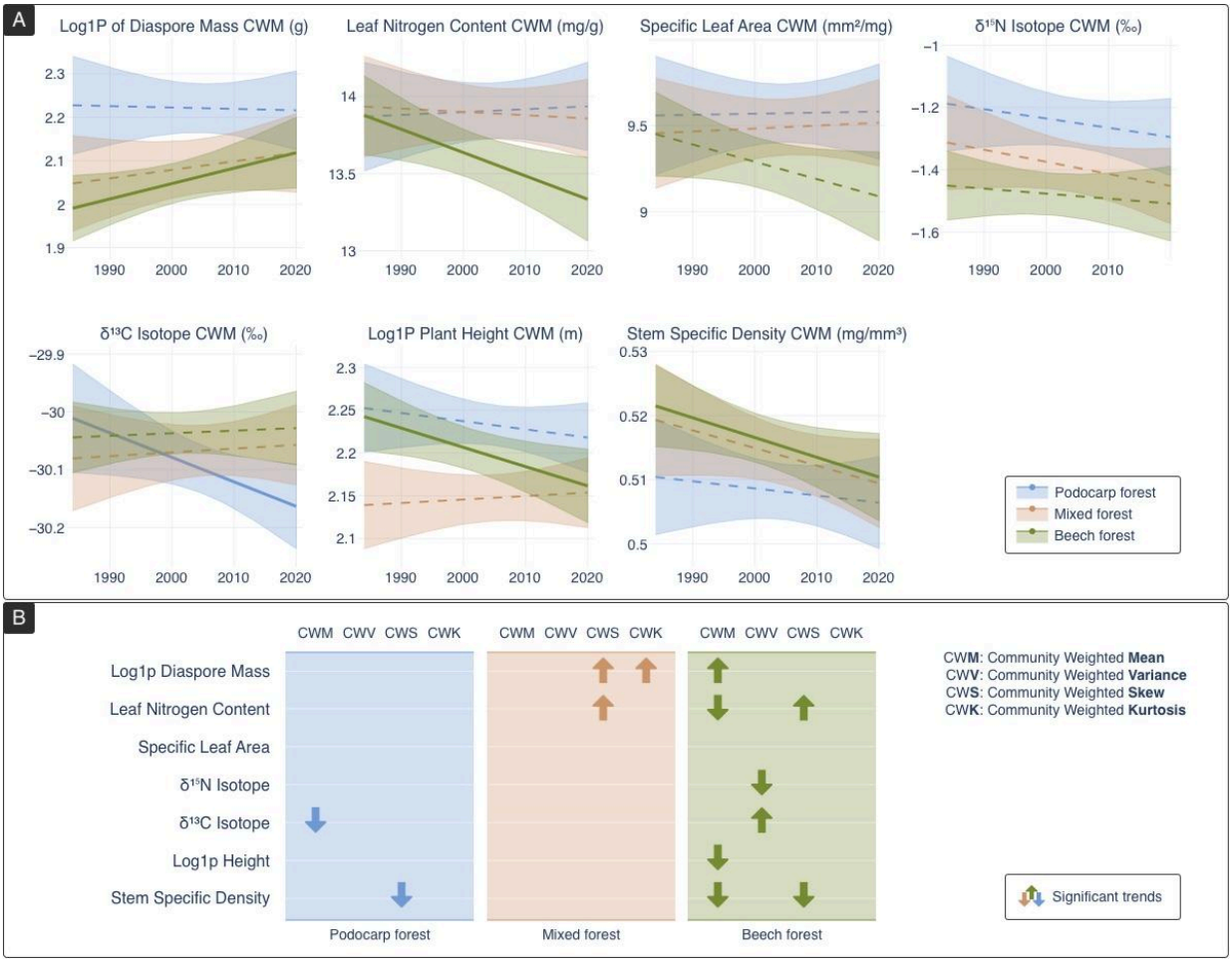


Figure 5.4: (A) Temporal trends of functional trait community weighted means for the three forest types (indicated by colour) over time. Significant relationships are displayed as solid lines (insignificant ones are dashed), 95% confidence intervals shaded. (B) Summary of trends observed in panel (A) and higher-order moments. Only significant trends are marked. Exact R^2 and p-values in supplementary table.

We identified species groups influencing (i.e. contributing more than expected by chance) temporal trends of trait CWMs (***Fig. B10***). In beech forests, increases in diaspore mass and reductions in leaf nitrogen were influenced less than expected by AM-associated species, indicating a stronger role for EcM-associated dominant beeches. The declining height trend was influenced by trees, which were not AM-associated. On the other hand,

the declining trend in stem-specific density was more strongly influenced by tree ferns (all of which have AM-associations). These findings suggest two parallel functional drivers underlying shifts in CWM trait values. In podocarp forests, the $\Delta^{13}C$ trend was influenced less than expected by podocarp forest endemic natives, indicating that other groups of species are responsible for the observed shift. Although not statistically significant, beech-forest-endemic shrubs showed above-average contributions to the $\Delta^{13}C$ trend.

5.5. Discussion

Our study revealed that climate-driven reorganisation of forests is differentially structured and progresses at varying rates across three forest types (warm-adapted podocarp, cold-adapted beech and ecotonal mixed forests (***Fig. B1***)). As New Zealand's climate became warmer, drier, with altered stability (***Fig. B5***), warm-adapted, lower-elevation species migrated southward (Fig. 5.1), driving increases in species richness (Fig. 5.2) and turnover (***Fig. B8***) that differed among forest types. Cold-adapted beech forests showed low turnover but strong functional changes (Fig. 5.4) driven by the proliferation of two contrasting strategies: Shorter ruderal species with low SSD and conservative species with higher diaspore mass and lower leaf nitrogen content. Despite higher turnover, podocarp and mixed forests showed limited functional changes. Functional richness increased with species richness but less than expected by chance, indicating expansion within an abiotically constrained functional envelope (Fig. 5.2). Across all forest types, acquisitive and exotic species, endemic to warm-adapted podocarp forests, disproportionately increased functional richness (Fig. 5.3), whereas growthform and mycorrhizal associations affected functional and taxonomic metrics differentially across forest types(***Fig. B9***). The context-dependent mechanisms underlying

uniform increases in taxonomic and functional richness demonstrate that trait-mediated assembly processes translate climate forcing into divergent biodiversity responses, with direct implications for the future structure and resilience of forests.

All forest types increased in species richness (Fig. 5.2), with similar shifts in community environmental preferences (Fig. 5.1) but their rate of turnover and changes in basal cover for affected species differed markedly (Fig. B8 B). These patterns match global observations of increasing regional richness (Dornelas et al. 2023; Steinbauer et al. 2018), and lower turnover in cold-adapted forests may reflect the greater ability of low-elevation species to track climate change compared to montane species (Freeman et al. 2021; Fadrique et al. 2018). However, in warm-adapted podocarp forests, seven widespread species (collectively accounting for 15% of basal cover) showed range contractions (Fig. B8 A), indicating that thermophilisation is partly driven by species loss rather than solely by expansion. These declining species are predominantly montane, cold-adapted species (Fig. B8 C), consistent with projected losses at the warm margins of montane species despite initially rising richness (Rumpf et al. 2019; Engler et al. 2011). Together, these findings suggest that thermophilisation in podocarp forests proceeds through the replacement of cold-adapted species by warm-adapted taxa, whereas other forest types primarily experience species additions without comparable losses.

Over time, species and functional richness (FRic) increased while trait differences (MNND) decreased (Fig. 5.2, top row), indicating that the functional space is becoming more densely packed with functionally similar species. This pattern is consistent with niche packing driven by biotic interactions within abiotic bounds found elsewhere (Swenson and Weiser 2014). Concurrently, rising functional dispersion (FDis) reflects more widely

scattered traits, reflecting alternative strategies under environmental stress during climate-driven reassembly (Spasojevic and Suding 2012; Griffin-Nolan et al. 2019). However, these metrics were below expectations given the increasing species richness (Fig. 5.2, centre row), suggesting that abiotic filtering constrained the expansion of trait space and subsequently compressed it. Taxonomic and functional evenness decreased in beech and podocarp forests, respectively, suggesting an accumulation of rare species at low abundances. In both cases, the observed changes are strongly driven by acquisitive species (Fig. 5.3), consistent with previous large-scale observations (Henn et al. 2024; Goury et al. 2025). This pattern may be facilitated by climate change–induced increases in disturbance frequency (Keegan et al. 2022), which initiate successional trajectories, inviting early-successional, acquisitive species and result in declining evenness (van der Sande et al. 2024). In beech forests, the declining functional divergence (i.e., clustering of trait values at the centre) suggests that disturbance severity and warming, in addition to permitting migrants and expanding trait space, increase abiotic filtering of the dominant species located at the centre of trait space. Indeed, endemic beech forest species contribute disproportionately to the FDiv trend compared to species from other forests (Fig. 5.3).

Podocarp forest communities shifted toward species associated with lower precipitation niches (Fig. 5.1) but lower $\Delta^{13}C$ CWM (Fig. 5.4), indicating a functional transition towards species with lower water-use efficiency (Farquhar et al. 1989), despite decreases in precipitation (***Fig. B5***). Importantly, this shift was caused by species expansion rather than contraction, as contracting species had higher-than-average $\Delta^{13}C$ values (***Fig. B8***). Our findings tentatively indicate that these changes were driven by a small group of

non-endemic shrubs (***Fig. B10***) and suggest an increase in isohydric, drought-avoidant, rather than drought-tolerant (i.e. high water-use-efficiency) species. However, this contrasts previous findings of increasing $\Delta^{13}C$ as precipitation decreases (Stewart et al. 1995; Song et al. 2008). One possible explanation is rising atmospheric CO_2, which acts as a buffer against drought stress and relaxes selection against low-efficiency strategies (Keenan et al. 2013) despite ultimately leaving isohydric species more sensitive to drought (Domec et al. 2017). This drought signal is further reflected in structural change, with declines in taller, denser-wooded trees, as evidenced by a negative trend in the community-weighted skew of SSD and weak declines in mean height and SSD (***Fig. B7***). Due to wider water-conducting conduits (Olson et al. 2018), taller trees have an increased risk of embolism, which makes them more susceptible to drought (Bruelheide et al. 2018; Greenwood et al. 2017). Together, these findings suggest that in podocarp forests, moisture limitation, possibly interacting with higher CO_2 levels, drives changes in community structure.

Cold-adapted forests, dominated by beech species, exhibited the slowest turnover rates (***Fig. B8*** B). This ecological inertia is well-documented (De Frenne et al. 2013; Cotto et al. 2017; Dullinger et al. 2012; Goury et al. 2025) and experimentally confirmed (Cox et al. 2024). However, beech forests also showed the largest number of species with significantly increasing plot occupancy (38 species in ***Fig. B8*** A), indicating an influx of migrants at low abundance, decreasing taxonomic evenness (Fig. 5.2). This resulted in conflicting functional changes. On the one hand, trait CWMs revealed an increase in conservative species with lower leaf nitrogen content, on the other hand, more acquisitive, shorter plants with lower-density wood. This could be explained by tree ferns, which disproportionately lowered the SSD trend (***Fig. B10***). Tree ferns require ample moisture,

and dominate canopy gaps for up to 30 years after disturbances (Brock et al. 2016), have conservative traits, but low SSD and lower height than dominant beeches. However, we also found a CWM trend towards larger seeds, which can increase seedling survival during drought (Moles and Westoby 2004) and an increased variance in Δ13C (i.e., a wider range of employed water-use strategies) (Fig. 5.4), indicating abiotic filtering along a moisture gradient, which, in contrast to podocarp forests, predominantly affects establishment, not survival.

Additionally, we observed a declining variance in $\Delta^{15}N$ and a weak trend toward lower CWM, indicating increasing convergence in nitrogen acquisition strategies. Foliar $\Delta^{15}N$ is reduced by ecto- and ericoid mycorrhizal (EcM and ErM) fungal associations (Hobbie and Hobbie 2008), and the group of EcM species indeed had the strongest impact on the $\Delta^{15}N$ CWV trend (***Fig. B11***). Along with two EcM-AM, early successional species (*Leptospermum scoparium* and *Kunzea ericoides)*, the dominant beech species are the only widespread, native EcM species in New Zealand. One potential explanation for the expansion of EcM species might be elevated CO_2, which shifts the C:N stoichiometry, heightening nitrogen limitation and favouring species that make greater use of EcM symbioses (Cambron et al. 2025). Under elevated CO_2, ectomycorrhizal fungi buffer associated species against nutrient stress (Usman et al. 2021) and can increase biomass (Bennett and Classen 2020; Terrer et al. 2016). Moreover, elevated CO_2 is expected to lead to declining SLA and leaf nitrogen content (Wang et al. 2020; Poorter et al. 2022), for which we also found evidence in beech forests (Fig. 5.4). While more data is needed, these results point towards a growing importance of mycorrhizal associations, potentially mediated through elevated CO_2 levels, and highlight how higher-order trait moments, can reveal these emerging functional shifts.

The mixed forest ecotone exhibited the highest turnover rate (***Fig. B8*** B) and functional diversity changes (Fig. 5.2), likely due to its position between cold- and warm-adapted communities and increased warming ***Fig. B5***. The drivers of functional changes largely matched podocarp forests, with a slightly greater importance of acquisitive species (Fig. 5.3) and no major functional changes (Fig. 5.4). One notable difference was the disproportionate role of tree ferns for the declining MNND trend (***Fig. B9***), likely due to their pioneer role leading to abundance increases in disturbed areas (Brock et al. 2016). New Zealand's broadleaved forests follow two main successional pathways, one dominated by the tree/shrub *Kunzea ericoides* and the other by the tree fern *Cyathea medullaris* *(Brock et al. 2018)*. The latter dominates on steeper slopes, at lower temperatures, and under lower water deficit, resulting in a consistent broad-leaved podocarp forest, whereas the *K. ericoides* pathway leads to variable trajectories characteristic of fire-prone systems. This indicates that, at present, mixed forests are transitioning into podocarp forests, which, however, may change in the future, as the direction of climate change is inconsistent with the abiotic requirements of the *C. medullaris* successional pathway. This dynamic might not be unique to New Zealand, as tree ferns of the *Dicksonia* and *Cyathea* genera are found throughout the Southern Hemisphere in similar early-successional roles (Arens and Baracaldo 1998).

Although this study benefited from a uniquely large and long-term forest dataset, several limitations warrant consideratio and highlight directions for future research. First, the inclusion of tree ferns with distinct functional strategies (e.g., very light diaspores) is unusual but necessary for New Zealand, given their central role as early-successional

species (Brock et al. 2018; Gaxiola et al. 2008). Moreover, excluding them did not produce significantly different results (***Fig. B12***), beyond what would be expected from early successional species. Second, all traits and, in particular rare and cost-limited, isotopic ratios $\Delta^{15}N$ and $\Delta^{13}C$ are subject to intraspecific variation, which we did not explicitly account for, as our study spans a broad spatial range (subtropical to montane forests, over ca. 1600km) at which interspecific variation is expected to exceed intraspecific variation (Albert et al. 2011; Lajoie and Vellend 2015). An avenue for future research is to expand trait measurements, which would allow the use of trait distributions rather than trait values and could reveal the extent to which intraspecific variation buffers climatic changes (Laughlin et al. 2012; Abrego et al. 2025). Finally, the proposed link between elevated CO_2 and shifts toward ectomycorrhizal associations and drought-avoidant strategies remains inferential, as it is supported by theory but could not be directly tested in this study (Terrer et al. 2016; Keenan et al. 2013). The dataset presented here, however, provides a basis to test these mechanisms through targeted experimental approaches. Despite these limitations, we consider the central insight of context-dependent biodiversity rearrangement and its inferred mechanisms to remain well supported.

5.6. Conclusion

Climate change is restructuring forest communities at different rates through divergent ecological pathways and abiotic constraints, despite consistent increases in species richness and thermophilisation. Warm-adapted podocarp forests exhibit pronounced declines of montane species and functional shifts toward drought-avoidant strategies, indicating moisture limitation as a dominant driver. In contrast, cold-adapted forests

change more slowly and show signs of nitrogen limitation, evidenced by isotope data and the proliferation of ectomycorrhizal (EcM) and ericoid associations (Hobbie and Hobbie 2008; Bennett and Classen 2020). Both trajectories are possibly linked to elevated CO_2, which can buffer isohydric species against drought stress (Keenan et al. 2013) and increase biomass by alleviating nitrogen limitation in EcM species (Bennett and Classen 2020; Terrer et al. 2016). Despite these differences across all forest types, acquisitive and exotic species contributed disproportionately to functional changes, matching recent findings (Goury et al. 2025) and indicating a global pattern of proliferation of novel strategies rather than redistribution of the native pool. Disturbance further reinforces these dynamics by promoting early-successional species that may define long-term successional trajectories (Brock et al. 2018). Methodologically, we demonstrate how imputation can increase the number of studied traits and species (Penone et al. 2014), and combined with higher-order moments, provide early signs of context-dependent responses needed to anticipate long-term ecosystem trajectories (Thuiller et al. 2013). Together, these findings reveal that apparently uniform biodiversity trends mask fundamentally different assembly processes along environmental gradients, with direct implications for predicting and managing forest responses to climate change.

5.7. References

Abrego, N., Niittynen, P., Kemppinen, J., & Ovaskainen, O. (2025). Joint species-trait distribution modeling: The role of intraspecific trait variation in community assembly. *Ecology*, *106*(9), e70174. https://doi.org/10.1002/ecy.70174

Albert, C. H., Grassein, F., Schurr, F. M., Vieilledent, G., & Violle, C. (2011). When and how

should intraspecific variability be considered in trait-based plant ecology? *Perspectives in Plant Ecology, Evolution and Systematics*, *13*(3), 217–225. https://doi.org/10.1016/j.ppees.2011.04.003

Arens, N. C., & Baracaldo, P. S. (1998). Distribution of tree ferns (Cyatheaceae) across the successional mosaic in an Andean cloud forest, narino, Colombia. *American Fern Journal*, *88*(2), 60. https://doi.org/10.2307/1547225

Bennett, A. E., & Classen, A. T. (2020). Climate change influences mycorrhizal fungal-plant interactions, but conclusions are limited by geographical study bias. *Ecology*, *101*(4), e02978. https://doi.org/10.1002/ecy.2978

Breshears, D. D., Huxman, T. E., Adams, H. D., Zou, C. B., & Davison, J. E. (2008). Vegetation synchronously leans upslope as climate warms. *Proceedings of the National Academy of Sciences of the United States of America*, *105*(33), 11591–11592. https://doi.org/10.1073/pnas.0806579105

Brock, J. M. R., Perry, G. L. W., Lee, W. G., & Burns, B. R. (2016). Tree fern ecology in New Zealand: A model for southern temperate rainforests. *Forest Ecology and Management*, *375*, 112–126. https://doi.org/10.1016/j.foreco.2016.05.030

Brock, J., Perry, G., Lee, W. G., Schwendenmann, L., & Burns, B. (2018). Pioneer tree ferns influence community assembly in northern New Zealand forests. *New Zealand Journal of Ecology*, *42*(1), 18–30. https://doi.org/10.20417/NZJECOL.42.5

Bruelheide, H., Dengler, J., Purschke, O., Lenoir, J., Jiménez-Alfaro, B., Hennekens, S. M., Botta-Dukát, Z., Chytrý, M., Field, R., Jansen, F., Kattge, J., Pillar, V. D., Schrodt, F., Mahecha, M. D., Peet, R. K., Sandel, B., van Bodegom, P., Altman, J., Alvarez-Dávila, E., … Jandt, U. (2018). Global trait-environment relationships of plant communities. *Nature Ecology & Evolution*, *2*(12), 1906–1917. https://doi.org/10.1038/s41559-018-0699-8

Cambron, T. W., Fisher, J. B., Hungate, B. A., Stocker, B. D., Keenan, T., Prentice, I. C., & Terrer, C. (2025). Plant nutrient acquisition under elevated CO2 and implications for the land carbon sink. *Nature Climate Change*, 1–12. https://doi.org/10.1038/s41558-025-02386-y

Carnicer, J., Domingo-Marimon, C., Ninyerola, M., Camarero, J. J., Bastos, A., López-Parages, J., Blanquer, L., Rodríguez-Fonseca, B., Lenton, T. M., Dakos, V., Ribas, M., Gutiérrez, E., Peñuelas, J., & Pons, X. (2019). Regime shifts of Mediterranean forest carbon uptake and reduced resilience driven by multidecadal ocean surface temperatures. *Global Change Biology*, *25*(8), 2825–2840. https://doi.org/10.1111/gcb.14664

Cornwell, W. K., & Ackerly, D. D. (2009). Community assembly and shifts in plant trait distributions across an environmental gradient in coastal California. *Ecological Monographs*, *79*(1), 109–126. https://doi.org/10.1890/07-1134.1

Cotto, O., Wessely, J., Georges, D., Klonner, G., Schmid, M., Dullinger, S., Thuiller, W., & Guillaume, F. (2017). A dynamic eco-evolutionary model predicts slow response of alpine plants to climate warming. *Nature Communications*, *8*(1), 15399. https://doi.org/10.1038/ncomms15399

Cox, A. J. F., González-Caro, S., Meir, P., Hartley, I. P., Restrepo, Z., Villegas, J. C., Sanchez, A., & Mercado, L. M. (2024). Variable thermal plasticity of leaf functional traits in Andean tropical montane forests. *Plant, Cell & Environment*, *47*(3), 731–750. https://doi.org/10.1111/pce.14778

Dawson, T. E., Mambelli, S., Plamboeck, A. H., Templer, P. H., & Tu, K. P. (2002). Stable isotopes in plant ecology. *Annual Review of Ecology and Systematics*, *33*(1), 507–559. https://doi.org/10.1146/annurev.ecolsys.33.020602.095451

Debastiani, V. J., Bastazini, V. A. G., & Pillar, V. D. (2021). Using phylogenetic information to

impute missing functional trait values in ecological databases. *Ecological Informatics*, *63*(101315), 101315. https://doi.org/10.1016/j.ecoinf.2021.101315

De Frenne, P., Rodríguez-Sánchez, F., Coomes, D. A., Baeten, L., Verstraeten, G., Vellend, M., Bernhardt-Römermann, M., Brown, C. D., Brunet, J., Cornelis, J., Decocq, G. M., Dierschke, H., Eriksson, O., Gilliam, F. S., Hédl, R., Heinken, T., Hermy, M., Hommel, P., Jenkins, M. A., … Verheyen, K. (2013). Microclimate moderates plant responses to macroclimate warming. *Proceedings of the National Academy of Sciences of the United States of America*, *110*(46), 18561–18565. https://doi.org/10.1073/pnas.1311190110

Devictor, V., Julliard, R., Couvet, D., & Jiguet, F. (2008). Birds are tracking climate warming, but not fast enough. *Proceedings. Biological Sciences*, *275*(1652), 2743–2748. https://doi.org/10.1098/rspb.2008.0878

Díaz, S., Kattge, J., Cornelissen, J. H. C., Wright, I. J., Lavorel, S., Dray, S., Reu, B., Kleyer, M., Wirth, C., Prentice, I. C., Garnier, E., Bönisch, G., Westoby, M., Poorter, H., Reich, P. B., Moles, A. T., Dickie, J., Gillison, A. N., Zanne, A. E., … Gorné, L. D. (2016). The global spectrum of plant form and function. *Nature*, *529*(7585), 167–171. https://doi.org/10.1038/nature16489

Díaz, S., Kattge, J., Cornelissen, J. H. C., Wright, I. J., Lavorel, S., Dray, S., Reu, B., Kleyer, M., Wirth, C., Prentice, I. C., Garnier, E., Bönisch, G., Westoby, M., Poorter, H., Reich, P. B., Moles, A. T., Dickie, J., Zanne, A. E., Chave, J., … Zotz, G. (2022). The global spectrum of plant form and function: enhanced species-level trait dataset. *Scientific Data*, *9*(1), 755. https://doi.org/10.1038/s41597-022-01774-9

Domec, J.-C., Smith, D. D., & McCulloh, K. A. (2017). A synthesis of the effects of atmospheric carbon dioxide enrichment on plant hydraulics: implications for whole-plant water use efficiency and resistance to drought. *Plant, Cell &*

Environment, *40*(6), 921–937. https://doi.org/10.1111/pce.12843

Dornelas, M., Chase, J. M., Gotelli, N. J., Magurran, A. E., McGill, B. J., Antão, L. H., Blowes, S. A., Daskalova, G. N., Leung, B., Martins, I. S., Moyes, F., Myers-Smith, I. H., Thomas, C. D., & Vellend, M. (2023). Looking back on biodiversity change: lessons for the road ahead. *Philosophical Transactions of the Royal Society of London. Series B, Biological Sciences*, *378*(1881), 20220199. https://doi.org/10.1098/rstb.2022.0199

Dornelas, M., Gotelli, N. J., McGill, B., Shimadzu, H., Moyes, F., Sievers, C., & Magurran, A. E. (2014). Assemblage time series reveal biodiversity change but not systematic loss. *Science*, *344*(6181), 296–299. https://doi.org/10.1126/science.1248484

Dullinger, S., Gattringer, A., Thuiller, W., Moser, D., Zimmermann, N. E., Guisan, A., Willner, W., Plutzar, C., Leitner, M., Mang, T., Caccianiga, M., Dirnböck, T., Ertl, S., Fischer, A., Lenoir, J., Svenning, J.-C., Psomas, A., Schmatz, D. R., Silc, U., … Hülber, K. (2012). Extinction debt of high-mountain plants under twenty-first-century climate change. *Nature Climate Change*, *2*(8), 619–622. https://doi.org/10.1038/nclimate1514

EcoTraits Landcare Research. (2005). https://ecotraits.landcareresearch.co.nz/WeedsIntro.aspx

Engler, R., Randin, C. F., Thuiller, W., Dullinger, S., Zimmermann, N. E., Araújo, M. B., Pearman, P. B., Le Lay, G., Piedallu, C., Albert, C. H., Choler, P., Coldea, G., De LAMO, X., Dirnböck, T., Gégout, J.-C., Gómez-García, D., Grytnes, J.-A., Heegaard, E., Høistad, F., … Guisan, A. (2011). 21st century climate change threatens mountain flora unequally across Europe: CLIMATE CHANGE IMPACTS ON MOUNTAIN FLORAE. *Global Change Biology*, *17*(7), 2330–2341. https://doi.org/10.1111/j.1365-2486.2010.02393.x

Enquist, B. J., Norberg, J., Bonser, S. P., Violle, C., Webb, C. T., Henderson, A., Sloat, L. L., & Savage, V. M. (2015). Chapter Nine - Scaling from Traits to Ecosystems: Developing a General Trait Driver Theory via Integrating Trait-Based and Metabolic Scaling

Theories. In S. Pawar, G. Woodward, & A. I. Dell (Eds.), *Advances in Ecological Research* (Vol. 52, pp. 249–318). Academic Press. https://doi.org/10.1016/bs.aecr.2015.02.001

Etherington, T. R., Perry, G. L. W., & Wilmshurst, J. M. (2022). HOTRUNZ: an open-access 1 km resolution monthly 1910–2019 time series of interpolated temperature and rainfall grids with associated uncertainty for New Zealand. *Earth System Science Data*, *14*(6), 2817–2832. https://doi.org/10.5194/essd-14-2817-2022

Fadrique, B., Báez, S., Duque, Á., Malizia, A., Blundo, C., Carilla, J., Osinaga-Acosta, O., Malizia, L., Silman, M., Farfán-Ríos, W., Malhi, Y., Young, K. R., Cuesta C, F., Homeier, J., Peralvo, M., Pinto, E., Jadan, O., Aguirre, N., Aguirre, Z., & Feeley, K. J. (2018). Widespread but heterogeneous responses of Andean forests to climate change. *Nature*, *564*(7735), 207–212. https://doi.org/10.1038/s41586-018-0715-9

Farquhar, G. D., Ehleringer, J. R., & Hubick, K. T. (1989). Carbon isotope discrimination and photosynthesis. *Annual Review of Plant Physiology and Plant Molecular Biology*, *40*(1), 503–537. https://www.academia.edu/download/42237597/Carbon_isotope_discrimination_and_photos20160206-11499-1s8u0ia.pdf

Fischer, H. S. (2015). On the combination of species cover values from different vegetation layers. *Applied Vegetation Science*, *18*(1), 169–170. https://doi.org/10.1111/avsc.12130

Flores, S., Forister, M. L., Sulbaran, H., Díaz, R., & Dyer, L. A. (2023). Extreme drought disrupts plant phenology: Insights from 35 years of cloud forest data in Venezuela. *Ecology*, *104*(5), e4012. https://doi.org/10.1002/ecy.4012

Freeman, B. G., Song, Y., Feeley, K. J., & Zhu, K. (2021). Montane species track rising temperatures better in the tropics than in the temperate zone. *Ecology Letters*.

https://doi.org/10.1111/ELE.13762

Funk, J. L., Larson, J. E., Ames, G. M., Butterfield, B. J., Cavender-Bares, J., Firn, J., Laughlin, D. C., Sutton-Grier, A. E., Williams, L., & Wright, J. (2017). Revisiting the Holy Grail: using plant functional traits to understand ecological processes. *Biological Reviews of the Cambridge Philosophical Society*, *92*(2), 1156–1173. https://doi.org/10.1111/brv.12275

García Criado, M., Myers-Smith, I. H., Bjorkman, A. D., Elmendorf, S. C., Normand, S., Aastrup, P., Aerts, R., Alatalo, J. M., Baeten, L., Björk, R. G., Björkman, M. P., Boulanger-Lapointe, N., Butler, E. E., Cooper, E. J., Cornelissen, J. H. C., Daskalova, G. N., Fadrique, B., Forbes, B. C., Henry, G. H. R., … Vellend, M. (2025). Plant diversity dynamics over space and time in a warming Arctic. *Nature*, 1–9. https://doi.org/10.1038/s41586-025-08946-8

Gaxiola, A., Burrows, L. E., & Coomes, D. A. (2008). Tree fern trunks facilitate seedling regeneration in a productive lowland temperate rain forest. *Oecologia*, *155*(2), 325–335. https://doi.org/10.1007/s00442-007-0915-8

Gottfried, M., Pauli, H., Futschik, A., Akhalkatsi, M., Barančok, P., Benito Alonso, J. L., Coldea, G., Dick, J., Erschbamer, B., Fernández Calzado, M. R., Kazakis, G., Krajči, J., Larsson, P., Mallaun, M., Michelsen, O., Moiseev, D., Moiseev, P., Molau, U., Merzouki, A., … Grabherr, G. (2012). Continent-wide response of mountain vegetation to climate change. *Nature Climate Change*, *2*(2), 111–115. https://doi.org/10.1038/nclimate1329

Goury, R., Thuiller, W., Abdulhak, S., Pache, G., Van Es, J., Bowler, D. E., Renaud, J., Violle, C., & Münkemüller, T. (2025). Recent vegetation shifts in the French Alps with winners outnumbering losers. *The Journal of Ecology*, *113*(11), 3275–3292. https://doi.org/10.1111/1365-2745.70159

Green, S. J., Brookson, C. B., Hardy, N. A., & Crowder, L. B. (2022). Trait-based approaches to global change ecology: moving from description to prediction. *Proceedings. Biological Sciences / The Royal Society*, *289*(1971), 20220071. https://doi.org/10.1098/rspb.2022.0071

Greenwood, S., Ruiz-Benito, P., Martínez-Vilalta, J., Lloret, F., Kitzberger, T., Allen, C. D., Fensham, R., Laughlin, D. C., Kattge, J., Bönisch, G., Kraft, N. J. B., & Jump, A. S. (2017). Tree mortality across biomes is promoted by drought intensity, lower wood density and higher specific leaf area. *Ecology Letters*, *20*(4), 539–553. https://doi.org/10.1111/ele.12748

Griffin-Nolan, R. J., Blumenthal, D. M., Collins, S. L., Farkas, T. E., Hoffman, A. M., Mueller, K. E., Ocheltree, T. W., Smith, M. D., Whitney, K. D., & Knapp, A. K. (2019). Shifts in plant functional composition following long- term drought in grasslands. *The Journal of Ecology*, *107*(5), 2133–2148. https://doi.org/10.1111/1365-2745.13252

Grime, J. P. (1977). Evidence for the Existence of Three Primary Strategies in Plants and Its Relevance to Ecological and Evolutionary Theory. *The American Naturalist*. https://doi.org/10.1086/283244

Gross, N., Le Bagousse-Pinguet, Y., Liancourt, P., Berdugo, M., Gotelli, N. J., & Maestre, F. T. (2017). Functional trait diversity maximizes ecosystem multifunctionality. *Nature Ecology & Evolution*, *1*(5), 0132–0132. https://doi.org/10.1038/s41559-017-0132

Hagan, J. G., Henn, J. J., & Osterman, W. H. A. (2023). Plant traits alone are good predictors of ecosystem properties when used carefully. *Nature Ecology & Evolution*, *7*(3), 332–334. https://doi.org/10.1038/s41559-022-01920-x

Henn, J. J., Anderson, K. E., Brigham, L. M., Bueno de Mesquita, C. P., Collins, C. G., Elmendorf, S. C., Green, M. D., Huxley, J. D., Rafferty, N. E., Rose-Person, A., & Spasojevic, M. J. (2024). Long-term alpine plant responses to global change drivers

depend on functional traits. *Ecology Letters*, *27*(10), e14518. https://doi.org/10.1111/ele.14518

Hobbie, E. A., & Hobbie, J. E. (2008). Natural abundance of 15N in nitrogen-limited forests and tundra can estimate nitrogen cycling through mycorrhizal fungi: A review. *Ecosystems (New York, N.Y.)*, *11*(5), 815–830. https://doi.org/10.1007/s10021-008-9159-7

Homeier, J., Seeler, T., Pierick, K., & Leuschner, C. (2021). Leaf trait variation in species-rich tropical Andean forests. *Scientific Reports*, *11*(1), 9993. https://doi.org/10.1038/s41598-021-89190-8

Hurst, J. M. (2022). *The Recce method for describing New Zealand vegetation - field manual*. Manaaki Whenua Press. https://doi.org/10.7931/P48H-ZB65

Kattge, J., Bönisch, G., Díaz, S., Lavorel, S., Prentice, I. C., Leadley, P., Tautenhahn, S., Werner, G. D. A., Aakala, T., Abedi, M., Acosta, A. T. R., Adamidis, G. C., Adamson, K., Aiba, M., Albert, C. H., Alcántara, J. M., Alcázar C, C., Aleixo, I., Ali, H., … Wirth, C. (2020). TRY plant trait database - enhanced coverage and open access. *Global Change Biology*, *26*(1), 119–188. https://doi.org/10.1111/gcb.14904

Keegan, L., School of Biological Sciences, University of Auckland, Private Bag 92019, Auckland 1142, New Zealand, White, R., & Macinnis-Ng, C. (2022). Current knowledge and potential impacts of climate change on New Zealand's biological heritage. *New Zealand Journal of Ecology*. https://doi.org/10.20417/nzjecol.46.10

Keenan, T. F., Hollinger, D. Y., Bohrer, G., Dragoni, D., Munger, J. W., Schmid, H. P., & Richardson, A. D. (2013). Increase in forest water-use efficiency as atmospheric carbon dioxide concentrations rise. *Nature*, *499*(7458), 324–327. https://doi.org/10.1038/nature12291

Kerr, M. R., Ordonez, A., Riede, F., Atkinson, J., Pearce, E. A., Sykut, M., Trepel, J., &

Svenning, J.-C. (2025). Widespread ecological novelty across the terrestrial biosphere. *Nature Ecology & Evolution*, *9*(4), 589–598. https://doi.org/10.1038/s41559-025-02662-2

Komatsu, K. J., Avolio, M. L., Lemoine, N. P., Isbell, F., Grman, E., Houseman, G. R., Koerner, S. E., Johnson, D. S., Wilcox, K. R., Alatalo, J. M., Anderson, J. P., Aerts, R., Baer, S. G., Baldwin, A. H., Bates, J., Beierkuhnlein, C., Belote, R. T., Blair, J., Bloor, J. M. G., … Zhang, Y. (2019). Global change effects on plant communities are magnified by time and the number of global change factors imposed. *Proceedings of the National Academy of Sciences of the United States of America*, *116*(36), 17867–17873. https://doi.org/10.1073/pnas.1819027116

Lajoie, G., & Vellend, M. (2015). Understanding context dependence in the contribution of intraspecific variation to community trait-environment matching. *Ecology*, *96*(11), 2912–2922. https://doi.org/10.1890/15-0156.1

Laliberté, E., & Legendre, P. (2010). A distance-based framework for measuring functional diversity from multiple traits. *Ecology*, *91*(1), 299–305. https://doi.org/10.1890/08-2244.1

Lamanna, C., Blonder, B., Violle, C., Kraft, N. J. B., Sandel, B., Šímová, I., Donoghue, J. C., 2nd, Svenning, J.-C., McGill, B. J., Boyle, B., Buzzard, V., Dolins, S., Jørgensen, P. M., Marcuse-Kubitza, A., Morueta-Holme, N., Peet, R. K., Piel, W. H., Regetz, J., Schildhauer, M., … Enquist, B. J. (2014). Functional trait space and the latitudinal diversity gradient. *Proceedings of the National Academy of Sciences of the United States of America*, *111*(38), 13745–13750. https://doi.org/10.1073/pnas.1317722111

Landcare Research. (2024). *Basic Ecosystems* [Dataset]. https://doi.org/10.7931/L1HM1

Laughlin, D. C. (2023). *Plant Strategies: The Demographic Consequences of Functional*

Traits in Changing Environments. Oxford University Press. https://play.google.com/store/books/details?id=0aakzwEACAAJ

Laughlin, D. C., Joshi, C., van Bodegom, P. M., Bastow, Z. A., & Fulé, P. Z. (2012). A predictive model of community assembly that incorporates intraspecific trait variation. *Ecology Letters*, *15*(11), 1291–1299. https://doi.org/10.1111/j.1461-0248.2012.01852.x

Lawlor, J. A., Comte, L., Grenouillet, G., Lenoir, J., Baecher, J. A., Bandara, R. M. W. J., Bertrand, R., Chen, I.-C., Diamond, S. E., Lancaster, L. T., Moore, N., Murienne, J., Oliveira, B. F., Pecl, G. T., Pinsky, M. L., Rolland, J., Rubenstein, M., Scheffers, B. R., Thompson, L. M., … Sunday, J. (2024). Mechanisms, detection and impacts of species redistributions under climate change. *Nature Reviews. Earth & Environment*, *5*(5), 351–368. https://doi.org/10.1038/s43017-024-00527-z

Le Bagousse-Pinguet, Y., Gross, N., Maestre, F. T., Maire, V., de Bello, F., Fonseca, C. R., Kattge, J., Valencia, E., Leps, J., & Liancourt, P. (2017). Testing the environmental filtering concept in global drylands. *The Journal of Ecology*, *105*(4), 1058–1069. https://doi.org/10.1111/1365-2745.12735

Lebrija-Trejos, E., Pérez-García, E. A., Meave, J. A., Bongers, F., & Poorter, L. (2010). Functional traits and environmental filtering drive community assembly in a species-rich tropical system. *Ecology*, *91*(2), 386–398. https://doi.org/10.1890/08-1449.1

Lenoir, J., & Svenning, J.-C. (2015). Climate- related range shifts – a global multidimensional synthesis and new research directions. *Ecography*, *38*(1), 15–28. https://doi.org/10.1111/ecog.00967

Li, L., McCormack, M. L., Ma, C., Kong, D., Zhang, Q., Chen, X., Zeng, H., Niinemets, Ü., & Guo, D. (2015). Leaf economics and hydraulic traits are decoupled in five species-rich tropical-subtropical forests. *Ecology Letters*, *18*(9), 899–906.

https://doi.org/10.1111/ele.12466

Locosselli, G. M., Brienen, R. J. W., Leite, M. de S., Gloor, M., Krottenthaler, S., Oliveira, A. A. de, Barichivich, J., Anhuf, D., Ceccantini, G., Schöngart, J., & Buckeridge, M. (2020). Global tree-ring analysis reveals rapid decrease in tropical tree longevity with temperature. *Proceedings of the National Academy of Sciences of the United States of America*, *117*(52), 33358–33364. https://doi.org/10.1073/pnas.2003873117

Luo, T., Zhang, L., Zhu, H., Daly, C., Li, M., & Luo, J. (2009). Correlations between net primary productivity and foliar carbon isotope ratio across a Tibetan ecosystem transect. *Ecography*, *32*(3), 526–538. https://doi.org/10.1111/j.1600-0587.2008.05735.x

Mao, F., Du, H., Zhou, G., Zheng, J., Li, X., Xu, Y., Huang, Z., & Yin, S. (2022). Simulated net ecosystem productivity of subtropical forests and its response to climate change in Zhejiang Province, China. *The Science of the Total Environment*, *838*(Pt 1), 155993. https://doi.org/10.1016/j.scitotenv.2022.155993

McCarthy, J., Leathwick, J., Roudier, P., Barringer, J., Etherington, T., Morgan, F., Odgers, N., Price, R., Wiser, S., & Richardson, S. (2021). New Zealand Environmental Data Stack (NZEnvDS): A standardised collection of spatial layers for environmental modelling and site characterisation. *New Zealand Journal of Ecology*, *45*, 3440.

McLauchlan, K. K., Ferguson, C. J., Wilson, I. E., Ocheltree, T. W., & Craine, J. M. (2010). Thirteen decades of foliar isotopes indicate declining nitrogen availability in central North American grasslands. *The New Phytologist*, *187*(4), 1135–1145. https://doi.org/10.1111/j.1469-8137.2010.03322.x

Moles, A. T., & Westoby, M. (2004). Seedling survival and seed size: a synthesis of the literature: Seedling survival and seed size. *The Journal of Ecology*, *92*(3), 372–383. https://doi.org/10.1111/j.0022-0477.2004.00884.x

Montràs-Janer, T., Suggitt, A. J., Fox, R., Jönsson, M., Martay, B., Roy, D. B., Walker, K. J., &

Auffret, A. G. (2024). Anthropogenic climate and land-use change drive short- and long-term biodiversity shifts across taxa. *Nature Ecology & Evolution*, *8*(4), 739–751. https://doi.org/10.1038/s41559-024-02326-7

Nakagawa, S., & Schielzeth, H. (2013). A general and simple method for obtainingR2from generalized linear mixed-effects models. *Methods in Ecology and Evolution*, *4*(2), 133–142. https://doi.org/10.1111/j.2041-210x.2012.00261.x

O'Donnel, M. S., & Ignizio, D. A. (2012). *Bioclimatic predictors for supporting ecological applications in the conterminous United States* (No. 691). U.S. Geological Survey. https://pubs.usgs.gov/publication/ds691

Oliver, T. H., Heard, M. S., Isaac, N. J. B., Roy, D. B., Procter, D., Eigenbrod, F., Freckleton, R., Hector, A., Orme, C. D. L., Petchey, O. L., Proença, V., Raffaelli, D., Suttle, K. B., Mace, G. M., Martín-López, B., Woodcock, B. A., & Bullock, J. M. (2015). Biodiversity and resilience of ecosystem functions. *Trends in Ecology & Evolution*, *30*(11), 673–684. https://doi.org/10.1016/j.tree.2015.08.009

Olson, M. E., Soriano, D., Rosell, J. A., Anfodillo, T., Donoghue, M. J., Edwards, E. J., León-Gómez, C., Dawson, T., Camarero Martínez, J. J., Castorena, M., Echeverría, A., Espinosa, C. I., Fajardo, A., Gazol, A., Isnard, S., Lima, R. S., Marcati, C. R., & Méndez-Alonzo, R. (2018). Plant height and hydraulic vulnerability to drought and cold. *Proceedings of the National Academy of Sciences of the United States of America*, *115*(29), 7551–7556. https://doi.org/10.1073/pnas.1721728115

Penone, C., Davidson, A. D., Shoemaker, K. T., Di Marco, M., Rondinini, C., Brooks, T. M., Young, B. E., Graham, C. H., & Costa, G. C. (2014). Imputation of missing data in life- history trait datasets: which approach performs the best? *Methods in Ecology and Evolution*, *5*(9), 961–970. https://doi.org/10.1111/2041-210x.12232

Pereira, H. M., Martins, I. S., Rosa, I. M. D., Kim, H., Leadley, P., Popp, A., van Vuuren, D. P.,

Hurtt, G., Quoss, L., Arneth, A., Baisero, D., Bakkenes, M., Chaplin-Kramer, R., Chini, L., Di Marco, M., Ferrier, S., Fujimori, S., Guerra, C. A., Harfoot, M., … Alkemade, R. (2024). Global trends and scenarios for terrestrial biodiversity and ecosystem services from 1900 to 2050. *Science*, *384*(6694), 458–465. https://doi.org/10.1126/science.adn3441

Pérez-Harguindeguy, N., Díaz, S., Garnier, E., Lavorel, S., Poorter, H., Jaureguiberry, P., Bret-Harte, M. S., Cornwell, W. K., Craine, J. M., Gurvich, D. E., Urcelay, C., Veneklaas, E. J., Reich, P. B., Poorter, L., Wright, I. J., Ray, P., Enrico, L., Pausas, J. G., de Vos, A. C., … Cornelissen, J. H. C. (2013). New handbook for standardised measurement of plant functional traits worldwide. *Australian Journal of Botany*, *61*(3), 167. https://doi.org/10.1071/bt12225

Pla, L., Casanoves, F., & Di Rienzo, J. (2012). Functional Diversity Indices. In *SpringerBriefs in Environmental Science* (pp. 27–51). Springer Netherlands. https://doi.org/10.1007/978-94-007-2648-2_3

Poorter, H., Knopf, O., Wright, I. J., Temme, A. A., Hogewoning, S. W., Graf, A., Cernusak, L. A., & Pons, T. L. (2022). A meta-analysis of responses of C3 plants to atmospheric CO2 : dose-response curves for 85 traits ranging from the molecular to the whole-plant level. *The New Phytologist*, *233*(4), 1560–1596. https://doi.org/10.1111/nph.17802

Pureswaran, D. S., Roques, A., & Battisti, A. (2018). Forest insects and climate change. *Current Forestry Reports*, *4*(2), 35–50. https://doi.org/10.1007/s40725-018-0075-6

Radeloff, V. C., Williams, J. W., Bateman, B. L., Burke, K. D., Carter, S. K., Childress, E. S., Cromwell, K. J., Gratton, C., Hasley, A. O., Kraemer, B. M., Latzka, A. W., Marin-Spiotta, E., Meine, C. D., Munoz, S. E., Neeson, T. M., Pidgeon, A. M., Rissman, A. R., Rivera, R. J., Szymanski, L. M., & Usinowicz, J. (2015). The rise of novelty in ecosystems. *Ecological Applications: A Publication of the Ecological Society of America*, *25*(8), 2051–2068.

https://doi.org/10.1890/14-1781.1

Rubenstein, M. A., Weiskopf, S. R., Bertrand, R., Carter, S. L., Comte, L., Eaton, M. J., Johnson, C. G., Lenoir, J., Lynch, A. J., Miller, B. W., Morelli, T. L., Rodriguez, M. A., Terando, A., & Thompson, L. M. (2023). Climate change and the global redistribution of biodiversity: substantial variation in empirical support for expected range shifts. *Environmental Evidence*, *12*(1), 1–21. https://doi.org/10.1186/s13750-023-00296-0

Rumpf, S. B., Hülber, K., Wessely, J., Willner, W., Moser, D., Gattringer, A., Klonner, G., Zimmermann, N. E., & Dullinger, S. (2019). Extinction debts and colonization credits of non-forest plants in the European Alps. *Nature Communications*, *10*(1), 4293. https://doi.org/10.1038/s41467-019-12343-x

Seabold, S., & Perktold, J. (2010). Statsmodels: Econometric and statistical modeling with python. *Proceedings of the Python in Science Conference*, 92–96. https://doi.org/10.25080/majora-92bf1922-011

Searle, E. B., & Chen, H. Y. H. (2020). Complementarity effects are strengthened by competition intensity and global environmental change in the central boreal forests of Canada. *Ecology Letters*, *23*(1), 79–87. https://doi.org/10.1111/ele.13411

Song, M., Duan, D., Chen, H., Hu, Q., Zhang, F., Xu, X., Tian, Y., Ouyang, H., & Peng, C. (2008). Leaf Δ^{13} C reflects ecosystem patterns and responses of alpine plants to the environments on the Tibetan Plateau. *Ecography*, *31*(4), 499–508. https://doi.org/10.1111/j.0906-7590.2008.05331.x

Song, W., & Zhou, Y. (2021). Linking leaf Δ15N and Δ13C with soil fungal biodiversity, ectomycorrhizal and plant pathogenic abundance in forest ecosystems of China. *Catena*, *200*(105176), 105176. https://doi.org/10.1016/j.catena.2021.105176

Soudzilovskaia, N. A., Vaessen, S., Barcelo, M., He, J., Rahimlou, S., Abarenkov, K., Brundrett, M. C., Gomes, S. I. F., Merckx, V., & Tedersoo, L. (2020). FungalRoot: global

online database of plant mycorrhizal associations. *The New Phytologist*, *227*(3), 955–966. https://doi.org/10.1111/nph.16569

Spasojevic, M. J., & Suding, K. N. (2012). Inferring community assembly mechanisms from functional diversity patterns: the importance of multiple assembly processes: Functional diversity along gradients. *The Journal of Ecology*, *100*(3), 652–661. https://doi.org/10.1111/j.1365-2745.2011.01945.x

Staples, T. L., Kiessling, W., & Pandolfi, J. M. (2022). Emergence patterns of locally novel plant communities driven by past climate change and modern anthropogenic impacts. *Ecology Letters*, *25*(6), 1497–1509. https://doi.org/10.1111/ele.14016

Steinbauer, M. J., Grytnes, J.-A., Jurasinski, G., Kulonen, A., Lenoir, J., Pauli, H., Rixen, C., Winkler, M., Bardy-Durchhalter, M., Barni, E., Bjorkman, A. D., Breiner, F. T., Burg, S., Czortek, P., Dawes, M. A., Delimat, A., Dullinger, S., Erschbamer, B., Felde, V. A., … Wipf, S. (2018). Accelerated increase in plant species richness on mountain summits is linked to warming. *Nature*, *556*(7700), 231–234. https://doi.org/10.1038/s41586-018-0005-6

Stephenson, N. L., & Mantgem, P. J. (2005). Forest turnover rates follow global and regional patterns of productivity: Patterns in forest turnover rates. *Ecology Letters*, *8*(5), 524–531. https://doi.org/10.1111/j.1461-0248.2005.00746.x

Stewart, G. R., Turnbull, M. H., Schmidt, S., & Erskine, P. D. (1995). 13C natural abundance in plant communities along a rainfall gradient: A biological integrator of water availability. *Australian Journal of Plant Physiology*, *22*(1), 51–55. https://doi.org/10.1071/pp9950051

Subedi, S. C., Ross, M. S., Sah, J. P., Redwine, J., & Baraloto, C. (2019). Trait- based community assembly pattern along a forest succession gradient in a seasonally dry tropical forest. *Ecosphere (Washington, D.C)*, *10*(4), e02719.

https://doi.org/10.1002/ecs2.2719

Swenson, N. G., & Weiser, M. D. (2014). On the packing and filling of functional space in eastern North American tree assemblages. *Ecography*, *37*(11), 1056–1062. https://doi.org/10.1111/ecog.00763

Terrer, C., Vicca, S., Hungate, B. A., Phillips, R. P., & Prentice, I. C. (2016). Mycorrhizal association as a primary control of the CO_2 fertilization effect. *Science (New York, N.Y.)*, *353*(6294), 72–74. https://doi.org/10.1126/science.aaf4610

Thuiller, W., Münkemüller, T., Lavergne, S., Mouillot, D., Mouquet, N., Schiffers, K., & Gravel, D. (2013). A road map for integrating eco-evolutionary processes into biodiversity models. *Ecology Letters*, *16 Suppl 1*(0 1), 94–105. https://doi.org/10.1111/ele.12104

Trumbore, S., Brando, P., & Hartmann, H. (2015). Forest health and global change. *Science (New York, N.Y.)*, *349*(6250), 814–818. https://doi.org/10.1126/science.aac6759

Usman, M., Ho-Plágaro, T., Frank, H. E. R., Calvo-Polanco, M., Gaillard, I., Garcia, K., & Zimmermann, S. D. (2021). Mycorrhizal symbiosis for better adaptation of trees to abiotic stress caused by climate change in temperate and boreal forests. *Frontiers in Forests and Global Change*, *4*, 742392. https://doi.org/10.3389/ffgc.2021.742392

Valdez, J. W., Callaghan, C. T., Junker, J., Purvis, A., Hill, S. L. L., & Pereira, H. M. (2023). The undetectability of global biodiversity trends using local species richness. *Ecography*, *2023*(3), e06604. https://doi.org/10.1111/ecog.06604

van der Sande, M. T., Poorter, L., Derroire, G., do Espirito Santo, M. M., Lohbeck, M., Müller, S. C., Bhaskar, R., van Breugel, M., Dupuy-Rada, J. M., Durán, S. M., Jakovac, C. C., Paz, H., Rozendaal, D. M. A., Brancalion, P., Craven, D., Mora Ardilla, F., Almeida, J. S., Balvanera, P., Becknell, J., … Bongers, F. (2024). Tropical forest succession increases tree taxonomic and functional richness but decreases evenness. *Global Ecology and Biogeography: A Journal of Macroecology*, *33*(8), e13856.

https://doi.org/10.1111/geb.13856

Vellend, M., Baeten, L., Myers-Smith, I. H., Elmendorf, S. C., Beauséjour, R., Brown, C. D., De Frenne, P., Verheyen, K., & Wipf, S. (2013). Global meta-analysis reveals no net change in local-scale plant biodiversity over time. *Proceedings of the National Academy of Sciences of the United States of America*, *110*(48), 19456–19459. https://doi.org/10.1073/pnas.1312779110

Villéger, S., Mason, N. W. H., & Mouillot, D. (2008). New multidimensional functional diversity indices for a multifaceted framework in functional ecology. *Ecology*, *89*(8), 2290–2301. https://doi.org/10.1890/07-1206.1

Violle, C., Reich, P. B., Pacala, S. W., Enquist, B. J., & Kattge, J. (2014). The emergence and promise of functional biogeography. *Proceedings of the National Academy of Sciences of the United States of America*, *111*(38), 13690–13696. https://doi.org/10.1073/pnas.1415442111

Wang, N., Gao, G., Wang, Y., Wang, D., Wang, Z., & Gu, J. (2020). Coordinated responses of leaf and absorptive root traits under elevated CO2 concentration in temperate woody and herbaceous species. *Environmental and Experimental Botany*, *179*(104199), 104199. https://doi.org/10.1016/j.envexpbot.2020.104199

Wieczynski, D. J., Boyle, B., Buzzard, V., Duran, S. M., Henderson, A. N., Hulshof, C. M., Kerkhoff, A. J., McCarthy, M. C., Michaletz, S. T., Swenson, N. G., Asner, G. P., Bentley, L. P., Enquist, B. J., & Savage, V. M. (2019). Climate shapes and shifts functional biodiversity in forests worldwide. *Proceedings of the National Academy of Sciences of the United States of America*, *116*(2), 587–592. https://doi.org/10.1073/pnas.1813723116

Wilson, S. V., Cebere, B., Myatt, J., & Wilson, S. (2023). *miceforest*. https://github.com/AnotherSamWilson/miceforest/

Wiser, S. K., Bellingham, P. J., & Burrows, L. E. (2001). Managing biodiversity information: development of New Zealand's National Vegetation Survey databank. *New Zealand Journal of Ecology*, *25*(2).

Wiser, S. K., & De Cáceres, M. (2018). New Zealand's plot-based classification of vegetation. *Phytocoenologia*, *48*(2), 153–161. https://doi.org/10.1127/phyto/2017/0180

Wyka, S. A., Munck, I. A., Brazee, N. J., & Broders, K. D. (2018). Response of eastern white pine and associated foliar, blister rust, canker and root rot pathogens to climate change. *Forest Ecology and Management*, *423*, 18–26. https://doi.org/10.1016/j.foreco.2018.03.011

Wyse, S., School of Environment, University of Auckland, Private Bag 92019, Auckland 1142, New Zealand, Wilmshurst, J., Burns, B., & Perry, G. (2018). New Zealand forest dynamics: a review of past and present vegetation responses to disturbance, and development of conceptual forest models. *New Zealand Journal of Ecology*, *42*(2). https://doi.org/10.20417/nzjecol.42.18

6. A Machine Learning Framework for Mapping Shifts in Species' Abundance from Long-term Monitoring Data (AtiP)

6.1. Abstract

1. Climate change has driven extensive reorganisation of plant communities as species adjust their ranges in response to changing conditions. Existing studies focus on the role of temperature, documenting shifts in range margins, but neglecting changes in abundance within the range. This results in unexplained patterns complicated by overlooked, interacting biotic and abiotic drivers, such as soil properties and herbivores, limiting our ability to predict forest response and vulnerability to climate change.
2. Here, we develop the Abundance Trend Indicator (ATI), a machine-learning approach that learns the conditions under which changes in species' abundance have occurred and, thus, the extent and location of the mismatch of a species' current range to its total realised habitat. The resulting abundance shift maps identify abundance shift directions, vulnerable species, and their drivers. We validate the algorithm on New Zealand's forest inventory data (2821 sites, 77 woody species, collectively accounting for 75% of forest canopy nationally) and 37 predictor variables, which include climatic, topographic, edaphic and biological factors.

3. ATI confirms globally observed trends of upward and poleward abundance shifts, but reveals drivers such as soil pH, grazing, and climate stability for species shifting in opposite directions. Moreover, our findings suggest that vulnerability is primarily explained by a plant's ability to tolerate or avoid stress resulting from climatic fluctuations and limited migration capacity.
4. Synthesis: Using existing forest inventory data, ATI models within-range abundance shifts, rather than changes in range margins, resulting in earlier detection of environmental drivers and geographical directions of plant migration. This enables the early identification of vulnerable species.

6.2. Introduction

Human activities drive climate change, biodiversity redistribution, and species introductions that are reshaping Earth's ecosystems at an unprecedented rate and creating novel climates (Williams et al. 2007) and communities (Gougherty et al. 2024). Species react to these environmental changes by expanding or contracting their geographic range, tracking more favourable conditions, or persisting in place due to phenotypic plasticity, genetic adaptation (Diamond 2018) or phenological shifts (Jakoby et al. 2019). Failure to adapt or migrate leads to various degrees of vulnerability or extinction

(Lenoir and Svenning 2015). Identifying the behaviour of species in relation to their biotic and abiotic environment, therefore, is key to conserving biodiversity.

The most well-documented trend of species range shifts (~50-80%) in response to recent climate change is a poleward and upward movement towards cooler temperatures (Rubenstein et al. 2023; Lawlor et al. 2024). Fewer than 20% of studies consider range-shift drivers beyond temperature (Taheri et al. 2021). Temperature, however, might not be a direct driver of range shifts. For example, the water balance of individual trees is influenced by factors such as topography, soil, and interspecific interactions (Stephenson 1998), making range shifts inherently local (Rapacciuolo et al. 2014). Consequently, many species may be responding not to temperature itself, but to other changing environmental factors, such as precipitation (Crimmins et al. 2011; Fei et al. 2017), biotic interactions (Lenoir et al. 2010; Louthan et al. 2015) or land-use change (Guo et al. 2018). Accurate range shift analyses, therefore, need to consider multiple drivers as well as their interactions (Lawlor et al. 2024).

In long-lived plant species, range shifts often lag behind within-range abundance shifts (Breshears et al. 2008), sometimes by centuries (Beckage et al. 2008), thereby masking the responses to climate change. Previous studies, however, have mainly documented range shifts at species' margins (Lenoir and Svenning 2015) as they only require presence-absence data. This neglects that a plant species' demographic performance varies across its geographic range, in response to local abiotic gradients (Doak and Morris 2010; Villellas et al. 2015; Lynn et al. 2021). Abundance shift observations across the species' entire range should therefore be preferred to range shift observations to assess climate change responses and identify vulnerable species.

Plant abundance and occurrence data are available from National Forest Inventories (NFIs), which monitor forest composition over time (Tomppo et al. 2009). However, these inventories often lack uniform methods for collecting, storing, and processing this data, especially for older observations (Chirici et al. 2012). New analytical approaches can unify conflicting protocols and handle missing data. For instance, seedlings and adults are usually surveyed using different methods (Wiser et al. 2001), but comparing their distributions can be used for range-shift assessments (Lenoir et al. 2009; Woodall et al. 2009). In another instance, to account for heterogeneous survey methodologies, multiple locations were combined into an artificial plot and abundances compared to reveal shifts and drivers of change (Fei et al. 2017). Analytical methods, therefore, will leverage larger datasets and yield more widely applicable insights if they are able to operate on protocol-independent representations of NFI data rather than relying on inventory-specific survey designs.

The most common methods used to assess range shifts are species distribution models (SDMs, (Guisan and Thuiller 2005)), which model the abiotic conditions of a species' presence and extrapolate it into the future (Foden et al. 2019). Since SDMs typically output habitat suitability, they fail to reliably predict abundances needed for effective conservation (Johnston et al. 2015), with only 42% of studies finding consistent positive correlations with independent abundance estimates (Lee-Yaw et al. 2022). Abundance can also be predicted by demographic rates (Ehrlén and Morris 2015) through process-based models (Connolly et al. 2017), but estimating them requires data of high spatiotemporal resolution (Dormann et al. 2012) and, for long-lived trees, in particular, at different life

stages (i.e. stage-dependent population models (Caswell 2006)). Despite growing data availability (e.g. COMPADRE database, (Salguero-Gómez et al. 2015)) data on vital rates remain scarce. For instance, COMPADRE contains only three native vascular plant species from New Zealand. More data and better methods are therefore needed to overcome these challenges and better predict the impact of climate change on species range and abundance shifts (Lenoir and Svenning 2015).

Here, we present a conceptually distinct machine learning approach, the "Abundance Trend Indicator (ATI)," which estimates the degree to which a specific climate is conducive to an increase in species abundance. The resulting ATI maps allow for estimation of geographical abundance gradients and numerous environmental drivers of these abundance changes. Moreover, vulnerability can be assessed if the abundance trend of a species is predominantly negative. We validate and exemplify the approach using New Zealand's forest inventory dataset comprised of 2,821 sites surveyed from 1969 to 2019 with individual counts of 77 woody species and 37 spatio-temporal, abiotic and biotic variables. We aimed to quantify the contribution of drivers other than temperature to abundance shifts, distinguish individual species responses from mean trends, and assess species vulnerability arising from species-specific environmental limits and stressors. Detailed species-level results and ATI maps are available on an interactive website: https://ati-nz-predictions-7e6f3d514735.herokuapp.com/.

6.3. Materials and Methods

The Abundance Trend Indicator (ATI) is a machine learning model that uses environmental (i.e. biotic and abiotic) predictor variables x_i to predict how conducive a location i is to a species abundance increase (Fig. 6.1). It is trained on resurveyed plots where the binary target labels $y_i \in \{0, 1\}$ corresponded to an increase or decrease of individual adult tree counts (Steps 1 and 2 in Fig. 6.1). Formulating y as a binary variable allows us to clean the training data using a well established framework (Brodley and Friedl 1999) (step 3) and to achieve higher accuracy in predicting y from x (step 4). The model, then, made binary yearly predictions over the species' entire range ati_{yr}: $\mathbb{R}^{N \times D} \rightarrow \{0, 1\}^N$, which were averaged over the years 1969 - 2019 (step 5). This step transformed binary into continuous predictions, indicating how conducive the environment in each grid cell was to abundance increases over the 50-year period. To avoid extrapolation, we limited predictions to the range of environmental conditions where the species has been previously observed (step 6). The final ATI map (step 7) thus consisted of the ATI predictions (step 5) masked with the similarity mask (step 6) and was used to reveal directions of increasing abundance (abundance gradients, along geographical or environmental variables) and assess how favourable a species' realised niche is to increased abundance (i.e. vulnerability, Steps 8 and 9).

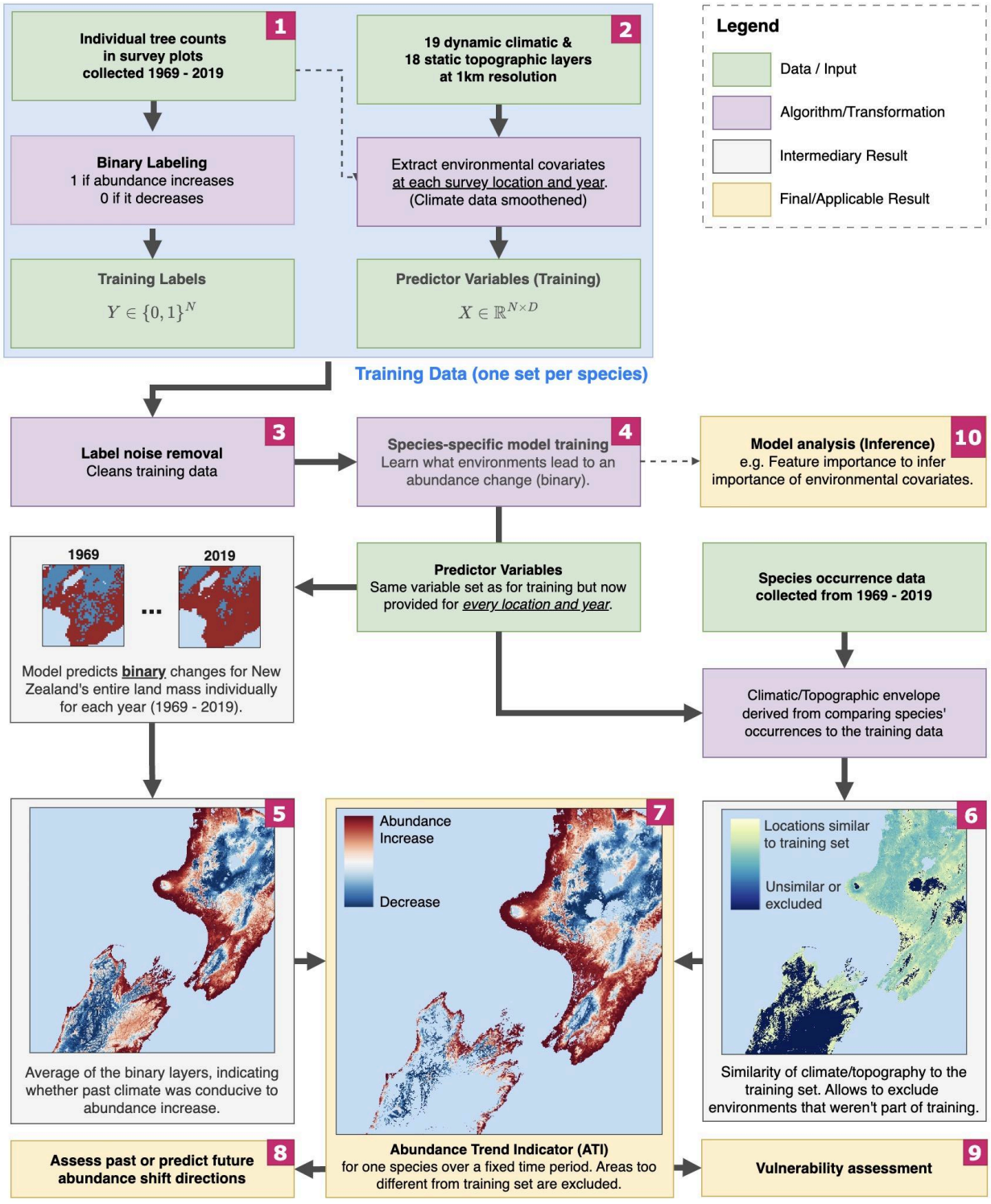

Legend
Data / Input
Algorithm/Transformation
Intermediary Result
Final/Applicable Result
1
Individual tree counts in survey plots collected 1969 - 2019
2
19 dynamic climatic & 18 static topographic layers at 1km resolution
Binary Labeling
1 if abundance increases
0 if it decreases
Extract environmental covariates at each survey location and year.
(Climate data smoothened)
Training Labels
$Y \in \{0,1\}^N$
Predictor Variables (Training)
$X \in \mathbb{R}^{N \times D}$
Training Data (one set per species)
3
Label noise removal
Cleans training data
4
Species-specific model training
Learn what environments lead to an abundance change (binary).
10
Model analysis (Inference)
e.g. Feature importance to infer importance of environmental covariates.
1969
2019
...
Model predicts binary changes for New Zealand's entire land mass individually for each year (1969 - 2019).
Predictor Variables
Same variable set as for training but now provided for every location and year.
Species occurrence data collected from 1969 - 2019
Climatic/Topographic envelope derived from comparing species' occurrences to the training data
5
Average of the binary layers, indicating whether past climate was conducive to abundance increase.
7
Abundance Increase
Decrease
6
Locations similar to training set
Unsimilar or excluded
Similarity of climate/topography to the training set. Allows to exclude environments that weren't part of training.
8
Assess past or predict future abundance shift directions
Abundance Trend Indicator (ATI)
for one species over a fixed time period. Areas too different from training set are excluded.
9
Vulnerability assessment

Figure 6.1: *Overview of the Abundance Trend Indicator (ATI) algorithm. The final ATI map (step 7) is the combination of the predictions of a (binary) classification model trained on tree count data and environmental variables (left path, steps 1-5) masked by areas similar in climate and topography to the training data (right path, step 6). ATI maps reveal environmental and geographical gradients of abundance shifts and species vulnerability (steps 8-9). Additionally, models can be analysed directly (step 10) to infer the importance of environmental covariates. A dashed line between steps 4 and 10 indicates that the models from step 4 are used for inference in step 10.*

6.3.1. Occurrence dataset and training labels (Step 1)

New Zealand, as a study area, is well-suited for studying climate-driven abundance shifts because its forests span a wide range of latitudinal, elevational, and temperature gradients (see Fig. 6.3) with intact forests largely managed for conservation (Heino et al. 2015; Ewers et al. 2006). The Southern Alps, spanning almost the entire length of the South Island, encompass alpine flora, cool-temperate forests, and lowland shrublands, whereas in the north the vegetation transitions from montane to subtropical. Long geographic isolation results in a very high level of endemism (82% of plant species (Murray and de Lange 2011)), many with limited dispersal capacity and distinct ecological strategies, which makes within-range demographic responses particularly informative (Pagel et al. 2020). In addition, introduced herbivores (e.g. red deer (Forsyth et al. 2010)), impose spatially heterogeneous top-down pressure on forest vegetation, providing an opportunity to assess how biotic regulation interacts with climatic gradients to shape climate change responses (Jia et al. 2018).

A training label is a binary number that refers to an outcome a model aims to predict, given a set of predictor variables (e.g., an increase or decrease in abundance under

certain environmental conditions). To obtain training labels for our model, we used a subset of 2,821 plots in New Zealand's nationwide forest inventory data (NVS, (Wiser et al. 2001)) containing 311 woody species with at least two surveys in the years 1969-2019, not more than 30 years and not less than 2 years apart (9,388 observations total). Importantly, this dataset contains a series of permanent plots covering all forested areas at regular spatial intervals, minimising spatial bias (visible as a grid pattern in Fig. C6). Moreover, the protocol ensures a consistent measurement of vegetation. Each plot measured 20 x 20 meters. If a plot was measured more than twice, each consecutive pair was treated independently. Each survey consisted of counts of mature individuals of shrubs, trees, tree ferns, and vines, and their diameter at breast height (DBH). Individuals under 120cm in height were not counted. Plots closer together than the resolution of our topographic data (100m) were treated as one combined plot.

We used two methods to extract training labels, resulting in two datasets:

1. Abundance Only: Based on whether the number of individuals increased or decreased, a 1 or 0 was assigned. Instances with an equal number of individuals were discarded.
2. Abundance and DBH: Expands the Abundance Only datasets by adding plots with an unchanged number of individuals, where a 1 was assigned if the sum of DBH of all individuals increased. In 74.9% of cases, equal individuals resulted in a DBH increase (i.e. individuals aged and grew). In 25.1% younger individuals replaced older individuals, and total DBH decreased.

The datasets yielded 65 species covering 69.37% and 86 species covering 75.59% of forest canopy cover, respectively (Fig. C1). The Abundance Only dataset records a '1' only when individual counts rise due to recruitment, survival, or reduced mortality. The Abundance and DBH

dataset broadens the criteria for a positive abundance trend by including an increase in biomass (i.e., an increase in total DBH, but not individuals).

We used another subset of NVS plots measured using the RECCE methodology (Hurst 2022) (18,664 observations in 15,095 plots) to estimate species cover, as they contained categorical cover estimates for every height tier category (1 through 6, for individuals > 25m down to < 60cm) and can be collapsed into a single cover estimate (Fischer 2015). The sum of these estimates was normalised to 1, yielding relative canopy cover values for each species. Given that abundance changes are approximately Gaussian distributed (Fig. C9) and following (Wisz et al. 2008; Pearson et al. 2007), we excluded species with fewer than 100 total or fewer than 20 observations in either class to avoid a strong class imbalance and an over-dependency of scores on the random choice of training and test data.

6.3.2. Predictor Variables and Training Data (Step 2)

We derived predictor variables from geospatial data. Variables that change over time (e.g. climate) need to be provided for each year, as otherwise ATI predictions would be identical every year and result in a binary output (see grey box between steps 4 and 5 in Fig. 6.1). We constructed 19 BioClim variables (O'Donnel and Ignizio 2012) obtained from monthly rainfall, minimum and maximum temperatures at 1km resolution from the HOTRUNZ dataset (Etherington et al. 2022). We then decomposed the time-dependent BioClim variables $v(t)$ into a linear trend and a stochastic component: $v(t) = m_v \cdot t + \eta$ retaining only the former for training. This reduces the effect of annual climate

fluctuations on species abundances in favour of slow decadal climate changes. Short-term fluctuations, however, are captured in dedicated BioClim variables, such as temperature seasonality. Additionally, we extracted 15 static topographic and edaphic variables (e.g. elevation) from the NZEnvDS dataset ([No author] [no date]). Since New Zealand's vegetation is subject to strong impacts from grazing by introduced mammals (Wyse et al. 2018; Zotov 1938), we included layers for rat, possum, and red deer distributions (Department of Conservation 2015; Department of Conservation 2015; Department of Conservation 2015).

We reduced the "Full" 37-variable dataset to an "Explain" 14-variable dataset using hierarchical clustering (see Section C1.2, Fig. C2 , and Table C1) to improve the interpretation of climatic drivers by removing highly correlated variables. Limiting collinearity additionally improves the fidelity of feature importance scores (Section 6.3.10) (Molnar 2022). PCA was considered but discarded due to poorer model performance and interpretability (Fig. C3). For applications where variable interpretation is secondary to model performance (e.g., spatial forecasting of locations of high canopy turnover), the "Full" dataset can be used, as it yields a slightly better model fit (Fig. C12). However, since our focus was on obtaining ecologically interpretable results, we used the "Explain" dataset for this study. The interactive website contains results for both datasets (https://ati-nz-predictions-7e6f3d514735.herokuapp.com/).

Because the model is trained to predict changes in abundance, it may be susceptible to regression to the mean (RTM), where extreme initial values can create spurious correlations with environmental predictors (see Section C1.7 for details). A common mitigation strategy is to include the initial abundance as a covariate (Mazalla and

Diekmann 2022). However, in our case, an initial abundance of zero would always produce a binary 'increase' label, thus revealing the labels in the training data and artificially inflating model performance. We therefore included mean abundance instead. Since abundance is only known for the training data, this adjustment can only be applied for inference (only Section 6.3.8 and Fig. 6.5), not for prediction. Overall, ATI's binarisation reduced RTM effects to a negligible level ($R^2 \approx 0.01$; Fig. S8 and Section C1.7).

6.3.3. Data cleaning (Step 3)

Our dataset contained data entry and collection errors (see Section C2), leading to erroneous target labels (i.e., labelling noise). Such issues are common in multi-decadal national forest inventories, where observer changes, taxonomic revisions, and disturbances introduce inconsistencies (Thompson et al. 2007). In our data, at least 2.7% of plots had unnaturally high species turnover, and 3.68% of congeneric species were misidentified. Labelling noise can also arise from the stochasticity of rare or hard-to-detect species, resulting in reported error rates of 5.9 to 21% (Scott and Hallam 2003; Verheyen et al. 2018). To reduce labelling noise, we modified an established editing procedure (Frénay and Verleysen 2014) to allow the exclusion of a flexible number of potentially erroneous observations. We found an effective cutoff rate of 10% and 15% for the Abundance Only and Abundance and DBH datasets, respectively (Fig. C12 C). Beyond these thresholds, the cleaning process rendered some species data-deficient, thereby reducing the dataset.

Our algorithm assigned each data point (i.e. plot pair) a continuous noise score $\epsilon_i \in [0, 1]$ based on its environmental predictors x_i and binary label y_i, relative to the K most similar neighbouring plots and their labels. Similarity was defined as the sum of differences of all environmental variables. High noise scores indicated plots whose labels contradicted those of environmentally similar neighbours (Fig. C4). Ranking observations by noise scores allowed for the flexible removal of the noisiest fraction of the dataset. Section C1.3 provides a detailed description of the data cleaning steps.

6.3.4. Model training (Step 4)

We used a random forest (RF) classifier implemented in the SciKit Python package (Pedregosa et al. 2011), due to its excellent predictive performance (Breiman 2001). Random forests classify data by aggregating predictions from many decision trees built during training. Three alternative models: logistic regression, support vector machines, and artificial neural networks showed poorer performance (Fig. C12) and were not pursued further (see Section C1.4). We identified optimal hyperparameters using an exhaustive grid search across all possible parameter combinations (Table C2). Model training employed 4-fold cross-validation, and predictive performance was evaluated using the mean Area Under the Receiver Operating Characteristic Curve (ROC AUC) (Fawcett 2006). In ecological applications, ROC AUC values below 0.7 are generally considered poor (Araújo et al. 2005). We therefore rejected classifiers scoring below this threshold. Final model performance was calculated asthe average ROC AUC score of the four test folds (see Table C5).

6.3.5. Unmasked ATI maps (Step 5)

The trained models make discrete predictions for each grid cell i and year $ati_{yr}: \mathbb{R}^{N \times D} \rightarrow \{0,1\}^{N}$. Taking the average over all years $Y = \{yr | 1969 \leq t \leq 2019\}$ yields a single continuous number between 0 and 1 $ATI = \frac{1}{|Y|} \sum_{yr} ati_{yr}$ for each grid cell i. This eliminates species-specific differences in the number or spacing of training data points. The predictions can be mapped. Locations with ATI < 0.5 indicate that environmental conditions averaged over the years Y led to a decrease in abundance, whereas locations with ATI > 0.5 indicate that conditions led to an increase in abundance. Importantly, the unmasked map contains areas far outside the training range (i.e. a species' realised niche), possibly leading to erroneous model behaviour (Bartley et al. 2019). We therefore discarded predictions outside the species range (see next section).

6.3.6. Similarity maps (Step 6)

Following (Owens et al. 2013), we identified and excluded grid cells whose environmental conditions fell outside those represented in the observed species records, thereby avoiding extrapolation into novel environmental space. The resulting binary similarity masks delineated each species' realised range, allowing a small, flexible margin around the observed conditions (Fig. C6). First, to assess how similar environmental conditions at a location x_i were to those at the observed locations, we calculated the average distance

in terms of environmental similarity to the $K = 3$ nearest observed locations $NN(x_i)$ for each year individually and then averaged over all years, yielding

$D_i = \frac{1}{|Y| \cdot K} \sum_{y \in Y} \sum_{x \in NN(x_i)} ||x - x_i||_1$. The result is a distance map (Fig. C6A) that assigns an environmental distance value to each grid cell i. Next, we defined a threshold S per species and excluded points where $D_i > S$. This yielded the binary similarity mask (Fig. C6C). We defined $S = \gamma S'$ with $\gamma = 1.2$ (Fig. C6C yellow area) where S' is the threshold containing 95% of a species occurrences (Fig. C6B) and corresponds to the range of the species without strong outliers (Fig. C6C orange area). However, since we are interested in predicting range shifts beyond the observed range, we set $\gamma > 1$ to include the periphery of the species range (Fig. C6C, yellow area added due to $\gamma > 1$).

6.3.7. Final ATI map (Step 7)

The final ATI map (Fig. 6.1, Step 7) comprises modelled predictions with environmentally dissimilar areas removed using the similarity mask (see previous two sections). This map indicates how frequently climatic conditions over the past 50 years have facilitated increases in abundance within and immediately surrounding a species' realised niche. The spatial mean of the ATI map provides an overall indicator of the species' climatic vulnerability, while its spatial gradients indicate the direction of abundance shifts. Interpretation depends on the training dataset used (see Section 6.3.1). We use the Abundance Only dataset to infer abundance gradients, as it provides a stronger signal of demographic expansion. For climate vulnerability assessments, we used the larger

Abundance and DBH dataset. The difference between the datasets is that ATI > 0.5 in the former suggests increasing population size, whereas in the latter, it reflects either population expansion or biomass growth (i.e., increased DBH without an increase in the number of individuals).

6.3.8. Abundance gradients (Step 8)

Abundance shifts are defined as transitions from areas of predicted decline to areas of predicted increase. These directions can be analysed along geographic gradients to determine where species are moving (e.g. to lower latitudes) or along environmental gradients to identify the climatic or biotic drivers of the abundance shift (e.g. towards lower temperatures, niche shifts). To quantify these directions, we first segment the grid cells in the ATI map into two subsets: $ATI^{+} = \{i \mid ATI_i > 0.5\}$ and $ATI^{-} = \{i \mid ATI_i \leq 0.5\}$ which correspond to spatially explicit areas of projected demographic gain or loss, respectively.

Next, for a variable of interest v, we calculate its average value within each subset, weighed by the predicted ATI values: $\mu(v)^{+} = \frac{1}{|ATI^{+}|} \sum_{i \in ATI^{+}} ati(i) \cdot v(i)$ and analogously for $\mu^{-}(v)$. These weighted means reflect the average conditions associated with predicted increases or decreases in abundance, respectively. Therefore, we can interpret the difference $\Delta v = \mu^{+}(v) - \mu^{-}(v)$ as an abundance gradient along the variable v. For example, if v is elevation and $\Delta\mu(v) > 0$ the abundance gradient points toward a higher elevation, indicating an uphill migration. If v is precipitation, the species expands into wetter climates (e.g., to escape an arid climate). Importantly, abundance gradients are not

range shifts, which are defined geographically. Rather, they describe the environmental or spatial direction within and around the realised niche toward which the abundance is predicted to increase. To synthesise patterns across variables, we used principal component analysis.

6.3.9. Climate vulnerability assessment (Step 9)

To assess species' vulnerability to climate-related extinction (hereafter: ‘vulnerability’), we computed the mean ATI across all predicted grid cells using the Abundance and DBH dataset. A median value < 0.5 indicates that predicted decreases outweigh increases within the species’ realised range. To estimate overall forest condition, we computed a canopy-weighted average ATI across species, using relative cover as weights. This provides an integrated indicator of forest demographic health. ATI value distributions will have heavy tails at the lower end, as the similarity mask allows for a slight extrapolation (factor $\gamma = 1.2$ in Section 6.3.6) outside of a species' realised niche (Fig. C6), which would naturally have very low ATI values. When assessing vulnerability, a slightly smaller quantile (e.g. 25-75% in Fig. 6.2), therefore, better approximates the ATI values within the species' currently occupied range. To interpret the drivers of vulnerability, we combined feature-importance scores (Section 6.3.10), which quantify the relative contribution of each predictor, with abundance gradient analyses (Section 6.3.8), which indicate the direction of demographic change along environmental axes.

6.3.10. Feature importance (Step 10)

Random forest models produce a positive feature importance value for each variable during training. These values sum to one and indicate the relative contribution of each variable to make correct predictions (Breiman 2001). We used SciKit's Python package to extract these values for our models. For the feature importance analysis, we added the species abundance as an additional variable, as this eliminates the regression to the mean (RTM) effect, which confounds inference (Mazalla and Diekmann 2022) (See Section C1.7 for details).

As environmental conditions relevant to a species' growth are expected to correlate well with the abundance trend, we computed correlations $r_s(v) \in [-1, 1]$ between ATI values and predictor variables v for every species s as an alternative importance metric. To highlight only the correlation's strength (and not the direction), we use the absolute value of the correlation $|r_s|$. To assess the importance of a variable in general, we average it across all species $|\widetilde{r(v)}| = \frac{1}{N}\sum_s |r_s(v)|$.

6.3.11. Synthetic species

To illustrate our method's applicability and correctness, we generated three synthetic species shifting their abundance exclusively up a precipitation, elevation or latitude gradient. We compared AUC scores of the synthetic predictions to those of natural species, presumably driven by multiple environmental drivers and their interactions.

Two Gaussian distributions (for the year 1990 and 2019) described the synthetic species' abundance distribution along each variable. The mean of these distributions was artificially offset to mirror globally observed speeds of range shift for latitude and elevation of 11.8km/decade and 9m/decade (Rubenstein et al. 2023). We used real-world climate data for this experiment. A detailed description is provided in Section C3.4.

6.4. Results

6.4.1. Assessing species' climate vulnerability

We identified 19 vulnerable species for which, on average across their ranges, observed environmental change has led to declines in their abundance over the study period (i.e. median ATI < 0.5, Fig. 6.2A). These species had a collective canopy cover of 20.51%. Across all 86 species, however, the ATI median was 0.66, indicating that collectively, recent environmental change contributes to increases in New Zealand's species richness locally. The climatically vulnerable species were predominantly predicted to shift their abundance towards higher elevation and precipitation and toward lower temperature and precipitation fluctuations (Fig. 6.22B). The most important directions of abundance changes occurred along latitude and temperature ranges. For four species, however, abundance shifts occurred along a precipitation seasonality gradient, an otherwise less

important variable.

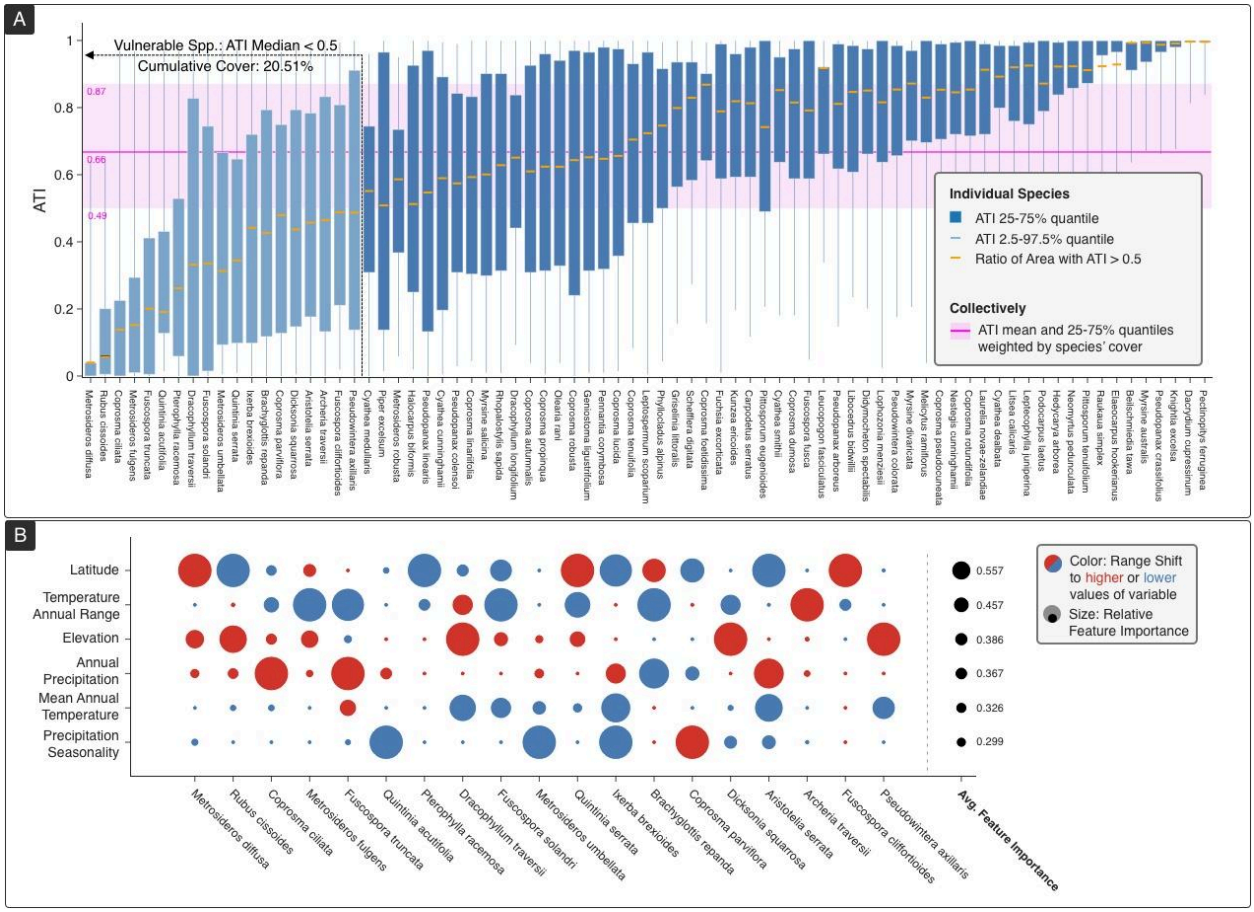


Figure 6.2: Vulnerability assessment through analysis of ATI distributions. (A): Bars indicate 25 - 75% percentiles of ATI values across individual species' realised niches. Yellow lines indicate the ratio of grid cells with ATI > 0.5 to total cells. The magenta line is the cover weighted mean for all species. 19 vulnerable species (light blue bars) have an ATI median below 0.5. (B): Feature importances and abundance gradients for the 19 vulnerable species. The size of markers indicates the importance of the feature for the species' model. Colours indicate abundance increases (red)/decreases(blue) towards larger values of this variable. The right column gives the average importance of each variable for all species.

6.4.2. Abundance shifts polewards and upwards towards steeper, wetter, cooler areas with lower isothermality

We identified abundance gradients for 62 species in the Abundance Only dataset (Fig. 6.3). In addition to abundance gradients along elevation, temperature, and precipitation, we found statistically significant abundance shifts (see Table C6 for test statistics) in the direction of areas with lower isothermality, more acidic soils and steeper slopes. Since the annual temperature range (a component of isothermality) showed no significant shifts, isothermality gradients might be explained by lower diurnal ranges. Precipitation seasonality, wind exposure and the distance to the nearest river were not associated with significant shifts in abundance. While species preferred the absence of red deer, the difference was non-significant across all species. Aspect showed no significant gradients along eastness but a small, significant shift along northness, corresponding to a rotation of ~5° closer to cooler, south-facing slopes.

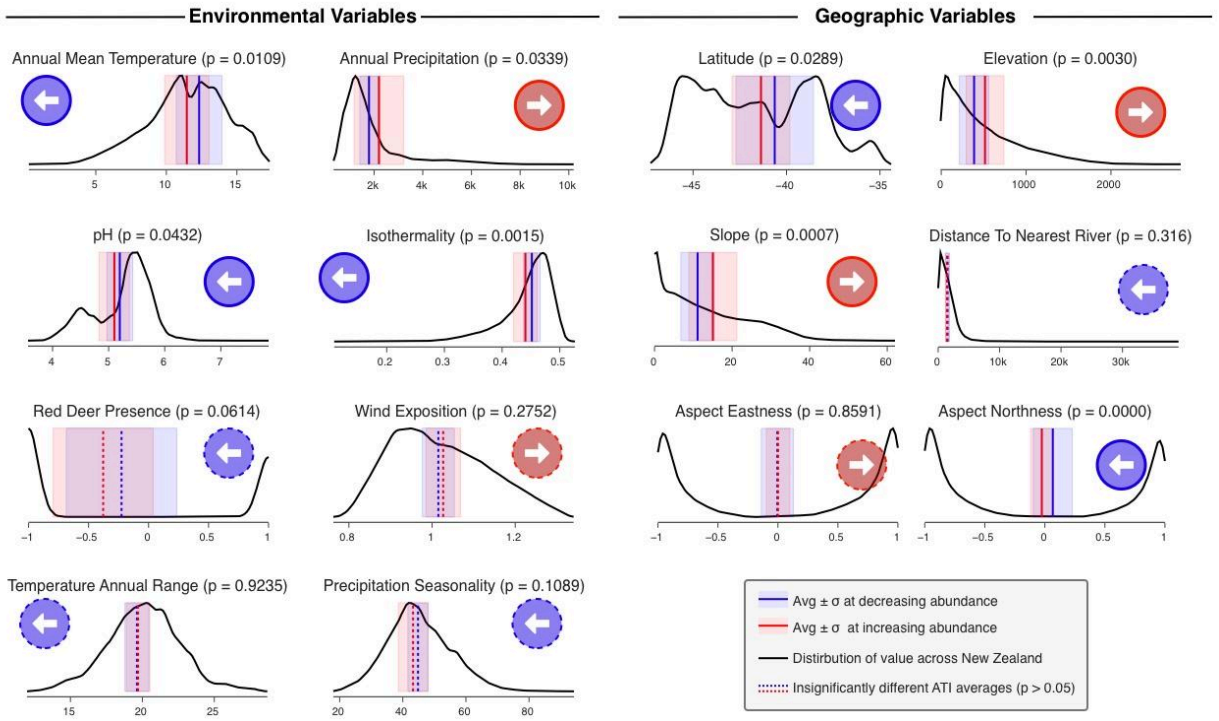


Figure 6.3: *Each subplot corresponds to abundance gradients along one environmental variable (e.g., Elevation, top right) and shows the average conditions correlated with increasing (red vertical line) and decreasing (blue vertical line) abundance trend prediction across all species. The shades represent ±1 the standard deviation among all 62 species. An arrow depicts the direction of the gradient along this variable (e.g., points rightwards, towards higher elevation). Dashed arrow outlines signify statistically non-significant changes. The black line indicates each variable's nationwide (New Zealand) distribution to provide context for the frequency of the habitat.*

6.4.3. Species respond individually and are far from the mean

For the six variables with the strongest abundance gradients, we additionally assessed the distribution of individual responses and compared them to the mean response (Fig. 6.4A-C). Across all six variables except precipitation seasonality, approximately two-thirds of species shifted in the average direction. For example, 63.8% of species shifted their abundance towards the average direction of wetter habitats, and 65.5% towards cooler habitats (i.e., towards the lower left of Fig. 6.4A). The remaining ~35% shifted into drier and warmer habitats. Likewise, 69.9% and 67.9% of species increased abundance polewards or towards higher elevations, respectively (i.e. towards the bottom and right of Fig. 6.4 B). The mean and standard deviation of responses across all species (red cross and ellipse, Fig. 6.4A-C) only poorly captured the accurate distribution of individual shifts (background heatmap), indicating species-specific rather than collective responses.

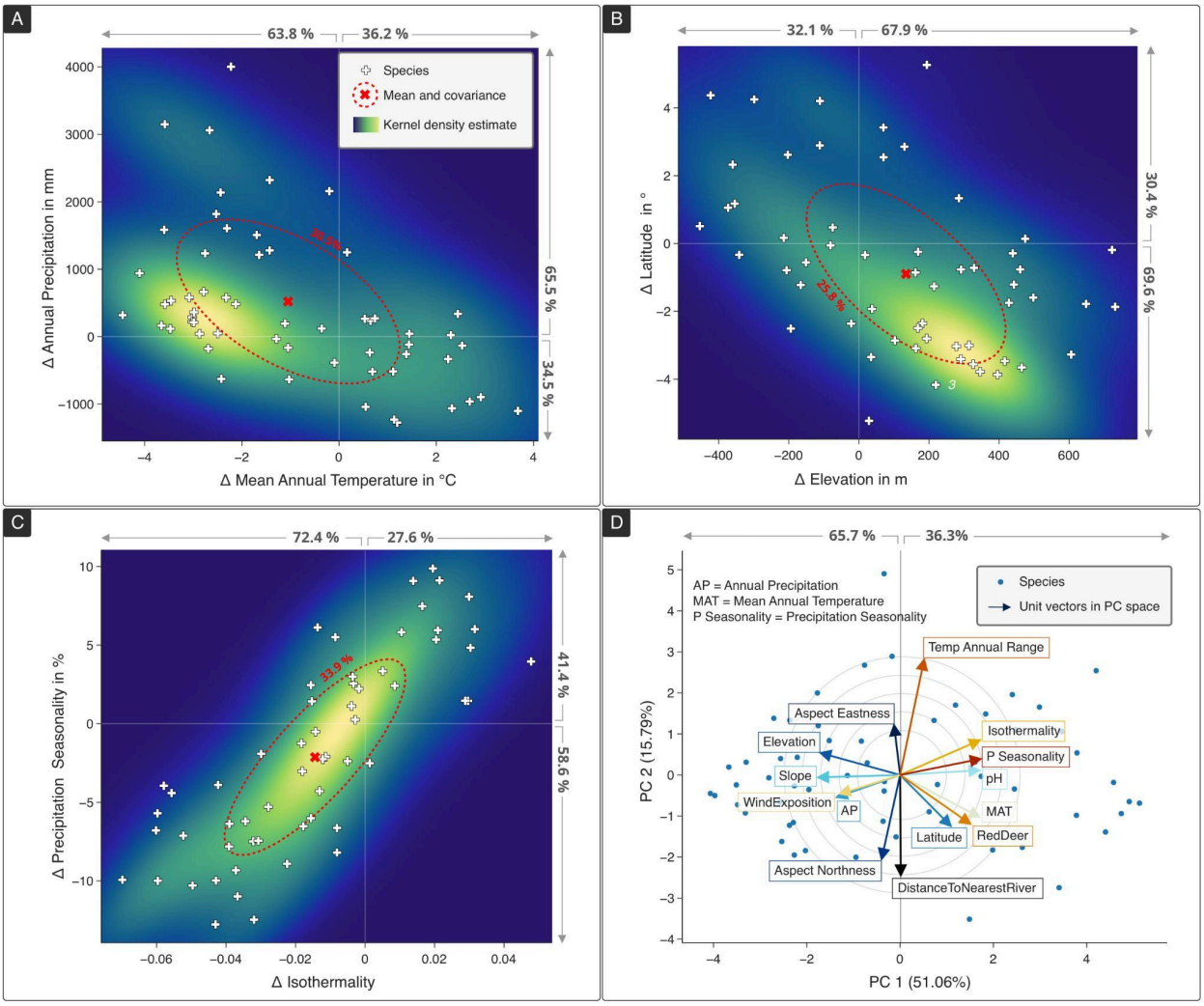


Figure 6.4: *Abundance shift directions for single species. A, B and C: Points are single species, and values on the axes give the difference in average conditions between areas of ATI > 0.5 (increasing abundance) and ATI ≤ 0.5 (decreasing abundance). For instance, if Δ Elevation = 100m, areas of decreasing and increasing ATI are on average separated by 100m in elevation. Background heatmap is a kernel density estimate across all species and is brighter in areas with more species. The mean and one standard deviation ellipse are shown in red. D: PCA biplot of abundance gradients along all 14 environmental variables, concentric circles for length comparison of unit vectors.*

A principal component analysis of all abundance gradients resulted in a dominant axis (PC1, explaining 51.06% of variation, Fig. 6.4D). Negative values on PC1 described abundance gradients aimed polewards, towards higher elevations and cooler climates, but also to harsher conditions (i.e., steeper, wind-exposed slopes and acidic soils). Positive values on PC1 reflected abundance gradients towards locations of stronger annual precipitation seasonality in precipitation and isothermality, and high grazing pressure and temperatures. Greater isothermality along PC1 is likely the result of increased diurnal ranges, as the annual temperature range is orthogonal to PC1. PC2 explained only a negligible 15.79% and was dominated by the temperature annual range and the distance to the nearest river (Fig. 6.5 B).

6.4.4. Elevation and temperature insufficiently explain abundance shifts

To understand which variables drive abundance increases, we assessed ATI correlations and feature importance scores (Fig. 6.5). While changes in species' abundance correlated most strongly with annual mean temperature ($|\widetilde{r}| = 0.40$), elevation ($|\widetilde{r}| = 0.34$), and latitude ($|\widetilde{r}| = 0.32$), almost all remaining climate and soil variables were comparably highly correlated (0.31 to 0.1). In contrast, the three synthetic species (Section 6.3.11 and S3.4) correlated with their main abundance driver elevation ($r = 0.75$), annual precipitation ($r = 0.63$), and latitude ($r = 0.81$) substantially better than any real-world species (green diamonds, Fig. 6.5 A). Feature importance (Fig. 6.5B), attributed comparably large importance to latitude, temperature, precipitation, and their

fluctuations. However, individual species' responses are concealed when the values are averaged. Striking examples of plant species whose abundance shifts occur strongly along a single variable are found among the outliers (highlights in Fig. 6.5B). Notably, *Lophozonia menziesii*, possibly the most abundant tree in New Zealand, was strongly driven by annual temperature.

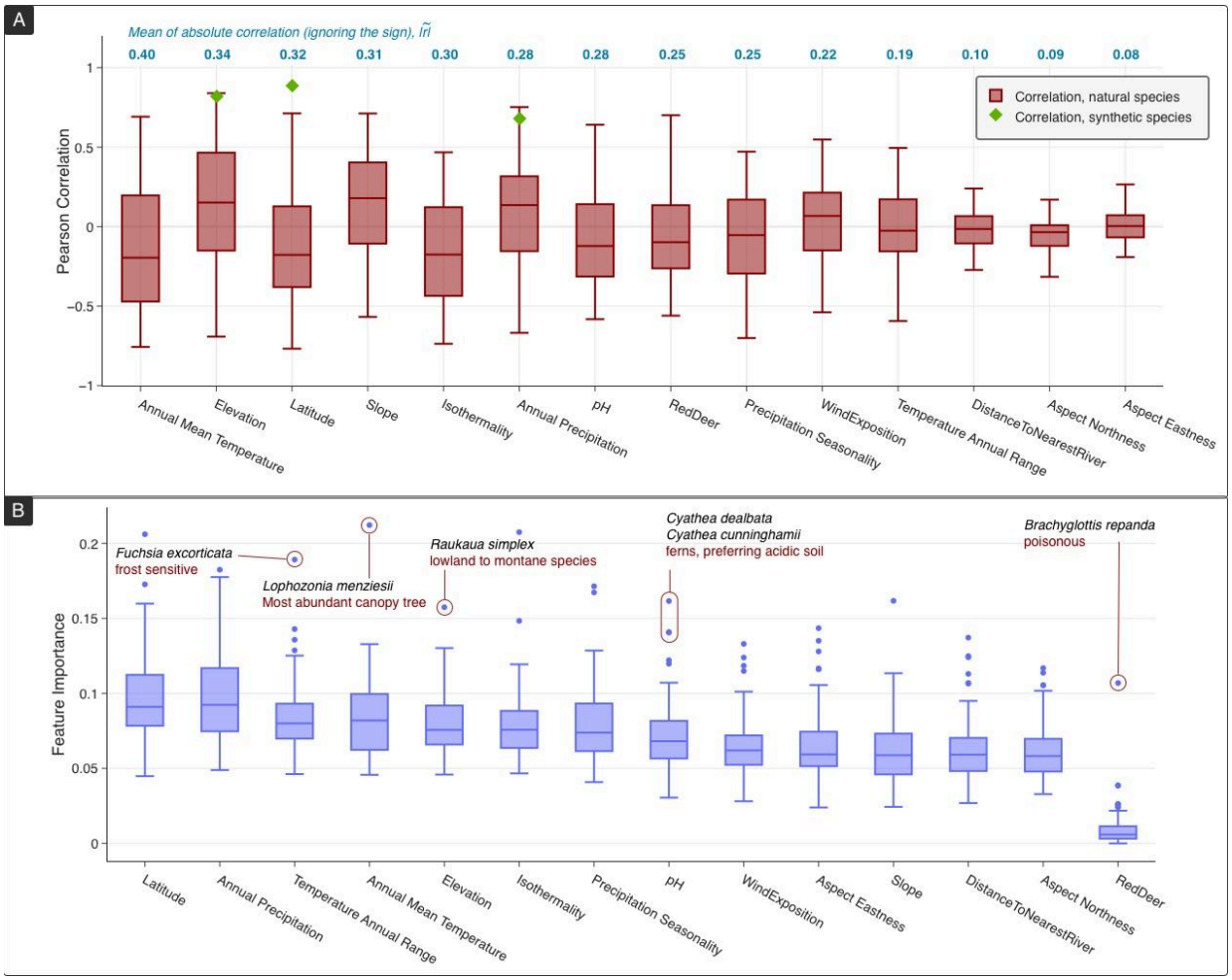


Figure 6.5: *Variable importance. A: Average Pearson's correlation of ATI and environmental variables within species' ranges (red). The average absolute values are displayed in blue text above. Correlation for synthetic species with their main drivers given as green diamonds. B: Feature importance scores from the random forest model. Higher scores indicate a stronger reliance of the model on the variable to predict ATI. Several outlier species are highlighted.*

6.5. Discussion

We present the Abundance Trend Indicator (ATI), a new method to identify and map areas of change in species abundance, which draws on historical tree count data common to many biological inventories (i.e, forestry inventories). We used ATI maps to reveal 19 vulnerable species in New Zealand and their environmental pressures. Abundance gradients, derived from ATI maps, showed that species abundance of New Zealand's woody species largely matched global trends with temperature, precipitation, isothermality and pH as primary drivers, resulting in abundance shifts polewards and upslope to higher elevations (Lawlor et al. 2024; Rubenstein et al. 2023), thus validating our method. However, ATI also revealed that these mean trends poorly matched individual responses, especially for specialist species, driven by less commonly significant variables such as grazing pressure. ATI is available as a Python package, and detailed maps for this dataset are accessible on: https://ati-nz-predictions-7e6f3d514735.herokuapp.com/.

6.5.1. Method interpretation

ATI identifies areas of repeated positive net change in adult abundance, thereby approximating a species' demographic niche when immigration is negligible. While it explicitly models the abiotic filter, biotic interactions are implicitly captured in the data (e.g., under given conditions, a species can decline due to either abiotic or biotic filtering), thereby linking it to the fundamental niche. The fundamental niche is defined as the species' growth rate under optimal conditions and no competition $r_0 > 0$ (Birch 1953; Ehrlén and Morris 2015). Although ATI does not estimate r_0 directly and includes biotic effects, an increase in adult abundance (i.e. ATI > 0) is a necessary (albeit not sufficient) empirical condition for positive population growth (i.e. $\lambda > 1$). ATI can therefore be considered a pragmatic proxy for identifying environments with $r_0 > 0$ at landscape scales, since directly measuring r_0 is challenging, especially for long-lived trees. For instance, the COMPADRE database (Salguero-Gómez et al. 2015), which compiles demographic models globally, contains only 792 species and only one from our dataset. By contrast, the ATI estimate uses only tree-count survey pairs, which are widely available in national forest inventories. This allows ATI to complement species distribution models (Guisan and Thuiller 2005), which do not explicitly model processes such as net population growth rate (Thuiller et al. 2013).

ATI is formulated as a binary classification model rather than a regression model. Its objective is to identify the direction of abundance change (increase vs. decrease) and to quantify the balance between positive and negative changes, which we interpret as (climate) vulnerability. The ATI score depends on the relative frequency and spatial

pattern of increases and declines, not on precise estimates of absolute abundance, and is largely insensitive to absolute abundance values given their approximately normal distribution (see Section C1.8 and Fig. C9). Accurate abundance modelling requires additional information on biotic interactions (Meier et al. 2010) and is context-dependent (Lynn et al. 2019), which a landscape model can't fully capture. However, binarisation offers three key advantages. First, it enables the use of an established label noise removal framework (Brodley and Friedl 1999; Frénay and Verleysen 2014), which counteracts errors in forest inventory datasets estimated from 5.9% (Scott and Hallam 2003) to 21% (Verheyen et al. 2018) (Section C2), and enables the model to capture underlying general trends with higher accuracy (Section C3.3). Second, classification models are inherently less sensitive to outliers (Loh 2011). Third, a fivefold reduction (to $R^2 \approx 0.01$; Fig. S8) in the effect of regression to the mean (RTM), where extreme initial abundance values bias the observed change in abundance (Mazalla and Diekmann 2022), masking the relationships between environment and abundance (Section C1.7). An expansion of ATI to three classes (increase, decrease or no change) is meaningful, but requires three separate classifiers (Galar et al. 2011), increasing data requirements threefold. ATI's binary approach should therefore be viewed as a landscape-scale screening tool to identify dominant environmental drivers of abundance change and to flag species at risk, but followed by finer-scale abundance analyses, such as joint species distribution models (Ovaskainen and Soininen 2011).

Binarisation of ATI necessitated addressing areas with unchanged individual counts, resolving this via total DBH changes, however, is problematic because DBH reflects biomass, not fitness. Long-lived adults can maintain and increase biomass despite

population decline (Tilman et al. 1994). Conversely, juveniles and seed banks contribute little to DBH but increase overall fitness through recruitment. Moreover, DBH change is site-specific, influenced by factors such as soil fertility and amplified by temporal factors, including gap dynamics (Bagnato et al. 2021). However, if ATI were used to predict carbon storage, productivity, or biomass dynamics, choosing DBH changes for label generation over the number of individuals would be meaningful and straightforward.

While ATI was developed on New Zealand plants, it can be applied to animals if survey protocols and detection biases are accounted for (e.g. seasonal bird migration should not count as an abundance change). A major advantage is that ATI can combine multiple abundance metrics (e.g. individual counts or detection probability changes convert equally into binary labels), solving a major issue for biodiversity tracking (Callaghan et al. 2024). Similarly to SDMs, ATI extensions would require taxon and location-specific variables (e.g. habitat structure for animals, or snow-related variables at high latitudes) (Guillera-Arroita et al. 2015), and should follow ODMAP guidelines (Zurell et al. 2020) for validation, training and documentation. We introduced a mutual information and clustering-based variable choice procedure, which incorporates training labels, is taxon-agnostic (Section C1.2) and reduces collinearity (Dormann et al. 2013). With minor adjustments, therefore, the ATI framework can be applied to other organisms and at other locations.

Our method has a few limitations that can be addressed in future implementations. First, data on land-use change would likely improve abundance predictions (Guo et al. 2018), but

were unavailable for New Zealand at the time of analysis. Recently developed global land-use datasets (e.g. (Woodman et al. 2026)) provide a clear next step for improving ATI predictions. Our method does not account for species interactions or density dependence (Chesson 2000), and likely removes their effects in the data cleaning step. Density dependence strongly influences abundance distributions (Ehrlén and Morris 2015) and, as we demonstrate for inference, can be accounted for in ATI by including abundance as a predictive variable, improving model performance (Fig. C12A). For the prediction case, it would need to be estimated or measured. Second, abundance shifts result from a change in fitness, mediated by a species' traits (Laughlin 2023; Funk et al. 2017). Incorporating trait data might, therefore, allow us to unify species-specific ATI models into a single model, vastly expanding the training dataset and enabling more complex models that can infer successful trait combinations (i.e., functional strategies). Finally, while ATI successfully recovers abundance gradients for synthetic species (Section C3.4), full ecological validation at the landscape scale will require future studies using independent or targeted datasets.

6.5.2. Ecological results

Our results align New Zealand's flora with global trends of abundance shifts towards the poles and to higher, cooler elevations ((Parmesan and Yohe 2003; Lenoir et al. 2020); Fig. 6.3). However, temperature and elevation had only a modest two-fold difference in feature importance to the least influential variables (Fig. 6.5. B). These variables contributed to within-range biodiversity rearrangement, especially for specialist species

(outliers in Fig. 6.5. B), pointing to their importance in predicting abundance shifts and consequent range shifts (Franklin 2023; Howard et al. 2014). The presence of multiple interacting abundance gradients is further exemplified by comparing the lower prediction accuracy of real-world species (average AUC = 0.62) to that of synthetic species (driven by a single variable, AUC > 0.85; Section C3.4, Fig. 6.5. A). These findings illustrate ATI's advantage in capturing the complex interplay of a wide array of environmental drivers within a species' range, addressing limitations of previous work, overlooking within-range abundance dynamics (Taheri et al. 2021; Rubenstein et al. 2023).

Abundance gradients for all species were predominantly distributed along an axis from stress tolerance (PC1 in Fig. 6.4D) to avoidance. The ability to move (i.e. avoid stress) or persist (i.e. tolerate stress) determines a species' demographic success (Lenoir and Svenning 2015). However, environmental conditions translate into stress differently for each species (Lichtenthaler 1998), and thus, predicting abundance changes requires consideration of what constitutes stress to each species within the studied habitat. For example, the toxic *Brachyglottis repanda* has a competitive advantage under grazing pressure (Mortimer and White 1967), and showed the strongest feature importance score for this variable (Fig. 6.5. B). This species-specificity is illustrated by the majority of abundance gradients lying outside the 1σ margin around the mean gradient (Fig. 6.4 A-C), in other words, the mean response of all species is not a common response of any species. This illustrates that a better understanding of biodiversity rearrangement needs to consider individual plant stressors caused by a diverse range of factors.

Vulnerability assessments for individual species at a landscape scale are often costly, time-consuming, and dependent on limited expert opinions (Ackerly et al. 2010) and might

not reflect species' shrinking ranges (Goury et al. 2025). Recently developed climate-based methods broadly assess biodiversity risk but sacrifice precision (Klausmeyer et al. 2011). ATI, on the other hand, enables broad-scale climate vulnerability assessments for individual species by identifying species with predominantly declining abundances. An important limitation of this metric is that it does not account for aspects of vulnerability beyond climate, such as introduced diseases, dispersal limitation, or habitat destruction and fragmentation, unless they are included as predictive variables (e.g., deer presence in our data). We identified 19 such species across New Zealand whose vulnerability is driven by climatic variability, particularly temperature range and precipitation seasonality. Despite mean annual temperature (MAT) being more important collectively (Fig. 6.5A), it was not of primary importance to any of the vulnerable species (Fig. 6.2B). This aligns with experimental evidence that limited adaptive phenotypic plasticity to climatic variability, rather than tolerance to mean climate, often determines population persistence under changing conditions (Reyer et al. 2013; Scheepens et al. 2018), highlighting that increasing fluctuations may pose a stronger risk than shifts in climatic means. Alarmingly, two of the most vulnerable species (*Metrosideros diffusa* and *Metrosideros fulgens*) belong to the Myrtaceae family, which is susceptible to the recently introduced invasive fungal pathogen *Austropuccinia psidii* (myrtle rust) (Toome-Heller et al. 2020). Given that only two years in our dataset overlap with the presence of myrtle rust, this may reflect interacting pressures of climate variability and disease, highlighting these species as priorities for closer monitoring under ongoing environmental change.

6.6. Conclusion

Our study underscores the necessity of examining within-range abundance changes to understand forest plant species' responses to recent climate change. The Abundance Trend Indicator (ATI) leverages freely available forest inventory data to identify spatially explicit changes in species abundance and reveals that species respond individually rather than following mean trends, often as a function of unstable environmental conditions. Moreover, the focus on abundance ties the model outputs closer to niche theory and enhances our ability to identify vulnerable species and the specific factors contributing to their decline. By using ATI alongside species distribution models, we can refine ecological predictions and inform conservation strategies more effectively. ATI is easily expanded to other organisms and locations, provided abundance changes can be detected reliably. A Python package for ATI is available, and an interactive website (https://ati-nz-predictions-7e6f3d514735.herokuapp.com/), showcases detailed results to foster broader familiarity with ATI.

6.7. References

Ackerly, D. D., Loarie, S. R., Cornwell, W. K., Weiss, S. B., Hamilton, H., Branciforte, R., & Kraft, N. J. B. (2010). The geography of climate change: implications for conservation biogeography: Geography of climate change. *Diversity & Distributions*, *16*(3), 476–487. https://doi.org/10.1111/j.1472-4642.2010.00654.x

Araújo, M. B., Pearson, R. G., Thuiller, W., & Erhard, M. (2005). Validation of species–climate impact models under climate change. *Global Change Biology*, *11*(9), 1504–1513. https://doi.org/10.1111/j.1365-2486.2005.01000.x

Bagnato, S., Marziliano, P. A., Sidari, M., Mallamaci, C., Marra, F., & Muscolo, A. (2021). Effects of gap size and cardinal directions on natural regeneration, growth dynamics of trees outside the gaps and soil properties in European beech forests of southern Italy. *Forests*, *12*(11), 1563. https://doi.org/10.3390/f12111563

Bartley, M. L., Hanks, E. M., Schliep, E. M., Soranno, P. A., & Wagner, T. (2019). Identifying and characterizing extrapolation in multivariate response data. *PloS One*, *14*(12), e0225715. https://doi.org/10.1371/journal.pone.0225715

Beckage, B., Osborne, B., Gavin, D. G., Pucko, C., Siccama, T., & Perkins, T. (2008). A rapid upward shift of a forest ecotone during 40 years of warming in the Green Mountains of Vermont. *Proceedings of the National Academy of Sciences of the United States of America*, *105*(11), 4197–4202. https://doi.org/10.1073/pnas.0708921105

Birch, L. C. (1953). EXPERIMENTAL BACKGROUND TO THE STUDY OF THE DISTRIBUTION AND ABUNDANCE OF INSECTS: III. The relation between innate capacity for increase and survival of different species of beetles living together on the same food. *Evolution; International Journal of Organic Evolution*, *7*(2), 136–144. https://doi.org/10.1111/j.1558-5646.1953.tb00072.x

Breiman, L. (2001). Random Forests. *Machine Learning*, *45*(1), 5–32. https://doi.org/10.1023/A:1010933404324

Breshears, D. D., Huxman, T. E., Adams, H. D., Zou, C. B., & Davison, J. E. (2008). Vegetation synchronously leans upslope as climate warms. *Proceedings of the National Academy of Sciences of the United States of America*, *105*(33), 11591–11592. https://doi.org/10.1073/pnas.0806579105

Brodley, C. E., & Friedl, M. A. (1999). Identifying Mislabeled Training Data. *Journal of Artificial Intelligence Research*, *11*, 131–167. https://doi.org/10.1613/jair.606

Callaghan, C. T., Santini, L., Spake, R., & Bowler, D. E. (2024). Population abundance estimates in conservation and biodiversity research. *Trends in Ecology & Evolution*, *39*(6), 515–523. https://doi.org/10.1016/j.tree.2024.01.012

Caswell, H. (2006). Matrix Population Models. In *Encyclopedia of Environmetrics*. John Wiley & Sons, Ltd. https://onlinelibrary.wiley.com/doi/abs/10.1002/9780470057339.vam006m

Chesson, P. (2000). Mechanisms of Maintenance of Species Diversity. *Annual Review of Ecology, Evolution, and Systematics*, *31*(Volume 31, 2000), 343–366. https://doi.org/10.1146/annurev.ecolsys.31.1.343

Chirici, G., McRoberts, R. E., Winter, S., Bertini, R., Brändli, U.-B., Asensio, I. A., Bastrup-Birk, A., Rondeux, J., Barsoum, N., & Marchetti, M. (2012). National forest inventory contributions to forest biodiversity monitoring. *Forest Science*, *58*(3), 257–268. https://doi.org/10.5849/forsci.12-003

Connolly, S. R., Keith, S. A., Colwell, R. K., & Rahbek, C. (2017). Process, mechanism, and modeling in macroecology. *Trends in Ecology & Evolution*, *32*(11), 835–844. https://doi.org/10.1016/j.tree.2017.08.011

Crimmins, S. M., Dobrowski, S. Z., Greenberg, J. A., Abatzoglou, J. T., & Mynsberge, A. R. (2011). Changes in climatic water balance drive downhill shifts in plant species' optimum elevations. *Science*, *331*(6015), 324–327. https://doi.org/10.1126/science.1199040

Department of Conservation. (2015a). *Distribution of possums 2002–2014* [Map]. New Zealand's Environmental Reporting Series: The Ministry for the Environment and Statistics New Zealand. https://data.mfe.govt.nz/x/NDiRh9

Department of Conservation. (2015b). *Distribution of rats 2002–2014* [Map]. New Zealand's Environmental Reporting Series: The Ministry for the Environment and Statistics New Zealand. https://data.mfe.govt.nz/x/zbW9de

Department of Conservation. (2015c). *Distribution of red deer 2002–2014* [Map]. New Zealand's Environmental Reporting Series: The Ministry for the Environment and Statistics New Zealand. https://data.mfe.govt.nz/x/dyKrZA

Diamond, S. E. (2018). Contemporary climate- driven range shifts: Putting evolution back on the table. *Functional Ecology*, *32*(7), 1652–1665. https://doi.org/10.1111/1365-2435.13095

Doak, D. F., & Morris, W. F. (2010). Demographic compensation and tipping points in climate-induced range shifts. *Nature*, *467*(7318), 959–962. https://doi.org/10.1038/nature09439

Dormann, C. F., Elith, J., Bacher, S., Buchmann, C., Carl, G., Carré, G., Marquéz, J. R. G., Gruber, B., Lafourcade, B., Leitão, P. J., Münkemüller, T., McClean, C., Osborne, P. E., Reineking, B., Schröder, B., Skidmore, A. K., Zurell, D., & Lautenbach, S. (2013). Collinearity: a review of methods to deal with it and a simulation study evaluating their performance. *Ecography*, *36*(1), 27–46. https://doi.org/10.1111/j.1600-0587.2012.07348.x

Dormann, C. F., Schymanski, S. J., Cabral, J., Chuine, I., Graham, C., Hartig, F., Kearney, M., Morin, X., Römermann, C., Schröder, B., & Singer, A. (2012). Correlation and process in species distribution models: bridging a dichotomy: Bridging the correlation-process dichotomy. *Journal of Biogeography*, *39*(12), 2119–2131. https://doi.org/10.1111/j.1365-2699.2011.02659.x

Ehrlén, J., & Morris, W. F. (2015). Predicting changes in the distribution and abundance of species under environmental change. *Ecology Letters*.

https://doi.org/10.1111/ELE.12410

Etherington, T. R., Perry, G. L. W., & Wilmshurst, J. M. (2022). HOTRUNZ: an open-access 1 km resolution monthly 1910–2019 time series of interpolated temperature and rainfall grids with associated uncertainty for New Zealand. *Earth System Science Data*, *14*(6), 2817–2832. https://doi.org/10.5194/essd-14-2817-2022

Ewers, R. M., Kliskey, A. D., Walker, S., Rutledge, D., Harding, J. S., & Didham, R. K. (2006). Past and future trajectories of forest loss in New Zealand. *Biological Conservation*, *133*(3), 312–325. https://doi.org/10.1016/j.biocon.2006.06.018

Fawcett, T. (2006). An introduction to ROC analysis. *Pattern Recognition Letters*, *27*(8), 861–874. https://doi.org/10.1016/j.patrec.2005.10.010

Fei, S., Desprez, J. M., Potter, K. M., Jo, I., Knott, J. A., & Oswalt, C. M. (2017). Divergence of species responses to climate change. *Science Advances*, *3*(5), e1603055. https://doi.org/10.1126/sciadv.1603055

Fischer, H. S. (2015). On the combination of species cover values from different vegetation layers. *Applied Vegetation Science*, *18*(1), 169–170. https://doi.org/10.1111/avsc.12130

Foden, W. B., Young, B. E., Akçakaya, H. R., Garcia, R. A., Hoffmann, A. A., Stein, B. A., Thomas, C. D., Wheatley, C. J., Bickford, D., Carr, J. A., Hole, D. G., Martin, T. G., Pacifici, M., Pearce-Higgins, J. W., Platts, P. J., Visconti, P., Watson, J. E. M., & Huntley, B. (2019). Climate change vulnerability assessment of species. *Wiley Interdisciplinary Reviews. Climate Change*, *10*(1), e551. https://doi.org/10.1002/wcc.551

Forsyth, D., Wilmshurst, J., Allen, R., & Coomes, D. (2010). Impacts of introduced deer and extinct moa on New Zealand ecosystems. *New Zealand Journal of Ecology*, *34*(1), 48–65.

Franklin, J. (2023). Species distribution modelling supports the study of past, present and

future biogeographies. *Journal of Biogeography*, *50*(9), 1533–1545. https://doi.org/10.1111/jbi.14617

Frénay, B., & Verleysen, M. (2014). Classification in the presence of label noise: a survey. *IEEE Transactions on Neural Networks and Learning Systems*, *25*(5), 845–869. https://doi.org/10.1109/TNNLS.2013.2292894

Funk, J. L., Larson, J. E., Ames, G. M., Butterfield, B. J., Cavender-Bares, J., Firn, J., Laughlin, D. C., Sutton-Grier, A. E., Williams, L., & Wright, J. (2017). Revisiting the Holy Grail: using plant functional traits to understand ecological processes. *Biological Reviews of the Cambridge Philosophical Society*, *92*(2), 1156–1173. https://doi.org/10.1111/brv.12275

Galar, M., Fernández, A., Barrenechea, E., Bustince, H., & Herrera, F. (2011). An overview of ensemble methods for binary classifiers in multi-class problems: Experimental study on one-vs-one and one-vs-all schemes. *Pattern Recognition*, *44*(8), 1761–1776. https://doi.org/10.1016/j.patcog.2011.01.017

Gougherty, A. V., Prasad, A. M., Peters, M. P., Matthews, S. N., & Adams, B. T. (2024). Climate change and the emergence of no-analog forest assemblages in North America. *Global Change Biology*, *30*(12), e17605. https://doi.org/10.1111/gcb.17605

Goury, R., Thuiller, W., Abdulhak, S., Pache, G., Van Es, J., Bowler, D. E., Renaud, J., Violle, C., & Münkemüller, T. (2025). Recent vegetation shifts in the French Alps with winners outnumbering losers. *The Journal of Ecology*, *113*(11), 3275–3292. https://doi.org/10.1111/1365-2745.70159

Guillera-Arroita, G., Lahoz-Monfort, J. J., Elith, J., Gordon, A., Kujala, H., Lentini, P. E., McCarthy, M. A., Tingley, R., & Wintle, B. A. (2015). Is my species distribution model fit for purpose? Matching data and models to applications: Matching distribution models to applications. *Global Ecology and Biogeography: A Journal of Macroecology*,

24(3), 276–292. https://doi.org/10.1111/geb.12268

Guisan, A., & Thuiller, W. (2005). Predicting species distribution: offering more than simple habitat models. *Ecology Letters*, *8*(9), 993–1009. https://doi.org/10.1111/j.1461-0248.2005.00792.x

Guo, F., Lenoir, J., & Bonebrake, T. C. (2018). Land-use change interacts with climate to determine elevational species redistribution. *Nature Communications*, *9*(1), 1315. https://doi.org/10.1038/s41467-018-03786-9

Heino, M., Kummu, M., Makkonen, M., Mulligan, M., Verburg, P. H., Jalava, M., & Räsänen, T. A. (2015). Forest loss in protected areas and intact forest landscapes: A global analysis. *PloS One*, *10*(10), e0138918. https://doi.org/10.1371/journal.pone.0138918

Howard, C., Stephens, P. A., Pearce-Higgins, J. W., Gregory, R. D., & Willis, S. G. (2014). Improving species distribution models: the value of data on abundance. *Methods in Ecology and Evolution*, *5*(6), 506–513. https://doi.org/10.1111/2041-210X.12184

Hurst, J. M. (2022). *The Recce method for describing New Zealand vegetation - field manual*. Manaaki Whenua Press. https://doi.org/10.7931/P48H-ZB65

Jakoby, O., Lischke, H., & Wermelinger, B. (2019). Climate change alters elevational phenology patterns of the European spruce bark beetle (Ips typographus). *Global Change Biology*, *25*(12), 4048–4063. https://doi.org/10.1111/gcb.14766

Jia, S., Wang, X., Yuan, Z., Lin, F., Ye, J., Hao, Z., & Luskin, M. S. (2018). Global signal of top-down control of terrestrial plant communities by herbivores. *Proceedings of the National Academy of Sciences of the United States of America*, *115*(24), 6237–6242. https://doi.org/10.1073/pnas.1707984115

Johnston, A., Fink, D., Reynolds, M. D., Hochachka, W. M., Sullivan, B. L., Bruns, N. E., Hallstein, E., Merrifield, M. S., Matsumoto, S., & Kelling, S. (2015). Abundance models

improve spatial and temporal prioritization of conservation resources. *Ecological Applications: A Publication of the Ecological Society of America*, *25*(7), 1749–1756. https://doi.org/10.1890/14-1826.1

Klausmeyer, K. R., Shaw, M. R., MacKenzie, J. B., & Cameron, D. R. (2011). Landscape-scale indicators of biodiversity's vulnerability to climate change. *Ecosphere (Washington, D.C)*, *2*(8), art88. https://doi.org/10.1890/es11-00044.1

Laughlin, D. C. (2023). *Plant Strategies: The Demographic Consequences of Functional Traits in Changing Environments*. Oxford University Press. https://play.google.com/store/books/details?id=0aakzwEACAAJ

Lawlor, J. A., Comte, L., Grenouillet, G., Lenoir, J., Baecher, J. A., Bandara, R. M. W. J., Bertrand, R., Chen, I.-C., Diamond, S. E., Lancaster, L. T., Moore, N., Murienne, J., Oliveira, B. F., Pecl, G. T., Pinsky, M. L., Rolland, J., Rubenstein, M., Scheffers, B. R., Thompson, L. M., … Sunday, J. (2024). Mechanisms, detection and impacts of species redistributions under climate change. *Nature Reviews. Earth & Environment*, *5*(5), 351–368. https://doi.org/10.1038/s43017-024-00527-z

Lee-Yaw, J. A., L. McCune, J., Pironon, S., & N. Sheth, S. (2022). Species distribution models rarely predict the biology of real populations. *Ecography*, *2022*(6). https://doi.org/10.1111/ecog.05877

Lenoir, J., Bertrand, R., Comte, L., Bourgeaud, L., Hattab, T., Murienne, J., & Grenouillet, G. (2020). Species better track climate warming in the oceans than on land. *Nature Ecology & Evolution*. https://doi.org/10.1038/S41559-020-1198-2

Lenoir, J., Gégout, J.-C., Guisan, A., Vittoz, P., Wohlgemuth, T., Zimmermann, N. E., Dullinger, S., Pauli, H., Willner, W., & Svenning, J.-C. (2010). Going against the flow: potential mechanisms for unexpected downslope range shifts in a warming climate. *Ecography*, *33*(2), 295–303. https://doi.org/10.1111/j.1600-0587.2010.06279.x

Lenoir, J., Gégout, J.-C., Pierrat, J.-C., Bontemps, J.-D., & Dhôte, J.-F. (2009). Differences between tree species seedling and adult altitudinal distribution in mountain forests during the recent warm period (1986-2006). *Ecography*, *32*(5), 765–777. https://doi.org/10.1111/j.1600-0587.2009.05791.x

Lenoir, J., & Svenning, J.-C. (2015). Climate- related range shifts – a global multidimensional synthesis and new research directions. *Ecography*, *38*(1), 15–28. https://doi.org/10.1111/ecog.00967

Lichtenthaler, H. K. (1998). The stress concept in plants: an introduction. *Annals of the New York Academy of Sciences*, *851*(1 STRESS OF LIF), 187–198. https://doi.org/10.1111/j.1749-6632.1998.tb08993.x

Loh, W.-Y. (2011). Classification and regression trees: Classification and regression trees. *Wiley Interdisciplinary Reviews. Data Mining and Knowledge Discovery*, *1*(1), 14–23. https://doi.org/10.1002/widm.8

Louthan, A. M., Doak, D. F., & Angert, A. L. (2015). Where and When do Species Interactions Set Range Limits? *Trends in Ecology & Evolution*, *30*(12), 780–792. https://doi.org/10.1016/j.tree.2015.09.011

Lynn, J. S., Kazenel, M. R., Kivlin, S. N., & Rudgers, J. A. (2019). Context- dependent biotic interactions control plant abundance across altitudinal environmental gradients. *Ecography*, *42*(9), 1600–1612. https://doi.org/10.1111/ecog.04421

Lynn, J. S., Klanderud, K., Telford, R. J., Goldberg, D. E., & Vandvik, V. (2021). Macroecological context predicts species' responses to climate warming. *Global Change Biology*, *27*(10), 2088–2101. https://doi.org/10.1111/gcb.15532

Mazalla, L., & Diekmann, M. (2022). Regression to the mean in vegetation science. *Journal of Vegetation Science: Official Organ of the International Association for Vegetation Science*, *33*(2), e13117. https://doi.org/10.1111/jvs.13117

Meier, E. S., Kienast, F., Pearman, P. B., Svenning, J.-C., Thuiller, W., Araújo, M. B., Guisan, A., & Zimmermann, N. E. (2010). Biotic and abiotic variables show little redundancy in explaining tree species distributions. *Ecography*, *33*(6), 1038–1048. https://doi.org/10.1111/j.1600-0587.2010.06229.x

Molnar, C. (2022). *Interpretable machine learning. A Guide for Making Black Box Models Explainable* (2nd ed.). https://christophm.github.io/interpretable-ml-book

Mortimer, P. H., & White, E. P. (1967). Hepatotoxic substance in Brachyglottis repanda. *Nature*, *214*(5094), 1255–1256. https://doi.org/10.1038/2141255a0

Murray, B. G., & de Lange, P. J. (2011). Chromosomes and evolution in New Zealand endemic angiosperms and gymnosperms. In D. Bramwell & J. Caujape-castells (Eds.), *The Biology of Island Floras* (pp. 265–283). Cambridge University Press. https://doi.org/10.1017/cbo9780511844270.012

New Zealand Environmental Data Stack (NZEnvDS) - Manaaki Whenua - Landcare Research DataStore. (n.d.). Retrieved February 13, 2024, from https://datastore.landcareresearch.co.nz/dataset/nzenvds

O'Donnel, M. S., & Ignizio, D. A. (2012). *Bioclimatic predictors for supporting ecological applications in the conterminous United States* (No. 691). U.S. Geological Survey. https://pubs.usgs.gov/publication/ds691

Ovaskainen, O., & Soininen, J. (2011). Making more out of sparse data: hierarchical modeling of species communities. *Ecology*, *92*(2), 289–295. https://doi.org/10.1890/10-1251.1

Owens, H. L., Campbell, L. P., Dornak, L. L., Saupe, E. E., Barve, N., Soberón, J., Ingenloff, K., Lira-Noriega, A., Hensz, C. M., Myers, C. E., & Peterson, A. T. (2013). Constraints on interpretation of ecological niche models by limited environmental ranges on calibration areas. *Ecological Modelling*, *263*, 10–18.

https://doi.org/10.1016/j.ecolmodel.2013.04.011

Pagel, J., Treurnicht, M., Bond, W. J., Kraaij, T., Nottebrock, H., Schutte-Vlok, A., Tonnabel, J., Esler, K. J., & Schurr, F. M. (2020). Mismatches between demographic niches and geographic distributions are strongest in poorly dispersed and highly persistent plant species. *Proceedings of the National Academy of Sciences of the United States of America*, *117*(7), 3663–3669. https://doi.org/10.1073/pnas.1908684117

Parmesan, C., & Yohe, G. (2003). A globally coherent fingerprint of climate change impacts across natural systems. *Nature*, *421*(6918), 37–42. https://doi.org/10.1038/nature01286

Pearson, R. G., Raxworthy, C. J., Nakamura, M., & Townsend Peterson, A. (2007). ORIGINAL ARTICLE: Predicting species distributions from small numbers of occurrence records: a test case using cryptic geckos in Madagascar: Predicting species distributions with low sample sizes. *Journal of Biogeography*, *34*(1), 102–117. https://doi.org/10.1111/j.1365-2699.2006.01594.x

Pedregosa, F., Varoquaux, G., Gramfort, A., Michel, V., Thirion, B., Grisel, O., Blondel, M., Prettenhofer, P., Weiss, R., Dubourg, V., Vanderplas, J., Passos, A., Cournapeau, D., Brucher, M., Perrot, M., & Duchesnay, E. (2011). Scikit-learn: Machine Learning in Python. *Journal of Machine Learning Research*, *12*, 2825–2830.

Rapacciuolo, G., Maher, S. P., Schneider, A. C., Hammond, T. T., Jabis, M. D., Walsh, R. E., Iknayan, K. J., Walden, G. K., Oldfather, M. F., Ackerly, D. D., & Beissinger, S. R. (2014). Beyond a warming fingerprint: individualistic biogeographic responses to heterogeneous climate change in California. *Global Change Biology*, *20*(9), 2841–2855. https://doi.org/10.1111/gcb.12638

Reyer, C. P. O., Leuzinger, S., Rammig, A., Wolf, A., Bartholomeus, R. P., Bonfante, A., de Lorenzi, F., Dury, M., Gloning, P., Abou Jaoudé, R., Klein, T., Kuster, T. M., Martins, M.,

Niedrist, G., Riccardi, M., Wohlfahrt, G., de Angelis, P., de Dato, G., François, L., … Pereira, M. (2013). A plant's perspective of extremes: terrestrial plant responses to changing climatic variability. *Global Change Biology*, *19*(1), 75–89. https://doi.org/10.1111/gcb.12023

Rubenstein, M. A., Weiskopf, S. R., Bertrand, R., Carter, S. L., Comte, L., Eaton, M. J., Johnson, C. G., Lenoir, J., Lynch, A. J., Miller, B. W., Morelli, T. L., Rodriguez, M. A., Terando, A., & Thompson, L. M. (2023). Climate change and the global redistribution of biodiversity: substantial variation in empirical support for expected range shifts. *Environmental Evidence*, *12*(1), 1–21. https://doi.org/10.1186/s13750-023-00296-0

Salguero-Gómez, R., Jones, O. R., Archer, C. R., Buckley, Y. M., Che-Castaldo, J., Caswell, H., Hodgson, D., Scheuerlein, A., Conde, D. A., Brinks, E., de Buhr, H., Farack, C., Gottschalk, F., Hartmann, A., Henning, A., Hoppe, G., Römer, G., Runge, J., Ruoff, T., … Vaupel, J. W. (2015). The compadrePlant Matrix Database: an open online repository for plant demography. *The Journal of Ecology*, *103*(1), 202–218. https://doi.org/10.1111/1365-2745.12334

Scheepens, J. F., Deng, Y., & Bossdorf, O. (2018). Phenotypic plasticity in response to temperature fluctuations is genetically variable, and relates to climatic variability of origin, in Arabidopsis thaliana. *AoB Plants*, *10*(4), ly043. https://doi.org/10.1093/aobpla/ply043

Scott, W. A., & Hallam, C. J. (2003). Assessing species misidentification rates through quality assurance of vegetation monitoring. *Plant Ecology*, *165*(1), 101–115. https://doi.org/10.1023/a:1021441331839

Stephenson, N. (1998). Actual evapotranspiration and deficit: biologically meaningful correlates of vegetation distribution across spatial scales. *Journal of Biogeography*, *25*(5), 855–870. https://doi.org/10.1046/j.1365-2699.1998.00233.x

Taheri, S., Naimi, B., Rahbek, C., & Araújo, M. B. (2021). Improvements in reports of species redistribution under climate change are required. *Science Advances*, *7*(15). https://doi.org/10.1126/sciadv.abe1110

Thompson, I. D., Maher, S. C., Rouillard, D. P., Fryxell, J. M., & Baker, J. A. (2007). Accuracy of forest inventory mapping: Some implications for boreal forest management. *Forest Ecology and Management*, *252*(1), 208–221. https://doi.org/10.1016/j.foreco.2007.06.033

Thuiller, W., Münkemüller, T., Lavergne, S., Mouillot, D., Mouquet, N., Schiffers, K., & Gravel, D. (2013). A road map for integrating eco-evolutionary processes into biodiversity models. *Ecology Letters*, *16 Suppl 1*(0 1), 94–105. https://doi.org/10.1111/ele.12104

Tilman, D., May, R. M., Lehman, C. L., & Nowak, M. A. (1994). Habitat destruction and the extinction debt. *Nature*, *371*(6492), 65–66. https://doi.org/10.1038/371065a0

Tomppo, E., Gschwantner, T., Lawrence, M., & McRoberts, R. E. (Eds.). (2009). *National forest inventories: Pathways for common reporting* [PDF]. Springer. https://doi.org/10.1007/978-90-481-3233-1

Toome-Heller, M., Ho, W. W. H., Ganley, R. J., Elliott, C. E. A., Quinn, B., Pearson, H. G., & Alexander, B. J. R. (2020). Chasing myrtle rust in New Zealand: host range and distribution over the first year after invasion. *Australasian Plant Pathology*, *49*(3), 221–230. https://doi.org/10.1007/s13313-020-00694-9

Verheyen, K., Bažány, M., Chećko, E., Chudomelová, M., Closset-Kopp, D., Czortek, P., Decocq, G., De Frenne, P., De Keersmaeker, L., Enríquez García, C., Fabšičová, M., Grytnes, J.-A., Hederová, L., Hédl, R., Heinken, T., Schei, F. H., Horváth, S., Jaroszewicz, B., Jermakowicz, E., … Baeten, L. (2018). Observer and relocation errors matter in resurveys of historical vegetation plots. *Journal of Vegetation Science: Official Organ of the International Association for Vegetation Science*, *29*(5), 812–823.

https://doi.org/10.1111/jvs.12673

Villellas, J., Doak, D. F., García, M. B., & Morris, W. F. (2015). Demographic compensation among populations: what is it, how does it arise and what are its implications? *Ecology Letters*, *18*(11), 1139–1152. https://doi.org/10.1111/ele.12505

Williams, J. W., Jackson, S. T., & Kutzbach, J. E. (2007). Projected distributions of novel and disappearing climates by 2100 AD. *Proceedings of the National Academy of Sciences of the United States of America*, *104*(14), 5738–5742. https://doi.org/10.1073/pnas.0606292104

Wiser, S. K., Bellingham, P. J., & Burrows, L. E. (2001). Managing biodiversity information: development of New Zealand's National Vegetation Survey databank. *New Zealand Journal of Ecology*, *25*(2).

Wisz, M. S., Hijmans, R. J., Li, J., Peterson, A. T., Graham, C. H., Guisan, A., & NCEAS Predicting Species Distributions Working Group†. (2008). Effects of sample size on the performance of species distribution models. *Diversity & Distributions*, *14*(5), 763–773. https://doi.org/10.1111/j.1472-4642.2008.00482.x

Woodall, C. W., Oswalt, C. M., Westfall, J. A., Perry, C. H., Nelson, M. D., & Finley, A. O. (2009). An indicator of tree migration in forests of the eastern United States. *Forest Ecology and Management*, *257*(5), 1434–1444. https://doi.org/10.1016/j.foreco.2008.12.013

Woodman, T. L., Arendarczyk, B., Winkler, K., Henry, R. C., Eigenbrod, F., Burslem, D. F. R. P., Alexander, P., & Travis, J. M. J. (2026). High-resolution land-use maps from 1960 to 2100. *One Earth (Cambridge, Mass.)*, *9*(2), 101525. https://doi.org/10.1016/j.oneear.2025.101525

Wyse, S., School of Environment, University of Auckland, Private Bag 92019, Auckland 1142, New Zealand, Wilmshurst, J., Burns, B., & Perry, G. (2018). New Zealand forest dynamics: a review of past and present vegetation responses to disturbance, and

development of conceptual forest models. *New Zealand Journal of Ecology*, *42*(2). https://doi.org/10.20417/nzjecol.42.18

Zotov, V. D. (1938). An Outline of the Vegetation and Flora of the Tararua Mountains. *Transactions and Proceedings of the NZ Institute*.

Zurell, D., Franklin, J., König, C., Bouchet, P. J., Dormann, C. F., Elith, J., Fandos, G., Feng, X., Guillera-Arroita, G., Guisan, A., Lahoz-Monfort, J. J., Leitão, P. J., Park, D. S., Peterson, A. T., Rapacciuolo, G., Schmatz, D. R., Schröder, B., Serra-Diaz, J. M., Thuiller, W., … Merow, C. (2020). A standard protocol for reporting species distribution models. *Ecography*. https://doi.org/10.1111/ECOG.04960

7. Summary of Results

This thesis is motivated by the goal of understanding changes in biodiversity from the local to the landscape scale across New Zealand from the recent past into the late 21st century. To maximise ecological and conservation relevance, these changes need to be understood in a spatially, temporally, and taxonomically explicit manner, identifying where, when, and which species will change, and how these changes compound to overall plant biodiversity. Second, the goal is to find mechanistic explanations of community changes, based on plant functional traits and metrics derived from them. Lastly, this thesis aims to implement and demonstrate the usability of several generic and broadly applicable methodological advances in the imputation of trait data, the cleaning of forest inventory surveys, assessment of community turnover and abundance shifts. In the following sections, I outline the key results from the three papers and relate them to the aforementioned goals. The discussion chapter outlines how these results interact.

7.1 Biodiversity paper (BdP)

BdP addresses the contradictions in biodiversity trends and shows how monotonous trends across different biomes compound into a unimodal or saturating global trend, which is highly influenced by socioeconomic choices. Using New Zealand as a model, it develops a two-part framework that first models area changes across biomes and then uses species distributions along different environmental gradients to assess how well-matched species are to these changing biomes (termed “affinity” in this paper). The biome area model captures the metapopulation aspect of shared feedback mechanisms across biomes, allowing them to maintain a species pool under nearly identical climatic conditions (e.g., grasslands and forests) (Pausas and Bond 2021). The species affinities, on the other hand, capture the responses of individual species and are more closely related to SDM models, following the recent findings that constraining taxon-specific responses through community properties can improve SDM performance (Caradima et al. 2019). This approach advances the field by linking habitat redistribution and niche matching into a unified, scale-explicit framework that can reveal non-linear, transient, and scenario-dependent biodiversity trajectories.

Key results of this paper are:

1. New Zealand’s flora is projected to undergo thermophilisation, with different biomes affected differently.
2. Cold-adapted biomes (alpine, tussock grasslands and beech forests) are projected to contract in spatial extent but, due to relaxed lower thermal limits, allow for a potential increase in species richness through colonisation by warm-adapted species.

3. Warm-adapted biomes are projected to expand in area but to become increasingly taxonomically homogenised. This is likely explained by increased filtering at the upper thermal limit, which favours generalists with broad thermal tolerances.
4. At the landscape scale, these contradictory responses combine to produce an initial increase in biodiversity potential, which, depending on the socioeconomic scenario, either saturates or declines, forming a “peak biodiversity” window.
5. The non-linear “peak biodiversity” response is only visible at the landscape scale encompassing the entirety of New Zealand, not at the biome scale, as most biomes exhibit monotonous, if not linear, projections.
6. Other variables (precipitation, precipitation seasonality, and temperature diurnal and annual ranges) have a much smaller, but predominantly negative, impact on biodiversity potential.
7. Biome area changes are expected to be driven by the expansion of shrubs and contraction of alpine biomes and progress at a pace comparable to 20th-century observations of global biodiversity, positioning New Zealand as a model for global biodiversity changes.
8. Projection uncertainty increases sharply toward the end of the century and is dominated by socioeconomic pathways (SSPs), creating an effective cut-off for projections around 2070 at SSP3-4.6.

This paper concludes that species richness change is projected to neither uniformly decline nor increase, but vary across different parts of the study area. While these trends might be confounded by interactions between climatic drivers, as well as species’ ability to effectively track the climate, it nonetheless provides an explanation of the broad trends species richness might take in New Zealand.

7.2 Traits paper (TrP)

TrP analyses changes in functional traits, moments and indices of 120 widespread species in New Zealand's forests from 1984 - 2020. Moving beyond species richness alone, it quantifies the rate of species turnover in distinct forest types, their functional reorganisation under warming and drying trends, and attributes these changes to specific taxonomic groups using a null-model approach. The studied traits pertain to growth form (plant height, stem specific density, diaspore mass), leaf morphology (specific leaf area, nitrogen content), and leaf isotope ratios ($\Delta^{15}N$ and $\Delta^{13}C$), which were obtained through field work, the TRY database (Kattge et al. 2020), and data imputation (Debastiani et al. 2021). Combining higher-order trait moments (Enquist et al. 2015) and multi-trait diversity indices (Pla et al. 2012). The study advances our understanding of biodiversity change from phenomenological thermophilisation patterns to biome-specific assembly mechanisms driven by specific taxonomic and functional groups.

Key findings of this paper are:

1. On average across all forest areas the mean temperatures increased and precipitation declined (albeit with a large variance including increases in some areas). This resulted in increases of taxonomic and functional richness and decreasing functional similarity between species.
2. These changes were collectively driven by lower-elevation, warm-adapted species migrating north to south.
3. The increase in functional richness and functional similarity between species was below expectations given the increase in species richness, indicating an abiotic limitation on the expansion of functional space.

4. Exotic species disproportionately expanded functional trait space, while native species primarily increased richness.
5. Warm-adapted podocarp forests shifted predominantly towards drought-avoidant strategies with low water use efficiency, which may be enabled by elevated CO_2.
6. Cold-adapted forests exhibited strong functional restructuring despite slower rates of turnover. The changes were likely caused by two mechanisms: a disturbance-driven increase in early-successional species with acquisitive traits, and an expansion of species with conservative traits but ectomycorrhizal associations, which provide a competitive advantage under elevated CO_2.
7. The mixed forests ecotone showed high species turnover but minimal directional functional change.

This paper also provides a few methodological advances:

8. A simple leave-one-out procedure for data imputation error assessment is developed and minimised using easily obtainable species' taxonomic rather than phylogenetic trees.
9. A null-model-based method for identifying groups with contributions to temporal trends of any metric above what is expected by chance (e.g. contribution of exotic species to functional richness increase).
10. A novel rate of turnover per year metric is developed, which quantifies the percentage of a species' currently occupied basal area that needs to shift per year to match the observed species turnover.

On the one hand, the findings confirm previously observed trends of thermophilisation (Feeley et al. 2020) and the expansion of exotic species (Goury et al. 2025), but on the other hand reveal distinct functional trajectories underlying these trends. This suggests that ecosystem functions (such as productivity) and services (such as carbon sequestration capacity) might change differently in different biomes, despite similar climatic pressures, warranting closer observation of functional aspects in the future to understand, quantify, and project these changes.

7.3 ATI Paper (AtiP)

This paper develops the Abundance Trend Indicator (ATI). This machine-learning framework infers the environmental conditions that cause species' within-range abundance shifts, which predate shifts in range margins and are thus early indicators of biodiversity rearrangement. ATI reveals environmental drivers of shifts in the 86 most common New Zealand species and quantifies their vulnerability by identifying species with predominantly declining abundance within their realised niche. The main contribution of this paper for New Zealand is the identification of climatically vulnerable species and drivers of abundance shifts, and more generally, the novel method utilising existing forest inventory data to model within-range abundance shifts, which typically require rarer time-series observations.

The main results are:

1. Based on climatic variables, 19 of 86 studied species, with a collective canopy cover of 20.51% of the forested area, are projected to decline, while all other

species abundances are projected to increase, indicating an increase in overall species richness.

2. The strongest abundance shifts happen towards lower mean annual temperature, higher precipitation, lower latitude, and higher elevation, matching global observations.
3. While the average shifts follow predictable patterns, species typically have highly individual responses, determined by their tolerance to various stresses such as grazing pressure, climate fluctuations, or soil pH.
4. Because of the individual responses, all 14 covariates have similar importance scores.

Methodical advances are:

5. Building on an established machine learning framework a procedure for removing presumably erroneous data is developed and applied.
6. Once or twice, resurveyed plots distributed across the landscape are combined into a single dataset to infer abundance changes for individual species. The validity of this method is validated using a synthetic species experiment.

ATI scales sparse forest inventory surveys into a spatially explicit framework capable of capturing and predicting subtle within-range abundance changes, and highlights the necessity of studying them to understand species' responses to climate change. Moreover, ATI revealed the multi-dimensional nature of these responses, which, while following the global mean of upwards and polewards migration, are typically far from the mean. In particular, this calls for the transition towards a more process and trait-based understanding of biodiversity rearrangement.

The three papers address complementary aspects of climate-driven biodiversity change. The ATI and Biodiversity papers focus on goal 1, providing a landscape-scale diagnosis of species richness, uncovering how individual biomes and species can differ in their responses, yet produce responses consistent with monotonous global trends. Their collective finding is that New Zealand's local species richness has increased and is projected to increase in the short term, but that this process is unsustainable and comes at the cost of losing habitat specialists living at the edges of the abiotic filter. The traits paper, focusing on goal 2, explains these observations and reveals the proliferation of generalist and early-successional species in a changing, increasingly unstable climate. The use of rarely employed isotope data additionally hints at the importance of mycorrhizal associations and CO_2 fertilisation in this process. Lastly, for goal 3, all papers contribute and validate methodical advancements focused on extracting deeper insights through new methods, data imputation, and cleaning, using forest inventory and trait data.

8. General Discussion

The collective findings of this thesis suggest that biodiversity change must be understood, predicted, and managed across multiple interacting spatial scales, each of which requires different data, methods, and conservation responses. Conceptually, this heterogeneity helps explain why biodiversity trajectories under climate change often appear inconclusive or contradictory across studies, while practically it implies that both

conservation strategies and methodological approaches must be tailored to scale (Table 1). The central argument of this chapter is therefore that biodiversity research should explicitly connect these nested scales rather than treat them in isolation. While the Biodiversity paper provides a first step towards realising such a nested modelling framework, this discussion extends the concept and outlines directions for developing a more complete and predictive nested scale model. Collectively, this thesis proposes that integrating models and existing data sources can unlock new insights from already abundant forest inventory data, deepening our understanding of climate-driven change and expanding the scope for effective mitigation.

Table 1*: Summary of the nested scale framework presented in this thesis and its implications on different ecological processes and questions.*

	Species Level	Community Level	Biome Level
Processes	Demographic responses to climate	Species interactions & assembly	Climate constraints & disturbance regimes
Biodiversity signal	Abundance trends & range shifts	Turnover & functional structure	Biome area shifts & species pools
Role of traits	Niche breadth & life-history strategy	Assembly mechanisms & resilience	Dominant strategies shaping biomes
Major threats	Pathogens, demographic decline	Invasions, interaction disruption	Climate tipping points, shrinking areas

Conservation focus	Protect vulnerable species	Maintain diversity & resilience	Preserve refugia & disturbance regimes

8.1 Mechanisms of forest reassembly across ecological scales

The results of this thesis address the question of spatial scale in biodiversity projections, proposing that accurate projections of biodiversity trajectories need to combine multiple nested levels of scale: Individual species responses (AtiP), which are constrained by regional species pools, species interactions, and assembly mechanisms at the community scale (Mouquet et al. 2003) (TrP), which in turn are constrained by spatially larger biome-specific stabilising mechanisms, such as seed-banks, recurring disturbances, and meta-population dynamics (Pausas and Bond 2020) (BdP). Due to interactions among responses across spatial scales, biodiversity becomes increasingly variable and difficult to interpret at larger scales. While local observations often show both increases and declines centred around zero, regional and global patterns integrate these heterogeneous dynamics, leading to greater ambiguity in the magnitude and direction of biodiversity change (Dornelas et al. 2023), raising the question of whether large-scale biodiversity trends can be inferred from local observations (Valdez et al. 2023). While each paper is primarily concerned with one level of this nested hierarchy, in the following discussion, I explore how these three levels interact to produce complex biodiversity

trajectories that yield contradictory findings about biodiversity, and propose how this framework can be cast as a predictive model.

The ATI analysis revealed highly individualistic responses of species to climate change (Figs 6.2 and 6.4), which regionally compounded into divergent biodiversity trajectories (Fig. 4.4C; (Midolo et al. 2025)). However, these species-level responses alone may not fully explain the resulting biodiversity patterns. Because species gains and losses occur asynchronously, they can disrupt or enhance interactions among species, such as pollination or pest dynamics (Weaver and Mallinger 2022). As a result, changes in ecological interactions do not necessarily track changes in species richness (Valiente-Banuet et al. 2015), and because ecological interactions influence species survival and reproduction rates, neglecting them confounds biodiversity estimates (Urban et al. 2016). Co-occurrence is an important interaction, as well. For example, the presence of bryophytes in alpine regions prevented the establishment of new colonists, thus indirectly mediating biodiversity trajectories (Vandvik et al. 2020). Consequently, bottom-up models that aggregate biodiversity projections from individual species are limited in their ability to capture long-term biodiversity dynamics, as exemplified by the stark contrast between overall increased species richness New Zealand-wide (AtiP) and very distinct increasing and decreasing trajectories when broken down by biome or environmental driver (BdP). The disconnect between local and regional patterns is a globally observed pattern (Dornelas et al. 2023), calling for the incorporation of community and biome-level assembly processes in biodiversity studies.

Community assembly processes and regional species pools jointly determine the species' ability and efficacy to respond to climate change and how this response translates to biodiversity change (Lawton 1999). For example, in cold-adapted beech forests, rising temperatures open previously unavailable climatic niches that can be filled by migrants from warmer-adapted forests possessing distinct functional traits, leading to strong functional shifts and declining taxonomic evenness (Figs. 5.3 and 5.4). Because these new warm-adapted species are regionally present and functionally different, the principle of limiting similarity (Abrams 1983) allows them to be continuously added to the community, resulting in projected increases in species richness (Fig. 4.4). In contrast, warm-adapted podocarp forests experience long-term species losses (Fig. 4.4). Here the same warm-adapted species are functionally redundant, limiting the establishment of species with new strategies and instead increasing functional similarity among species (Figs. 5.2 and 5.3). Across both systems, exotic species and their unique trait combinations are consistently able to proliferate and reshape community trait structure (Fig. 5.3). Because assembly rules depend on trait distributions, they remain informative even under increasingly novel species compositions and environmental conditions (Kerr et al. 2025; Staples et al. 2022), offering a mechanistic basis for anticipating regional biodiversity outcomes.

At the landscape scale, community assembly processes are constrained by biome-level dynamics. Biomes encompass not only species assemblages but also shared disturbance regimes, often mediated by the species themselves (e.g. fire-prone grasslands), persistent seed banks, and networks of mutualists and antagonists that collectively stabilise ecosystem structure and define biome identity (Pausas and Bond 2021). These shared

properties can synchronise community responses to environmental change and produce threshold dynamics, where gradual climatic shifts trigger abrupt transitions in vegetation state, such as forests converting to savannas (Lenton et al. 2023; Trisos et al. 2020). Because such stable state transitions involve strong ecological feedbacks, they are rarely reversible and therefore represent critical constraints on future biodiversity trajectories (Mata et al. 2025). Since these thresholds are initiated by climatic stressors such as drought (Van Passel et al. 2024), the biodiversity paper modelled the biome distribution directly from climate data (Fig. 4.2), successfully reproducing globally observed patterns of shrub expansion (Myers-Smith et al. 2011) and contraction of temperature-limited ecosystems (Keenan and Riley 2018). Differences in biome area trajectories (Fig 4.4) and their associated species pools compounded to a non-linear trajectory, not apparent from the predominantly increasing individual species tendencies (Fig 6.2), helping reconcile often contradictory biodiversity observations (Steinbauer et al. 2018; Pereira et al. 2024; García Criado et al. 2025). Biome-level processes therefore, shape biodiversity trajectories beyond the effects of individual species responses or community processes.

The presented three-layer framework suggests that large-scale biodiversity change cannot be understood from local species-level responses, because responses to climate change, even for the same species, will differ depending on the regional community and abiotic context in which it is nested. Conversely, inferring local species responses fails without adequate data editing, as implemented by the ATI, suggesting that larger-scale assembly processes manifest as noise in local species responses and similarly preclude inferring species-specific responses. Species-specific responses will trigger higher-level community feedback. In New Zealand, for instance, the dominance of the

early-successional tree fern *Cyathea medullaris* in disturbed landscapes initiates a successional trajectory towards podocarp forests, whereas the shrub *Kunzea ericoides* leads to more fire-prone shrublands (Brock et al. 2018). Presently, climate change may be altering the relative contributions of these two successional pathways in New Zealand (Fig. B9 and discussion in TrP), highlighting how individual species' responses may influence communities of hundreds of species over decades. At the biome level, forest canopies buffer climatic extremes more efficiently than shrublands, if sufficient moisture is available (Davis et al. 2019; De Frenne et al. 2019), thus providing long-term stability for their species assemblages. Unifying species responses, community assembly mechanisms, and biome redistribution within a single conceptual and modelling framework will therefore enable more precise biodiversity forecasts and, in turn, more efficiently guide conservation.

BdP projects a ~16.5% contraction of beech forest and transition towards mixed broadleaf forest, consistent with earlier projections of upslope lowland migration and broadleaf invasion of Nothofagus forests (Leathwick et al. 1996) and with the more recent 12.1% decline in climatically suitable Nothofagus habitat under SSP3-7.0 (Mathias et al. 2023). Its projected reorganisation of tussock grasslands towards beech forest also aligns with observed grassland-to-shrubland succession in eastern Otago (Ropars et al. 2018), a proposed intermediate stage towards beech forest (Wyse et al. 2018), although climate-based projections compress the successional stages. However, *Nothofagus* species were a relative outlier in AtiP[1], with abundance shifting downslope against the dominant direction of change, potentially explaining previously observed static treelines (Cullen et al. 2001). AtiP also showed negative climate impacts on kāmahi (*Pterophylla*

[1] These results refer to the accompanying website: https://ati-nz-predictions-7e6f3d514735.herokuapp.com/

reacemosa), thus explaining its higher mortality reported by (Richardson et al. 2009), but only on the North Island, where that study was conducted. On the South Island, where kāmahi is far more widespread, climate effects were reversed. Together, these comparisons indicate that local or species-specific responses may not generalise across New Zealand and that direct climatic effects may be more important than their limited representation in the existing literature suggests (Macinnis-Ng et al. 2021). My analyses therefore provide a first nationwide attempt to address this long-standing gap in New Zealand ecology.

8.2 The role of Functional Traits in Biodiversity Projections

Plant functional traits mediate biodiversity trajectories at all three levels (species, communities and biomes) and are therefore central to understanding how local and global biodiversity are connected (Liu et al. 2024). At the species level, functional traits mediate the range of environmental conditions a species can tolerate (niche breadth) and life-history strategy (Laughlin 2023). For example, depending on whether climate shifts towards or away from a species' optimal conditions, specialists with narrow niches either thrive or go extinct, while generalists merely expand or contract (Zhigila et al. 2023); TrP). Since specialists are more common in harsh environments, such as mountains (Boulangeat et al. 2012), biodiversity changes are typically more pronounced there (Fig. 4.4C). Similar contrasts can occur across life-history strategies, where annual species (such as those typical of grasslands) have lower extinction risk due to better adaptation to an increasingly unstable climate (Poppenwimer et al. 2023). Species traits can therefore

determine which sets of species are more or less likely to persist in a changing climate, and have the potential to improve biodiversity forecasts.

At the community levels, functional traits can be combined to functional diversity indices, which capture the community assembly mechanisms driving change (Villéger et al. 2008), and ecosystem properties, such as resilience to climate stress (Anderegg et al. 2018), while community-weighted trait distributions reveal where these changes occur spatially and temporally (Wieczynski et al. 2019; Enquist et al. 2015). Using this method, we found strong functional shifts (Fig. 5.4) driven by disturbances as well as filtering along a moisture availability gradient in cold-adapted forests, despite their slow rates of turnover (Fig. B8) and only modest increase in species richness (Fig. 5.2). Warm-adapted podocarp forests, on the other hand, showed higher species turnover rates, but almost no functional changes (Fig 5.4). If projecting into the future, cold-adapted biomes gained species, warm-adapted forests lost them (Fig 4.4C). As higher functional and taxonomic diversity usually confers a protective effect on ecosystems (de Bello et al. 2021), the functional analysis suggests a loss of resilience in warm-adapted forests due to a lack of species with traits that confer greater fitness at elevated temperatures. Moreover, the functional analysis of New Zealand's forests revealed the protective effect of ectomycorrhizal fungal associations of the dominant beeches,under elevated CO_2 levels, and might explain why these forests change more slowly, despite rising temperatures. Collectively, these findings demonstrate how trait studies can help explain changes in biodiversity.

Despite the insights functional traits can provide, using them for prediction has eluded researchers (Funk et al. 2017; Lavorel and Garnier 2002), resulting in largely descriptive studies (Wieczynski et al. 2019; Li and Prentice 2024; Díaz et al. 2016), which do not always live up to the promise of predicting demographic outcomes needed for biodiversity projections (Yang et al. 2018). One reason is the prevalence of easily measured leaf traits (Green et al. 2022) in trait databases such as TRY (Kattge et al. 2020), which limits what can be predicted from trait studies. For instance, measuring carbon and nitrogen isotope ratios in the traits paper revealed the impacts of elevated CO_2 under moisture limitation. Including them in biodiversity predictions, however, is currently infeasible because these traits are available for only a small number of species (Fig B3). While trait databases keep improving, and methodical innovations such as imputation (Poyatos et al. 2018; Penone et al. 2014) enable larger-scale syntheses (Andrew et al. 2025), at the present moment, the complexity of the trait-biodiversity relationship (Liu et al. 2024) and lack of data suggest using them primarily for the inference of community assembly mechanisms and as early indicators of change, rather than to predict biodiversity trajectories.

8.3 Opportunities for Conservation

Because biodiversity responses are governed by different processes at different spatial scales, conservation strategies must also operate across multiple levels. At the species level, monitoring demographic trends can identify species at risk before range contractions occur (Fig. 6.2). Combined with future projections, this approach can also reveal species that are currently thriving but will become mismatched with future climates (e.g. *C. pseudocuneata* in Fig. 1), indicating an accumulation of extinction debt

(Tilman et al. 1994). At the community level, functional analyses can reveal which communities would benefit from structural interventions, such as invasive species removal or predator control, to maintain functional and taxonomic diversity (Petri and Ibáñez 2025). Finally, biome-level biodiversity projections can guide spatial conservation planning by identifying climate refugia that enable the long-term persistence of many species (Hoffmann 2022), as well as informing disturbance management, such as grazing regulation or controlled burning, to support ecosystem recovery (Múgica et al. 2021). Integrating these three levels enables conservation strategies that protect vulnerable species, maintain resilient communities, and safeguard landscapes capable of sustaining biodiversity in the long term.

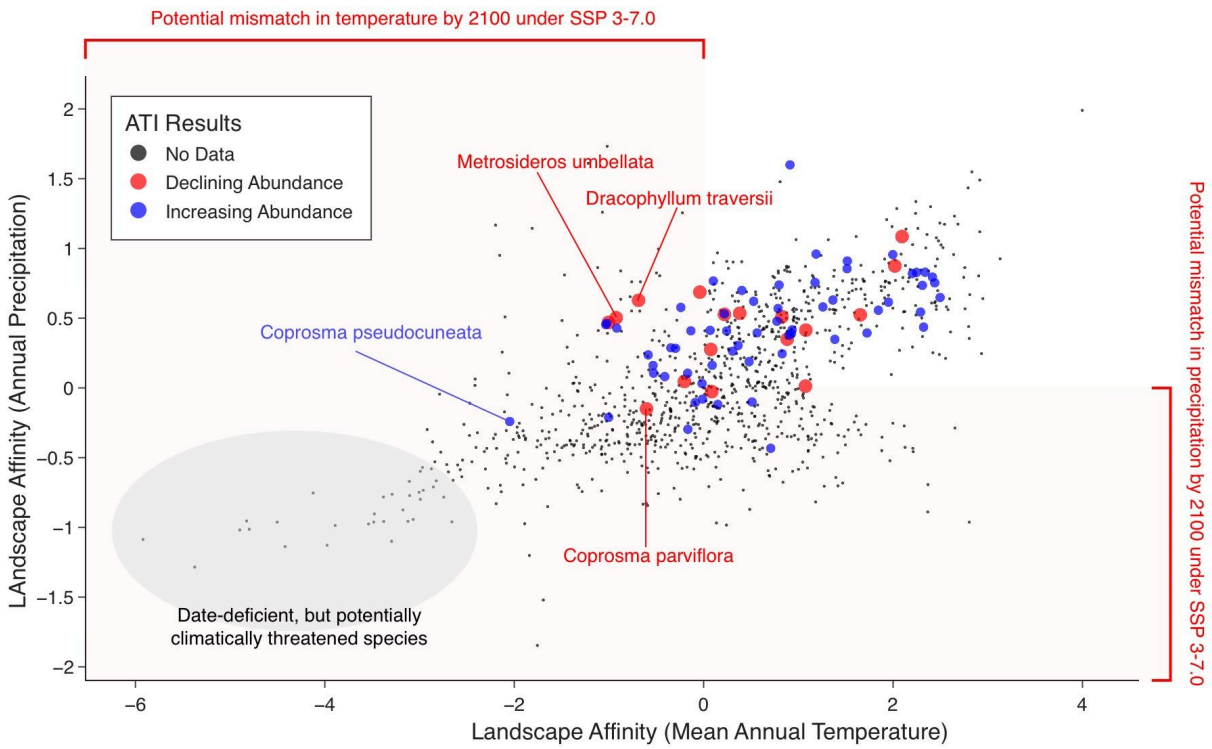


Figure 1: Vulnerability projections on the basis of landscape affinity derived from mean annual temperature (x-axis) and annual precipitation (y-axis) from the Biodiversity Paper for the year bracket 2080-2100 under SSP3-7.0. Negative values indicate the strength of a potential climatic mismatch between species' climatic preferences and the projected climatic conditions. Species with sufficient data to be analysed in the ATI paper (1960-2000) are displayed as red or blue dots depending on whether the mean ATI value was above 0.5 (species predominantly increasing in abundance) or below 0.5. Declining species are not expected to be clustered in the lower-right quadrant, as the ATI results use 20th century climate data, while landscape affinities are future projections.

While the results of this thesis require further refinement, particularly for rare species, they nevertheless illustrate how insights from multiple ecological scales can inform conservation decisions. At the species level, the ATI analysis identified species with declining abundance (Fig. 1 red dots). However, combined with a biome-level analysis from BdP, some of these species are projected to encounter improving climatic conditions (top right quadrant), whereas others face both declining abundance and worsening climatic suitability, and thus a risk for accelerated decline (e.g. *C. parviflora*, *M. umbellata*, or *D. traversii*). This perspective highlights how present demographic trajectories and future climate projections together can reveal emerging extinction debts long before range contractions become visible, and point to species, which are data-deficient but may become threatened in the future (Fig. 1 grey area). In a practical sense this approach also helps communicate to the public and policy makers why biodiversity can initially increase (Walther et al. 2002; Goury et al. 2025) but may eventually decline, broadening our potential for climate change mitigation and the communication around it (Jackson and Sax 2010).

Individual conservation responses for these patterns depend on their species traits and ecological context. For example, *M. umbellata* (Fig. 1) is susceptible to the recently introduced pathogen *Austropuccinia psidii* (myrtle rust) (Toome-Heller et al. 2020), as well as browsing by introduced bushtail possum (Coleman et al. 1985), suggesting interventions like fungicides (Pathan et al. 2020) to maintain viable populations or genetically informed breeding (Chen et al. 2025) to prevent inbreeding within disconnected habitat patches (Balkwill et al. 2025), and predator control (Byrom et al. 2016). *D. traversii*, on the other hand is a montane species, which will experience shrinking habitats invaded by lowland species (Fig 4.2D), suggesting interventions such as removal of invading shrubs (Kudo et al. 2017; Losapio et al. 2024). Finally, lowland species such as *C. pseudocuneata* and *C. parviflora* are subject to habitat fragmentation from land-use change and can be supported through careful choice of spatially connected conservation areas (Domisch et al. 2019; Segan et al. 2016). At the community level, the increasing homogeneity of warm-adapted forests (Fig. 4.4C), paired with a strong influence of exotic species on functional changes in all forests (Fig 5.3), suggests that limiting the impact of invasive species, and particularly in New Zealand, predator control (Byrom et al. 2016), are key for maintaining long-term forest health and resilience. These preliminary findings illustrate how conservation strategies can emerge from integrating species-level vulnerability with community and biome-scale ecological dynamics.

8.3.1 Implications for New Zealand

Although the analyses presented here operate at broad spatial and conceptual scales, they can contribute to conservation decisions in New Zealand. For instance, a growing concern in the face of climate change is the identification of “sleeper weeds”, species which persist at low density until specific climate conditions cause rapid proliferation

(Hulme 2020; Groves 1999) and could be realised using existing forest inventory data within a climate affinity framework (BdP). Similarly, AtiP quantified the impact of invasive mammalian herbivores on tree distribution, and if applied using finer-scale maps and distribution models (Shepherd et al. 2018), this approach could make pest management more efficient by identifying habitats and communities severely limited by herbivore pressure. Finally, the trait data presented here could be used to design functionally coherent communities adapted to future climates, an approach already applied in restoration using trait-based species selection (Ostertag et al. 2015), and consistent with a broader shift away from restoring historical states toward managing future-proof ecosystem function (Hobbs et al. 2011). These applications suggest that the main contribution of this thesis to conservation in New Zealand lies in improving the tools available to detect emerging risks, interpret ecological change, and guide future decision-making.

8.4 Methodological and conceptual advances

Ecological inference is often limited by noise in observational data, which confounds the relationship between environmental predictors and biodiversity responses. To address this, the ATI paper applied an established editing framework (Frénay and Verleysen 2014) to identify and remove unlikely observations prior to modelling species responses, which remains uncommon in ecology. By filtering out noisy data points using a separate model, this approach reduces the signal-to-noise ratio (Section C1.3 and Fig. C4) and allows underlying trends to emerge more clearly (Fig. C11). This contrasts with the alternative of increasing model complexity or adding predictors, which requires more training data

(Ferchichi et al. 2022) and may not improve inference if most variation is driven by a few dominant patterns (Transtrum et al. 2015), allowing simpler and more interpretable models to recover the main signal. Data editing approaches are broadly applicable to classification problems. For example, the BdP paper classified biomes using satellite-derived maps and interpolated climate data (Fig. A3), which can contain erroneous pixels, detectable by the editing procedure. This type of data is ubiquitous in ecology (Amiraslanova et al. 2025), and errors strongly influence classification outcomes (Pelletier et al. 2017). Data editing, as explored by AtiP, therefore has the potential to improve the reliability of large-scale ecological inference for a wide range of problems, without increasing the data requirements of more complex algorithms, such as deep neural networks (Pichler and Hartig 2023).

Trait-based analyses are often constrained by limited data availability, as many ecologically informative traits are costly or difficult to measure (Green et al. 2022). TrP addressed this by combining field data, the TRY database (Kattge et al. 2020), and data imputation to fill 16.75% of missing trait values, thereby almost doubling the number of species with a full set of traits from 59 to 108. The proposed leave-one-out metric estimated imputation errors at ~3.5–15% of interspecific variation, with the highest errors for $\Delta^{15}N$ and the lowest for diaspore mass. In lieu of phylogenetic data, we used taxonomic eigenvectors (Diniz-Filho et al. 1998) enabled by readily available taxonomies (https://phylot.biobyte.de/), to leverage evolutionary trait conservation and improve performance. This approach allowed reaching the four to eight trait threshold required to accurately capture community assembly processes (Laughlin 2014) and apply functional diversity metrics (Villéger et al. 2008) more broadly (Fig. B3). Importantly, including rare

traits such as carbon and nitrogen isotopes revealed otherwise overlooked processes related to CO_2 fertilisation and mycorrhizal associations. While implemented at the species level, this framework can be extended to individual-level data, enabling analyses at finer spatial scales where intraspecific variation is important (Albert et al. 2011). Overall, taxonomically informed trait imputation provides a simple and effective way to expand trait coverage and improve inference of community-level biodiversity change.

Biodiversity projections include thousands of species, increasing their data demand, especially when pairwise interactions, which scale as $O(N^2)$, are modelled. The BdP addressed this problem by combining two data sources into a hierarchical model that uses abundant satellite data to model biome-wide communities and forest inventory data to model individual species' climatic preferences. This hierarchical integration of community and individual responses is known to improve accuracy in biodiversity models (Caradima et al. 2019; D'Amen et al. 2017) and may be an efficient alternative to stacked SDMs, which ignore biotic interactions, or joint SDMs, which require more data (Cowans et al. 2025), but do not always improve performance (Zurell et al. 2020). Despite their often better performance, hierarchical models are often constrained by higher complexity (Mokany et al. 2011; Zipkin et al. 2023; D'Amen et al. 2017). A recently developed alternative are nested SDMs, which model single species at multiple spatial resolutions, improving generalisation performance (Goicolea et al. 2025; Guisan et al. 2025). In contrast, the BdP framework introduces a conceptual shift by modelling biome identity as an upper-level community composition constraint on individual species responses in a geographical area. However, borrowing from nested SDMs, both levels can be modelled with an established SDM-type algorithm, reducing complexity, while explicitly incorporating biotic

community structure into biodiversity predictions, yet without substantially increasing data or computational demands.

Since neither ecological data nor mechanisms are precise, biodiversity projections should explicitly incorporate uncertainty from multiple sources (Brodie et al. 2022; Thuiller et al. 2019). In this thesis, uncertainty was addressed through null models in TrP and through decomposition and explicit quantification in BdP (Morley et al. 2020; Velazco et al. 2024). Importantly, uncertainty itself provides ecological insight. For example, uncertainty in shrubland expansion was primarily driven by SSP scenarios, whereas in forests it was more sensitive to the choice of climate model (Fig A6), pointing to different levers for improvement of predictions: policy action versus better climate models. Uncertainty analysis also revealed that changes in cold-adapted biomes are easier to predict than those in warm-adapted biomes (Fig. 4.2C) and that predictions to 2100 are feasible only under SSP2-4.5 or below. In TrP, null models revealed that increases in functional richness were largely driven by rising species richness and identified the contributing species groups, thereby reducing uncertainty by distinguishing deterministic assembly processes from patterns expected under stochastic variation (Fig 5.2 and 5.3). Finally, modelling biodiversity trajectories in BdP with a non-linear approach reduced uncertainty and uncovered potential saturation or peak dynamics that linear models fail to capture. Collectively, these approaches demonstrate how, rather than being a limitation, uncertainty can be a tool for diagnosing drivers of change, improving predictive accuracy, and increasing confidence in biodiversity forecasts.

The methodical advances in this thesis illustrate how ecologists can obtain deeper insights from existing datasets, through various methods: by removing noise (AtiP),

imputing missing values (TrP), combining simple models into more powerful hierarchical models (BdP), and leveraging uncertainty as a feature (BdP, TrP). Collectively, these approaches can help address major challenges of growing but error-prone public databases (Maldonado et al. 2015), which can be edited, sparse past occurrence data, which can be leveraged through novel algorithms (Guo et al. 2024), AtiP), and the need for more meaningful trait data, which can be extended by imputation (Urban et al. 2016). This suggests choosing a shift in ecological modelling towards integration of results across scales, a combination of data sets and transparent uncertainty quantification over increasing algorithmic complexity.

8.5 Limitations and future research

Data availability constrained all approaches in this thesis, requiring the omission of several key biological processes that are likely to influence biodiversity trajectories. Disturbance regimes and the frequency of climatic events such as thunderstorms, droughts, or wildfires interact with a changing climate, affecting successional trajectories and the composition of future forests (Brock et al. 2018; Viljur et al. 2022). Similarly, spatially-explicit projections of land-use change remain rare, despite being recognised as a major driver of species' range shifts and biodiversity patterns (Titeux et al. 2016; Guo et al. 2018). Finally, data on the distribution and abundance of herbivores, pollinators and pests, can improve predictions, as exemplified by the importance of red deer presence for abundance changes of some species (Fig. 6.5B). These missing layers represent important drivers of biodiversity change that are currently mostly unavailable

for New Zealand in a spatially-explicit form, but could be readily implemented into the AtiP and BdP frameworks should they become available in the future. Incorporating these drivers could improve both predictive accuracy and ecological realism, and enable spatially-explicit assessments of management interventions. For instance, local explanation techniques (Ryo et al. 2021) can quantify how herbivore presence influences species pools at each location and guide pest control by identifying locations where interventions are most effective (Byrom et al. 2016).

Both AtiP and BdP rely on occurrence and abundance data that may be in disequilibrium with current environmental conditions, leading the models to deviate from underlying ecological responses (Elith et al. 2010; Sandel et al. 2025), especially for rare or rapidly spreading exotic species. Moreover, increasingly novel global climatic and biotic conditions (Kerr et al. 2025) force the models to extrapolate beyond what is captured by the training data, degrading their performance as dissimilarity increases (Charney et al. 2021). While carefully limited in both papers, extrapolation fundamentally limits the forecast horizon of the models (Fig 4.2A) (Petchey et al. 2015). As biodiversity rearrangements result from changes in fitness, which are mediated by traits (Laughlin 2023), these traits can be incorporated into our models to yield a more mechanistic model that explicitly captures physiological constraints and vital rates, providing more robust predictions for novel environments. However, the availability of data, the understanding of trait-environment associations, and the complexity of the modelling approaches make this step challenging (Fenollosa et al. 2025; Comte et al. 2024; Evans et al. 2016). Efforts to aggregate necessary data in databases, such as COMPADRE for demographic rates (Salguero-Gómez et al. 2015) or TRY for functional traits (Kattge et al. 2020) are underway

and motivate the transition towards more mechanistic predictions, although coverage remains limited for remote regions such as New Zealand.

While functional traits provide a pathway towards more mechanistic predictions, their application is subject to important limitations. First, intraspecific variation (ITV) was not accounted for in TrP, as the paper focused on a broad spatial scale, at which between-species differences likely overtake ITV (Albert et al. 2011; Lajoie and Vellend 2015). However, especially for plastic and context-dependent traits such as $\Delta^{15}N$ and $\Delta^{13}C$, this can significantly influence outcomes (Henn et al. 2018; Körner et al. 2016). Second, trait values can change through evolutionary processes, which can improve predictions if modelled (Cotto et al. 2017). Both of these processes could be integrated to transform the singular values of functional indices and community-weighted means, currently implemented by TrP, into probability distributions. The first approach, likely limited by data availability, is the use of Bayesian frameworks, which become increasingly demanding as the number of traits and species increases (Laughlin et al. 2012). Alternatively, Monte Carlo methods, which repeatedly run the model with varying trait values according to ITV, offer a more flexible, model-agnostic approach (Abrego et al. 2025). While computationally intensive, this approach could be integrated into TrP to propagate uncertainty in trait values and assess the conditions under which species persistence requires shifts in trait values, thereby linking trait variability to potential evolutionary or plastic responses.

Aside from incorporating additional data and more complex models, a major opportunity for generating further insights lies in combining the approaches developed across the

three papers. For instance, AtiP or an SDM in general, could incorporate functional traits as additional predictor variables, which has been shown to improve performance (Pollock et al. 2012; Wang and Wan 2021), particularly for exotic species that play a major role in the functional reorganisation of New Zealand's forests (Fig. 5.3). These models could replace the single-dimensional environmental affinity used in BdP with a multidimensional representation of species suitability, integrating multiple environmental drivers into a unified metric. Because the fitness advantage conferred by specific traits is context-dependent (Pérez-Ramos et al. 2019; Thomas and Vesk 2017) (e.g. frost tolerance becomes less relevant under warming climates), and BdP assumes static climatic envelopes for biomes, such models could be trained separately for each biome and combined into an ensemble prediction weighted by biome likelihood. Ensemble approaches have been shown to improve predictive performance (Hao et al. 2020; El Alaoui and Idri 2025), and importantly, provide an estimate of uncertainty (Noce et al. 2017). Lastly, implementing model-agnostic local explanation techniques (Ryo et al. 2021) would allow spatially explicit attribution of environmental drivers, improving interpretability. Collectively, integrating these approaches into a unified framework offers a pathway towards a more mechanistic, scalable, and explainable model for predicting biodiversity change under future environmental conditions.

8.6 Conclusion

Biodiversity change does not unfold at a single level of organisation. As this thesis has shown, it emerges through nested processes operating across individual species, communities, and biomes, each with distinct mechanisms, signals, and conservation

implications (Table 1). Species respond through range and abundance shifts, communities show altered functional structure as they are filtered by different abiotic filters, whereas biomes constrain these changes through broader climatic limits, disturbance regimes, and persistent feedbacks. Understanding climate-driven forest reassembly, therefore, requires linking these mechanisms into a unified framework that can explain why biodiversity may increase in one place, decline in another, and how these trajectories develop over time, forming sometimes transient peaks, as identified here. Seen in this way, apparently contradictory biodiversity trends are not evidence of failure in ecological understanding, but of a complex, interconnected system whose responses are inherently scale-dependent, nonlinear, context-specific, and dynamic.

This thesis suggests, that while our understanding of natural ecosystems will certainly benefit from more and better data, we can already extract practically relevant insights from what we have to guide conservation decisions at every level of spatial hierarchy: From protecting vulnerable species, to maintaining community resilience by controlling herbivores and invasive species, and safeguarding climatic refugia and biome processes at larger spatial scales. Indeed, many of these ideas are already realised in New Zealand (Byrom et al. 2016; McCarthy et al. 2021). The challenge for ecological restoration might therefore lie in translating existing understanding into sustained action, as scientific evidence alone is only the first and smallest component of impact (Posner et al. 2016). Climate change and biodiversity loss are ultimately human-made problems that need human-made solutions, including broad public education, policy change, and, most importantly, entrepreneurs able to catalyse this change (Veleva 2021). The need to align human activity with ecological limits has long been recognised, both in early accounts of human environmental impact (Marsh 1874) and in visions of a more holistic,

science-informed society a century later (Marquis 1968). Yet, despite this longstanding awareness, meaningful change keeps eluding us. The advances presented in this thesis will therefore only matter if they are acted upon.

9. Acknowledgements

I acknowledge the use of ChatGPT-5 (accessed in 2025 and 2026) to support creation of the outline for this thesis, suggest reorganization of segments and improve the clarity and flow of the wording. All AI-generated suggestions were reviewed, revised, and approved by the authors, who take full responsibility for the accuracy and integrity of the work. Analysis scripts were partially generated using Claude 3.5 Sonnet and Github CoPilot (February 2026). All AI-generated code was reviewed, tested, and revised by me, to confirm accuracy and reproducibility of results. I acknowledge the use of data drawn from the Natural Forest plot data collected between January 1969 and December 2024 by the Land Use and Carbon Analysis System (LUCAS) program for the Ministry for the Environment, and the NZ Department of Conservation. Data were acquired using the National Vegetation Survey databank (https://nvs.landcareresearch.co.nz/).

10. References

Abrams, P. (1983). The theory of limiting similarity. *Annual Review of Ecology and Systematics*, *14*(1), 359–376. https://doi.org/10.1146/annurev.es.14.110183.002043

Abrego, N., Niittynen, P., Kemppinen, J., & Ovaskainen, O. (2025). Joint species-trait distribution modeling: The role of intraspecific trait variation in community assembly. *Ecology*, *106*(9), e70174. https://doi.org/10.1002/ecy.70174

Ackerly, D. d., & Monson, R. k. (2003). Waking the Sleeping Giant: The Evolutionary Foundations of Plant Function. *International Journal of Plant Sciences*, *164*(S3), S1–S6. https://doi.org/10.1086/374729

Adde, A., Rey, P.-L., Fopp, F., Petitpierre, B., Schweiger, A. K., Broennimann, O., Lehmann, A., Zimmermann, N. E., Altermatt, F., Pellissier, L., & Guisan, A. (2023). Too many candidates: Embedded covariate selection procedure for species distribution modelling with the covsel R package. *Ecological Informatics*, *75*(102080), 102080. https://doi.org/10.1016/j.ecoinf.2023.102080

Albert, C. H., Grassein, F., Schurr, F. M., Vieilledent, G., & Violle, C. (2011). When and how should intraspecific variability be considered in trait-based plant ecology? *Perspectives in Plant Ecology, Evolution and Systematics*, *13*(3), 217–225. https://doi.org/10.1016/j.ppees.2011.04.003

Alexander, J. M., Chalmandrier, L., Lenoir, J., Burgess, T. I., Essl, F., Haider, S., Kueffer, C., McDougall, K., Milbau, A., Nuñez, M. A., Pauchard, A., Rabitsch, W., Rew, L. J., Sanders, N.

J., & Pellissier, L. (2018). Lags in the response of mountain plant communities to climate change. *Global Change Biology*, *24*(2), 563–579. https://doi.org/10.1111/gcb.13976

Amiraslanova, M., Hasanova, R., & Macnunlu, K. (2025). Vegetation mapping by satellite, drone imagery, machine learning and deep learning. *Dokladi Na Blgarskata Akademiya Na Naukite. Comptes Rendus de l'Academie Bulgare Des Sciences*, *78*(4), 571–578. https://doi.org/10.7546/crabs.2025.04.10

Anderegg, L. D. L. (2023). Why can't we predict traits from the environment? *The New Phytologist*, *237*(6), 1998–2004. https://doi.org/10.1111/nph.18586

Anderegg, L. D. L., Berner, L. T., Badgley, G., Sethi, M. L., Law, B. E., & HilleRisLambers, J. (2018). Within-species patterns challenge our understanding of the leaf economics spectrum. *Ecology Letters*, *21*(5), 734–744. https://doi.org/10.1111/ele.12945

Anderegg, W. R. L., Konings, A. G., Trugman, A. T., Yu, K., Bowling, D. R., Gabbitas, R., Karp, D. S., Pacala, S., Sperry, J. S., Sulman, B. N., & Zenes, N. (2018). Hydraulic diversity of forests regulates ecosystem resilience during drought. *Nature*, *561*(7724), 538–541. https://doi.org/10.1038/s41586-018-0539-7

Andrew, S. C., Martín-Forés, I., Guerin, G. R., Coleman, D., Falster, D. S., Wenk, E., Wright, I. J., & Gallagher, R. V. (2025). Mapping plant functional traits using gap- filled datasets to inform management and modelling. *Global Ecology and Biogeography: A Journal of Macroecology*, *34*(10), e70136. https://doi.org/10.1111/geb.70136

Balkwill, C. G., Koot, E., Ritchie, P., Chagné, D., & Deslippe, J. R. (2025). Adaptive potential of Syzygium maire, a critically threatened habitat specialist tree species in Aotearoa New Zealand. *Evolutionary Applications*, *18*(10), e70161. https://doi.org/10.1111/eva.70161

Beaumont, L. J., Graham, E., Duursma, D. E., Wilson, P. D., Cabrelli, A., Baumgartner, J. B., Hallgren, W., Esperón-Rodríguez, M., Nipperess, D. A., Warren, D. L., Laffan, S. W., & VanDerWal, J. (2016). Which species distribution models are more (or less) likely to

project broad-scale, climate-induced shifts in species ranges? *Ecological Modelling*, *342*, 135–146. https://doi.org/10.1016/j.ecolmodel.2016.10.004

Beckage, B., Osborne, B., Gavin, D. G., Pucko, C., Siccama, T., & Perkins, T. (2008). A rapid upward shift of a forest ecotone during 40 years of warming in the Green Mountains of Vermont. *Proceedings of the National Academy of Sciences of the United States of America*, *105*(11), 4197–4202. https://doi.org/10.1073/pnas.0708921105

Bertness, M. D., & Callaway, R. (1994). Positive interactions in communities. *Trends in Ecology & Evolution*, *9*(5), 191–193. https://doi.org/10.1016/0169-5347(94)90088-4

Boënnec, M., Dakos, V., & Devictor, V. (2024). Sources of confusion in global biodiversity trends. *Oikos (Copenhagen, Denmark)*, *2024*(6), e10732. https://doi.org/10.1111/oik.10732

Bohner, T., & Diez, J. (2020). Extensive mismatches between species distributions and performance and their relationship to functional traits. *Ecology Letters*, *23*(1), 33–44. https://doi.org/10.1111/ele.13396

Boulangeat, I., Lavergne, S., Van Es, J., Garraud, L., & Thuiller, W. (2012). Niche breadth, rarity and ecological characteristics within a regional flora spanning large environmental gradients: Plant niche breadth and ecological characteristics. *Journal of Biogeography*, *39*(1), 204–214. https://doi.org/10.1111/j.1365-2699.2011.02581.x

Bourel, B., Joly, A., Servajean, M., Bettinger, S., Sanabria-Fernández, J. A., & Mouillot, D. (2025). From presence-only to abundance species Distribution Models using transfer learning. *Ecology Letters*, *28*(7), e70177. https://doi.org/10.1111/ele.70177

Breiman, L. (2001). Random Forests. *Machine Learning*, *45*(1), 5–32. https://doi.org/10.1023/A:1010933404324

Breshears, D. D., Huxman, T. E., Adams, H. D., Zou, C. B., & Davison, J. E. (2008). Vegetation synchronously leans upslope as climate warms. *Proceedings of the National Academy*

of Sciences of the United States of America, *105*(33), 11591–11592. https://doi.org/10.1073/pnas.0806579105

Brock, J., Perry, G., Lee, W. G., Schwendenmann, L., & Burns, B. (2018). Pioneer tree ferns influence community assembly in northern New Zealand forests. *New Zealand Journal of Ecology*, *42*(1), 18–30. https://doi.org/10.20417/NZJECOL.42.5

Brockerhoff, E. G., Barbaro, L., Castagneyrol, B., Forrester, D. I., Gardiner, B., González-Olabarria, J. R., Lyver, P. O., Meurisse, N., Oxbrough, A., Taki, H., Thompson, I. D., van der Plas, F., & Jactel, H. (2017). Forest biodiversity, ecosystem functioning and the provision of ecosystem services. *Biodiversity and Conservation*, *26*(13), 3005–3035. https://doi.org/10.1007/s10531-017-1453-2

Brodie, S. J., Thorson, J. T., Carroll, G., Hazen, E. L., Bograd, S., Haltuch, M. A., Holsman, K. K., Kotwicki, S., Samhouri, J. F., Willis-Norton, E., & Selden, R. L. (2020). Trade- offs in covariate selection for species distribution models: a methodological comparison. *Ecography*, *43*(1), 11–24. https://doi.org/10.1111/ecog.04707

Brodie, S., Smith, J. A., Muhling, B. A., Barnett, L. A. K., Carroll, G., Fiedler, P., Bograd, S. J., Hazen, E. L., Jacox, M. G., Andrews, K. S., Barnes, C. L., Crozier, L. G., Fiechter, J., Fredston, A., Haltuch, M. A., Harvey, C. J., Holmes, E., Karp, M. A., Liu, O. R., … Kaplan, I. C. (2022). Recommendations for quantifying and reducing uncertainty in climate projections of species distributions. *Global Change Biology*, *28*(22), 6586–6601. https://doi.org/10.1111/gcb.16371

Bruelheide, H., Dengler, J., Purschke, O., Lenoir, J., Jiménez-Alfaro, B., Hennekens, S. M., Botta-Dukát, Z., Chytrý, M., Field, R., Jansen, F., Kattge, J., Pillar, V. D., Schrodt, F., Mahecha, M. D., Peet, R. K., Sandel, B., van Bodegom, P., Altman, J., Alvarez-Dávila, E., … Jandt, U. (2018). Global trait-environment relationships of plant communities. *Nature Ecology & Evolution*, *2*(12), 1906–1917. https://doi.org/10.1038/s41559-018-0699-8

Bu, W., Huang, J., Xu, H., Zang, R., Ding, Y., Li, Y., Lin, M., Wang, J., & Zhang, C. (2018). Plant Functional Traits Are the Mediators in Regulating Effects of Abiotic Site Conditions on Aboveground Carbon Stock-Evidence From a 30 ha Tropical Forest Plot. *Frontiers in Plant Science*, *9*, 1958. https://doi.org/10.3389/fpls.2018.01958

Buckley, L. B., Cannistra, A. F., & John, A. (2018). Leveraging organismal biology to forecast the effects of climate change. *Integrative and Comparative Biology*, *58*(1), 38–51. https://doi.org/10.1093/icb/icy018

Buisson, L., Thuiller, W., Casajus, N., Lek, S., & Grenouillet, G. (2010). Uncertainty in ensemble forecasting of species distribution. *Global Change Biology*, *16*(4), 1145–1157. https://doi.org/10.1111/j.1365-2486.2009.02000.x

Byrom, A. E., Innes, J., & Binny, R. N. (2016). A review of biodiversity outcomes from possum-focused pest control in New Zealand. *Wildlife Research (East Melbourne, Melbourne, Vic.)*, *43*(3), 228. https://doi.org/10.1071/wr15132

Caradima, B., Schuwirth, N., & Reichert, P. (2019). From individual to joint species distribution models: A comparison of model complexity and predictive performance. *Journal of Biogeography*, *46*(10), 2260–2274. https://doi.org/10.1111/jbi.13668

Cardinale, B. J., Duffy, J. E., Gonzalez, A., Hooper, D. U., Perrings, C., Venail, P., Narwani, A., Mace, G. M., Tilman, D., Wardle, D. A., Kinzig, A. P., Daily, G. C., Loreau, M., Grace, J. B., Larigauderie, A., Srivastava, D. S., & Naeem, S. (2012). Biodiversity loss and its impact on humanity. *Nature*, *486*(7401), 59–67. https://doi.org/10.1038/nature11148

Carnicer, J., Domingo-Marimon, C., Ninyerola, M., Camarero, J. J., Bastos, A., López-Parages, J., Blanquer, L., Rodríguez-Fonseca, B., Lenton, T. M., Dakos, V., Ribas, M., Gutiérrez, E., Peñuelas, J., & Pons, X. (2019). Regime shifts of Mediterranean forest carbon uptake and reduced resilience driven by multidecadal ocean surface temperatures. *Global Change Biology*, *25*(8), 2825–2840.

https://doi.org/10.1111/gcb.14664

Carta, A., Fernández-Pascual, E., Gioria, M., Müller, J. V., Rivière, S., Rosbakh, S., Saatkamp, A., Vandelook, F., & Mattana, E. (2022). Climate shapes the seed germination niche of temperate flowering plants: a meta-analysis of European seed conservation data. *Annals of Botany*, *129*(7), 775–786. https://doi.org/10.1093/aob/mcac037

Caruso, C. M., Maherali, H., & Martin, R. A. (2020). A Meta-analysis of Natural Selection on Plant Functional Traits. *International Journal of Plant Sciences*, *181*(1), 44–55. https://doi.org/10.1086/706199

Caruso, C. M., Mason, C. M., & Medeiros, J. S. (2020). The Evolution of Functional Traits in Plants: Is the Giant Still Sleeping? *International Journal of Plant Sciences*, *181*(1), 1–8. https://doi.org/10.1086/707141

Castro-Díez, P., Pauchard, A., Traveset, A., & Vilà, M. (2016). Linking the impacts of plant invasion on community functional structure and ecosystem properties. *Journal of Vegetation Science: Official Organ of the International Association for Vegetation Science*, *27*(6), 1233–1242. https://doi.org/10.1111/jvs.12429

Cavanaugh, K. C., Kellner, J. R., Forde, A. J., Gruner, D. S., Parker, J. D., Rodriguez, W., & Feller, I. C. (2014). Poleward expansion of mangroves is a threshold response to decreased frequency of extreme cold events. *Proceedings of the National Academy of Sciences of the United States of America*, *111*(2), 723–727. https://doi.org/10.1073/pnas.1315800111

Chacón-Labella, J., Hinojo-Hinojo, C., Bohner, T., Castorena, M., Violle, C., Vandvik, V., & Enquist, B. J. (2023). How to improve scaling from traits to ecosystem processes. *Trends in Ecology & Evolution*, *38*(3), 228–237. https://doi.org/10.1016/j.tree.2022.10.007

Chapin, F. S., 3rd, Zavaleta, E. S., Eviner, V. T., Naylor, R. L., Vitousek, P. M., Reynolds, H. L.,

Hooper, D. U., Lavorel, S., Sala, O. E., Hobbie, S. E., Mack, M. C., & Díaz, S. (2000). Consequences of changing biodiversity. *Nature*, *405*(6783), 234–242. https://doi.org/10.1038/35012241

Charney, N. D., Record, S., Gerstner, B. E., Merow, C., Zarnetske, P. L., & Enquist, B. J. (2021). A test of species distribution model transferability across environmental and geographic space for 108 western north American tree species. *Frontiers in Ecology and Evolution*, *9*(689295). https://doi.org/10.3389/fevo.2021.689295

Chauvier, Y., Descombes, P., Guéguen, M., Boulangeat, L., Thuiller, W., & Zimmermann, N. E. (2022). Resolution in species distribution models shapes spatial patterns of plant multifaceted diversity. *Ecography*, *2022*(10), e05973. https://doi.org/10.1111/ecog.05973

Chauvier, Y., Thuiller, W., Brun, P., Lavergne, S., Descombes, P., Karger, D. N., Renaud, J., & Zimmermann, N. E. (2021). Influence of climate, soil, and land cover on plant species distribution in the European Alps. *Ecological Monographs*, *91*(2), e01433. https://doi.org/10.1002/ecm.1433

Chave, J., Coomes, D., Jansen, S., Lewis, S. L., Swenson, N. G., & Zanne, A. E. (2009). Towards a worldwide wood economics spectrum. *Ecology Letters*, *12*(4), 351–366. https://doi.org/10.1111/j.1461-0248.2009.01285.x

Chen, I.-C., Hill, J. K., Ohlemüller, R., Roy, D. B., & Thomas, C. D. (2011). Rapid range shifts of species associated with high levels of climate warming. *Science*, *333*(6045), 1024–1026. https://doi.org/10.1126/science.1206432

Chen, S. H., Yap, J.-Y. S., Viler, V., Stehn, C., Sandhu, K. S., Percival, J., Pegg, G. S., Menzies, T., Jones, A., Guo, K., Giblin, F. R., Cohen, J., Edwards, R. J., Rossetto, M., & Bragg, J. G. (2025). Pathways to recovery: Genomics and resistance assays for tree species devastated by the myrtle rust pathogen. *Molecular Ecology*, *34*(16), e70030.

https://doi.org/10.1111/mec.70030

Chirici, G., McRoberts, R. E., Winter, S., Bertini, R., Brändli, U.-B., Asensio, I. A., Bastrup-Birk, A., Rondeux, J., Barsoum, N., & Marchetti, M. (2012). National forest inventory contributions to forest biodiversity monitoring. *Forest Science*, *58*(3), 257–268. https://doi.org/10.5849/forsci.12-003

Clark, C. M., Flynn, D. F. B., Butterfield, B. J., & Reich, P. B. (2012). Testing the link between functional diversity and ecosystem functioning in a Minnesota grassland experiment. *PloS One*, *7*(12), e52821. https://doi.org/10.1371/journal.pone.0052821

Coleman, J., Green, W. Q., & Polson, J. (1985). Diet of brushtail possums over a pasture-alpine gradient in Westland, New Zealand. *New Zealand Journal of Ecology*, *8*, 21–35. https://newzealandecology.org/nzje/1644

Comte, L., Bertrand, R., Diamond, S., Lancaster, L. T., Pinsky, M. L., Scheffers, B. R., Baecher, J. A., Bandara, R. M. W. J., Chen, I.-C., Lawlor, J. A., Moore, N. A., Oliveira, B. F., Murienne, J., Rolland, J., Rubenstein, M. A., Sunday, J., Thompson, L. M., Villalobos, F., Weiskopf, S. R., & Lenoir, J. (2024). Bringing traits back into the equation: A roadmap to understand species redistribution. *Global Change Biology*, *30*(4), e17271. https://doi.org/10.1111/gcb.17271

Connolly, S. R., Keith, S. A., Colwell, R. K., & Rahbek, C. (2017). Process, mechanism, and modeling in macroecology. *Trends in Ecology & Evolution*, *32*(11), 835–844. https://doi.org/10.1016/j.tree.2017.08.011

Cornwell, W. K., Schwilk, L. D. W., & Ackerly, D. D. (2006). A trait-based test for habitat filtering: convex hull volume. *Ecology*, *87*(6), 1465–1471. https://doi.org/10.1890/0012-9658(2006)87%255B1465:attfhf%255D2.0.co;2

Cotto, O., Wessely, J., Georges, D., Klonner, G., Schmid, M., Dullinger, S., Thuiller, W., & Guillaume, F. (2017). A dynamic eco-evolutionary model predicts slow response of

alpine plants to climate warming. *Nature Communications*, *8*(1), 15399. https://doi.org/10.1038/ncomms15399

Cowans, A., Bigatà, A. B., & Sutherland, C. (2025). Sample size considerations for species co-occurrence models. *Ecology*, *106*(8), e70175. https://doi.org/10.1002/ecy.70175

Crase, B., Liedloff, A., Vesk, P. A., Fukuda, Y., & Wintle, B. A. (2014). Incorporating spatial autocorrelation into species distribution models alters forecasts of climate-mediated range shifts. *Global Change Biology*, *20*(8), 2566–2579. https://doi.org/10.1111/gcb.12598

Crimmins, S., Dobrowski, S., Greenberg, J., Abatzoglou, J., & Mynsberge, A. R. (2011). Changes in Climatic Water Balance Drive Downhill Shifts in Plant Species' Optimum Elevations. *Science*. https://doi.org/10.1126/SCIENCE.1199040

Cullen, L. E., Stewart, G. H., Duncan, R. P., & Palmer, J. G. (2001). Disturbance and climate warming influences on New Zealand Nothofagus tree- line population dynamics: *Disturbance and climate warming at tree line*. *The Journal of Ecology*, *89*(6), 1061–1071. https://doi.org/10.1111/j.1365-2745.2001.00628.x

Da, R., Hao, M., Qiao, X., Zhang, C., & Zhao, X. (2022). Unravelling trait-environment relationships at local and regional scales in temperate forests. *Frontiers in Plant Science*, *13*, 907839. https://doi.org/10.3389/fpls.2022.907839

D'Amen, M., Rahbek, C., Zimmermann, N. E., & Guisan, A. (2017). Spatial predictions at the community level: from current approaches to future frameworks: Methods for community-level spatial predictions. *Biological Reviews of the Cambridge Philosophical Society*, *92*(1), 169–187. https://doi.org/10.1111/brv.12222

Davies, S. C., Thompson, P. L., Gomez, C., Nephin, J., Knudby, A., Park, A. E., Friesen, S. K., Pollock, L. J., Rubidge, E. M., Anderson, S. C., Iacarella, J. C., Lyons, D. A., MacDonald, A., McMillan, A., Ward, E. J., Holdsworth, A. M., Swart, N., Price, J., & Hunter, K. L. (2023).

Addressing uncertainty when projecting marine species' distributions under climate change. *Ecography*, *2023*(11), e06731. https://doi.org/10.1111/ecog.06731

Davis, K. T., Dobrowski, S. Z., Holden, Z. A., Higuera, P. E., & Abatzoglou, J. T. (2019). Microclimatic buffering in forests of the future: the role of local water balance. *Ecography*, *42*(1), 1–11. https://doi.org/10.1111/ecog.03836

Dawson, T. E., Mambelli, S., Plamboeck, A. H., Templer, P. H., & Tu, K. P. (2002). Stable isotopes in plant ecology. *Annual Review of Ecology and Systematics*, *33*(1), 507–559. https://doi.org/10.1146/annurev.ecolsys.33.020602.095451

de Bello, F., Lavorel, S., Hallett, L. M., Valencia, E., Garnier, E., Roscher, C., Conti, L., Galland, T., Goberna, M., Májeková, M., Montesinos-Navarro, A., Pausas, J. G., Verdú, M., E-Vojtkó, A., Götzenberger, L., & Lepš, J. (2021). Functional trait effects on ecosystem stability: assembling the jigsaw puzzle. *Trends in Ecology & Evolution*, *36*(9), 822–836. https://doi.org/10.1016/j.tree.2021.05.001

De Frenne, P., Zellweger, F., Rodríguez-Sánchez, F., Scheffers, B. R., Hylander, K., Luoto, M., Vellend, M., Verheyen, K., & Lenoir, J. (2019). Global buffering of temperatures under forest canopies. *Nature Ecology & Evolution*, *3*(5), 744–749. https://doi.org/10.1038/s41559-019-0842-1

Debastiani, V. J., Bastazini, V. A. G., & Pillar, V. D. (2021). Using phylogenetic information to impute missing functional trait values in ecological databases. *Ecological Informatics*, *63*(101315), 101315. https://doi.org/10.1016/j.ecoinf.2021.101315

Di Febbraro, M., Sallustio, L., Vizzarri, M., De Rosa, D., De Lisio, L., Loy, A., Eichelberger, B. A., & Marchetti, M. (2018). Expert-based and correlative models to map habitat quality: Which gives better support to conservation planning? *Global Ecology and Conservation*, *16*(e00513), e00513. https://doi.org/10.1016/j.gecco.2018.e00513

Díaz, S. (2025). Plant functional traits and the entangled phenotype. *Functional Ecology*,

39(5), 1144–1159. https://doi.org/10.1111/1365-2435.70017

Díaz, S., Kattge, J., Cornelissen, J. H. C., Wright, I. J., Lavorel, S., Dray, S., Reu, B., Kleyer, M., Wirth, C., Prentice, I. C., Garnier, E., Bönisch, G., Westoby, M., Poorter, H., Reich, P. B., Moles, A. T., Dickie, J., Gillison, A. N., Zanne, A. E., … Gorné, L. D. (2016). The global spectrum of plant form and function. *Nature*, *529*(7585), 167–171. https://doi.org/10.1038/nature16489

Díaz, S., Settele, J., Brondízio, E. S., Ngo, H. T., Agard, J., Arneth, A., Balvanera, P., Brauman, K. A., Butchart, S. H. M., Chan, K. M. A., Garibaldi, L. A., Ichii, K., Liu, J., Subramanian, S. M., Midgley, G. F., Miloslavich, P., Molnár, Z., Obura, D., Pfaff, A., … Zayas, C. N. (2019). Pervasive human-driven decline of life on Earth points to the need for transformative change. *Science (New York, N.Y.)*, *366*(6471), eaax3100. https://doi.org/10.1126/science.aax3100

Diniz-Filho, J. A. F., de Sant'Ana, C. E. R., & Bini, L. M. (1998). An eigenvector method for estimating phylogenetic inertia. *Evolution; International Journal of Organic Evolution*, *52*(5), 1247–1262. https://doi.org/10.1111/j.1558-5646.1998.tb02006.x

Díaz, S., & Cabido, M. (2001). Vive la différence: plant functional diversity matters to ecosystem processes. *Trends in Ecology & Evolution*, *16*(11), 646–655. https://doi.org/10.1016/s0169-5347(01)02283-2

Doak, D. F., & Morris, W. F. (2010). Demographic compensation and tipping points in climate-induced range shifts. *Nature*, *467*(7318), 959–962. https://doi.org/10.1038/nature09439

Dollinger, J., Brun, P., Sainte Fare Garnot, V., & Wegner, J. D. (2024). Sat-SINR: High-resolution species distribution models through satellite imagery. *ISPRS Annals of Photogrammetry Remote Sensing and Spatial Information Sciences*, *X-2–2024*, 41–48. https://doi.org/10.5194/isprs-annals-x-2-2024-41-2024

Domisch, S., Friedrichs, M., Hein, T., Borgwardt, F., Wetzig, A., Jähnig, S. C., & Langhans, S. D. (2019). Spatially explicit species distribution models: A missed opportunity in conservation planning? *Diversity & Distributions*, *25*(5), 758–769. https://doi.org/10.1111/ddi.12891

Dormann, C. F. (2007). Effects of incorporating spatial autocorrelation into the analysis of species distribution data. *Global Ecology and Biogeography: A Journal of Macroecology*, *16*(2), 129–138. https://doi.org/10.1111/j.1466-8238.2006.00279.x

Dormann, C. F., Elith, J., Bacher, S., Buchmann, C., Carl, G., Carré, G., Marquéz, J. R. G., Gruber, B., Lafourcade, B., Leitão, P. J., Münkemüller, T., McClean, C., Osborne, P. E., Reineking, B., Schröder, B., Skidmore, A. K., Zurell, D., & Lautenbach, S. (2013). Collinearity: a review of methods to deal with it and a simulation study evaluating their performance. *Ecography*, *36*(1), 27–46. https://doi.org/10.1111/j.1600-0587.2012.07348.x

Dornelas, M., Chase, J. M., Gotelli, N. J., Magurran, A. E., McGill, B. J., Antão, L. H., Blowes, S. A., Daskalova, G. N., Leung, B., Martins, I. S., Moyes, F., Myers-Smith, I. H., Thomas, C. D., & Vellend, M. (2023). Looking back on biodiversity change: lessons for the road ahead. *Philosophical Transactions of the Royal Society of London. Series B, Biological Sciences*, *378*(1881), 20220199. https://doi.org/10.1098/rstb.2022.0199

Dornelas, M., Gotelli, N. J., McGill, B., Shimadzu, H., Moyes, F., Sievers, C., & Magurran, A. E. (2014). Assemblage time series reveal biodiversity change but not systematic loss. *Science*, *344*(6181), 296–299. https://doi.org/10.1126/science.1248484

Dyderski, M. K., Paź, S., Frelich, L. E., & Jagodziński, A. M. (2018). How much does climate change threaten European forest tree species distributions? *Global Change Biology*, *24*(3), 1150–1163. https://doi.org/10.1111/gcb.13925

EcoTraits Landcare Research. (2005).

https://ecotraits.landcareresearch.co.nz/WeedsIntro.aspx

El Alaoui, O., & Idri, A. (2025). Impacts of base learners selection of heterogeneous ensemble for habitat suitability modeling. *Biodiversity and Conservation*, *34*(4), 1259–1290. https://doi.org/10.1007/s10531-025-03015-y

Elith, J., Graham, C., Valavi, R., Abegg, M., Bruce, C., Ford, A., Guisan, A., Hijmans, R. J., Huettmann, F., Lohmann, L., Loiselle, B., Moritz, C., Overton, J., Peterson, A. T., Phillips, S., Richardson, K., Williams, S., Wiser, S. K., Wohlgemuth, T., & Zimmermann, N. E. (2020). Presence-only and presence-absence data for comparing species distribution modeling methods. *Biodiversity Informatics*, *15*(2), 69–80. https://doi.org/10.17161/bi.v15i2.13384

Elith, J., Kearney, M., & Phillips, S. (2010). The art of modelling range-shifting species. *Methods in Ecology and Evolution / British Ecological Society*, *1*(4), 330–342. https://doi.org/10.1111/j.2041-210X.2010.00036.x

Enquist, B. J., Norberg, J., Bonser, S. P., Violle, C., Webb, C. T., Henderson, A., Sloat, L. L., & Savage, V. M. (2015). Chapter Nine - Scaling from Traits to Ecosystems: Developing a General Trait Driver Theory via Integrating Trait-Based and Metabolic Scaling Theories. In S. Pawar, G. Woodward, & A. I. Dell (Eds.), *Advances in Ecological Research* (Vol. 52, pp. 249–318). Academic Press. https://doi.org/10.1016/bs.aecr.2015.02.001

Evans, M. E. K., Merow, C., Record, S., McMahon, S. M., & Enquist, B. J. (2016). Towards process-based range modeling of many species. *Trends in Ecology & Evolution*, *31*(11), 860–871. https://doi.org/10.1016/j.tree.2016.08.005

Eyring, V., Bony, S., Meehl, G. A., Senior, C. A., Stevens, B., Stouffer, R. J., & Taylor, K. E. (2016). Overview of the Coupled Model Intercomparison Project Phase 6 (CMIP6) experimental design and organization. *Geoscientific Model Development*, *9*(5), 1937–1958. https://doi.org/10.5194/gmd-9-1937-2016

F. Dormann, C., M. McPherson, J., B. Araújo, M., Bivand, R., Bolliger, J., Carl, G., G. Davies, R., Hirzel, A., Jetz, W., Daniel Kissling, W., Kühn, I., Ohlemüller, R., R. Peres-Neto, P., Reineking, B., Schröder, B., M. Schurr, F., & Wilson, R. (2007). Methods to account for spatial autocorrelation in the analysis of species distributional data: a review. *Ecography*, *30*(5), 609–628. https://doi.org/10.1111/j.2007.0906-7590.05171.x

Feeley, K. J., Bravo-Avila, C., Fadrique, B., Perez, T. M., & Zuleta, D. (2020). Climate-driven changes in the composition of New World plant communities. *Nature Climate Change*, *10*(10), 965–970. https://doi.org/10.1038/s41558-020-0873-2

Fei, S., Desprez, J. M., Potter, K. M., Jo, I., Knott, J. A., & Oswalt, C. M. (2017). Divergence of species responses to climate change. *Science Advances*, *3*(5), e1603055. https://doi.org/10.1126/sciadv.1603055

Fenollosa, E., Pang, S. E. H., Briscoe, N. J., Guisan, A., & Salguero-Gómez, R. (2025). Powerful yet challenging: mechanistic niche models for predicting invasive species potential distribution under climate change. *Ecography*, e07775. https://doi.org/10.1002/ecog.07775

Ferchichi, A., Abbes, A. B., Barra, V., & Farah, I. R. (2022). Forecasting vegetation indices from spatio-temporal remotely sensed data using deep learning-based approaches: A systematic literature review. *Ecological Informatics*, *68*(101552), 101552. https://doi.org/10.1016/j.ecoinf.2022.101552

Ferrier, S., Watson, G., Pearce, J., & Drielsma, M. (2002). Extended statistical approaches to modelling spatial pattern in biodiversity in northeast New South Wales. I. Species-level modelling. *Biodiversity and Conservation*, *11*(12), 2275–2307. https://doi.org/10.1023/a:1021302930424

Finderup Nielsen, T., Sand-Jensen, K., Dornelas, M., & Bruun, H. H. (2019). More is less: net gain in species richness, but biotic homogenization over 140 years. *Ecology Letters*,

22(10), 1650–1657. https://doi.org/10.1111/ele.13361

Forrest, J. R. K. (2015). Plant–pollinator interactions and phenological change: what can we learn about climate impacts from experiments and observations? *Oikos (Copenhagen, Denmark)*, *124*(1), 4–13. https://doi.org/10.1111/oik.01386

Franklin, J. (2023). Species distribution modelling supports the study of past, present and future biogeographies. *Journal of Biogeography*, *50*(9), 1533–1545. https://doi.org/10.1111/jbi.14617

Frans, V. F., Augé, A. A., Fyfe, J., Zhang, Y., McNally, N., Edelhoff, H., Balkenhol, N., & Engler, J. O. (2022). Integrated SDM database: Enhancing the relevance and utility of species distribution models in conservation management. *Methods in Ecology and Evolution / British Ecological Society*, *13*(1), 243–261. https://doi.org/10.1111/2041-210x.13736

Frans, V. F., & Liu, J. (2024). Gaps and opportunities in modelling human influence on species distributions in the Anthropocene. *Nature Ecology & Evolution*, *8*(7), 1365–1377. https://doi.org/10.1038/s41559-024-02435-3

Frénay, B., & Verleysen, M. (2014). Classification in the presence of label noise: a survey. *IEEE Transactions on Neural Networks and Learning Systems*, *25*(5), 845–869. https://doi.org/10.1109/TNNLS.2013.2292894

Fricke, E. C., Ordonez, A., Rogers, H. S., & Svenning, J.-C. (2022). The effects of defaunation on plants' capacity to track climate change. *Science (New York, N.Y.)*, *375*(6577), 210–214. https://doi.org/10.1126/science.abk3510

Funk, J. L., Larson, J. E., Ames, G. M., Butterfield, B. J., Cavender-Bares, J., Firn, J., Laughlin, D. C., Sutton-Grier, A. E., Williams, L., & Wright, J. (2017). Revisiting the Holy Grail: using plant functional traits to understand ecological processes. *Biological Reviews of the Cambridge Philosophical Society*, *92*(2), 1156–1173. https://doi.org/10.1111/brv.12275

García Criado, M., Myers-Smith, I. H., Bjorkman, A. D., Elmendorf, S. C., Normand, S., Aastrup, P., Aerts, R., Alatalo, J. M., Baeten, L., Björk, R. G., Björkman, M. P., Boulanger-Lapointe, N., Butler, E. E., Cooper, E. J., Cornelissen, J. H. C., Daskalova, G. N., Fadrique, B., Forbes, B. C., Henry, G. H. R., … Vellend, M. (2025). Plant diversity dynamics over space and time in a warming Arctic. *Nature*, 1–9. https://doi.org/10.1038/s41586-025-08946-8

Gaul, W., Sadykova, D., White, H. J., Leon-Sanchez, L., Caplat, P., Emmerson, M. C., & Yearsley, J. M. (2020). Data quantity is more important than its spatial bias for predictive species distribution modelling. *PeerJ*, *8*, e10411. https://doi.org/10.7717/peerj.10411

Goberville, E., Beaugrand, G., Hautekèete, N.-C., Piquot, Y., & Luczak, C. (2015). Uncertainties in the projection of species distributions related to general circulation models. *Ecology and Evolution*, *5*(5), 1100–1116. https://doi.org/10.1002/ece3.1411

Goicolea, T., Adde, A., Broennimann, O., García-Viñas, J. I., Gastón, A., José Aroca-Fernández, M., Guisan, A., & G. Mateo, R. (2025). Spatially- nested hierarchical species distribution models to overcome niche truncation in national- scale studies. *Ecography*, *2025*(3), e07328. https://doi.org/10.1111/ecog.07328

González-Melo, A., Posada, J. M., Beauchêne, J., Lehnebach, R., Levionnois, S., Derroire, G., & Clair, B. (2024). The links between wood traits and species demography change during tree development in a lowland tropical rainforest. *AoB Plants*, *16*(1), lad090. https://doi.org/10.1093/aobpla/plad090

Gottfried, M., Pauli, H., Futschik, A., Akhalkatsi, M., Barančok, P., Benito Alonso, J. L., Coldea, G., Dick, J., Erschbamer, B., Fernández Calzado, M. R., Kazakis, G., Krajči, J., Larsson, P., Mallaun, M., Michelsen, O., Moiseev, D., Moiseev, P., Molau, U., Merzouki, A., … Grabherr, G. (2012). Continent-wide response of mountain vegetation to climate

change. *Nature Climate Change*, *2*(2), 111–115. https://doi.org/10.1038/nclimate1329

Goury, R., Thuiller, W., Abdulhak, S., Pache, G., Van Es, J., Bowler, D. E., Renaud, J., Violle, C., & Münkemüller, T. (2025). Recent vegetation shifts in the French Alps with winners outnumbering losers. *The Journal of Ecology*, *113*(11), 3275–3292. https://doi.org/10.1111/1365-2745.70159

Graham, C. H., Elith, J., Hijmans, R. J., Guisan, A., Townsend Peterson, A., Loiselle, B. A., & The Nceas Predicting Species Distributions Working Group. (2008). The influence of spatial errors in species occurrence data used in distribution models: Spatial error in occurrence data for predictive modelling. *The Journal of Applied Ecology*, *45*(1), 239–247. https://doi.org/10.1111/j.1365-2664.2007.01408.x

Green, S. J., Brookson, C. B., Hardy, N. A., & Crowder, L. B. (2022). Trait-based approaches to global change ecology: moving from description to prediction. *Proceedings. Biological Sciences / The Royal Society*, *289*(1971), 20220071. https://doi.org/10.1098/rspb.2022.0071

Grime, J. P. (1977). Evidence for the Existence of Three Primary Strategies in Plants and Its Relevance to Ecological and Evolutionary Theory. *The American Naturalist*, *111*(982), 1169–1194. https://doi.org/10.1086/283244

Grime, J. P. (1998). Benefits of plant diversity to ecosystems: immediate, filter and founder effects. *The Journal of Ecology*, *86*(6), 902–910. https://doi.org/10.1046/j.1365-2745.1998.00306.x

Groves, R. (1999). *Sleeper weeds*. 632–636. https://caws.org.nz/old-site/awc/1999/awc199916321.pdf

Guélat, J., & Kéry, M. (2018). Effects of spatial autocorrelation and imperfect detection on species distribution models. *Methods in Ecology and Evolution*, *9*(6), 1614–1625. https://doi.org/10.1111/2041-210x.12983

Guillerme, T., Cardoso, P., Jørgensen, M. W., Mammola, S., & Matthews, T. J. (2025). The what, how, and why of trait- based analyses in ecology. *Ecography*, *2025*(7), e07580. https://doi.org/10.1111/ecog.07580

Guisan, A., Chevalier, M., Adde, A., Zarzo-Arias, A., Goicolea, T., Broennimann, O., Petitpierre, B., Scherrer, D., Rey, P.-L., Collart, F., Riva, F., Steen, B., & Mateo, R. G. (2025). Spatially nested species distribution models (N- SDM): An effective tool to overcome niche truncation for more robust inference and projections. *The Journal of Ecology*, *113*(7), 1588–1605. https://doi.org/10.1111/1365-2745.70063

Guisan, A., & Thuiller, W. (2005). Predicting species distribution: offering more than simple habitat models. *Ecology Letters*, *8*(9), 993–1009. https://doi.org/10.1111/j.1461-0248.2005.00792.x

Guisan, A., Tingley, R., Baumgartner, J. B., Naujokaitis-Lewis, I., Sutcliffe, P. R., Tulloch, A. I. T., Regan, T. J., Brotons, L., McDonald-Madden, E., Mantyka-Pringle, C., Martin, T. G., Rhodes, J. R., Maggini, R., Setterfield, S. A., Elith, J., Schwartz, M. W., Wintle, B. A., Broennimann, O., Austin, M., … Buckley, Y. M. (2013). Predicting species distributions for conservation decisions. *Ecology Letters*, *16*(12), 1424–1435. https://doi.org/10.1111/ele.12189

Guo, F., Lenoir, J., & Bonebrake, T. C. (2018). Land-use change interacts with climate to determine elevational species redistribution. *Nature Communications*, *9*(1), 1315. https://doi.org/10.1038/s41467-018-03786-9

Guo, K., Cornwell, W. K., & Bragg, J. G. (2024). Using machine learning to link climate, phylogeny and leaf area in eucalypts through a 50- fold expansion of leaf trait datasets. *The Journal of Ecology*. https://doi.org/10.1111/1365-2745.14354

Hagan, J. G., Henn, J. J., & Osterman, W. H. A. (2023). Plant traits alone are good predictors of ecosystem properties when used carefully. *Nature Ecology & Evolution*, *7*(3),

332–334. https://doi.org/10.1038/s41559-022-01920-x

Halladin-Dąbrowska, A., Kania, A., & Kopeć, D. (2019). The t-SNE algorithm as a tool to improve the quality of reference data used in accurate mapping of heterogeneous non-forest vegetation. *Remote Sensing*, *12*(1), 39. https://doi.org/10.3390/rs12010039

Hao, T., Elith, J., Lahoz-Monfort, J. J., & Guillera-Arroita, G. (2020). Testing whether ensemble modelling is advantageous for maximising predictive performance of species distribution models. *Ecography*, *43*(4), 549–558. https://doi.org/10.1111/ecog.04890

Hawcroft, A., Bellingham, P. J., Jo, I., Richardson, S. J., & Wright, E. F. (2024). Are populations of trees threatened by non-native herbivorous mammals more secure in New Zealand's national parks? *Biological Conservation*, *295*(110637), Not Available. https://doi.org/10.1016/j.biocon.2024.110637

Henn, J. J., Anderson, K. E., Brigham, L. M., Bueno de Mesquita, C. P., Collins, C. G., Elmendorf, S. C., Green, M. D., Huxley, J. D., Rafferty, N. E., Rose-Person, A., & Spasojevic, M. J. (2024). Long-term alpine plant responses to global change drivers depend on functional traits. *Ecology Letters*, *27*(10), e14518. https://doi.org/10.1111/ele.14518

Henn, J. J., Buzzard, V., Enquist, B. J., Halbritter, A. H., Klanderud, K., Maitner, B. S., Michaletz, S. T., Pötsch, C., Seltzer, L., Telford, R. J., Yang, Y., Zhang, L., & Vandvik, V. (2018). Intraspecific trait variation and phenotypic plasticity mediate alpine plant species response to climate change. *Frontiers in Plant Science*, *9*, 1548. https://doi.org/10.3389/fpls.2018.01548

Hisano, M., Searle, E. B., & Chen, H. Y. H. (2018). Biodiversity as a solution to mitigate climate change impacts on the functioning of forest ecosystems: Biodiversity to mitigate climate change impacts. *Biological Reviews of the Cambridge Philosophical Society*, *93*(1), 439–456. https://doi.org/10.1111/brv.12351

Hobbs, R. J., Hallett, L. M., Ehrlich, P. R., & Mooney, H. A. (2011). Intervention ecology:

Applying ecological science in the twenty-first century. *Bioscience*, *61*(6), 442–450. https://doi.org/10.1525/bio.2011.61.6.6

Hoffmann, S. (2022). Challenges and opportunities of area-based conservation in reaching biodiversity and sustainability goals. *Biodiversity and Conservation*, *31*(2), 325–352. https://doi.org/10.1007/s10531-021-02340-2

Huard, D., Fyke, J., Capellán-Pérez, I., Matthews, H. D., & Partanen, A.-I. (2022). Estimating the likelihood of GHG concentration scenarios from probabilistic integrated assessment model simulations. *Earth's Future*, *10*(10), e2022EF002715. https://doi.org/10.1029/2022ef002715

Hulme, P. E. (2020). Plant invasions in New Zealand: global lessons in prevention, eradication and control. *Biological Invasions*, *22*(5), 1539–1562. https://doi.org/10.1007/s10530-020-02224-6

Jackson, S. T., & Sax, D. F. (2010). Balancing biodiversity in a changing environment: extinction debt, immigration credit and species turnover. *Trends in Ecology & Evolution*, *25*(3), 153–160. https://doi.org/10.1016/j.tree.2009.10.001

Jakoby, O., Lischke, H., & Wermelinger, B. (2019). Climate change alters elevational phenology patterns of the European spruce bark beetle (Ips typographus). *Global Change Biology*, *25*(12), 4048–4063. https://doi.org/10.1111/gcb.14766

Jo, I., Bellingham, P. J., Richardson, S. J., Hawcroft, A., & Wright, E. F. (2025). Tree demographic drivers across temperate rain forests, after accounting for site-, species-, and stem-level attributes. *Ecology*, *106*(1), e4471. https://doi.org/10.1002/ecy.4471

Johnson, T. F., Beckerman, A. P., Childs, D. Z., Webb, T. J., Evans, K. L., Griffiths, C. A., Capdevila, P., Clements, C. F., Besson, M., Gregory, R. D., Thomas, G. H., Delmas, E., & Freckleton, R. P. (2024). Revealing uncertainty in the status of biodiversity change.

Nature, *628*(8009), 788–794. https://doi.org/10.1038/s41586-024-07236-z

Jump, A. S., Huang, T.-J., & Chou, C.-H. (2012). Rapid altitudinal migration of mountain plants in Taiwan and its implications for high altitude biodiversity. *Ecography*, *35*(3), 204–210. https://doi.org/10.1111/j.1600-0587.2011.06984.x

Jung, V., Violle, C., Mondy, C., Hoffmann, L., & Muller, S. (2010). Intraspecific variability and trait-based community assembly. *The Journal of Ecology*, *98*(5), 1134–1140. https://doi.org/10.1111/j.1365-2745.2010.01687.x

Kattge, J., Bönisch, G., Díaz, S., Lavorel, S., Prentice, I. C., Leadley, P., Tautenhahn, S., Werner, G. D. A., Aakala, T., Abedi, M., Acosta, A. T. R., Adamidis, G. C., Adamson, K., Aiba, M., Albert, C. H., Alcántara, J. M., Alcázar C, C., Aleixo, I., Ali, H., … Wirth, C. (2020). TRY plant trait database - enhanced coverage and open access. *Global Change Biology*, *26*(1), 119–188. https://doi.org/10.1111/gcb.14904

Keegan, L., School of Biological Sciences, University of Auckland, Private Bag 92019, Auckland 1142, New Zealand, White, R., & Macinnis-Ng, C. (2022). Current knowledge and potential impacts of climate change on New Zealand's biological heritage. *New Zealand Journal of Ecology*. https://doi.org/10.20417/nzjecol.46.10

Keenan, T. F., & Riley, W. J. (2018). Greening of the land surface in the world's cold regions consistent with recent warming. *Nature Climate Change*, *8*(9), 825–828. https://doi.org/10.1038/s41558-018-0258-y

Kemppinen, J., Niittynen, P., le Roux, P. C., Momberg, M., Happonen, K., Aalto, J., Rautakoski, H., Enquist, B. J., Vandvik, V., Halbritter, A. H., Maitner, B., & Luoto, M. (2021). Consistent trait-environment relationships within and across tundra plant communities. *Nature Ecology & Evolution*, *5*(4), 458–467. https://doi.org/10.1038/s41559-021-01396-1

Kerr, M. R., Ordonez, A., Riede, F., Atkinson, J., Pearce, E. A., Sykut, M., Trepel, J., & Svenning, J.-C. (2025). Widespread ecological novelty across the terrestrial biosphere.

Nature Ecology & Evolution, *9*(4), 589–598. https://doi.org/10.1038/s41559-025-02662-2

Kim, H., Rosa, I. M. D., Alkemade, R., Leadley, P., Hurtt, G., Popp, A., van Vuuren, D. P., Anthoni, P., Arneth, A., Baisero, D., Caton, E., Chaplin-Kramer, R., Chini, L., De Palma, A., Di Fulvio, F., Di Marco, M., Espinoza, F., Ferrier, S., Fujimori, S., … Pereira, H. M. (2018). A protocol for an intercomparison of biodiversity and ecosystem services models using harmonized land-use and climate scenarios. *Geoscientific Model Development*, *11*(11), 4537–4562. https://doi.org/10.5194/gmd-11-4537-2018

Knutti, R., Furrer, R., Tebaldi, C., Cermak, J., & Meehl, G. A. (2010). Challenges in combining projections from multiple climate models. *Journal of Climate*, *23*(10), 2739–2758. https://doi.org/10.1175/2009jcli3361.1

Kong, D., Wang, J., Wu, H., Valverde-Barrantes, O. J., Wang, R., Zeng, H., Kardol, P., Zhang, H., & Feng, Y. (2019). Nonlinearity of root trait relationships and the root economics spectrum. *Nature Communications*, *10*(1), 2203. https://doi.org/10.1038/s41467-019-10245-6

Körner, C., Leuzinger, S., Riedl, S., Siegwolf, R. T., & Streule, L. (2016). Carbon and nitrogen stable isotope signals for an entire alpine flora, based on herbarium samples. *Alpine Botany*, *126*(2), 153–166. https://doi.org/10.1007/s00035-016-0170-x

Kudo, G., Kawai, Y., Amagai, Y., & Winkler, D. E. (2017). Degradation and recovery of an alpine plant community: experimental removal of an encroaching dwarf bamboo. *Alpine Botany*, *127*(1), 75–83. https://doi.org/10.1007/s00035-016-0178-2

Kuebbing, S. E., Maynard, D. S., & Bradford, M. A. (2018). Linking functional diversity and ecosystem processes: A framework for using functional diversity metrics to predict the ecosystem impact of functionally unique species. *The Journal of Ecology*, *106*(2), 687–698. https://doi.org/10.1111/1365-2745.12835

Kühn, N., Tovar, C., Carretero, J., Vandvik, V., Enquist, B. J., & Willis, K. J. (2021). Globally important plant functional traits for coping with climate change. *Frontiers of Biogeography*, *13*(4). https://doi.org/10.21425/F5FBG53774

Lajoie, G., & Vellend, M. (2015). Understanding context dependence in the contribution of intraspecific variation to community trait-environment matching. *Ecology*, *96*(11), 2912–2922. https://doi.org/10.1890/15-0156.1

Lalechère, E., Lenoir, J., Marrec, R., Essl, F., Kühn, I., & Ergon, T. (2025). Assessing biodiversity trends in a quasi-permanent non-equilibrium state. *Trends in Ecology & Evolution*, *40*(10), 949–959. https://doi.org/10.1016/j.tree.2025.07.003

Laliberté, E., & Legendre, P. (2010). A distance-based framework for measuring functional diversity from multiple traits. *Ecology*, *91*(1), 299–305. https://doi.org/10.1890/08-2244.1

Lamouroux, N., Poff, N. L., & Angermeier, P. L. (2002). Intercontinental convergence of stream fish community traits along geomorphic and hydraulic gradients. *Ecology*, *83*(7), 1792. https://doi.org/10.2307/3071765

Laughlin, D. C. (2014). The intrinsic dimensionality of plant traits and its relevance to community assembly. *The Journal of Ecology*, *102*(1), 186–193. https://doi.org/10.1111/1365-2745.12187

Laughlin, D. C. (2023). *Plant Strategies: The Demographic Consequences of Functional Traits in Changing Environments*. Oxford University Press. https://play.google.com/store/books/details?id=0aakzwEACAAJ

Laughlin, D. C. (2024). Unifying functional and population ecology to test the adaptive value of traits. *Biological Reviews of the Cambridge Philosophical Society*, *99*(6), 1976–1991. https://doi.org/10.1111/brv.13107

Laughlin, D. C., Joshi, C., van Bodegom, P. M., Bastow, Z. A., & Fulé, P. Z. (2012). A predictive

model of community assembly that incorporates intraspecific trait variation. *Ecology Letters*, *15*(11), 1291–1299. https://doi.org/10.1111/j.1461-0248.2012.01852.x

Lavorel, S., & Garnier, E. (2002). Predicting changes in community composition and ecosystem functioning from plant traits: revisiting the Holy Grail. *Functional Ecology*, *16*(5), 545–556. https://doi.org/10.1046/j.1365-2435.2002.00664.x

Lawlor, J. A., Comte, L., Grenouillet, G., Lenoir, J., Baecher, J. A., Bandara, R. M. W. J., Bertrand, R., Chen, I.-C., Diamond, S. E., Lancaster, L. T., Moore, N., Murienne, J., Oliveira, B. F., Pecl, G. T., Pinsky, M. L., Rolland, J., Rubenstein, M., Scheffers, B. R., Thompson, L. M., … Sunday, J. (2024). Mechanisms, detection and impacts of species redistributions under climate change. *Nature Reviews. Earth & Environment*, *5*(5), 351–368. https://doi.org/10.1038/s43017-024-00527-z

Lawton, J. H. (1999). Are There General Laws in Ecology? *Oikos*, *84*(2), 177–192. https://doi.org/10.2307/3546712

Leathwick, J. R. (1998). Are New Zealand's Nothofagus species in equilibrium with their environment? *Journal of Vegetation Science: Official Organ of the International Association for Vegetation Science*, *9*(5), 719–732. https://doi.org/10.2307/3237290

Leathwick, J. R., Whitehead, D., & McLeod, M. (1996). Predicting changes in the composition of New Zealand's indigenous forests in response to global warming: a modelling approach. *Environmental Software*, *11*(1–3), 81–90. https://doi.org/10.1016/s0266-9838(96)00045-7

Lee-Yaw, J. A., L. McCune, J., Pironon, S., & N. Sheth, S. (2022). Species distribution models rarely predict the biology of real populations. *Ecography*, *2022*(6). https://doi.org/10.1111/ecog.05877

Lenoir, J., Gégout, J.-C., Guisan, A., Vittoz, P., Wohlgemuth, T., Zimmermann, N. E., Dullinger, S., Pauli, H., Willner, W., & Svenning, J.-C. (2010). Going against the flow: potential

mechanisms for unexpected downslope range shifts in a warming climate. *Ecography*, *33*(2), 295–303. https://doi.org/10.1111/j.1600-0587.2010.06279.x

Lenton, T. M., Armstrong McKay, D. I., Loriani, S., Abrams, J. F., Lade, S. J., Donges, J. F., Milkoreit, M., Powell, T., Smith, S. R., Zimm, C., Buxton, J. E., Bailey, E., Laybourn, L., Ghadiali, A., & Dyke, J. G. (2023). *The Global Tipping Points Report 2023*. University of Exeter. https://global-tipping-points.org/

Li, H., Luo, P., Yang, H., Ni, M., Cheng, Y., Huang, Y., & Xie, W. (2025). Multidimensional β-diversity responses to global change: a meta-analysis highlighting divergent effects on plant communities. *Nature Communications*, 1–10. https://doi.org/10.1038/s41467-025-66574-2

Li, J., & Prentice, I. C. (2024). Global patterns of plant functional traits and their relationships to climate. *Communications Biology*, *7*(1), 1136. https://doi.org/10.1038/s42003-024-06777-3

Liang, J., Crowther, T. W., Picard, N., Wiser, S., Zhou, M., Alberti, G., Schulze, E.-D., McGuire, A. D., Bozzato, F., Pretzsch, H., de-Miguel, S., Paquette, A., Hérault, B., Scherer-Lorenzen, M., Barrett, C. B., Glick, H. B., Hengeveld, G. M., Nabuurs, G.-J., Pfautsch, S., … Reich, P. B. (2016). Positive biodiversity-productivity relationship predominant in global forests. *Science (New York, N.Y.)*, *354*(6309), aaf8957–aaf8957. https://doi.org/10.1126/science.aaf8957

Lima, J. S., Lenoir, J., & Hylander, K. (2024). Potential migration pathways of broadleaved trees across the receding boreal biome under future climate change. *Global Change Biology*, *30*(8), e17471. https://doi.org/10.1111/gcb.17471

Liu, C., White, M., & Newell, G. (2018). Detecting outliers in species distribution data. *Journal of Biogeography*, *45*(1), 164–176. https://doi.org/10.1111/jbi.13122

Liu, H., Yin, D., He, P., Cadotte, M. W., & Ye, Q. (2024). Linking plant functional traits to

biodiversity under environmental change. *Biological Diversity*, *1*(1), 22–28. https://doi.org/10.1002/bod2.12004

Losapio, G., De Moraes, C. M., Dirzo, R., Tscheulin, T., Zouros, N., & Mescher, M. C. (2024). Habitat protection and removal of encroaching shrubs support the recovery of biodiversity and ecosystem functioning. *Conservation Science and Practice*, *6*(4), e13111. https://doi.org/10.1111/csp2.13111

Lu, W.-X., Wang, Z.-Z., Hu, X.-Y., & Rao, G.-Y. (2024). Incorporating eco-evolutionary information into species distribution models provides comprehensive predictions of species range shifts under climate change. *The Science of the Total Environment*, *912*(169501), 169501. https://doi.org/10.1016/j.scitotenv.2023.169501

Lubiana Botelho, L., Jeynes-Smith, C., Vollert, S. A., & Bode, M. (2025). Calibrated ecosystem models cannot predict the consequences of conservation management decisions. *Ecology Letters*, *28*(1), e70034. https://doi.org/10.1111/ele.70034

Macinnis-Ng, C., Mcintosh, A. R., Monks, J. M., Waipara, N., White, R. S. A., Boudjelas, S., Clark, C. D., Clearwater, M. J., Curran, T. J., Dickinson, K. J. M., Nelson, N., Perry, G. L. W., Richardson, S. J., Stanley, M. C., & Peltzer, D. A. (2021). Climate- change impacts exacerbate conservation threats in island systems: New Zealand as a case study. *Frontiers in Ecology and the Environment*, *19*(fee.2285), 216–224. https://doi.org/10.1002/fee.2285

Mahaut, L., Violle, C., Shihan, A., Pélissier, R., Morel, J.-B., de Tombeur, F., Rahajaharilaza, K., Fabre, D., Luquet, D., Hartley, S., Thorne, S. J., Ballini, E., & Fort, F. (2023). Beyond trait distances: Functional distinctiveness captures the outcome of plant competition. *Functional Ecology*, *37*(9), 2399–2412. https://doi.org/10.1111/1365-2435.14397

Maldonado, C., Molina, C. I., Zizka, A., Persson, C., Taylor, C. M., Albán, J., Chilquillo, E., Rønsted, N., & Antonelli, A. (2015). Estimating species diversity and distribution in the

era of Big Data: to what extent can we trust public databases?: Species diversity and distribution in the era of Big Data. *Global Ecology and Biogeography: A Journal of Macroecology*, *24*(8), 973–984. https://doi.org/10.1111/geb.12326

Mammola, S., Carmona, C. P., Guillerme, T., & Cardoso, P. (2021). Concepts and applications in functional diversity. *Functional Ecology*, *35*(9), 1869–1885. https://doi.org/10.1111/1365-2435.13882

Maréchaux, I., Langerwisch, F., Huth, A., Bugmann, H., Morin, X., Reyer, C. P. O., Seidl, R., Collalti, A., Dantas de Paula, M., Fischer, R., Gutsch, M., Lexer, M. J., Lischke, H., Rammig, A., Rödig, E., Sakschewski, B., Taubert, F., Thonicke, K., Vacchiano, G., & Bohn, F. J. (2021). Tackling unresolved questions in forest ecology: The past and future role of simulation models. *Ecology and Evolution*, *11*(9), 3746–3770. https://doi.org/10.1002/ece3.7391

Marmion, M., Parviainen, M., Luoto, M., Heikkinen, R. K., & Thuiller, W. (2009). Evaluation of consensus methods in predictive species distribution modelling. *Diversity & Distributions*, *15*(1), 59–69. https://doi.org/10.1111/j.1472-4642.2008.00491.x

Marquis, S. (1968). Ecosystems, societies, and cities. *The American Behavioral Scientist*, *11*(6), 11–15. https://doi.org/10.1177/000276426801100604

Marsh, G. P. (1874). *The earth as modified by human action / by George P. Marsh: 1874 edition*. Scribner, Armstrong & Co. https://doi.org/10.5962/bhl.title.53722

Martínez-Minaya, J., Cameletti, M., Conesa, D., & Pennino, M. G. (2018). Species distribution modeling: a statistical review with focus in spatio-temporal issues. *Stochastic Environmental Research and Risk Assessment: Research Journal*, *32*(11), 3227–3244. https://doi.org/10.1007/s00477-018-1548-7

Martínez-Vilalta, J., García-Valdés, R., Jump, A., Vilà-Cabrera, A., & Mencuccini, M. (2023). Accounting for trait variability and coordination in predictions of drought-induced range shifts in woody plants. *The New Phytologist*, *240*(1), 23–40.

https://doi.org/10.1111/nph.19138

Mason, N. W. H., & de Bello, F. (2013). Functional diversity: a tool for answering challenging ecological questions. *Journal of Vegetation Science: Official Organ of the International Association for Vegetation Science*, *24*(5), 777–780. https://doi.org/10.1111/jvs.12097

Mason, N. W. H., Mouillot, D., Lee, W. G., & Wilson, J. B. (2005). Functional richness, functional evenness and functional divergence: the primary components of functional diversity. *Oikos (Copenhagen, Denmark)*, *111*(1), 112–118. https://doi.org/10.1111/j.0030-1299.2005.13886.x

Mata, S., Braga, J. M. A., Flores, B. M., & Sansevero, J. B. B. (2025). Use of the alternative stable states concept in tropical terrestrial ecosystem research—A systematic literature review. *Biotropica*, *57*(2), e70025. https://doi.org/10.1111/btp.70025

Mathias, S., van Galen, L. G., Jarvie, S., & Larcombe, M. J. (2023). Range reshuffling: Climate change, invasive species, and the case of *Nothofagus* forests in Aotearoa New Zealand. *Diversity & Distributions*, *29*(11), 1402–1419. https://doi.org/10.1111/ddi.13767

McCarthy, J. K., Wiser, S. K., Bellingham, P. J., Beresford, R. M., Campbell, R. E., Turner, R., & Richardson, S. J. (2021). Using spatial models to identify refugia and guide restoration in response to an invasive plant pathogen. *The Journal of Applied Ecology*, *58*(1), 192–201. https://doi.org/10.1111/1365-2664.13756

McCrea, R., King, R., Graham, L., & Börger, L. (2023). Realising the promise of large data and complex models. *Methods in Ecology and Evolution*, *14*(1), 4–11. https://doi.org/10.1111/2041-210x.14050

McGlone, M. S., Buitenwerf, R., & Richardson, S. J. (2016). The formation of the oceanic temperate forests of New Zealand. *New Zealand Journal of Botany*, *54*(2), 128–155. https://doi.org/10.1080/0028825x.2016.1158196

McLauchlan, K. K., Ferguson, C. J., Wilson, I. E., Ocheltree, T. W., & Craine, J. M. (2010). Thirteen decades of foliar isotopes indicate declining nitrogen availability in central North American grasslands. *The New Phytologist*, *187*(4), 1135–1145. https://doi.org/10.1111/j.1469-8137.2010.03322.x

Medeiros, C. D., Scoffoni, C., John, G. P., Bartlett, M. K., Inman-Narahari, F., Ostertag, R., Cordell, S., Giardina, C., & Sack, L. (2019). An extensive suite of functional traits distinguishes Hawaiian wet and dry forests and enables prediction of species vital rates. *Functional Ecology*, *33*(4), 712–734. https://doi.org/10.1111/1365-2435.13229

Medeiros, J. S., Hewins, C. R., Baumgardner, A. W., & Burns, J. H. (2020). Shifts in phenology and plant architecture across genus rhododendron highlight different ways to become more acquisitive despite universally conservative xylem anatomy. *International Journal of Plant Sciences*, *181*(1), 103–115. https://doi.org/10.1086/706188

Midolo, G., Clark, A. T., Chytrý, M., Essl, F., Dullinger, S., Jandt, U., Bruelheide, H., Argagnon, O., Biurrun, I., Chiarucci, A., Ćušterevska, R., De Frenne, P., De Sanctis, M., Dengler, J., Divíšek, J., Dziuba, T., Ejrnæs, R., Garbolino, E., Illa, E., … Keil, P. (2025). Six decades of losses and gains in alpha diversity of European plant communities. *Ecology Letters*, *28*(11), e70248. https://doi.org/10.1111/ele.70248

Mokany, K., Harwood, T. D., Overton, J. M., Barker, G. M., & Ferrier, S. (2011). Combining α - and β -diversity models to fill gaps in our knowledge of biodiversity: Filling gaps in biodiversity knowledge. *Ecology Letters*, *14*(10), 1043–1051. https://doi.org/10.1111/j.1461-0248.2011.01675.x

Montràs-Janer, T., Suggitt, A. J., Fox, R., Jönsson, M., Martay, B., Roy, D. B., Walker, K. J., & Auffret, A. G. (2024). Anthropogenic climate and land-use change drive short- and long-term biodiversity shifts across taxa. *Nature Ecology & Evolution*, *8*(4), 739–751.

https://doi.org/10.1038/s41559-024-02326-7

Morley, J. W., Frölicher, T. L., & Pinsky, M. L. (2020). Characterizing uncertainty in climate impact projections: a case study with seven marine species on the North American continental shelf. *ICES Journal of Marine Science: Journal Du Conseil*, *77*(6), 2118–2133. https://doi.org/10.1093/icesjms/fsaa103

Mouchet, M. A., Villéger, S., Mason, N. W. H., & Mouillot, D. (2010). Functional diversity measures: an overview of their redundancy and their ability to discriminate community assembly rules: Functional diversity measures. *Functional Ecology*, *24*(4), 867–876. https://doi.org/10.1111/j.1365-2435.2010.01695.x

Mouillot, D., Villéger, S., Scherer-Lorenzen, M., & Mason, N. W. H. (2011). Functional structure of biological communities predicts ecosystem multifunctionality. *PloS One*, *6*(3), e17476. https://doi.org/10.1371/journal.pone.0017476

Mouquet, N., Munguia, P., Kneitel, J. M., & Miller, T. E. (2003). Community assembly time and the relationship between local and regional species richness. *Oikos (Copenhagen, Denmark)*, *103*(3), 618–626. https://doi.org/10.1034/j.1600-0706.2003.12772.x

Mueller, K. E., Kray, J. A., & Blumenthal, D. M. (2024). Coordination of leaf, root, and seed traits shows the importance of whole plant economics in two semiarid grasslands. *The New Phytologist*, *241*(6), 2410–2422. https://doi.org/10.1111/nph.19529

Múgica, L., Canals, R. M., San Emeterio, L., & Peralta, J. (2021). Decoupling of traditional burnings and grazing regimes alters plant diversity and dominant species competition in high-mountain grasslands. *The Science of the Total Environment*, *790*(147917), 147917. https://doi.org/10.1016/j.scitotenv.2021.147917

Muscatello, A., Elith, J., & Kujala, H. (2021). How decisions about fitting species distribution models affect conservation outcomes. *Conservation Biology: The Journal of the Society for Conservation Biology*, *35*(4), 1309–1320. https://doi.org/10.1111/cobi.13669

Myers-Smith, I. H., Forbes, B. C., Wilmking, M., Hallinger, M., Lantz, T., Blok, D., Tape, K. D., Macias-Fauria, M., Sass-Klaassen, U., Lévesque, E., Boudreau, S., Ropars, P., Hermanutz, L., Trant, A., Collier, L. S., Weijers, S., Rozema, J., Rayback, S. A., Schmidt, N. M., … Hik, D. S. (2011). Shrub expansion in tundra ecosystems: dynamics, impacts and research priorities. *Environmental Research Letters*, *6*(4), 045509. https://doi.org/10.1088/1748-9326/6/4/045509

Nepstad, D. C., Stickler, C. M., Filho, B. S.-, & Merry, F. (2008). Interactions among Amazon land use, forests and climate: prospects for a near-term forest tipping point. *Philosophical Transactions of the Royal Society of London. Series B, Biological Sciences*, *363*(1498), 1737–1746. https://doi.org/10.1098/rstb.2007.0036

Noce, S., Collalti, A., & Santini, M. (2017). Likelihood of changes in forest species suitability, distribution, and diversity under future climate: The case of Southern Europe. *Ecology and Evolution*, *7*(22), 9358–9375. https://doi.org/10.1002/ece3.3427

Norberg, A., Abrego, N., Blanchet, F. G., Adler, F. R., Anderson, B. J., Anttila, J., Araújo, M. B., Dallas, T., Dunson, D., Elith, J., Foster, S. D., Fox, R., Franklin, J., Godsoe, W., Guisan, A., O'Hara, B., Hill, N. A., Holt, R. D., Hui, F. K. C., … Ovaskainen, O. (2019). A comprehensive evaluation of predictive performance of 33 species distribution models at species and community levels. *Ecological Monographs*, *89*(3), e01370. https://doi.org/10.1002/ecm.1370

Ostertag, R., Warman, L., Cordell, S., & Vitousek, P. M. (2015). Using plant functional traits to restore Hawaiian rainforest. *The Journal of Applied Ecology*, *52*(4), 805–809. https://doi.org/10.1111/1365-2664.12413

Ovaskainen, O. (2020). *Joint Species Distribution Modelling: With Applications in R*. Cambridge University Press. https://play.google.com/store/books/details?id=zbxSzQEACAAJ

Owens, H. L., Campbell, L. P., Dornak, L. L., Saupe, E. E., Barve, N., Soberón, J., Ingenloff, K., Lira-Noriega, A., Hensz, C. M., Myers, C. E., & Peterson, A. T. (2013). Constraints on interpretation of ecological niche models by limited environmental ranges on calibration areas. *Ecological Modelling*, *263*, 10–18. https://doi.org/10.1016/j.ecolmodel.2013.04.011

Paine, C. E. T., Amissah, L., Auge, H., Baraloto, C., Baruffol, M., Bourland, N., Bruelheide, H., Daïnou, K., de Gouvenain, R. C., Doucet, J.-L., Doust, S., Fine, P. V. A., Fortunel, C., Haase, J., Holl, K. D., Jactel, H., Li, X., Kitajima, K., Koricheva, J., … Hector, A. (2015). Globally, functional traits are weak predictors of juvenile tree growth, and we do not know why. *The Journal of Ecology*, *103*(4), 978–989. https://doi.org/10.1111/1365-2745.12401

Pan, Y., Cieraad, E., & van Bodegom, P. M. (2019). Are ecophysiological adaptive traits decoupled from leaf economics traits in wetlands? *Functional Ecology*, *33*(7), 1202–1210. https://doi.org/10.1111/1365-2435.13329

Parducci, L., Jørgensen, T., Tollefsrud, M. M., Elverland, E., Alm, T., Fontana, S. L., Bennett, K. D., Haile, J., Matetovici, I., Suyama, Y., Edwards, M. E., Andersen, K., Rasmussen, M., Boessenkool, S., Coissac, E., Brochmann, C., Taberlet, P., Houmark-Nielsen, M., Larsen, N. K., … Willerslev, E. (2012). Glacial survival of boreal trees in northern Scandinavia. *Science (New York, N.Y.)*, *335*(6072), 1083–1086. https://doi.org/10.1126/science.1216043

Pathan, A. K., Cuddy, W., Kimberly, M. O., Adusei-Fosu, K., Rolando, C. A., & Park, R. F. (2020). Efficacy of fungicides applied for protectant and curative activity against myrtle rust. *Plant Disease*, *104*(8), 2123–2129. https://doi.org/10.1094/PDIS-10-19-2106-RE

Pausas, J. G., & Bond, W. J. (2020). Alternative biome states in terrestrial ecosystems. *Trends in Plant Science*, *25*(3), 250–263. https://doi.org/10.1016/j.tplants.2019.11.003

Pausas, J. G., & Bond, W. J. (2021). Alternative biome states challenge the modelling of

species' niche shifts under climate change. *The Journal of Ecology*, *109*(12), 3962–3971. https://doi.org/10.1111/1365-2745.13781

Pelletier, C., Valero, S., Inglada, J., Champion, N., Marais Sicre, C., & Dedieu, G. (2017). Effect of training class label noise on classification performances for land cover mapping with satellite image time series. *Remote Sensing*, *9*(2), 173. https://doi.org/10.3390/rs9020173

Penone, C., Davidson, A. D., Shoemaker, K. T., Di Marco, M., Rondinini, C., Brooks, T. M., Young, B. E., Graham, C. H., & Costa, G. C. (2014). Imputation of missing data in life- history trait datasets: which approach performs the best? *Methods in Ecology and Evolution*, *5*(9), 961–970. https://doi.org/10.1111/2041-210x.12232

Pereira, H. M., Martins, I. S., Rosa, I. M. D., Kim, H., Leadley, P., Popp, A., van Vuuren, D. P., Hurtt, G., Quoss, L., Arneth, A., Baisero, D., Bakkenes, M., Chaplin-Kramer, R., Chini, L., Di Marco, M., Ferrier, S., Fujimori, S., Guerra, C. A., Harfoot, M., … Alkemade, R. (2024). Global trends and scenarios for terrestrial biodiversity and ecosystem services from 1900 to 2050. *Science*, *384*(6694), 458–465. https://doi.org/10.1126/science.adn3441

Pérez-Ramos, I. M., Matías, L., Gómez-Aparicio, L., & Godoy, Ó. (2019). Functional traits and phenotypic plasticity modulate species coexistence across contrasting climatic conditions. *Nature Communications*, *10*(1), 2555. https://doi.org/10.1038/s41467-019-10453-0

Perry, G., Wilmshurst, J., & McGlone, M. (2014). Ecology and long-term history of fire in New Zealand. *New Zealand Journal of Ecology*, *38*, 157–176. https://newzealandecology.org/nzje/3198

Petchey, O. L., Pontarp, M., Massie, T. M., Kéfi, S., Ozgul, A., Weilenmann, M., Palamara, G. M., Altermatt, F., Matthews, B., Levine, J. M., Childs, D. Z., McGill, B. J., Schaepman, M. E., Schmid, B., Spaak, P., Beckerman, A. P., Pennekamp, F., & Pearse, I. S. (2015). The

ecological forecast horizon, and examples of its uses and determinants. *Ecology Letters*, *18*(7), 597–611. https://doi.org/10.1111/ele.12443

Petri, L., & Ibáñez, I. (2025). Successful recovery of native plants post-invasive removal in forest understories is driven by native community features. *Ecological Applications*, *35*(2), e70012. https://doi.org/10.1002/eap.70012

Phillips, S. J., Anderson, R. P., & Schapire, R. E. (2006). Maximum entropy modeling of species geographic distributions. *Ecological Modelling*, *190*(3), 231–259. https://doi.org/10.1016/j.ecolmodel.2005.03.026

Pianka, E. R. (1970). On r- and K-Selection. *The American Naturalist*, *104*(940), 592–597. https://doi.org/10.1086/282697

Pichler, M., & Hartig, F. (2023). Machine learning and deep learning—A review for ecologists. *Methods in Ecology and Evolution / British Ecological Society*, *14*(4), 994–1016. https://doi.org/10.1111/2041-210x.14061

Pla, L., Casanoves, F., & Di Rienzo, J. (2012). Functional Diversity Indices. In *SpringerBriefs in Environmental Science* (pp. 27–51). Springer Netherlands. https://doi.org/10.1007/978-94-007-2648-2_3

Pollock, L. J., Morris, W. K., & Vesk, P. A. (2012). The role of functional traits in species distributions revealed through a hierarchical model. *Ecography*, *35*(8), 716–725. https://doi.org/10.1111/j.1600-0587.2011.07085.x

Poppenwimer, T., Mayrose, I., & DeMalach, N. (2023). Revising the global biogeography of annual and perennial plants. *Nature*, *624*(7990), 109–114. https://doi.org/10.1038/s41586-023-06644-x

Pörtner, H.-O., Scholes, R. J., Arneth, A., Barnes, D. K. A., Burrows, M. T., Diamond, S. E., Duarte, C. M., Kiessling, W., Leadley, P., Managi, S., McElwee, P., Midgley, G., Ngo, H. T., Obura, D., Pascual, U., Sankaran, M., Shin, Y. J., & Val, A. L. (2023). Overcoming the

coupled climate and biodiversity crises and their societal impacts. *Science (New York, N.Y.)*, *380*(6642), eabl4881. https://doi.org/10.1126/science.abl4881

Posner, S. M., McKenzie, E., & Ricketts, T. H. (2016). Policy impacts of ecosystem services knowledge. *Proceedings of the National Academy of Sciences of the United States of America*, *113*(7), 1760–1765. https://doi.org/10.1073/pnas.1502452113

Poyatos, R., Sus, O., Badiella, L., Mencuccini, M., & Martínez-Vilalta, J. (2018). Gap-filling a spatially explicit plant trait database: comparing imputation methods and different levels of environmental information. *Biogeosciences*, *15*(9), 2601–2617. https://doi.org/10.5194/bg-15-2601-2018

Proença, V., & Pereira, H. M. (2017). Comparing extinction rates: Past, present, and future ☆. In *Reference Module in Life Sciences*. Elsevier. https://doi.org/10.1016/b978-0-12-809633-8.02128-2

Qazi, A. W., Saqib, Z., & Zaman-ul-Haq, M. (2022). Trends in species distribution modelling in context of rare and endemic plants: a systematic review. *Ecological Processes*, *11*(1), 40. https://doi.org/10.1186/s13717-022-00384-y

Raiter, K. G., & Hawlena, D. (2024). Managing multiple uncertainties in species distribution modelling. *Diversity & Distributions*, *30*(9), e13857. https://doi.org/10.1111/ddi.13857

Rapacciuolo, G., Maher, S. P., Schneider, A. C., Hammond, T. T., Jabis, M. D., Walsh, R. E., Iknayan, K. J., Walden, G. K., Oldfather, M. F., Ackerly, D. D., & Beissinger, S. R. (2014). Beyond a warming fingerprint: individualistic biogeographic responses to heterogeneous climate change in California. *Global Change Biology*, *20*(9), 2841–2855. https://doi.org/10.1111/gcb.12638

Richardson, S., Smale, M., Hurst, J. M., Fitzgerald, N., Peltzer, D., Allen, R., Bellingham, P., & McKelvey, P. (2009). Large-tree growth and mortality rates in forests of the central North Island, New Zealand. *New Zealand Journal of Ecology*, *33*, 208–215.

https://newzealandecology.org/nzje/2901

Ricotta, C., & Pavoine, S. (2024). *What do functional diversity, redundancy, rarity, and originality actually measure? A theoretical guide for ecologists and conservationists*. https://ecoevorxiv.org/repository/view/7493/

Ropars, P., Département de biologie, chimie et géographie, Université du Québec à Rimouski, 300 allée des Ursulines, Rimouski, QC, Canada, G5L 3A1, Comeau, É., Lee, W., & Boudreau, S. (2018). Biome transition in a changing world: from indigenous grasslands to shrub-dominated communities. *New Zealand Journal of Ecology*, *42*(2), 229–239. https://doi.org/10.20417/nzjecol.42.26

Rose, M. B., Velazco, S. J. E., Regan, H. M., Flint, A. L., Flint, L. E., Thorne, J. H., & Franklin, J. (2024). Uncertainty in consensus predictions of plant species' vulnerability to climate change. *Diversity & Distributions*, *30*(8), e13898. https://doi.org/10.1111/ddi.13898

Rosenfield, M. F., & Müller, S. C. (2020). Plant traits rather than species richness explain ecological processes in subtropical forests. *Ecosystems (New York, N.Y.)*, *23*(1), 52–66. https://doi.org/10.1007/s10021-019-00386-6

Rubenstein, M. A., Weiskopf, S. R., Bertrand, R., Carter, S. L., Comte, L., Eaton, M. J., Johnson, C. G., Lenoir, J., Lynch, A. J., Miller, B. W., Morelli, T. L., Rodriguez, M. A., Terando, A., & Thompson, L. M. (2023). Climate change and the global redistribution of biodiversity: substantial variation in empirical support for expected range shifts. *Environmental Evidence*, *12*(1), 1–21. https://doi.org/10.1186/s13750-023-00296-0

Ryo, M., Angelov, B., Mammola, S., Kass, J. M., Benito, B. M., & Hartig, F. (2021). Explainable artificial intelligence enhances the ecological interpretability of black- box species distribution models. *Ecography*, *44*(2), 199–205. https://doi.org/10.1111/ecog.05360

Sack, L., & Buckley, T. N. (2020). Trait Multi-Functionality in Plant Stress Response. *Integrative and Comparative Biology*, *60*(1), 98–112.

https://doi.org/10.1093/icb/icz152

Salguero-Gómez, R., Jones, O. R., Archer, C. R., Buckley, Y. M., Che-Castaldo, J., Caswell, H., Hodgson, D., Scheuerlein, A., Conde, D. A., Brinks, E., de Buhr, H., Farack, C., Gottschalk, F., Hartmann, A., Henning, A., Hoppe, G., Römer, G., Runge, J., Ruoff, T., … Vaupel, J. W. (2015). The compadrePlant Matrix Database: an open online repository for plant demography. *The Journal of Ecology*, *103*(1), 202–218. https://doi.org/10.1111/1365-2745.12334

Salguero-Gómez, R., Jones, O. R., Jongejans, E., Blomberg, S. P., Hodgson, D. J., Mbeau-Ache, C., Zuidema, P. A., de Kroon, H., & Buckley, Y. M. (2016). Fast-slow continuum and reproductive strategies structure plant life-history variation worldwide. *Proceedings of the National Academy of Sciences of the United States of America*, *113*(1), 230–235. https://doi.org/10.1073/pnas.1506215112

Sandel, B., Merow, C., Serra-Diaz, J. M., & Svenning, J.-C. (2025). Disequilibrium in plant distributions: Challenges and approaches for species distribution models. *The Journal of Ecology*, *113*(4), 782–794. https://doi.org/10.1111/1365-2745.70009

Schipper, A. M., Hilbers, J. P., Meijer, J. R., Antão, L. H., Benítez-López, A., de Jonge, M. M. J., Leemans, L. H., Scheper, E., Alkemade, R., Doelman, J. C., Mylius, S., Stehfest, E., van Vuuren, D. P., van Zeist, W.-J., & Huijbregts, M. A. J. (2020). Projecting terrestrial biodiversity intactness with GLOBIO 4. *Global Change Biology*, *26*(2), 760–771. https://doi.org/10.1111/gcb.14848

Schmera, D., Ricotta, C., & Podani, J. (2023). Components of functional diversity revisited: A new classification and its theoretical and practical implications. *Ecology and Evolution*, *13*(10), e10614. https://doi.org/10.1002/ece3.10614

Schratz, P., Muenchow, J., Iturritxa, E., Richter, J., & Brenning, A. (2019). Hyperparameter tuning and performance assessment of statistical and machine-learning algorithms

using spatial data. *Ecological Modelling*, *406*, 109–120. https://doi.org/10.1016/j.ecolmodel.2019.06.002

Scott, W. A., & Hallam, C. J. (2003). Assessing species misidentification rates through quality assurance of vegetation monitoring. *Plant Ecology*, *165*(1), 101–115. https://doi.org/10.1023/a:1021441331839

Segan, D. B., Murray, K. A., & Watson, J. E. M. (2016). A global assessment of current and future biodiversity vulnerability to habitat loss–climate change interactions. *Global Ecology and Conservation*, *5*, 12–21. https://doi.org/10.1016/j.gecco.2015.11.002

Segurado, P., Araújo, M. B., & Kunin, W. E. (2006). Consequences of spatial autocorrelation for niche- based models. *The Journal of Applied Ecology*, *43*(3), 433–444. https://doi.org/10.1111/j.1365-2664.2006.01162.x

Seliger, B. J., McGill, B. J., Svenning, J.-C., & Gill, J. L. (2021). Widespread underfilling of the potential ranges of North American trees. *Journal of Biogeography*, *48*(2), 359–371. https://doi.org/10.1111/jbi.14001

Shepherd, J. D., Gillingham, S., Heuer, T., Barron, M. C., Byrom, A. E., & Pech, R. P. (2018). Multi-scale dynamic maps for the management of invading and established wildlife populations: brushtail possums in New Zealand. *Wildlife Research (East Melbourne, Melbourne, Vic.)*, *45*(4), 336–343. https://doi.org/10.1071/wr17135

Shipley, B., De Bello, F., Cornelissen, J. H. C., Laliberté, E., Laughlin, D. C., & Reich, P. B. (2016). Reinforcing loose foundation stones in trait-based plant ecology. *Oecologia*, *180*(4), 923–931. https://doi.org/10.1007/s00442-016-3549-x

Siefert, A., Violle, C., Chalmandrier, L., Albert, C. H., Taudiere, A., Fajardo, A., Aarssen, L. W., Baraloto, C., Carlucci, M. B., Cianciaruso, M. V., de L Dantas, V., de Bello, F., Duarte, L. D. S., Fonseca, C. R., Freschet, G. T., Gaucherand, S., Gross, N., Hikosaka, K., Jackson, B., … Wardle, D. A. (2015). A global meta-analysis of the relative extent of intraspecific trait

variation in plant communities. *Ecology Letters*, *18*(12), 1406–1419. https://doi.org/10.1111/ele.12508

Sillero, N., Arenas-Castro, S., Enriquez-Urzelai, U., Vale, C. G., Sousa-Guedes, D., Martínez-Freiría, F., Real, R., & Barbosa, A. M. (2021). Want to model a species niche? A step-by-step guideline on correlative ecological niche modelling. *Ecological Modelling*, *456*(109671), 109671. https://doi.org/10.1016/j.ecolmodel.2021.109671

Simmonds, E. G., Jarvis, S. G., Henrys, P. A., Isaac, N. J. B., & O'Hara, R. B. (2020). Is more data always better? A simulation study of benefits and limitations of integrated distribution models. *Ecography*, *43*(10), 1413–1422. https://doi.org/10.1111/ecog.05146

Sofaer, H. R., Jarnevich, C. S., Flather, C. H., & Kark, S. (2018). Misleading prioritizations from modelling range shifts under climate change. *Global Ecology and Biogeography: A Journal of Macroecology*, *27*(6), 658–666. https://doi.org/10.1111/geb.12726

Soley-Guardia, M., Alvarado-Serrano, D. F., & Anderson, R. P. (2024). Top ten hazards to avoid when modeling species distributions: a didactic guide of assumptions, problems, and recommendations. *Ecography*, *2024*(4), e06852. https://doi.org/10.1111/ecog.06852

Song, W., & Zhou, Y. (2021). Linking leaf Δ15N and Δ13C with soil fungal biodiversity, ectomycorrhizal and plant pathogenic abundance in forest ecosystems of China. *Catena*, *200*(105176), 105176. https://doi.org/10.1016/j.catena.2021.105176

Spasojevic, M. J., & Suding, K. N. (2012). Inferring community assembly mechanisms from functional diversity patterns: the importance of multiple assembly processes: Functional diversity along gradients. *The Journal of Ecology*, *100*(3), 652–661. https://doi.org/10.1111/j.1365-2745.2011.01945.x

Staples, T. L., Kiessling, W., & Pandolfi, J. M. (2022). Emergence patterns of locally novel

plant communities driven by past climate change and modern anthropogenic impacts. *Ecology Letters*, *25*(6), 1497–1509. https://doi.org/10.1111/ele.14016

Steinbauer, M. J., Grytnes, J.-A., Jurasinski, G., Kulonen, A., Lenoir, J., Pauli, H., Rixen, C., Winkler, M., Bardy-Durchhalter, M., Barni, E., Bjorkman, A. D., Breiner, F. T., Burg, S., Czortek, P., Dawes, M. A., Delimat, A., Dullinger, S., Erschbamer, B., Felde, V. A., … Wipf, S. (2018). Accelerated increase in plant species richness on mountain summits is linked to warming. *Nature*, *556*(7700), 231–234. https://doi.org/10.1038/s41586-018-0005-6

Stephenson, N. (1998). Actual evapotranspiration and deficit: biologically meaningful correlates of vegetation distribution across spatial scales. *Journal of Biogeography*, *25*(5), 855–870. https://doi.org/10.1046/j.1365-2699.1998.00233.x

Sun, C., Yao, J., Huang, Y., & Zang, R. (2025). Variation in functional traits of woody plants across successional stages in subtropical forests. *Forests*, *16*(5), 868. https://doi.org/10.3390/f16050868

Svenning, J.-C., & Skov, F. (2004). Limited filling of the potential range in European tree species: Limited range filling in European trees. *Ecology Letters*, *7*(7), 565–573. https://doi.org/10.1111/j.1461-0248.2004.00614.x

Swenson, N. G., Worthy, S. J., Eubanks, D., Iida, Y., Monks, L., Petprakob, K., Rubio, V. E., Staiger, K., & Zambrano, J. (2020). A Reframing of Trait–Demographic Rate Analyses for Ecology and Evolutionary Biology. *International Journal of Plant Sciences*, *181*(1), 33–43. https://doi.org/10.1086/706189

Taheri, S., Naimi, B., Rahbek, C., & Araújo, M. B. (2021). Improvements in reports of species redistribution under climate change are required. *Science Advances*, *7*(15). https://doi.org/10.1126/sciadv.abe1110

Ten Caten, C., & Dallas, T. (2023). Thinning occurrence points does not improve species distribution model performance. *Ecosphere (Washington, D.C)*, *14*(12), e4703.

https://doi.org/10.1002/ecs2.4703

Thomas, F. M., & Vesk, P. A. (2017). Are trait-growth models transferable? Predicting multi-species growth trajectories between ecosystems using plant functional traits. *PloS One*, *12*(5), e0176959. https://doi.org/10.1371/journal.pone.0176959

Thompson, P. R., Fagan, W. F., & Staniczenko, P. P. A. (2020). Predictor species: Improving assessments of rare species occurrence by modeling environmental co-responses. *Ecology and Evolution*, *10*(7), 3293–3304. https://doi.org/10.1002/ece3.6096

Thuiller, W., Guéguen, M., Renaud, J., Karger, D. N., & Zimmermann, N. E. (2019). Uncertainty in ensembles of global biodiversity scenarios. *Nature Communications*, *10*(1), 1446. https://doi.org/10.1038/s41467-019-09519-w

Thuiller, W., Münkemüller, T., Lavergne, S., Mouillot, D., Mouquet, N., Schiffers, K., & Gravel, D. (2013). A road map for integrating eco-evolutionary processes into biodiversity models. *Ecology Letters*, *16 Suppl 1*(0 1), 94–105. https://doi.org/10.1111/ele.12104

Tilman, D., May, R. M., Lehman, C. L., & Nowak, M. A. (1994). Habitat destruction and the extinction debt. *Nature*, *371*(6492), 65–66. https://doi.org/10.1038/371065a0

Titeux, N., Henle, K., Mihoub, J.-B., Regos, A., Geijzendorffer, I. R., Cramer, W., Verburg, P. H., & Brotons, L. (2016). Biodiversity scenarios neglect future land-use changes. *Global Change Biology*, *22*(7), 2505–2515. https://doi.org/10.1111/gcb.13272

Toome-Heller, M., Ho, W. W. H., Ganley, R. J., Elliott, C. E. A., Quinn, B., Pearson, H. G., & Alexander, B. J. R. (2020). Chasing myrtle rust in New Zealand: host range and distribution over the first year after invasion. *Australasian Plant Pathology*, *49*(3), 221–230. https://doi.org/10.1007/s13313-020-00694-9

Transtrum, M. K., Machta, B. B., Brown, K. S., Daniels, B. C., Myers, C. R., & Sethna, J. P. (2015). Perspective: Sloppiness and emergent theories in physics, biology, and beyond. *The Journal of Chemical Physics*, *143*(1), 010901. https://doi.org/10.1063/1.4923066

Trisos, C. H., Merow, C., & Pigot, A. L. (2020). The projected timing of abrupt ecological disruption from climate change. *Nature*, *580*(7804), 496–501. https://doi.org/10.1038/s41586-020-2189-9

Turnbull, L. A., Isbell, F., Purves, D. W., Loreau, M., & Hector, A. (2016). Understanding the value of plant diversity for ecosystem functioning through niche theory. *Proceedings. Biological Sciences / The Royal Society*, *283*(1844), 20160536. https://doi.org/10.1098/rspb.2016.0536

Turner, M. G., & Seidl, R. (2023). Novel Disturbance Regimes and Ecological Responses. *Annual Review of Ecology, Evolution, and Systematics*, *54*(Volume 54, 2023), 63–83. https://doi.org/10.1146/annurev-ecolsys-110421-101120

Urban, D. L. (2024). Species distribution modeling. In *Landscape Ecology* (pp. 29–79). Springer Nature Switzerland. https://doi.org/10.1007/978-3-031-72251-6_2

Urban, M. C. (2024). Climate change extinctions. *Science (New York, N.Y.)*, *386*(6726), 1123–1128. https://doi.org/10.1126/science.adp4461

Urban, M. C., Bocedi, G., Hendry, A. P., Mihoub, J.-B., Pe'er, G., Singer, A., Bridle, J. R., Crozier, L. G., De Meester, L., Godsoe, W., Gonzalez, A., Hellmann, J. J., Holt, R. D., Huth, A., Johst, K., Krug, C. B., Leadley, P. W., Palmer, S. C. F., Pantel, J. H., … Travis, J. M. J. (2016). Improving the forecast for biodiversity under climate change. *Science (New York, N.Y.)*, *353*(6304), aad8466–aad8466. https://doi.org/10.1126/science.aad8466

Valavi, R., Elith, J., Lahoz-Monfort, J. J., & Guillera-Arroita, G. (2021). Modelling species presence- only data with random forests. *Ecography*, *44*(12), 1731–1742. https://doi.org/10.1111/ecog.05615

Valavi, R., Guillera-Arroita, G., Lahoz-Monfort, J. J., & Elith, J. (2022). Predictive performance of presence- only species distribution models: a benchmark study with reproducible code. *Ecological Monographs*, *92*(1), e01486.

https://doi.org/10.1002/ecm.1486

Valdez, J. W., Callaghan, C. T., Junker, J., Purvis, A., Hill, S. L. L., & Pereira, H. M. (2023). The undetectability of global biodiversity trends using local species richness. *Ecography*, *2023*(3), e06604. https://doi.org/10.1111/ecog.06604

Valiente-Banuet, A., Aizen, M. A., Alcántara, J. M., Arroyo, J., Cocucci, A., Galetti, M., García, M. B., García, D., Gómez, J. M., Jordano, P., Medel, R., Navarro, L., Obeso, J. R., Oviedo, R., Ramírez, N., Rey, P. J., Traveset, A., Verdú, M., & Zamora, R. (2015). Beyond species loss: the extinction of ecological interactions in a changing world. *Functional Ecology*, *29*(3), 299–307. https://doi.org/10.1111/1365-2435.12356

Van Bodegom, P. M., Douma, J. C., Witte, J. P. M., Ordoñez, J. C., Bartholomeus, R. P., & Aerts, R. (2012). Going beyond limitations of plant functional types when predicting global ecosystem–atmosphere fluxes: exploring the merits of traits- based approaches: Merits of traits-based vegetation modelling. *Global Ecology and Biogeography: A Journal of Macroecology*, *21*(6), 625–636. https://doi.org/10.1111/j.1466-8238.2011.00717.x

van der Sande, M. T., Poorter, L., Derroire, G., do Espirito Santo, M. M., Lohbeck, M., Müller, S. C., Bhaskar, R., van Breugel, M., Dupuy-Rada, J. M., Durán, S. M., Jakovac, C. C., Paz, H., Rozendaal, D. M. A., Brancalion, P., Craven, D., Mora Ardilla, F., Almeida, J. S., Balvanera, P., Becknell, J., … Bongers, F. (2024). Tropical forest succession increases tree taxonomic and functional richness but decreases evenness. *Global Ecology and Biogeography: A Journal of Macroecology*, *33*(8), e13856. https://doi.org/10.1111/geb.13856

Van Passel, J., Bernardino, P. N., Lhermitte, S., Rius, B. F., Hirota, M., Conradi, T., de Keersmaecker, W., Van Meerbeek, K., & Somers, B. (2024). Critical slowing down of the Amazon forest after increased drought occurrence. *Proceedings of the National*

Academy of Sciences of the United States of America, *121*(22), e2316924121. https://doi.org/10.1073/pnas.2316924121

van Steenderen, C. J. M., & Sutton, G. F. (2024). Climate covariate selection influences MaxEnt model predictions and predictive accuracy under current and future climates. *Ecological Modelling*, *498*(110872), 110872. https://doi.org/10.1016/j.ecolmodel.2024.110872

Vandvik, V., Skarpaas, O., Klanderud, K., Telford, R. J., Halbritter, A. H., & Goldberg, D. E. (2020). Biotic rescaling reveals importance of species interactions for variation in biodiversity responses to climate change. *Proceedings of the National Academy of Sciences of the United States of America*, *117*(37), 22858–22865. https://doi.org/10.1073/pnas.2003377117

Velazco, S. J. E., Ribeiro, B. R., Laureto, L. M. O., & De Marco Júnior, P. (2020). Overprediction of species distribution models in conservation planning: A still neglected issue with strong effects. *Biological Conservation*, *252*(108822), 108822. https://doi.org/10.1016/j.biocon.2020.108822

Velazco, S. J. E., Rose, M. B., De Marco, P., Jr, Regan, H. M., & Franklin, J. (2024). How far can I extrapolate my species distribution model? Exploring shape, a novel method. *Ecography*, *2024*(3). https://doi.org/10.1111/ecog.06992

Veleva, V. (2021). The role of entrepreneurs in advancing sustainable lifestyles: Challenges, impacts, and future opportunities. *Journal of Cleaner Production*, *283*(124658), 124658. https://doi.org/10.1016/j.jclepro.2020.124658

Verberk, W. C. E. P., van Noordwijk, C. G. E., & Hildrew, A. G. (2013). Delivering on a promise: integrating species traits to transform descriptive community ecology into a predictive science. *Freshwater Science*, *32*(2), 531–547. https://doi.org/10.1899/12-092.1

Verheyen, K., Bažány, M., Chećko, E., Chudomelová, M., Closset-Kopp, D., Czortek, P.,

Decocq, G., De Frenne, P., De Keersmaeker, L., Enríquez García, C., Fabšičová, M., Grytnes, J.-A., Hederová, L., Hédl, R., Heinken, T., Schei, F. H., Horváth, S., Jaroszewicz, B., Jermakowicz, E., … Baeten, L. (2018). Observer and relocation errors matter in resurveys of historical vegetation plots. *Journal of Vegetation Science: Official Organ of the International Association for Vegetation Science*, *29*(5), 812–823. https://doi.org/10.1111/jvs.12673

Vetaas, O. R. (2002). Realized and Potential Climate Niches: A Comparison of Four Rhododendron Tree Species. *Journal of Biogeography*, *29*(4), 545–554. http://www.jstor.org/stable/827583

Viljur, M.-L., Abella, S. R., Adámek, M., Alencar, J. B. R., Barber, N. A., Beudert, B., Burkle, L. A., Cagnolo, L., Campos, B. R., Chao, A., Chergui, B., Choi, C.-Y., Cleary, D. F. R., Davis, T. S., Dechnik-Vázquez, Y. A., Downing, W. M., Fuentes-Ramirez, A., Gandhi, K. J. K., Gehring, C., … Thorn, S. (2022). The effect of natural disturbances on forest biodiversity: an ecological synthesis. *Biological Reviews of the Cambridge Philosophical Society*, *97*(5), 1930–1947. https://doi.org/10.1111/brv.12876

Villéger, S., Mason, N. W. H., & Mouillot, D. (2008). New multidimensional functional diversity indices for a multifaceted framework in functional ecology. *Ecology*, *89*(8), 2290–2301. https://doi.org/10.1890/07-1206.1

Villellas, J., Doak, D. F., García, M. B., & Morris, W. F. (2015). Demographic compensation among populations: what is it, how does it arise and what are its implications? *Ecology Letters*, *18*(11), 1139–1152. https://doi.org/10.1111/ele.12505

Violle, C., Enquist, B. J., McGill, B. J., Jiang, L., Albert, C. H., Hulshof, C., Jung, V., & Messier, J. (2012). The return of the variance: intraspecific variability in community ecology. *Trends in Ecology & Evolution*, *27*(4), 244–252. https://doi.org/10.1016/j.tree.2011.11.014

Violle, C., Navas, M.-L., Vile, D., Kazakou, E., Fortunel, C., Hummel, I., & Garnier, E. (2007). Let the concept of trait be functional! *Oikos (Copenhagen, Denmark)*, *116*(5), 882–892. https://doi.org/10.1111/j.0030-1299.2007.15559.x

Visser, M. D., Bruijning, M., Wright, S. J., Muller-Landau, H. C., Jongejans, E., Comita, L. S., & Kroon, H. (2016). Functional traits as predictors of vital rates across the life cycle of tropical trees. *Functional Ecology*, *30*(2), 168–180. https://doi.org/10.1111/1365-2435.12621

Walther, G.-R., Post, E., Convey, P., Menzel, A., Parmesan, C., Beebee, T. J. C., Fromentin, J.-M., Hoegh-Guldberg, O., & Bairlein, F. (2002). Ecological responses to recent climate change. *Nature*, *416*(6879), 389–395. https://doi.org/10.1038/416389a

Wang, C.-J., & Wan, J.-Z. (2021). Functional trait perspective on suitable habitat distribution of invasive plant species at a global scale. *Perspectives in Ecology and Conservation*, *19*(4), 475–486. https://doi.org/10.1016/j.pecon.2021.07.002

Wardle, P., & Coleman, M. C. (1992). Evidence for rising upper limits of four native New Zealand forest trees. *New Zealand Journal of Botany*, *30*(3), 303–314. https://doi.org/10.1080/0028825X.1992.10412909

Watts, J. L., & Watkins, J. E. (2022). New Zealand fern distributions from the last glacial maximum to 2070: A dynamic tale of migration and community turnover. *American Fern Journal*, *112*(4), 354–372. https://doi.org/10.1640/0002-8444-112.4.354

Weaver, S. A., & Mallinger, R. E. (2022). A specialist bee and its host plants experience phenological shifts at different rates in response to climate change. *Ecology*, *103*(5), e3658. https://doi.org/10.1002/ecy.3658

Weiher, E., & Keddy, P. A. (1995). Assembly Rules, Null Models, and Trait Dispersion: New Questions from Old Patterns. *Oikos*, *74*(1), 159–164. https://doi.org/10.2307/3545686

Westerband, A. C., Funk, J. L., & Barton, K. E. (2021). Intraspecific trait variation in plants: a

renewed focus on its role in ecological processes. *Annals of Botany*, *127*(4), 397–410. https://doi.org/10.1093/aob/mcab011

Wieczynski, D. J., Boyle, B., Buzzard, V., Duran, S. M., Henderson, A. N., Hulshof, C. M., Kerkhoff, A. J., McCarthy, M. C., Michaletz, S. T., Swenson, N. G., Asner, G. P., Bentley, L. P., Enquist, B. J., & Savage, V. M. (2019). Climate shapes and shifts functional biodiversity in forests worldwide. *Proceedings of the National Academy of Sciences of the United States of America*, *116*(2), 587–592. https://doi.org/10.1073/pnas.1813723116

Wilkes, M. A., Mckenzie, M., Johnson, A., Hassall, C., Kelly, M., Willby, N., & Brown, L. E. (2025). Revealing hidden sources of uncertainty in biodiversity trend assessments. *Ecography*, *2025*(5), e07441. https://doi.org/10.1111/ecog.07441

Wiser, S. K., Bellingham, P. J., & Burrows, L. E. (2001). Managing biodiversity information: development of New Zealand's National Vegetation Survey databank. *New Zealand Journal of Ecology*, *25*(2).

Woodstock, M. S., & Harris, H. E. (2025). Ecosystem models can predict the consequences of conservation management decisions. *Ecology Letters*, *28*(4), e70116. https://doi.org/10.1111/ele.70116

Wookey, P. A., Aerts, R., Bardgett, R. D., Baptist, F., Bråthen, K. A., Cornelissen, J. H. C., Gough, L., Hartley, I. P., Hopkins, D. W., Lavorel, S., & Shaver, G. R. (2009). Ecosystem feedbacks and cascade processes: understanding their role in the responses of Arctic and alpine ecosystems to environmental change. *Global Change Biology*, *15*(5), 1153–1172. https://doi.org/10.1111/j.1365-2486.2008.01801.x

Wooliver, R., Pfennigwerth, A. A., Bailey, J. K., & Schweitzer, J. A. (2016). Plant functional constraints guide macroevolutionary trade- offs in competitive and conservative growth responses to nitrogen. *Functional Ecology*, *30*(7), 1099–1108.

https://doi.org/10.1111/1365-2435.12648

Wright, I. J., Reich, P. B., Westoby, M., Ackerly, D. D., Baruch, Z., Bongers, F., Cavender-Bares, J., Chapin, T., Cornelissen, J. H. C., Diemer, M., Flexas, J., Garnier, E., Groom, P. K., Gulias, J., Hikosaka, K., Lamont, B. B., Lee, T., Lee, W., Lusk, C., … Villar, R. (2004). The worldwide leaf economics spectrum. *Nature*, *428*(6985), 821–827. https://doi.org/10.1038/nature02403

Wyse, S., School of Environment, University of Auckland, Private Bag 92019, Auckland 1142, New Zealand, Wilmshurst, J., Burns, B., & Perry, G. (2018). New Zealand forest dynamics: a review of past and present vegetation responses to disturbance, and development of conceptual forest models. *New Zealand Journal of Ecology*, *42*(2). https://doi.org/10.20417/nzjecol.42.18

Yachi, S., & Loreau, M. (1999). Biodiversity and ecosystem productivity in a fluctuating environment: the insurance hypothesis. *Proceedings of the National Academy of Sciences of the United States of America*, *96*(4), 1463–1468. https://doi.org/10.1073/pnas.96.4.1463

Yan, P., He, N., Yu, K., Xu, L., & Van Meerbeek, K. (2023). Integrating multiple plant functional traits to predict ecosystem productivity. *Communications Biology*, *6*(1), 239. https://doi.org/10.1038/s42003-023-04626-3

Yang, J., Cao, M., & Swenson, N. G. (2018). Why Functional Traits Do Not Predict Tree Demographic Rates. *Trends in Ecology & Evolution*, *33*(5), 326–336. https://doi.org/10.1016/j.tree.2018.03.003

Yang, J., Lu, J., Chen, Y., Yan, E., Hu, J., Wang, X., & Shen, G. (2020). Large underestimation of intraspecific trait variation and its improvements. *Frontiers in Plant Science*, *11*, 53. https://doi.org/10.3389/fpls.2020.00053

Zeng, Y.-F., Wang, W.-T., Liao, W.-J., Wang, H.-F., & Zhang, D.-Y. (2015). Multiple glacial

refugia for cool-temperate deciduous trees in northern East Asia: the Mongolian oak as a case study. *Molecular Ecology*, *24*(22), 5676–5691. https://doi.org/10.1111/mec.13408

Zhigila, D. A., Muasya, A. M., & Verboom, G. A. (2023). Extinction risk patterns in a biodiversity hotspot—The case of *Thesium* (Santalaceae) in the Greater Cape Floristic Region. *Conservation Science and Practice*, *5*(6), e12932. https://doi.org/10.1111/csp2.12932

Zipkin, E. F., Doser, J. W., Davis, C. L., Leuenberger, W., Ayebare, S., & Davis, K. L. (2023). Integrated community models: A framework combining multispecies data sources to estimate the status, trends and dynamics of biodiversity. *The Journal of Animal Ecology*, *92*(12), 2248–2262. https://doi.org/10.1111/1365-2656.14012

Zurell, D., Zimmermann, N. E., Gross, H., Baltensweiler, A., Sattler, T., & Wüest, R. O. (2020). Testing species assemblage predictions from stacked and joint species distribution models. *Journal of Biogeography*, *47*(1), 101–113. https://doi.org/10.1111/jbi.13608

Appendix A: Supplementary Materials for BdP

A1. Variable Choice

We adopted an objective approach to variable selection. From each highly correlated pair (r > 0.7), we discarded the variable with the higher average correlation to all other variables until no more highly correlated pairs remained. The only exceptions were the mean annual temperature and total annual precipitation, which were always preferentially included to aid model interpretation.

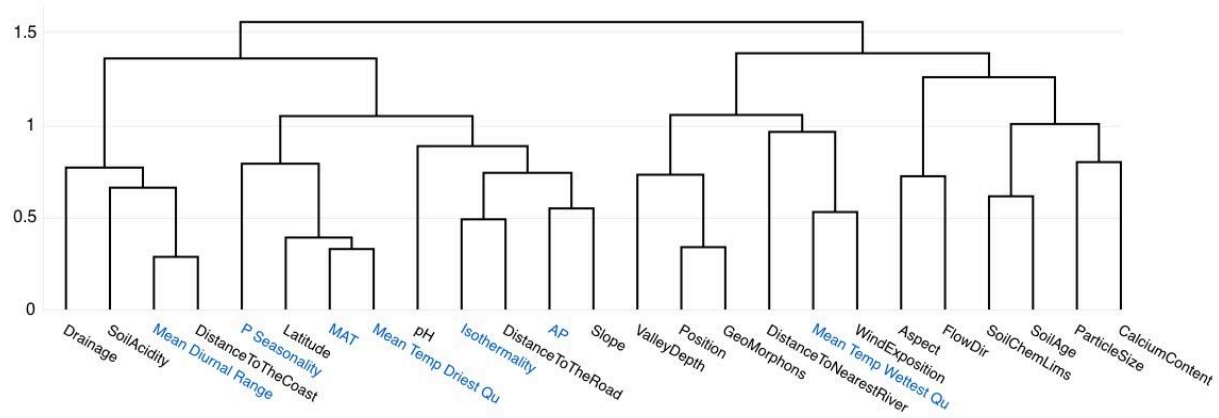


Figure A1*: Variable correlation structure. The y-axis gives the correlation between variables and clusters of variables. Climatic variables, subject to change in future climate projections, are highlighted in blue. MAT = Mean annual temperature, AP = total annual precipitation, P = precipitation, Qu = quarter.*

Model	Modeling Center	Year

MPI-ESM1-2-HR	German Climate Computing Centre, Germany	2017
MRI-ESM2-0	Meteorological Research Institute, Japan	2017
UKESM1-0-LL	Met Office Hadley Center, United Kingdom	2018

Table A1: The three climate models from WorldClim that were averaged for future climate projections, obtained from WorldClim 2.1 under the Coupled Model Inter-comparison Project phase 6 (CMIP6).

A2. Available Biomes

The distribution of the six biomes used in this study is displayed in (***Fig. A12***), with occupied area in (***Fig. A2***).

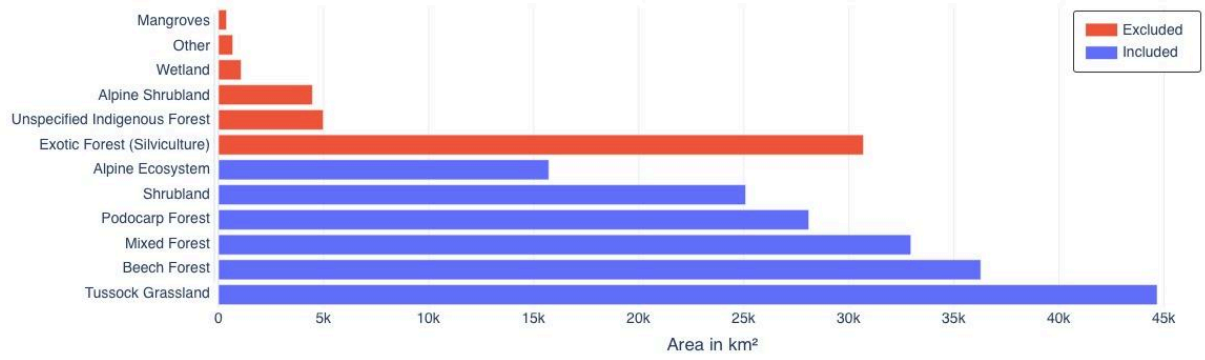


Figure A2*: Area occupied by natural ecosystems and silviculture forests in New Zealand. Colours indicate the six biomes used in this study.*

A3. Model Scores

We employed the True Skill Statistic (TSS) as the primary measure of model performance, as it is less sensitive to class imbalance than the more common ROC-AUC score and provides an established reliability threshold of 0.6(Yoon & Lee, 2023). Because ecological datasets are typically spatially autocorrelated, which can produce overoptimistic performance estimates (Ploton et al., 2020), we used five-fold spatial cross-validation with a 76-km block size, determined using the variogram method implemented in the blockCV package(Valavi et al., 2019) (***Fig. A3*** D). At this block size, the model achieved a TSS of 0.63, exceeding the established reliability threshold of 0.6 (***Fig. A3*** B). Model performance declined as block distance increased (***Fig. A3*** C), indicating reduced predictive performance under increasing spatial separation between training and test data.

We further examined the confusion matrix to identify class-specific sources of prediction error (***Fig. A3*** A). Notably, mixed forests were frequently misclassified as either beech or podocarp forests (5–14%), likely because these forest types can form continuous compositional gradients that are difficult to delineate from aerial imagery, potentially introducing classification noise into the training data. The largest classification error occurred for alpine ecosystems, 22% of which were misclassified as tussock grasslands (equivalent to 5% of observations classified as tussock grasslands). Similarly, shrublands were misclassified as other biomes, excluding alpine ecosystems, at rates of 5–12%. This confusion may reflect the ecological heterogeneity of shrublands, which encompass extensive vegetation and disturbed states associated with multiple biomes. Overall, the spatial cross-validation and class-specific error patterns indicate that the model retained useful predictive capacity under spatially independent evaluation, although potential data noise might improve its ability to distinguish ecologically continuous and heterogeneous classes.


A
Alpine
Tussock
Shrub
Podocarp
Beech
Mixed
True Class
75.9 %
22.3 %
0.5 %
0.1 %
1.0 %
0.2 %
5.3 %
86.6 %
1.3 %
0.1 %
6.0 %
0.7 %
0.0 %
5.8 %
69.8 %
12.6 %
5.7 %
6.1 %
0.0 %
0.2 %
5.8 %
80.2 %
3.9 %
9.9 %
0.1 %
4.3 %
2.5 %
1.4 %
80.6 %
11.0 %
0.0 %
0.4 %
5.3 %
6.4 %
14.3 %
73.6 %
Predicted Class
B
TSS across folds
Block size 76 km
Alpine
Beech
Mixed
Podocarp
Shrub
Tussock
Average*
* across biomes, weighted by biome area
C
76 km
True Skill Statistic
Spatial block distance (km)
D
Autocorrelation range (km)
Median: 76.3 km
WindExposition
Position
SoilChemLims
FlowDir
Aspect
ValleyDepth
SoilAge
GeoMorphons
DistanceToTheRoad
Slope
Mean Temp Driest Qu
CalciumContent
Mean Temp Wettest Qu
MAT
pH
DistanceToTheCoast
Drainage
Mean Diurnal Range
P Seasonality
ParticleSize
AP
Isothermality
SoilAcidity
DistanceToNearestRiver

Figure A3: Model performance and spatial cross-validation. (A) Confusion matrix showing the percentage of observations from each true class (rows) assigned to each predicted class (columns). Diagonal values represent correct classifications (class-specific recall), whereas off-diagonal values indicate misclassifications. (B) True Skill Statistic (TSS) across five folds of spatial cross-validation using a 76 km spatial block size. Boxplots show variation among folds for each biome; the overall average is weighted by biome area. (C) TSS for individual biomes across increasing spatial block distances. The vertical dashed line indicates the 76-km block size selected from the estimated spatial autocorrelation ranges. (D) Spatial autocorrelation ranges of predictor variables estimated using the blockCV package(Valavi et al., 2019). The dashed horizontal line indicates the median autocorrelation range (76.3 km), which was used to define the spatial block size for cross-validation.

We also used, the more common, Area Under the Receiver Operating Characteristic Curve (ROC AUC) (Fawcett, 2006) score. However, while SDMs typically predict a single class (presence/absence of one species), our model deals with a six-class problem, which makes the ROC-AUC overly optimistic due to the stark imbalance when comparing instances of the target class (positives) versus all other classes (negatives) (Wang & Carvalho, 2024). This led to scores above 0.9 (A value above 0.7 is considered reliable (Araújo et al., 2005)) even at larger block sizes, indicating ROC-AUC is not a good measure of model performance for the biome classification.

A4. Prediction Probability Uncertainty

The output of our model per pixel is six numbers (0-1) for each biome. The pixel is assigned the biome with the highest output. While the output is a number between 0 and 1, it is not a probability, but a score that can't be interpreted meaningfully. To obtain interpretable probabilities, the model outputs were calibrated using a sigmoid function (Platt scaling; (Niculescu-Mizil & Caruana, 2005)),

which fits a logistic model to align predicted scores with observed class frequencies. Calibration does not significantly change which class has the highest probability/score, and thus does not strongly alter the model's categorical class predictions. However, the raw numeric score becomes meaningful and interpretable as a class probability.

The model's uncertainty at each pixel will depend on how close the probability values are. For instance, if all probability values were equal, any small perturbation in input variables would likely tip the prediction in a different direction, making predictions unstable. To assess stability, we ranked class probabilities for each pixel and plotted the mean probability for each rank (***Fig. A4*** A). Regardless of SSP and time period, the model remained certain, with the predicted class probability 3-4 times higher than that of the second-ranked class. Next, we evaluated the difference between the highest-ranked and second-ranked classes across all time periods and SSPs (***Fig. A4*** B). While this difference diminished over time and with SSP, it remained high. However, the 95% confidence interval expanded to almost 0, meaning that for ~2.5% of pixels the model remained undecided. This is expected, as transitions between classes lead to changes in class ranks and thus a threshold at which the two probabilities are equal.

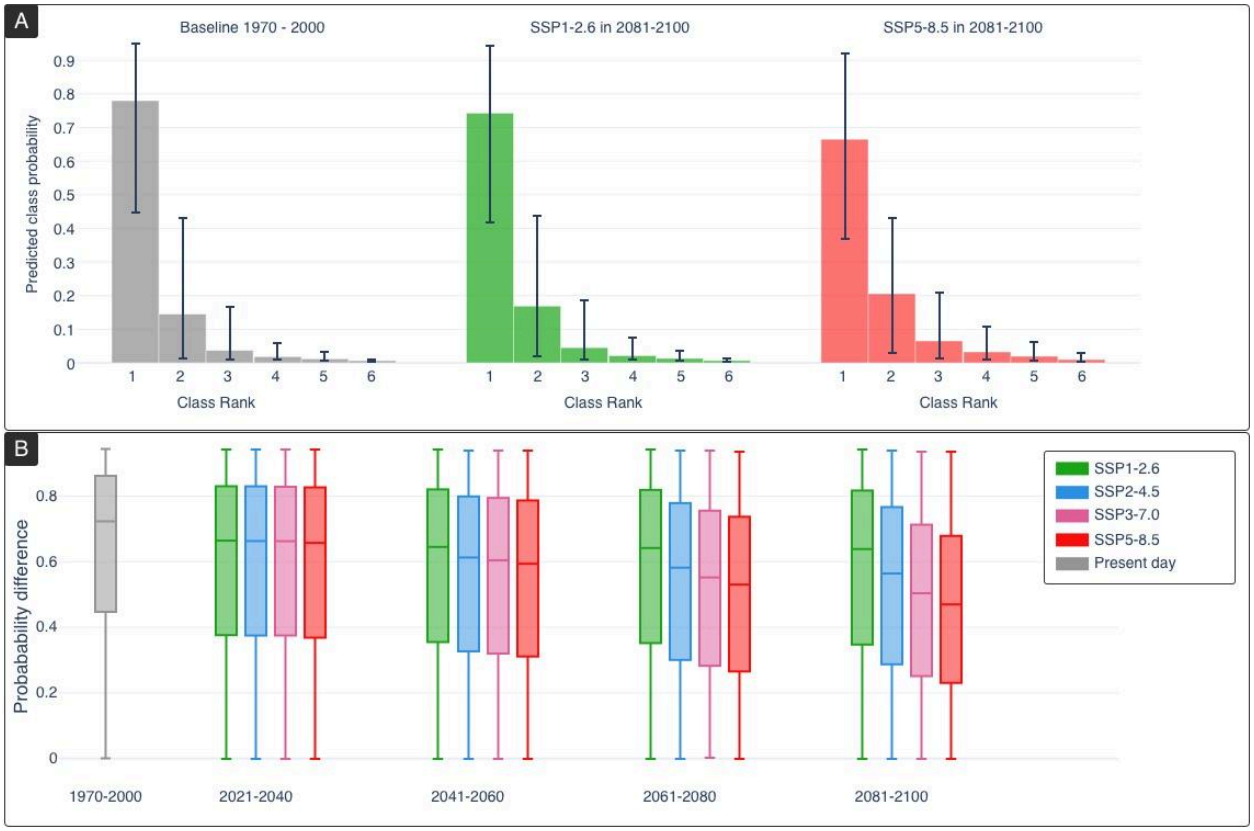


Figure A4*: Uncertainty in the model's class probability assignments. (A) The average probability of a class based on rank (e.g, rank 1 = predicted class with highest probability). Whiskers indicate 95% quantile. Three scenarios are shown as indicated by plot titles. (B) The difference in probability between the two top-ranked class probabilities (e.g. predicted class to the next most probable class) over time and SSPs. Whiskers indicate 95% confidence intervals.*

Additionally, we explored how the three climate models (Table A1) influence class predictions. Since a common approach to assessing likelihood in a multi-model scenario is to identify the consensus prediction between them (Capinha & Anastácio, 2011; Marmion et al., 2009; Noce et al., 2017), we identified no-consensus pixels where all three climate models predict different classes and used it as a measure of disagreement between models. The average disagreement across all SSPs and time brackets was 1.7% and increased to 2.9% at the end of the century. This indicates that a consensus

approach, rather than using the mean of the climate predictions, yields very similar results for biome area projections. The resulting landscape affinities are similarly only minimally affected by choice of model (see Section S6.1 and ***Fig. A8***)

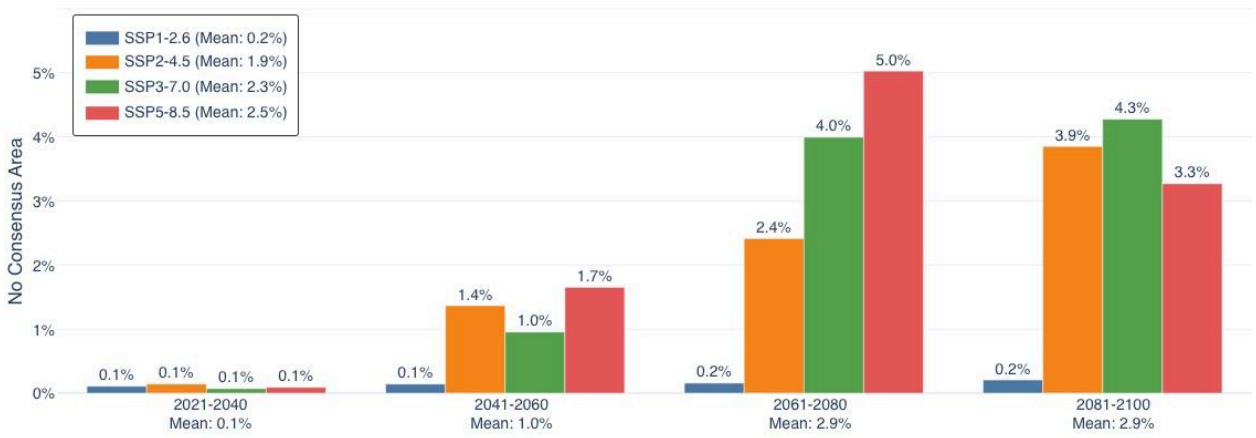


Figure A5*: Disagreement between climate models as percentage of pixels where class predictions for all three models differ (no-consensus area) by SSP (colour) over time. Means for year brackets are indicated on the x-axis and means for the SSPs in the legend. Total average is 1.7%*

A5. Affinity Trends

Two problems need to be addressed to efficiently estimate and compare affinity and landscape affinity trends. First, different variables (e.g., temperature, precipitation, etc.) yield different baseline affinities and therefore are not directly comparable. (If the biome distribution were to be uniform $p_b(T) = \frac{1}{T^+ - T^-}$ in the range (T^-, T^+), affinity would depend linearly on the constant factor $\frac{1}{T^+ - T^-}$ and thus would change in magnitude simply by a wider or narrower distribution, which does not affect the species' environmental match). Second, since species differ strongly in their absolute affinities, this produces large between-species intercept differences that are irrelevant to the temporal trend we aim to estimate. We developed a set of normalisation procedures to address these issues:

Variable Normalisation: To make variables comparable, for each SSP we computed the mean μ_0 and variance σ_0 of the affinity distribution for the first-year bracket (labelled "Pres." in Fig. 5) and transformed all affinity values using the formula $laV = \frac{la-\mu_0}{\sigma_0}$. This resulted in the first-year bracket distribution (across all species) always having a zero mean and unit variance, and the consequent timestamp reflecting the relative change in units of standard deviation, thus showing the change in affinity for this variable in an identical way across all variables.

Species Normalisation: To remove species-specific offsets while keeping all species on a comparable numerical scale, we offset each species by its present-day affinity, where $la_0(s)$ is the affinity of species s in the present day. This collapses the present-day affinity distribution across species to zero, but emphasises the trends species follow in subsequent years.

Full Normalisation: When applying the variable normalisation first, then the species normalisation, we get a fully normalised affinity trajectory, which is comparable across species and variables (Fig. 5A and B): $laF(s,t) = laV(s,t) - laV(s,0)$. Unless otherwise stated, this normalisation is used throughout the paper.

Both transformations are analogous for affinity and landscape affinity, except that for affinity, we need to apply the transformation to each SSP and biome, whereas for landscape affinity, we only need to apply it to each SSP.

A5.1 Affinity Regression

To identify trends in the affinity distributions of species across years, we fitted a bent cable regression (Chiu et al., 2006) to the affinity values $a(s,t)$ and computed their goodness of fit using:

$$R^2 = 1 - \frac{\sum_{s,t}(a(s,t) - pa(s,t))^2}{\sum_{s,t}(a(s,t) - \bar{a})^2}$$

Where $pa(s,t)$ are the model predictions and $\bar{a}$ the global mean. The process is analogous for fitting the normalised landscape affinity $laF(s,t)$ or affinities for subgroups (e.g. dominant and subordinate).

The goodness of fit for the fully normalised landscape affinity are stated in Table A2:

Variable	SSP1-2.6	SSP2-4.5	SSP3-7.0	SSP5-8.5
Annual Precipitation	0.006	0.023	0.011	0.047
Mean Annual Temperature	0.078	0.035	0.020	0.028
Mean Diurnal Range	0.029	0.019	0.012	0.019
Precipitation Seasonality	0.050	0.076	0.092	0.063
Temperature Annual Range	0.031	0.021	0.017	0.023

Table A2: Goodness of fits (R^2) for the fully normalised landscape affinity trends using bent cable regression.

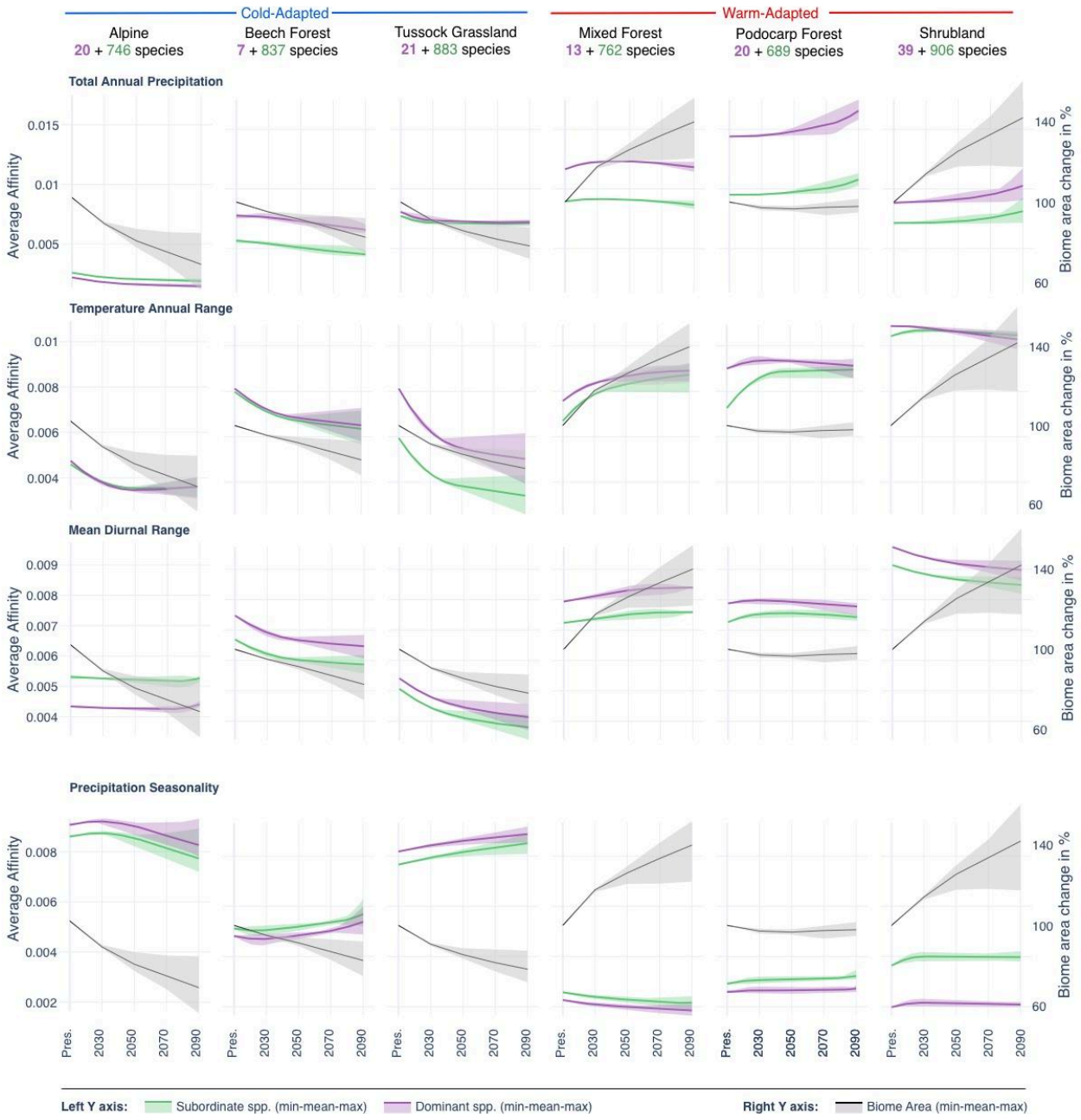


Figure A6: Species' biome affinity in relation to four climatic variables (rows). Lines show the mean across SSP scenarios, with shaded areas indicating minimum–maximum ranges. Regressions were fitted separately for dominant species (≈50% of total cover; purple) and subordinate species (green). Numbers below each biome indicate counts of dominant and subordinate species. Affinity values are not normalised (see Section S5) to emphasise differences between groups. The secondary y-axis (grey) shows projected mean biome area change from the present-day baseline in % with min–max shading.

A6. Uncertainty Partitioning

Beyond the extrapolation distance, the choice of climate model (CM), SSP, and SDM has a significant impact on projection accuracy (Thuiller et al., 2019). Since our choice of SDM was motivated by its ability to generalise and extrapolate (see the previous two sections), we did not use an ensemble SDM approach. We acknowledge but cannot assess other known sources of uncertainty, such as training methods and data (present-day climate data and biome identity), as well as endogenous factors (e.g., biotic feedbacks) influencing biome projections (Dietze, 2017). This leaves SSP and CM as sources of uncertainty.

Following (Morley et al., 2020), we assessed uncertainty by fitting a linear model to the predicted area $A_{b,y}$ for each biome and future year bracket $A_{b,y} \sim SSP + CM + \epsilon$ for the four SSPs and three CMs. Next, we computed the sum of squares (SS) error for each factor (SSP and CM) by summing the squared differences between each factor level and the overall mean. The SS values were divided by the number of pixels assigned to a biome to make them comparable across biomes. This yields, for

each biome and time bracket, the fractional contributions of SSP and CM to the projection uncertainty. The absolute magnitude of the sum of squares error indicates the overall variability of area projections across a biome, allowing the identification of biomes with stronger fluctuations.

Projections of uncertainty in alpine biomes and mixed forests were strongest and predominantly depended on the SSP, while climate models played a stronger role in near-term predictions (***Fig. A7***). Compared to other biomes, SSP was a disproportionately large source of uncertainty in shrublands. The other three biomes (beech forest, podocarp forests and tussock grasslands) showed relatively stable predictions, with beech forest variability more dependent on SSP and podocarp forests more on the choice of climate model. Projection uncertainty increased up to 10-fold between 2030 and 2090, constituting the strongest factor.

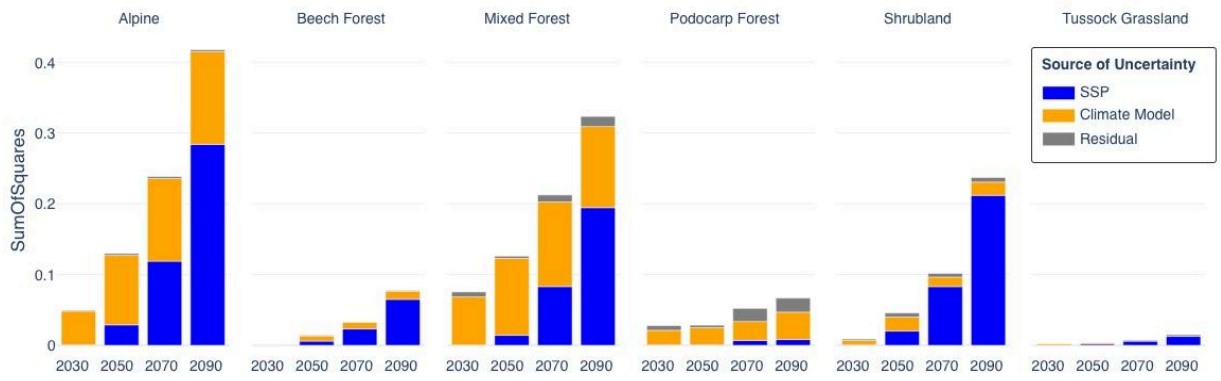


Figure A7: Partitioning of the sum of squares of biome area change (estimate of uncertainty) across SSP and climate model impact, as well as the unexplained residual.

A6.1 Agreement between Climate Models

To evaluate the difference the employed climate models have on the inferred landscape affinity trajectory, we reran the affinity calculation using each model individually and compared it to the

multi-model mean. Mean annual temperature, which had the strongest impact on landscape affinity, yielded almost identical trajectories and trends (plateau below SSP2-4.5 and collapse above). However, for SSP5-8.5 the landscape affinity for total annual precipitation and precipitation seasonality landscape affinity exhibited variation between models. Water deficit is an important driver of New Zealand's tree species and exhibits particularly strong gradients due to the east–west divide imposed by the Southern Alps(Leathwick & Whitehead, 2001), suggesting that the observed discrepancies among climate models may reflect differences in how they represent these precipitation gradients, as well as differences introduced during the projection downscaling process (Gibson et al., 2024).

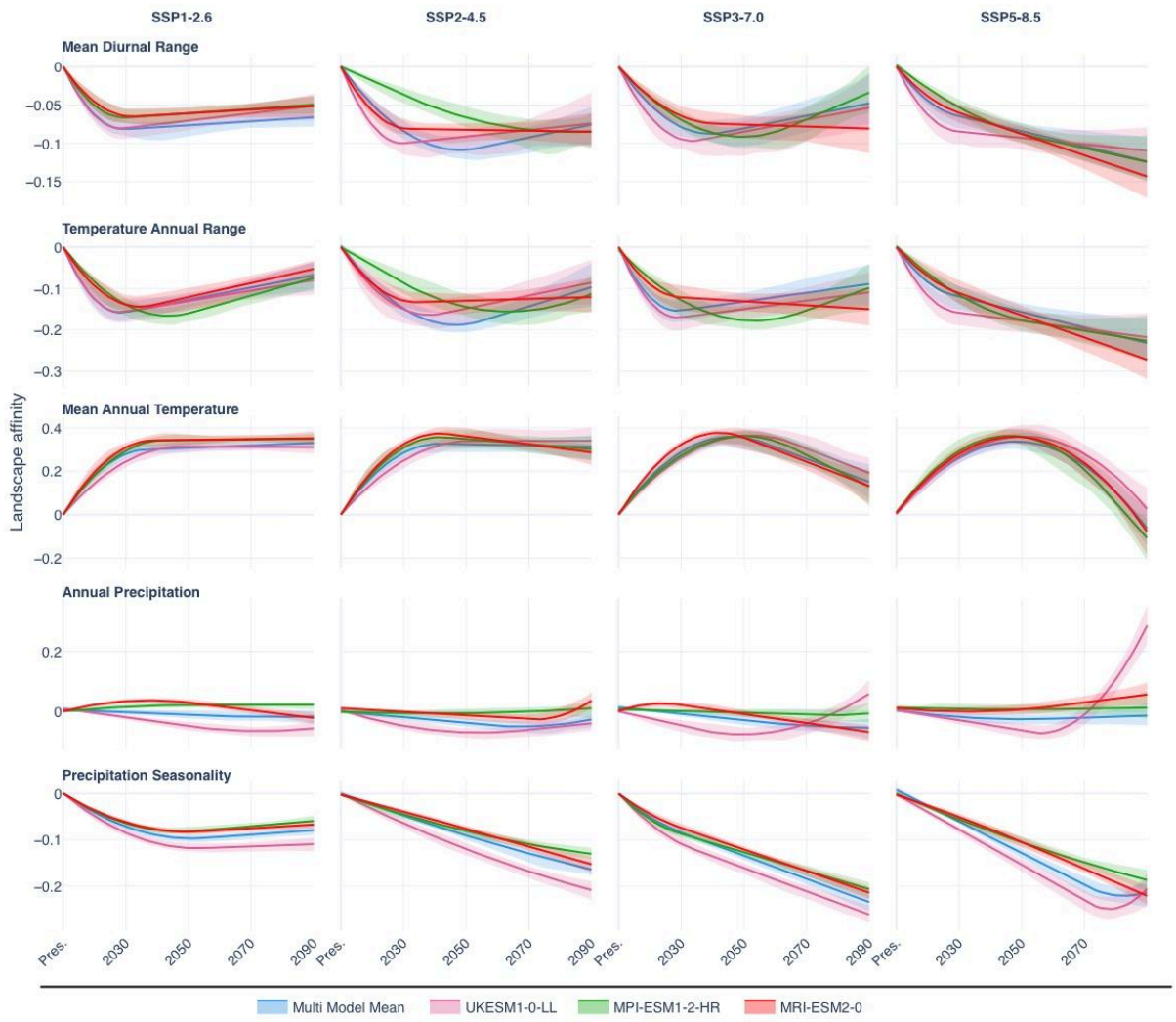


Figure A8: Comparison of fully normalised landscape affinity trajectories for all environmental variables based on the multi-model mean (main result) and individual global circulation models with 95% confidence intervals, by SSP (columns).

Similarly to landscape affinities the area projections of the six biomes were predominantly determined by SSP, with the exception of alpine and mixed forests biomes, where especially for the second half of the century climate model uncertainty rose to levels comparable to differences caused by SSP scenarios (***Fig. A9***). However, the climate model differences did not qualitatively

change the direction of the major area trends: shrinking cold-adapted biomes and expansion of mixed forests and shrublands.

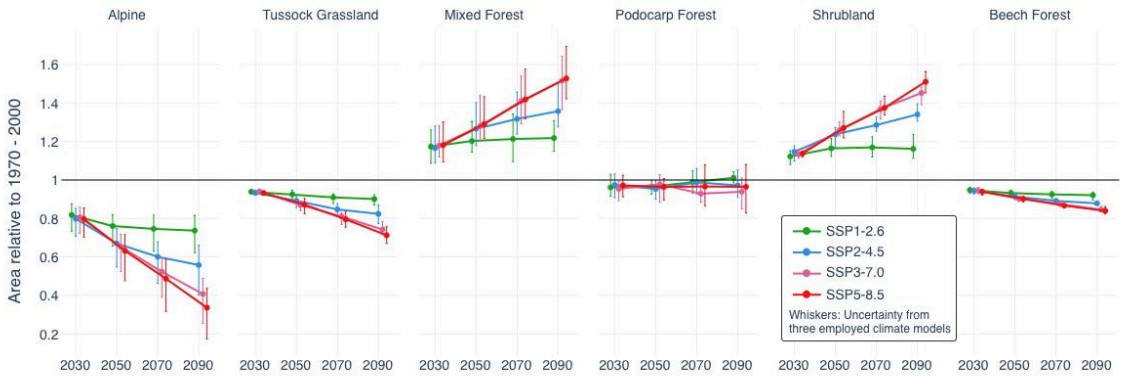


Figure A9: Area change relative to baseline for each SSP, with markers indicating the cross-model mean and whiskers the min–max range between the three climate models.

A7. Forecast Horizon

Extrapolating predictions on data dissimilar to the training set leads to unpredictable results and degraded performance, the farther the extrapolation extends ("extrapolation distance") (Charney et al., 2021; Owens et al., 2013), forming a forecast horizon threshold (FHT) beyond which model accuracy drops below an unacceptable threshold. For every point in an N-dimensional climate space, the extrapolation distance can be assessed as the distance (Euclidean or Mahalanobis) to the centroid of the training data (MESS, (Elith et al., 2010)) or to several nearest neighbours (MOP, (Owens et al., 2013)). Shape (Velazco et al., 2024) combines these approaches and normalises the nearest neighbour distance by the average distance to the centroid. The Shape distance is moreover interpretable because all training data points are 0, and a value of 1 indicates that the new data

point is as distant from the nearest training point as the training points are to the centroid of the training data. However, all metrics depend strongly on which input variables are used, making the choice of FHT ambiguous and the threshold value difficult to validate or transfer across studies.

To motivate our choice of an FHT method, we calculated the FHT needed for 90% of pixels to fall below it for all year brackets, four SSPs, two sets of variables, and two methods for assessing the extrapolation distance (z-score used in (Charney et al., 2021) and Shape proposed in (Velazco et al., 2024)). Since the variable choice also influences model performance, we plotted the FHT against the true skill statistic of the biome with the lowest score (***Fig. A10***). Both methods produced similar patterns, with one notable difference. In Shape, adding geographic variables lowered the FHT (magenta vs red lines in ***Fig. A10***), while using z-score led to a stark increase. A lowered FHT value in Shape is intuitively correct, as a specific climate might not be entirely novel unless specified by geographic variables like elevation and latitude, making it novel locally and thus increasing FHT. The z-score method did not show this pattern because it computes average standardised differences, which are reduced by adding static variables, diluting the climate's novelty. This motivated us to use Shape as the FHT metric with a set of 25 decorrelated variables (blue line), which combined good performance with lower FHT and, due to the reduced number of variables, better explainability and interpretability.



Figure A10: Assessment of how far into the future model predictions can be trusted under various forecast horizon thresholds. The X-axis represents the needed forecast horizon threshold to encompass 90% of the area. Two different extrapolation distance techniques are compared: z-score (right, (Charney et al., 2021)) or shape value (left, (Velazco et al., 2024)). The marker and line represent the mean and range across all sixteen SSPs and future period combinations. The y-axis shows the model's predictive performance, measured as the True Skill Statistic (TSS) for the shrubland biome (the hardest to predict across all biomes).

No general rule exists for setting the FHT value, and because it assesses climate novelty not observed in the training data, objective validation is impossible. One previous study found that across many SDM algorithms, performance degraded to an unacceptable level beyond an extrapolation distance of ~2-3σ (in climate space) from the training centroid (Charney et al., 2021). This neglects spatial covariates, which typically improve predictions (Brodie et al., 2022) and were necessary to achieve acceptable reliability at TSS > 0.6, making this finding inapplicable to our study. However, the typical horizon for comparable landscape-wide vegetation studies includes predictions to 2070 under most SSP scenarios (e.g., (Ali et al., 2023; Dyderski et al., 2018; Noce et al., 2017), which we used as a guideline. In our data, this corresponded to a Shape distance of ~1 with some variation across biomes. The authors of Shape note that the extrapolation threshold can be relaxed

with increasing niche breadth, as in biome classes modelled in this study (relative to single-species SDMs), suggesting that our threshold of 1 is a conservative choice. Collectively, these choices provide a conservative and transparent basis for defining the forecast horizon. Since no universally valid extrapolation threshold can be objectively established, our FHT represents a pragmatic limit on interpretation rather than a definitive boundary of model reliability.

A8. Range and Niche Shifts supplement

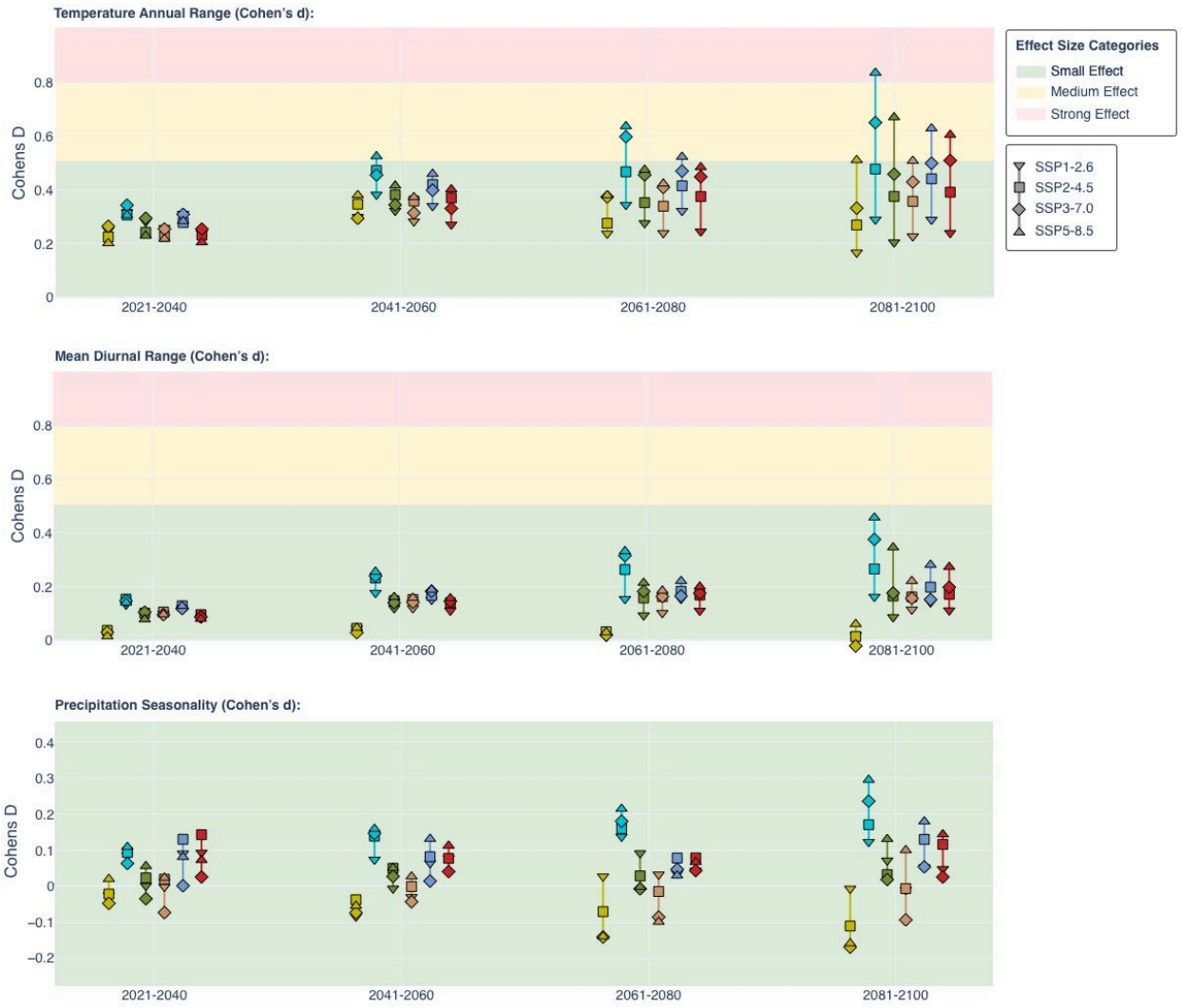


Figure A11: Change of distribution along climatic variables as Cohen's d between present-day distributions and projected future distributions. SSP scenarios are indicated by marker shape. Colours refer to biomes. Absolute strength of Cohen's d is colour-coded in the background.

A9. Species Abundances

To measure the abundance of species, we used 10,128 forest inventory plots (20x20m) from New Zealand's national vegetation survey (Wiser et al., 2001) surveyed a total of 13159 times from 1983 to 2022 (***Fig. A12***) using the RECCE methodology (Hurst, 2022). Locations are largely (but not

exclusively) spaced on an 8x8km grid and span the entirety of the three main islands in New Zealand. For each species, the RECCE method consists of a categorical cover estimate for every height tier category (1 through 6, for individuals > 25m down to < 60cm). These two values are collapsed into a single cover estimate using an established method (Fischer, 2015) and normalised to sum up to 1 across all species in plot i, yielding a relative cover $r(s, i)$ for a species. Using the biome data (Landcare Research, 2024), each plot can be assigned to a biome. Only species with more than 20 occurrences in a biome were retained to maintain accuracy.

Next, we determined the distribution of the mean annual temperature, annual precipitation, isothermality, pH and precipitation seasonality (collectively: variable) for each biome $p_b(V)$ across all pixels belonging to this forest type by using a kernel density estimate across the variable in each pixel assigned to this biome (***Fig. A13***). While New Zealand's forest biomes have a wide temperature and latitudinal spread, their temperature preference allows for a broader classification into warm-adapted (shrublands, podocarp forests, mixed forests) and cold-adapted (alpine, beech forests, tussock grasslands) biomes.

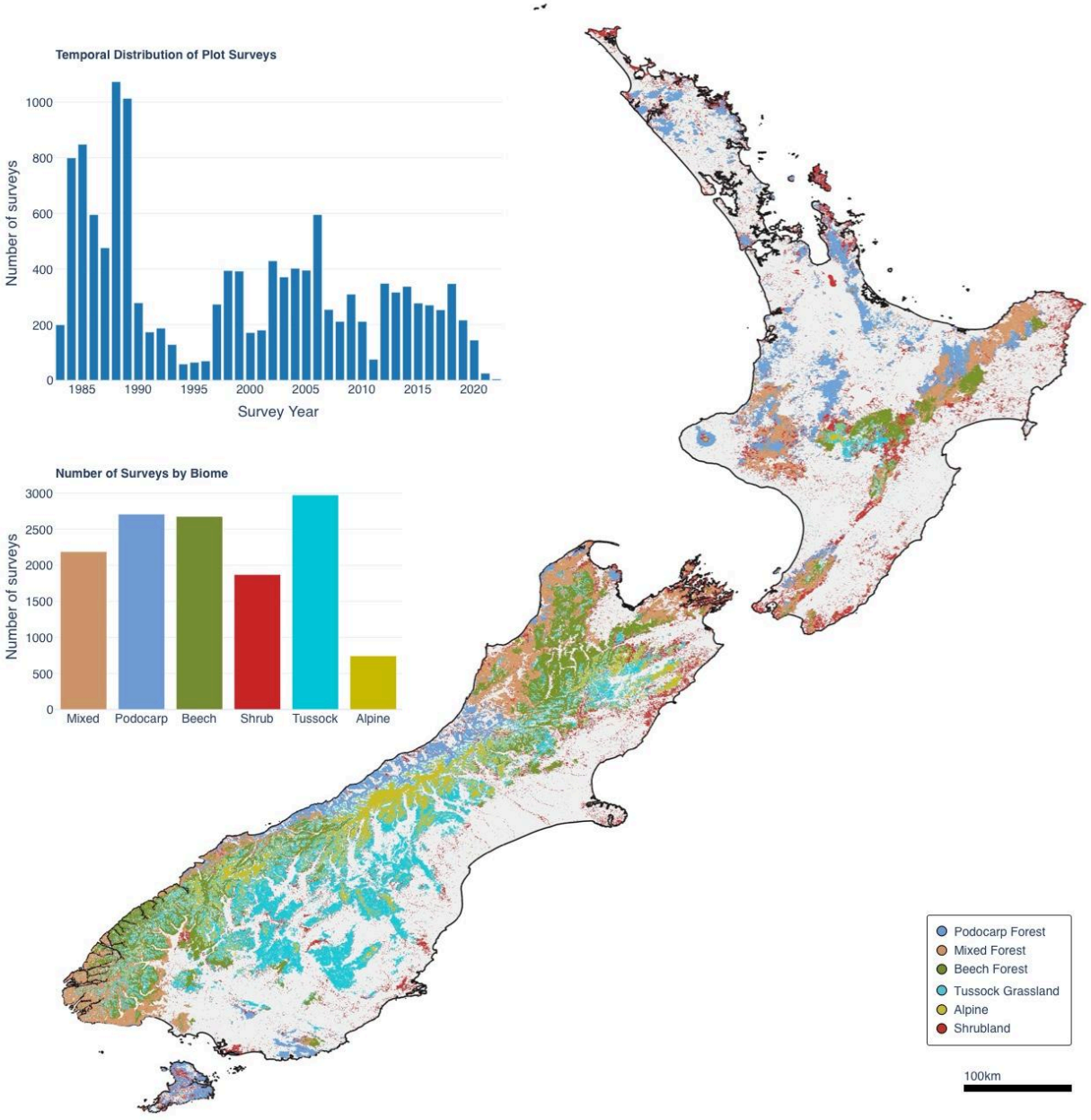

Temporal Distribution of Plot Surveys
Number of surveys
0
200
400
600
800
1000
1985
1990
1995
2000
2005
2010
2015
2020
Survey Year
Number of Surveys by Biome
Number of surveys
0
500
1000
1500
2000
2500
3000
Mixed
Podocarp
Beech
Shrub
Tussock
Alpine
Podocarp Forest
Mixed Forest
Beech Forest
Tussock Grassland
Alpine
Shrubland
100km

Figure A12: The map shows the distribution of the biomes, with colour corresponding to the biome assignment from satellite data. Pixels that are not one of the six biomes are gray. The upper histogram shows the survey year of the plots used in this study. The lower histogram shows the number of surveys per biome. The survey plot location is not shown.

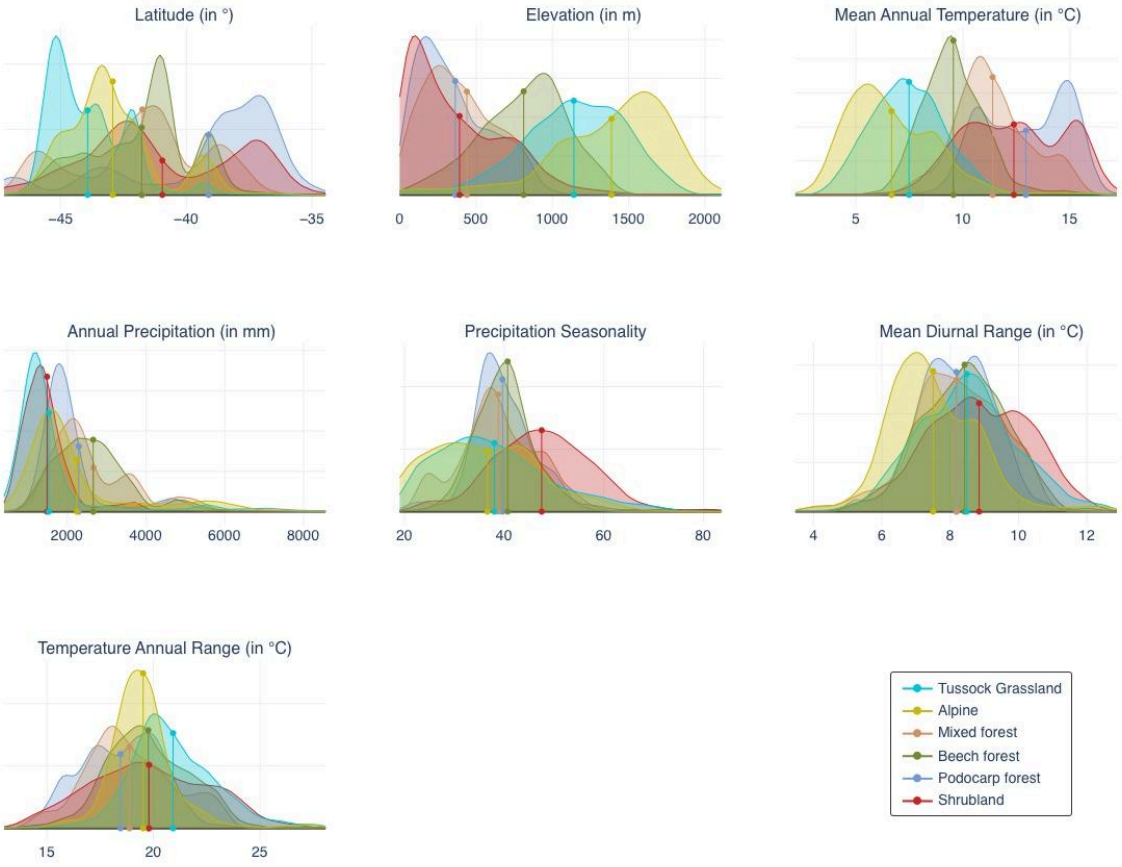


Figure A13: Distributions of environmental variables across the six studied biomes. Curves generated via kernel density estimate. Latitude multimodality is due to the three separate islands in New Zealand (North, South, and Stewart Islands).

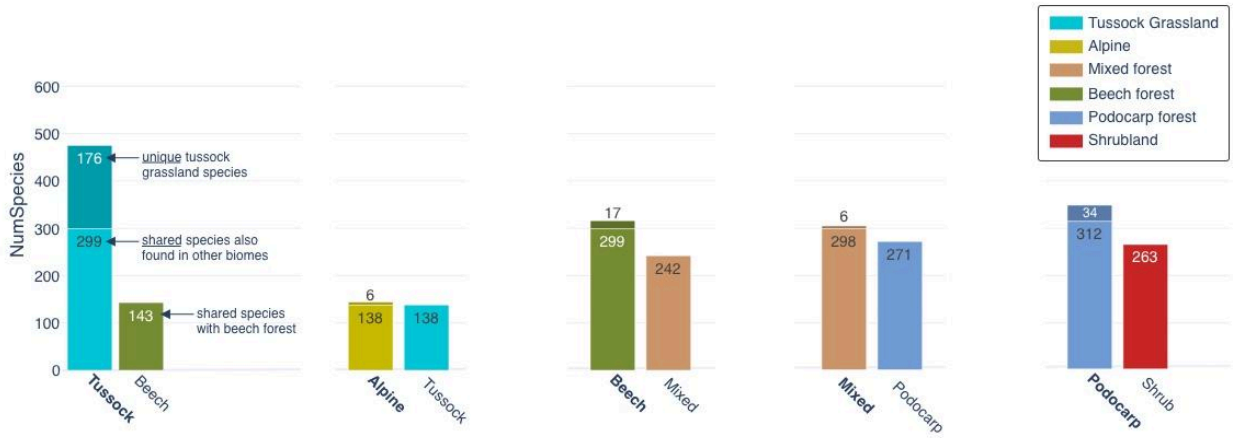


Figure A14: Shared species across biome pairs. The pairs are chosen to match the main biome transitions according to Fig. 3 of the main results. The left bar in each pair shows the number of species found in that biome and observed in at least 20 plots broken down into two categories: Shared species found in this and other biomes (brighter shade), unique species found only in that biome (darker shade). The other bar indicates how many of the shared species are found in the respective other biome. Arrows in the top left panel exemplify this. A high overlap of species between biomes indicates lower dispersal constraints, as the species are already present in both biomes.

A10. References

Ali, F., Khan, N., Khan, A. M., Ali, K., & Abbas, F. (2023). Species distribution modelling of Monotheca buxifolia (Falc.) A. DC.: Present distribution and impacts of potential climate change. *Heliyon*, *9*(2), e13417.

Araújo, M. B., Pearson, R. G., Thuiller, W., & Erhard, M. (2005). Validation of species–climate impact

models under climate change. *Global Change Biology*, *11*(9), 1504–1513.

Brodie, S., Smith, J. A., Muhling, B. A., Barnett, L. A. K., Carroll, G., Fiedler, P., Bograd, S. J., Hazen, E. L., Jacox, M. G., Andrews, K. S., Barnes, C. L., Crozier, L. G., Fiechter, J., Fredston, A., Haltuch, M. A., Harvey, C. J., Holmes, E., Karp, M. A., Liu, O. R., … Kaplan, I. C. (2022). Recommendations for quantifying and reducing uncertainty in climate projections of species distributions. *Global Change Biology*, *28*(22), 6586–6601.

Capinha, C., & Anastácio, P. (2011). Assessing the environmental requirements of invaders using ensembles of distribution models: Environmental requirements from ensembles of models. *Diversity & Distributions*, *17*(1), 13–24.

Charney, N. D., Record, S., Gerstner, B. E., Merow, C., Zarnetske, P. L., & Enquist, B. J. (2021). A test of species distribution model transferability across environmental and geographic space for 108 western north American tree species. *Frontiers in Ecology and Evolution*, *9*(689295). https://doi.org/10.3389/fevo.2021.689295

Chiu, G., Lockhart, R., & Routledge, R. (2006). Bent-cable regression theory and applications. *Journal of the American Statistical Association*, *101*(474), 542–553.

Dietze, M. C. (2017). Prediction in ecology: a first-principles framework. *Ecological Applications: A Publication of the Ecological Society of America*, *27*(7), 2048–2060.

Dyderski, M. K., Paź, S., Frelich, L. E., & Jagodziński, A. M. (2018). How much does climate change threaten European forest tree species distributions? *Global Change Biology*, *24*(3), 1150–1163.

Elith, J., Kearney, M., & Phillips, S. (2010). The art of modelling range-shifting species. *Methods in Ecology and Evolution / British Ecological Society*, *1*(4), 330–342.

Fawcett, T. (2006). An introduction to ROC analysis. *Pattern Recognition Letters*, *27*(8), 861–874.

Fischer, H. S. (2015). On the combination of species cover values from different vegetation layers. *Applied Vegetation Science*, *18*(1), 169–170.

Gibson, P. B., Rampal, N., Dean, S. M., & Morgenstern, O. (2024). Storylines for future projections of precipitation over New Zealand in CMIP6 models. *Journal of Geophysical Research Atmospheres*, *129*(5), e2023JD039664.

Hurst, J. M. (2022). *The Recce method for describing New Zealand vegetation - field manual*. Manaaki Whenua Press. https://doi.org/10.7931/P48H-ZB65

Landcare Research. (2024). *Basic Ecosystems* [Dataset]. https://doi.org/10.7931/L1HM1

Leathwick, & Whitehead, D. (2001). Soil and atmospheric water deficits and the distribution of New Zealand's indigenous tree species: Water deficits and tree distribution. *Functional Ecology*, *15*(2), 233–242.

Marmion, M., Parviainen, M., Luoto, M., Heikkinen, R. K., & Thuiller, W. (2009). Evaluation of consensus methods in predictive species distribution modelling. *Diversity & Distributions*, *15*(1), 59–69.

Morley, J. W., Frölicher, T. L., & Pinsky, M. L. (2020). Characterizing uncertainty in climate impact projections: a case study with seven marine species on the North American continental shelf. *ICES Journal of Marine Science: Journal Du Conseil*, *77*(6), 2118–2133.

Niculescu-Mizil, A., & Caruana, R. (2005). Predicting good probabilities with supervised learning. *Proceedings of the 22nd International Conference on Machine Learning - ICML '05*, 625–632.

Noce, S., Collalti, A., & Santini, M. (2017). Likelihood of changes in forest species suitability, distribution, and diversity under future climate: The case of Southern Europe. *Ecology and Evolution*, *7*(22), 9358–9375.

Owens, H. L., Campbell, L. P., Dornak, L. L., Saupe, E. E., Barve, N., Soberón, J., Ingenloff, K., Lira-Noriega, A., Hensz, C. M., Myers, C. E., & Peterson, A. T. (2013). Constraints on interpretation of ecological niche models by limited environmental ranges on calibration areas. *Ecological Modelling*, *263*, 10–18.

Ploton, P., Mortier, F., Réjou-Méchain, M., Barbier, N., Picard, N., Rossi, V., Dormann, C., Cornu, G., Viennois, G., Bayol, N., Lyapustin, A., Gourlet-Fleury, S., & Pélissier, R. (2020). Spatial validation reveals poor predictive performance of large-scale ecological mapping models. *Nature Communications*, *11*(1), 4540.

Thuiller, W., Guéguen, M., Renaud, J., Karger, D. N., & Zimmermann, N. E. (2019). Uncertainty in ensembles of global biodiversity scenarios. *Nature Communications*, *10*(1), 1446.

Valavi, R., Elith, J., Lahoz-Monfort, J. J., & Guillera-Arroita, G. (2019). block CV : An r package for generating spatially or environmentally separated folds for *k* -fold cross-validation of species distribution models. *Methods in Ecology and Evolution*, *10*(2), 225–232.

Velazco, S. J. E., Rose, M. B., De Marco, P., Jr, Regan, H. M., & Franklin, J. (2024). How far can I extrapolate my species distribution model? Exploring shape, a novel method. *Ecography*, *2024*(3). https://doi.org/10.1111/ecog.06992

Wang, L., & Carvalho, L. (2024). Multiclass ROC. In *arXiv [stat.ML]*. arXiv. http://arxiv.org/abs/2404.13147

Wiser, S. K., Bellingham, P. J., & Burrows, L. E. (2001). Managing biodiversity information: development of New Zealand's National Vegetation Survey databank. *New Zealand Journal of Ecology*, *25*(2).

Yoon, S., & Lee, W.-H. (2023). Application of true skill statistics as a practical method for quantitatively assessing CLIMEX performance. *Ecological Indicators*, *146*(109830), 109830.

Appendix B: Supplementary Materials for TrP

B1. Data

The three forest types differ in their climatic preferences. Podocarp forests are predominant on the warmer North Island of New Zealand and appear in more coastal areas at lower elevations and slopes. On average, they are more humid. Beech forests on the other hand are more seasonal (lower isothermality), drier, higher in elevation and cooler. They predominate on New Zealand's South Island.

Mixed forests lean towards one or the other type. For example, they have a similar elevational profile as podocarp forests, but their mean latitude is closer to that of beech forests. Their temperature preference is naturally between the other types. On average, the three forest types are along a gradient from a subtropical to a temperate forest.

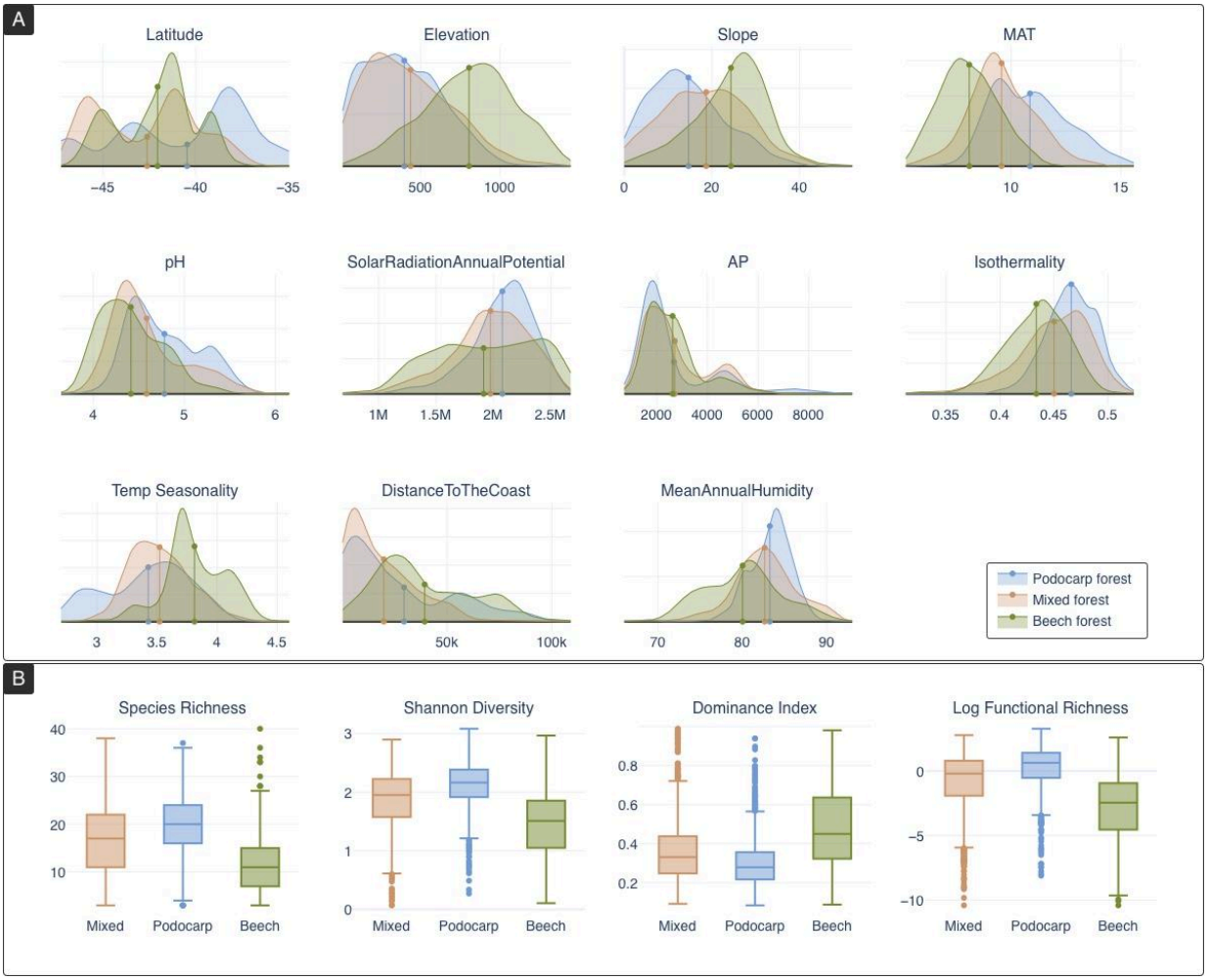


Figure B1: Properties of the studied forest types. (A) Distributions of environmental variables across the three forest types. Curves generated via kernel density estimate. Latitude multimodality is due to the three separate islands in New Zealand (North, South, and Stewart Islands). (B) Species richness, Shannon-Weiner Index (measures diversity), Dominance Index (basal cover of dominant species in the plot), and log-transformed functional richness.

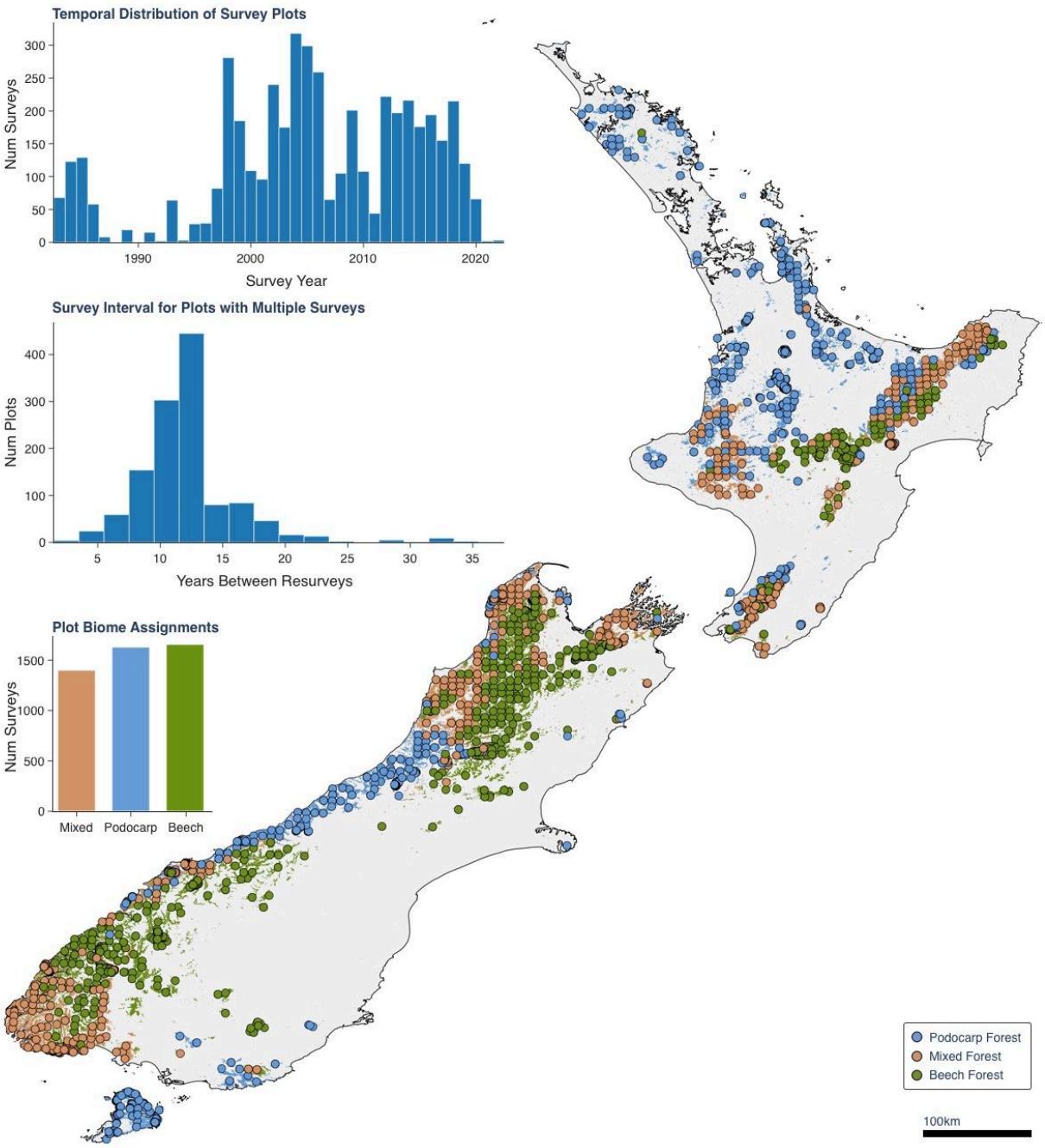

Temporal Distribution of Survey Plots
Num Surveys
0
50
100
150
200
250
300
1990
2000
2010
2020
Survey Year
Survey Interval for Plots with Multiple Surveys
Num Plots
0
100
200
300
400
5
10
15
20
25
30
35
Years Between Resurveys
Plot Biome Assignments
Num Surveys
0
500
1000
1500
Mixed
Podocarp
Beech
Podocarp Forest
Mixed Forest
Beech Forest
100km

Figure B2: Spatial and temporal distribution of surveyed plots across New Zealand. The map shows the distribution of the plots, with colour corresponding to the assigned biome. Background colouring indicates the biome assignment from satellite data. Pixels that are not one of the three biomes are gray. The upper histogram shows the survey year of the plots used in this study. For plots that have been surveyed more than twice, the histogram of the time between the surveys is indicated by the middle histogram. The lower histogram displays the number of surveys in each biome.

B2. Imputation

In *miceforest* *(Wilson et al. 2023)*, multiple imputation works by iteratively filling in missing values using a random forest algorithm (Breiman 2001). The basis is a species-trait matrix with each row corresponding to the trait values of a single species. This matrix contains missing values. For each missing value, the algorithm uses the observed data to build a series of decision trees that predict the missing values based on the patterns learned from the complete data. During each iteration, the imputed values are updated by considering both the relationships between variables and the uncertainty associated with the missing data. The algorithm thus exploits correlations between known trait values to impute missing values.

The number of iterations I is a hyperparameter that can positively impact performance, at the expense of runtime. Performance can be further improved by adding phylogenetic or taxonomic information, if available, as a species vector and adding it as additional columns to the species-trait matrix (Debastiani et al. 2021). This is typically done using phylogenetic eigenvectors (Diniz-Filho et al. 1998).

B2.1 Taxonomic Eigenvectors

We constructed a taxonomic tree (with equal distances on each branch) for our species using the PhyloT(https://phylot.biobyte.de/) website and transformed it into an ordinal distance matrix (i.e., one constructed from a taxonomic tree where all branch lengths are equal to one). This distance matrix was transformed into a set of vectors using phylogenetic eigenvector regression (Diniz-Filho et al. 1998), which yields better imputation results (Penone et al. 2014) and has been successfully utilised previously (Debastiani et al. 2021). The number of available phylogenetic eigenvectors (PVRs) is equal to the number of species. We utilized $E = 20$ eigenvectors as this resulted in the best performance.

B2.2. Imputation Error

To assess the quality of the imputation and optimise the hyperparameters, we implemented a leave-one-out error scheme:

1. From each trait, we removed a single value (of a random species), leading to $T = 7$ additional missing values in the species-trait matrix. This value is denoted by a_{ti} for the trait t and species i.
2. We add E PVRs as columns to the amputated species-trait matrix
3. The MICE algorithm imputes missing values, resulting in the previously amputated values a_{ti} now having a value b_{ti}. If the imputation were perfect $a_{ti} = b_{ti}$.
4. Steps 1 to 3 are repeated N times until every known trait value is amputated at least once. N in our dataset is therefore the number of species where $\delta^{15}N$ is missing, as this trait has the highest missingness (***Fig. B3*** B).
5. A root mean square error (RMSE) between the imputation value and the true value is computed for each trait t individually and normalised (NRMSE) by the standard deviation of the

known trait values across all species σ_t:

$$nrmse_t = \sqrt{\frac{1}{N}\sum_i (b_{ti} - a_{ti})^2} \cdot \frac{1}{\sigma_t}$$

The NRMSE expresses the imputation error in relation to the variation of the trait expressed in %. Since known data is removed to compute the NRMSE, the imputation performance using all available values will be better than when computing the NRMSE. This makes our NRMSE calculation an upper bound of the error.

6. An average across all traits of $nrmse_t$ yields a single error metric for the entire imputation process.

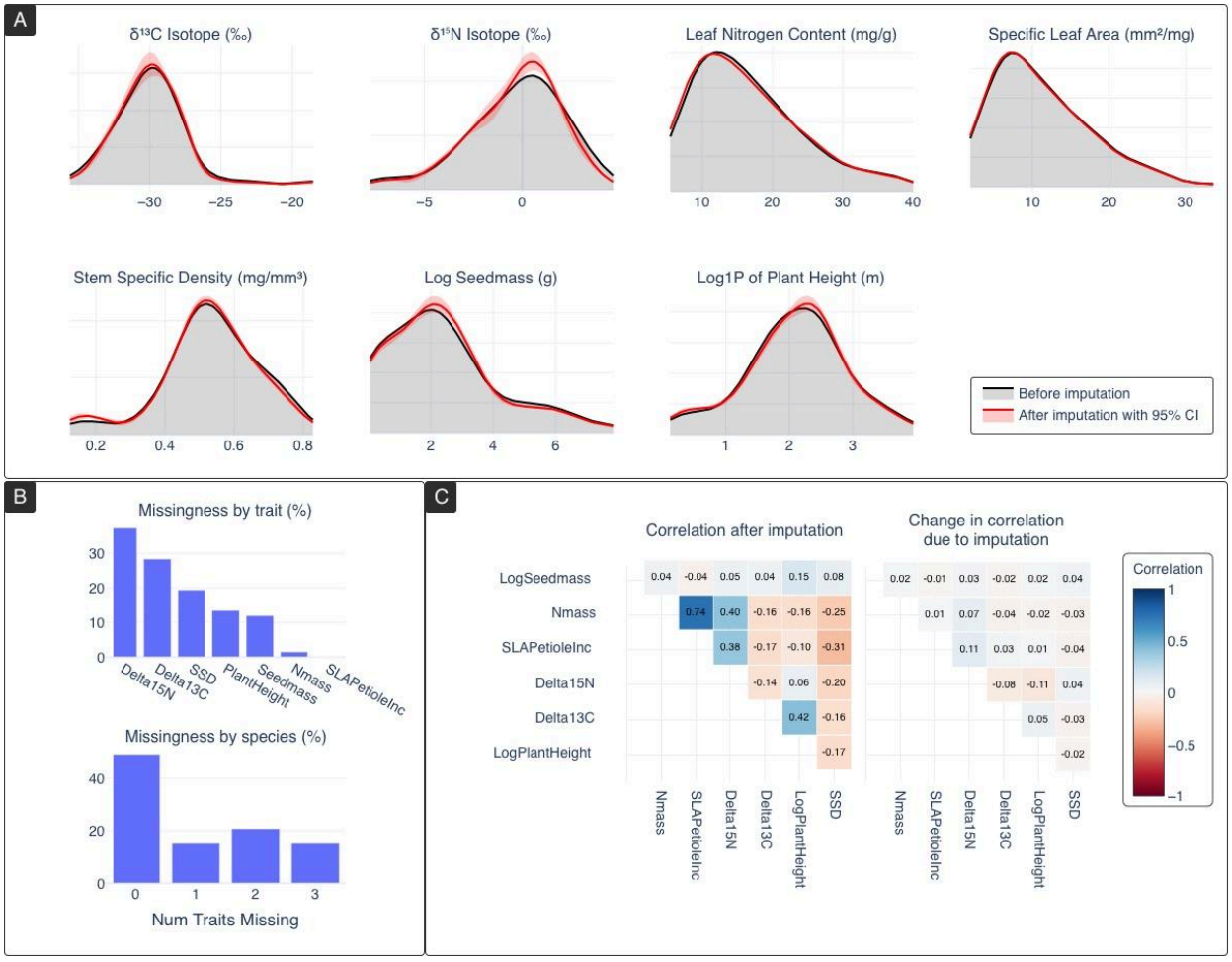


Figure B3: Impacts of imputation on trait distributions. (A) Distributions of traits before and after imputation. (B) Missingness. Top: Percentage of species missing a specific trait. Bottom: Percentage of species missing a certain number of traits. (C) Correlation matrix of the traits. Left: After imputation. Right: Difference between the correlation matrix before and after imputation. i.e. changes in correlation induced by the imputation procedure.

B2.3. Error and Hyperparameter Choice

The number of MICE iterations I (see (Wilson et al. 2023)) and PVRs E are hyperparameters optimised by exhaustively trying out various combinations (grid search) and comparing the average NRMSE. The lowest mean error across all traits was 10.68% at five iterations and 20 PVRs.

B3. Supplementary Methods

B3.1 Formulae for computing trait moments

Let t_s be the value of the focal trait of species s and a_{si} be the abundance of this species in the plot i. The abundances are normalised such that $\sum_s a_{si} = 1$. The community weighted moments are then defined as follows (Wieczynski et al. 2019):

Community weighted mean (CWM):

$$CWM_i = \sum_s a_{si} \cdot t_s$$

Community weighted variance (CWV):

$$CWV_i = \sum_s a_{si}(t_s - CWM_i)^2$$

Community weighted skew (CWS):

$$CWS_i = \sum_s a_{si}\left(\frac{t_s - CWM_i}{\sqrt{CWV_i}}\right)^3$$

Community weighted kurtosis (CWK):

$$CWS_i = \sum_s a_{si}\left(\frac{t_s - CWM_i}{\sqrt{CWV_i}}\right)^4 - 3$$

B3.2. Rate of Directional Change: plot occupancy over time

To estimate whether a species has increased its plot occupancy over time, we calculated the ratio of plots containing this species to the total number of plots measured in that year, yielding a single plot occupancy value of 0-1 for each year (omitting years where the species was not detected). This is done for each forest type separately. We then ran a linear regression to determine whether plot occupancy had a significant positive trend (species becomes more common) or a negative trend (species becomes less common). We used the slope of the linear regression to indicate the rate of change in occupancy, interpreting only slopes statistically significantly different from zero. This allows us to qualitatively compare occupancy trends of species across forest types. As the location of the plots is not considered, the rate of occupancy change does not differentiate a species becoming more common within its geographical range from an expansion of the species' range. In both cases, a positive rate of occupancy change indicates an increase in individuals of this species in response to climate change.

B3.3. Rate of Turnover: Index of Dissimilarity change per Year

To assess aim three, we modified the Index of Dissimilarity (Taeuber and Taeuber 1976), IoD) which measures what proportion of individuals (or basal area in our case) would need to move to achieve the observed species rearrangement. A value of 1 indicates that all individuals would need to relocate, while a value of 0 means no change. We used IoD as a metric of turnover for single species. It was determined by using the abundances of species in remeasured plot pairs ($a_i^0(s)$ and $a_i^1(s)$) and their sums across all plots (e.g. $A^1(s) = \sum a_i^1(s)$). Giving the index: $IoD(s) = \frac{1}{2}\sum_i^N \left| \frac{a_i^0(s)}{A^0(s)} - \frac{a_i^1(s)}{A^1(s)} \right|$. Since IoD would be expected to be higher if the remeasurement interval is increased, we calculated an IoD per year using the following scheme:

1. Binning all plot pairs based on their remeasurement interval ($P_{\Delta y}$)
2. Computing the IoD for each subset $IoD(s, \Delta y)$ separately
3. Combining the IoDs divided by Δy and weighed by the number of plots for each interval $|P_{\Delta y}|$:

   $$IoDpY(s) = \frac{1}{|P|} \sum_{\Delta y} \frac{IoD(s,\Delta y)}{|P_{\Delta y}| \cdot \Delta y}$$

   The resulting metric is independent of the remeasurement interval.

IoDpY can be interpreted as the percentage of a species' currently occupied basal area that needs to shift per year to match the observed species turnover. However, it does not inform whether a species expands or contracts its range.

B3.4. Null Models

To calculate the standardised effect sizes we employed the following algorithm:

1. Let i denote the survey of a forest plot located in a biome b, containing a set of N species $S_i = \{s_k\}$ and $M(S_i)$ be a metric of interest measured on this species assemblage (e.g. functional richness). The metric of the true assemblage is denoted by M_i^{True}
2. Based on the total number of observations of a species s in all plots located in forest type f define a probability distribution $P_f(s)$, where $\sum_s P_f(s) = 1$.
3. Draw a random assemblage of species S_i^{α} of length N according to the probability $P_f(s)$ and compute the metric of interest on the random assemblage $M(S_i^{\alpha}) = M_i^{\alpha}$. This step ensures that rare species are not over-represented in S_i^{α}.
4. Repeat step three 1000 times to yield a null distribution for the metric $P_i^{Null} = \{M_i^{\alpha} | \alpha = B..1000\}$
5. Determine the mean and variance of the null distribution: μ_i^{Null} and σ_i^{Null}.
6. The standardised effect size (SES) is defined as $SES_i(M) = \left(M_i^{True} - \mu_i^{Null}\right) \cdot \frac{1}{\sigma_i^{Null}}$.

The SES captures the importance of the identities of the species found in plot i to the metric M. For instance, if any combination of species would yield the exact same value of M, the identity of the species is irrelevant and $SES_i(M) = 0$. This is only true for the species richness as a metric, and deviates from zero to a different degree for all other metrics, allowing to decouple neutral

processes, where species identity is assumed irrelevant to the metric, and functional changes, where species traits' determine their success in a given environment.

We evaluated whether the standardised effect size computation removed the correlation of the functional metrics with species richness and found that this was the case for all employed metrics (***Fig. B4***). This is expected, as the goal of the standardised effect size is to decouple the metric from the functional richness (Swenson and Weiser 2014).

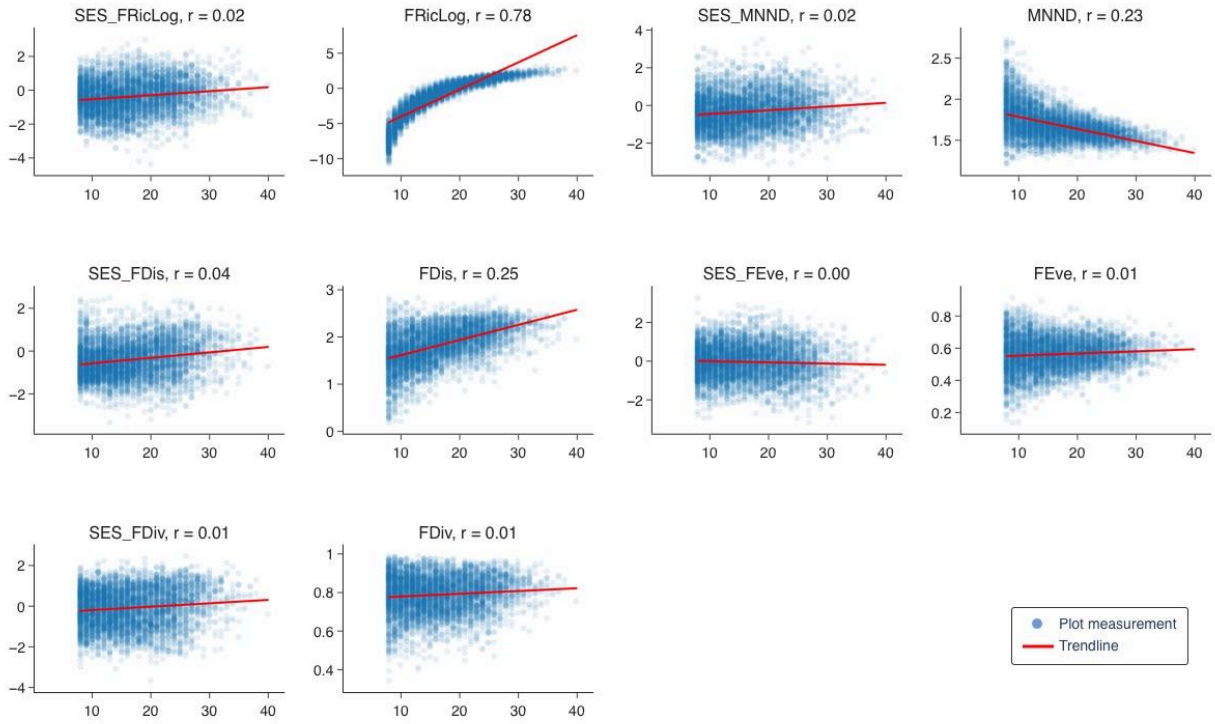


Figure B4: Correlation of species richness (x-axis) and functional metrics (FRicLog, MNND, FDis, FEve and FDiv), as well as their standardised effect sizes (SES prefix). The Pearson correlation is given in the title of each subplot.

B4. Supplementary Results

B4.1 Changes in climate

Over the last 50 years, mean temperatures have been increasing across all forest types at a rate of ~0.12°C per decade or 0.6°C over 50 years, while seasonality decreased (***Fig. B5***). Precipitation in all forest types decreased by ~22 mm per decade, corresponding to a decrease of 0.87% of the mean annual precipitation or ~4.8% over the last 50 years.

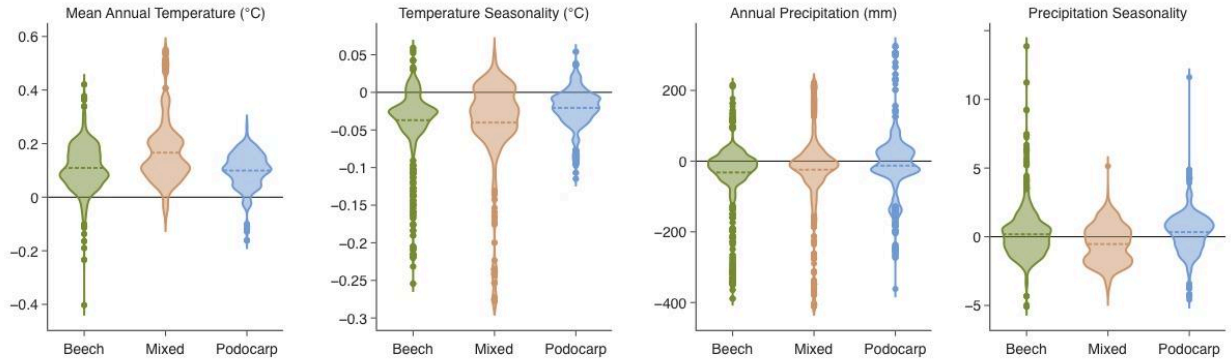


Figure B5: Changes in temperature, precipitation, and their respective seasonality values per decade. Distribution derived from changes at single forest plots. The dashed line indicates the mean, and the black line is at zero.

B4.2. Community environmental preferences

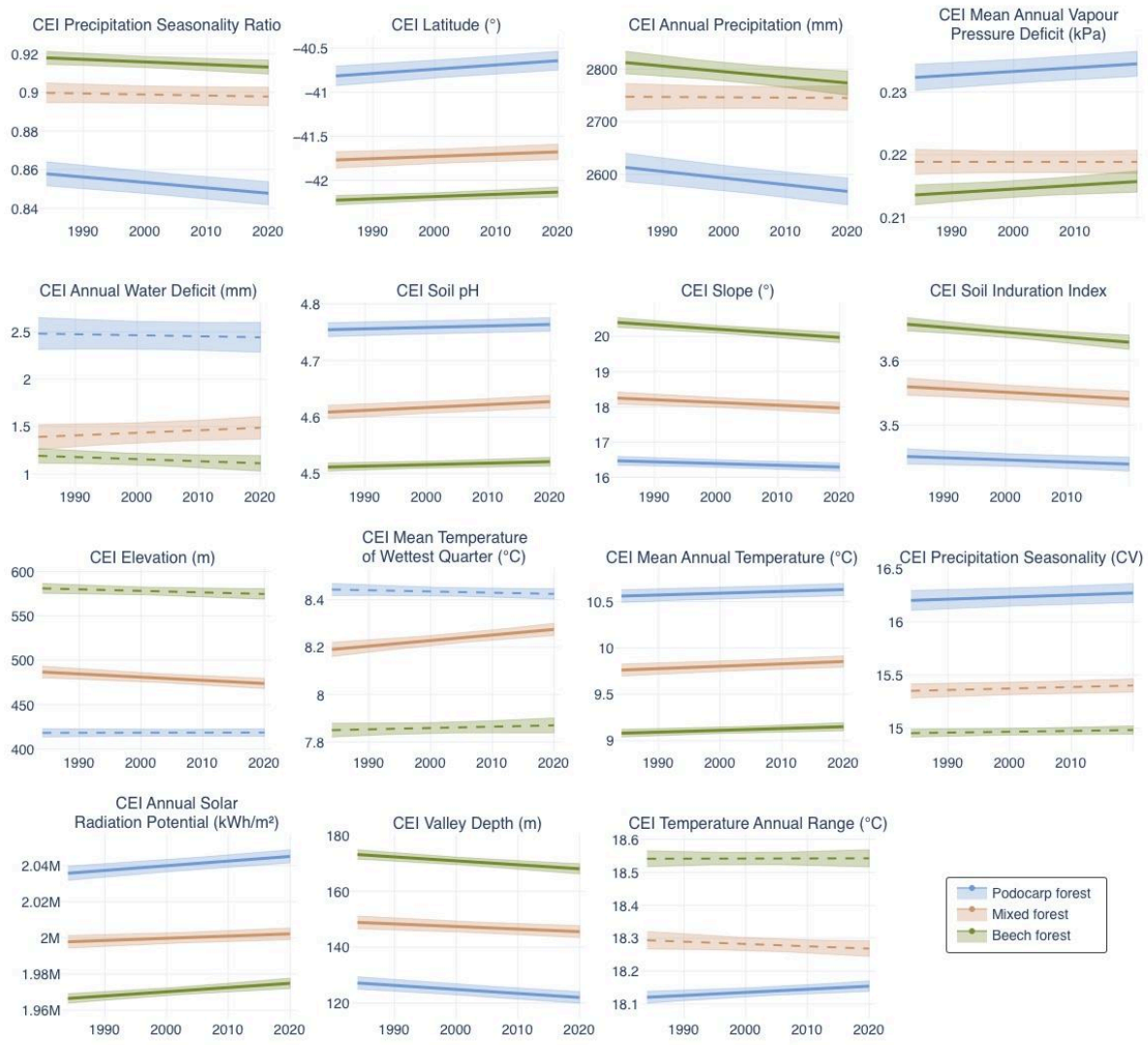


Figure B6: Community environmental preferences of all environmental variable traits used in this study over time by forest type. Shaded areas are 95% confidence intervals. Dashed lines imply a non-significant relationship. Exact R^2 and p-values in supplementary table.

B4.3. Temporal Trends of Trait Moments

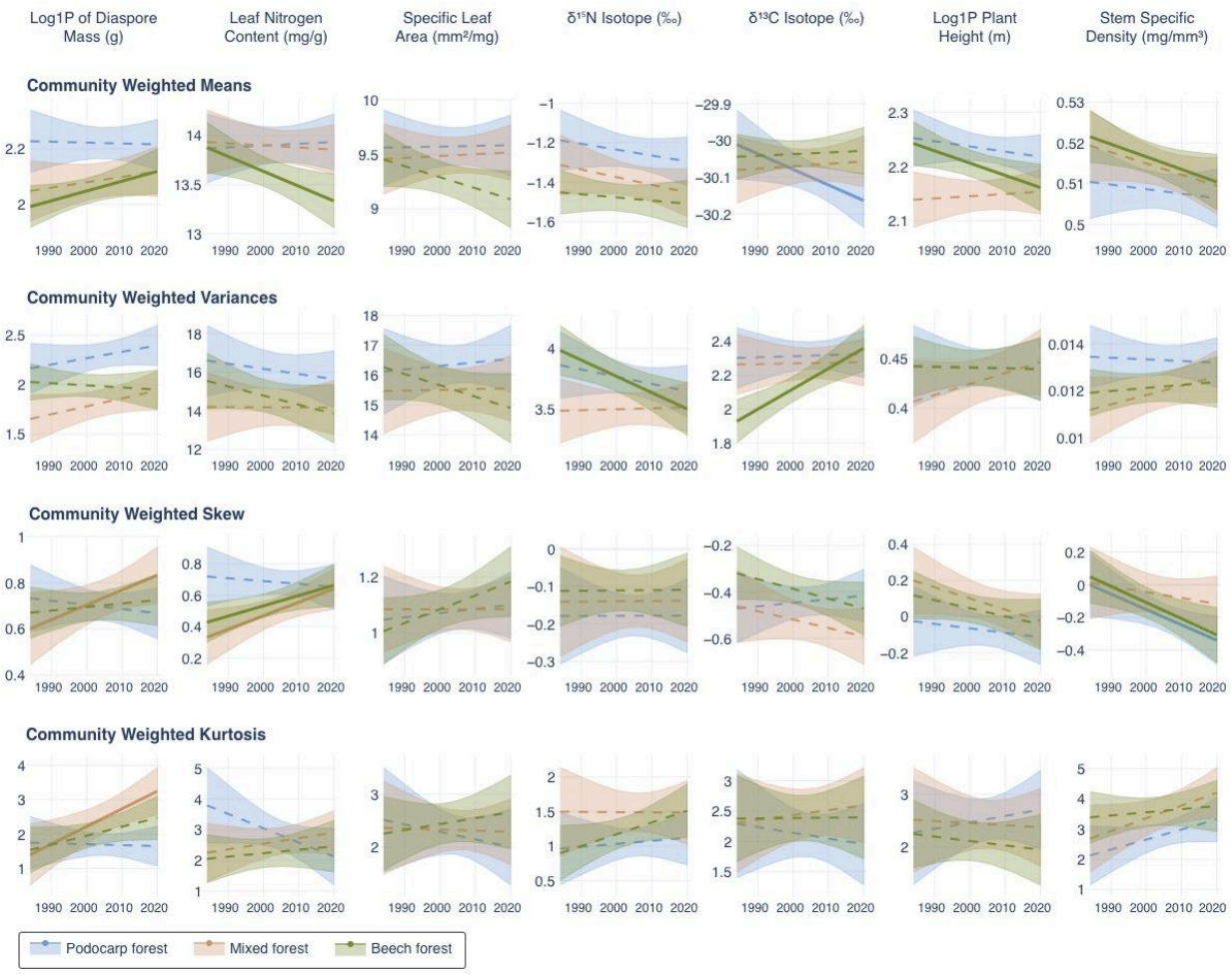


Figure B7: Trait moments (top to bottom: mean, variance, skew and kurtosis) of all functional traits used in this study over time by forest type. Shaded areas are 95% confidence intervals. Dashed lines imply a non-significant relationship. Exact R^2 and p-values in supplementary table.

B4.4. The rate and identity of species change and turnover differ by forest

Across forest types, a similar number of species showed non-zero rates of change (29-38, ***Fig. B8***A, left). However, weighing these species by the cover they occupy revealed that in podocarp and mixed forests, the shifting species are more widespread, leading to larger changes overall (***Fig. B8***A, right). The rate of turnover was highest in mixed forests (***Fig. B8***B). The rate of turnover between species within the three forest types was only weakly correlated (R^2 = 0.07-0.18), indicating that species shifted differentially across forest types.

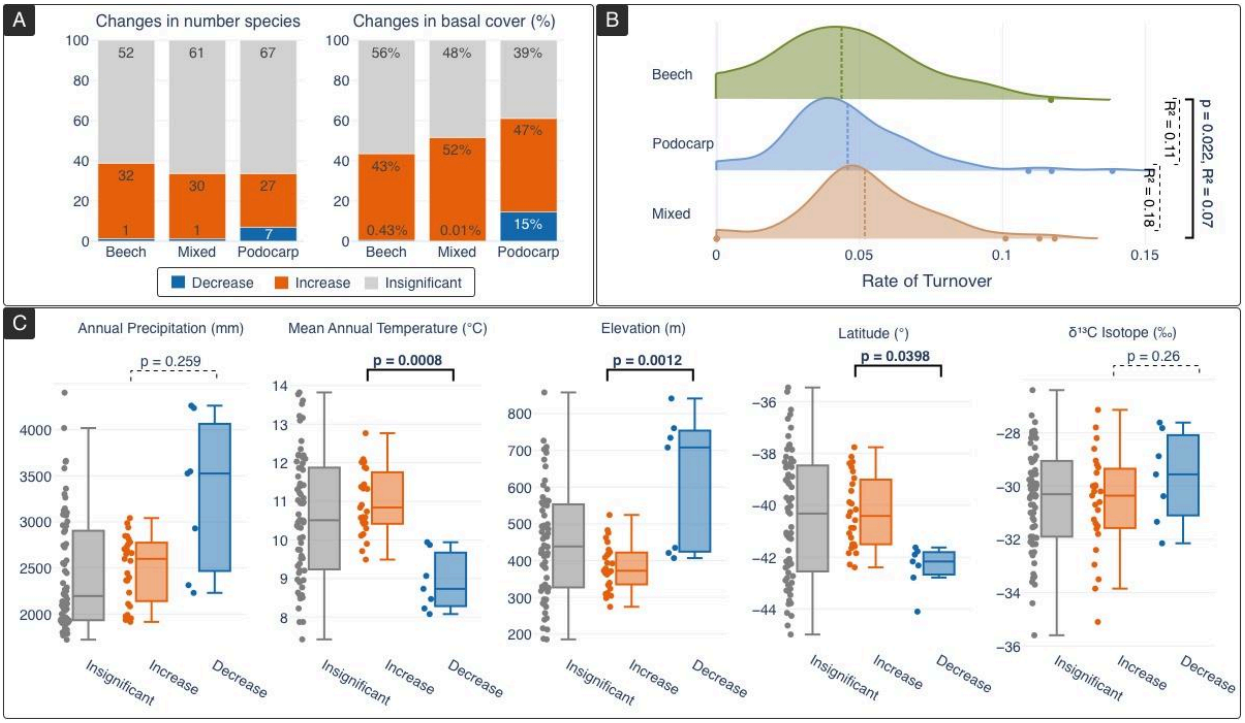


Figure B8: (A) Left: Number of species experiencing significant directional changes. Right: Total cover occupied by these species. (B) The rate of turnover for all species found in plots of a forest type. As species often occur in all forest types, their turnover rates can be correlated. Correlation value provided in brackets. (C) Species environmental preferences (AP, MAT, elevation, and latitude) and $\delta^{13}C$ Isotope ratio for species in podocarp forests by the class of their directional change (from panel A). P values for the one-sided Wilcoxon rank-sum are displayed between the increase and decrease class only.

B4.5. Trend Contribution by Species Group

To assess whether species with specific mycorhizal associations contribute more than expected by random to the trends of functional and taxonomic richness and diversity, we extracted the mycorrhizal type for species in our dataset from the FungalRoot database (Soudzilovskaia et al. 2020). To reduce the number of groups, we assigned one species classified as "uncertain" and five species classified as facultative arbuscular (NM-AM) to the arbuscular mycorrhizal group. Of the 120 studied species, 101 were arbuscular mycorrhizal (AM), 8 ectomycorrhizal (EcM), 5 ericoid mycorrhizal (ErM), 4 EcM and AM, and 2 non-mycorrhizal. Due to this imbalance, AM species had overwhelmingly strong effects on all metrics (***Fig. B9***). An exception to this pattern is the species richness trend (increasing) in beech forests, which is more strongly dominated by EcM-associated species (which include the dominant beeches). Indicating that despite already being dominant, beech expansion contributed to an increase in species richness over time.



Figure B9: Standardised effect sizes by mycorrhizal association and growth form for all significantly changing functional and taxonomic diversity metrics. An arrow next to the metric name indicates the trend direction. Positive values indicate that this group contributes more to the trend than expected by chance. Only values for which the metrics exhibit significant trends are shown. An asterisk indicates groups that have a statistically significant deviation from the null distribution ($p < 0.05$).



Figure B10: Standardised effect sizes by bio status, mycorrhizal association, growth form and primary biome for all significant CWM trends. An arrow next to the trait name indicates the trend direction. Positive values indicate that this group contributes more to the trend than expected by chance. Only values for which the metrics exhibit significant trends are shown. An asterisk indicates groups that have a statistically significant deviation from the null distribution ($p < 0.05$). Note: Functional strategy is not displayed, as the group membership is determined by the trait values themselves.

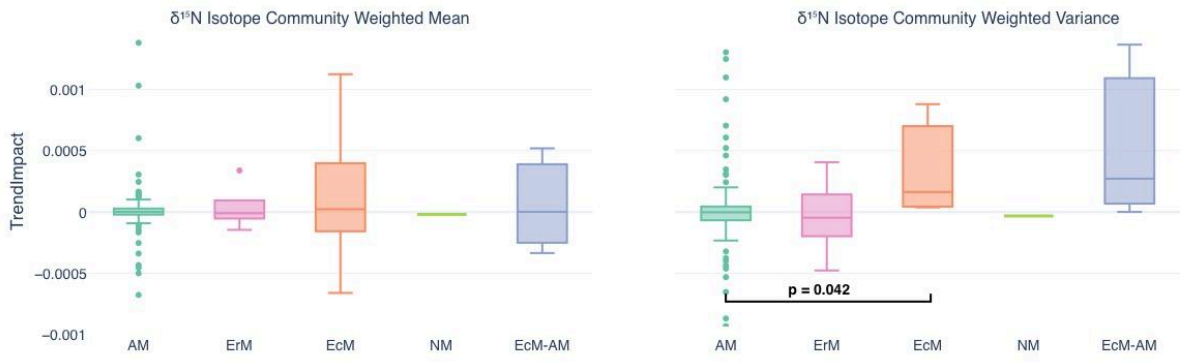


Figure B11: Trend impacts (see methods section 2.9) of species grouped by mycorrhizal association on the CWM (left) and CWV (right) of the $\delta^{15}N$ isotope ratio in beech forests. Positive values indicate that the presence of the group contributes to making the trends steeper (i.e. decline faster over time). The only statistically significant difference between groups was between AM and EcM for $\delta^{15}N$ CWV and is highlighted with its p-value (using the Mann–Whitney U test).

B4.6. Impact of tree ferns on trends

Tree ferns are a prominent part of New Zealand's forest ecosystems, especially in early successional and disturbed ecosystems, where they influence community assembly (Brock et al. 2016; Brock et al. 2018). However, tree ferns are phylogenetically distant from woody species and retaining them in the species collection can, in theory, lead to substantial changes in trait moments and diversity indices, due to their different functional strategies. To assess how tree ferns affect our results, we examined temporal trends without including them (***Fig. B12***). While none of the functional or taxonomic diversity or richness indices showed changes in trend from this exclusion, some trait moments did. The largest difference was found in SLA and Nmass trends, which switched from no significant trend to a downward trend in podocarp forests. As tree ferns have an above-average SLA (thicker, rougher leaves), and their absence leads to lower SLA over time, tree ferns are presumably expanding in podocarp forests, which might be a result of increasing disturbances (Keegan et al.

2022). A declining Nmass in the absence of tree ferns points towards community compositions consisting of tree ferns combined with more conservative species (lower Nmass than tree ferns). This is common in New Zealand and leads to disturbance and browsing-driven oscillations in tree fern abundance (Wyse et al. 2018). In beech forests, the inclusion of tree ferns yields a downward trend of plant height, which also indicates a disturbance-driven expansion of ferns at the expense of much taller, dominant beech tree species (e.g. *Fuscospora* or *Lophozonia spp.,* synonymously: *Nothofagus spp*). The trend in SSD follows the same logic, as trees have a higher SSD than tree ferns. If tree ferns are more widespread in the present than in the past, their removal from the data results in a declining SSD trend. Since tree ferns are more predominant in warmer northern forests, their exclusion from the data also diminished the community environmental index for latitude and pH in mixed forests, indicating their increasing abundance over time.

Collectively we do not find surprising effects by removing tree ferns, aside from what would be expected from species in the regenarative niche, and the data indicates that tree ferns (like most species in our data) are expanding from the warmer north to the colder south, are gaining in abundance, possibly due to increased disturbance severity, and lead to slight functional shifts, which however do not compound to significant changes in trends of functional and taxonomic indices.

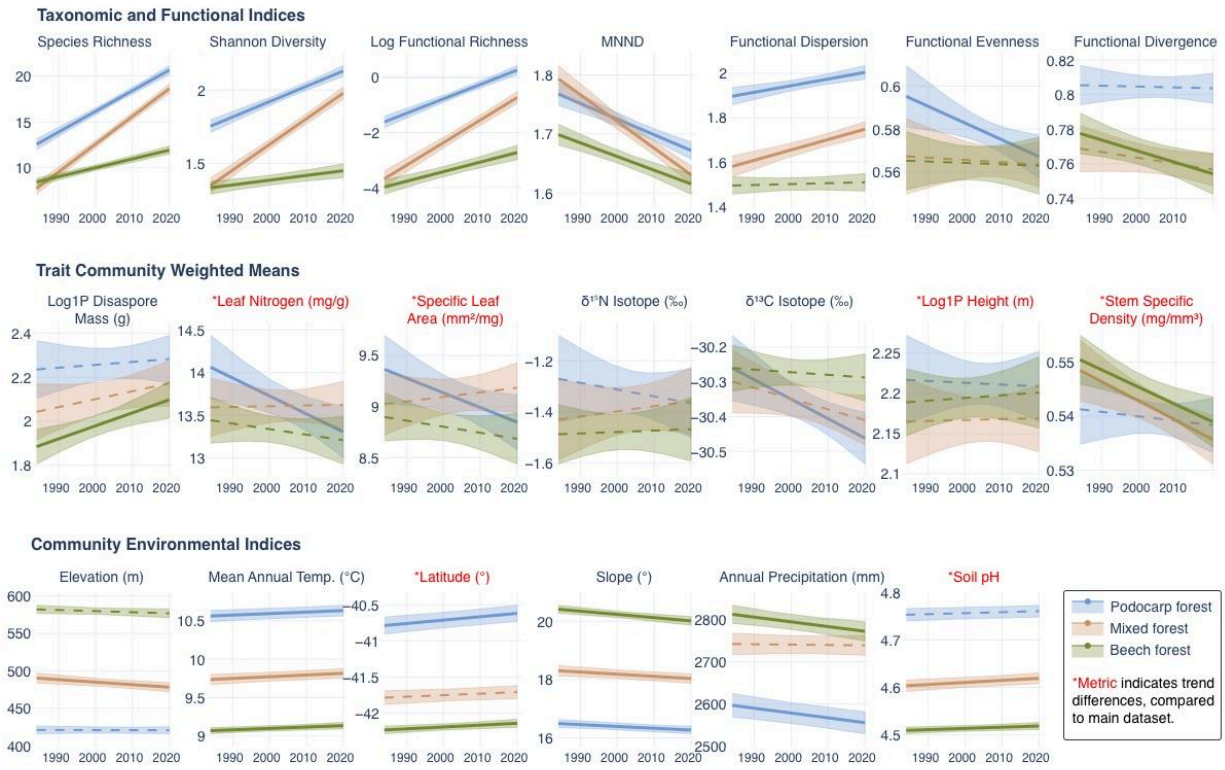


Figure B12: Results when excluding tree ferns. Temporal trends of taxonomic and functional richness and diversity indices, trait community weighted means and community environmental indices, analogously to the main result figures. Metrics where a trend changes in significance compared to the main dataset (including tree ferns) are highlighted in red and with an asterisk. Exact R^2 and p-values in supplementary table.

B5. References

Breiman, L. (2001). Random Forests. *Machine Learning*, *45*(1), 5–32. https://doi.org/10.1023/A:1010933404324

Brock, J. M. R., Perry, G. L. W., Lee, W. G., & Burns, B. R. (2016). Tree fern ecology in New Zealand: A model for southern temperate rainforests. *Forest Ecology and Management*, *375*, 112–126. https://doi.org/10.1016/j.foreco.2016.05.030

Brock, J., Perry, G., Lee, W. G., Schwendenmann, L., & Burns, B. (2018). Pioneer tree ferns influence community assembly in northern New Zealand forests. *New Zealand Journal of Ecology*, *42*(1), 18–30. https://doi.org/10.20417/NZJECOL.42.5

Debastiani, V. J., Bastazini, V. A. G., & Pillar, V. D. (2021). Using phylogenetic information to impute missing functional trait values in ecological databases. *Ecological Informatics*, *63*(101315), 101315. https://doi.org/10.1016/j.ecoinf.202B101315

Diniz-Filho, J. A. F., de Sant'Ana, C. E. R., & Bini, L. M. (1998). An eigenvector method for estimating phylogenetic inertia. *Evolution; International Journal of Organic Evolution*, *52*(5), 1247–1262. https://doi.org/10.1111/j.1558-5646.1998.tb02006.x

Keegan, L., School of Biological Sciences, University of Auckland, Private Bag 92019, Auckland 1142, New Zealand, White, R., & Macinnis-Ng, C. (2022). Current knowledge and potential impacts of climate change on New Zealand's biological heritage. *New Zealand Journal of Ecology*. https://doi.org/10.20417/nzjecol.46.10

Penone, C., Davidson, A. D., Shoemaker, K. T., Di Marco, M., Rondinini, C., Brooks, T. M., Young, B. E., Graham, C. H., & Costa, G. C. (2014). Imputation of missing data in life-history trait datasets: which approach performs the best? *Methods in Ecology and Evolution*, *5*(9), 961–970. https://doi.org/10.1111/2041-210x.12232

Soudzilovskaia, N. A., Vaessen, S., Barcelo, M., He, J., Rahimlou, S., Abarenkov, K., Brundrett, M. C., Gomes, S. I. F., Merckx, V., & Tedersoo, L. (2020). FungalRoot: global online database of plant mycorrhizal associations. *The New Phytologist*, *227*(3), 955–966. https://doi.org/10.1111/nph.16569

Swenson, N. G., & Weiser, M. D. (2014). On the packing and filling of functional space in eastern North American tree assemblages. *Ecography*, *37*(11), 1056–1062. https://doi.org/10.1111/ecog.00763

Taeuber, K. E., & Taeuber, A. F. (1976). A practitioner's perspective on the index of dissimilarity. *American Sociological Review*, *41*(5), 884. https://doi.org/10.2307/2094734

Wieczynski, D. J., Boyle, B., Buzzard, V., Duran, S. M., Henderson, A. N., Hulshof, C. M., Kerkhoff, A. J., McCarthy, M. C., Michaletz, S. T., Swenson, N. G., Asner, G. P., Bentley, L. P., Enquist, B. J., & Savage, V. M. (2019). Climate shapes and shifts functional biodiversity in forests worldwide. *Proceedings of the National Academy of Sciences of the United States of America*, *116*(2), 587–592. https://doi.org/10.1073/pnas.1813723116

Wilson, S. V., Cebere, B., Myatt, J., & Wilson, S. (2023). *miceforest*. https://github.com/AnotherSamWilson/miceforest/

Wyse, S., School of Environment, University of Auckland, Private Bag 92019, Auckland 1142, New Zealand, Wilmshurst, J., Burns, B., & Perry, G. (2018). New Zealand forest dynamics: a review of past and present vegetation responses to disturbance, and development of conceptual forest models. *New Zealand Journal of Ecology*, *42*(2). https://doi.org/10.20417/nzjecol.42.18

Appendix C: Supplementary materials for AtiP

C1. Supplementary Methods

C1. Dataset Statistics

We formulated the abundance trend as a binary classification problem. Three sets of predictor variables were used to predict a binary target label: Increase (1) or decrease (0). Increase or decrease is determined by comparing two surveys of the same site. **Fig. C1** describes the distribution of labels by species (Panel A), total (Panel B), a histogram of time between remeasurements (Panel C) and the frequency of remeasurement for plot pairs (Panel D).

Our dataset was slightly imbalanced, leaning towards the "increase" class due to the assignment of plots without a change in abundance (survival) primarily to "increase" (see Abundance and DBH dataset discussion in Section 7.3.1). Approximately 50% of sites are remeasured within seven years or less, with a long tail extending up to 30 years. About half the surveys consisted of plots measured twice; sites with more than four surveys were extremely uncommon.

We analysed whether the remeasurement interval dY biased the class label by computing the correlation between dY and the class label ratio $cl(dY) = \frac{I}{D+I}$ where D and I are the counts of decrease or increase labels for all observations that were dY years apart, regardless of species. To assess general bias, species must not be taken into account, because declining species would be expected to have more "Decrease" labels the farther back in time the first measurement is (and vice versa for expanding species), reflecting ecological trends rather than data bias. The correlation

between dY and $cl(dY)$ was low (r=0.12), and the slightly positive trend likely reflects the increasing local species richness and thus expansion of a majority of species (**Fig. 2**).

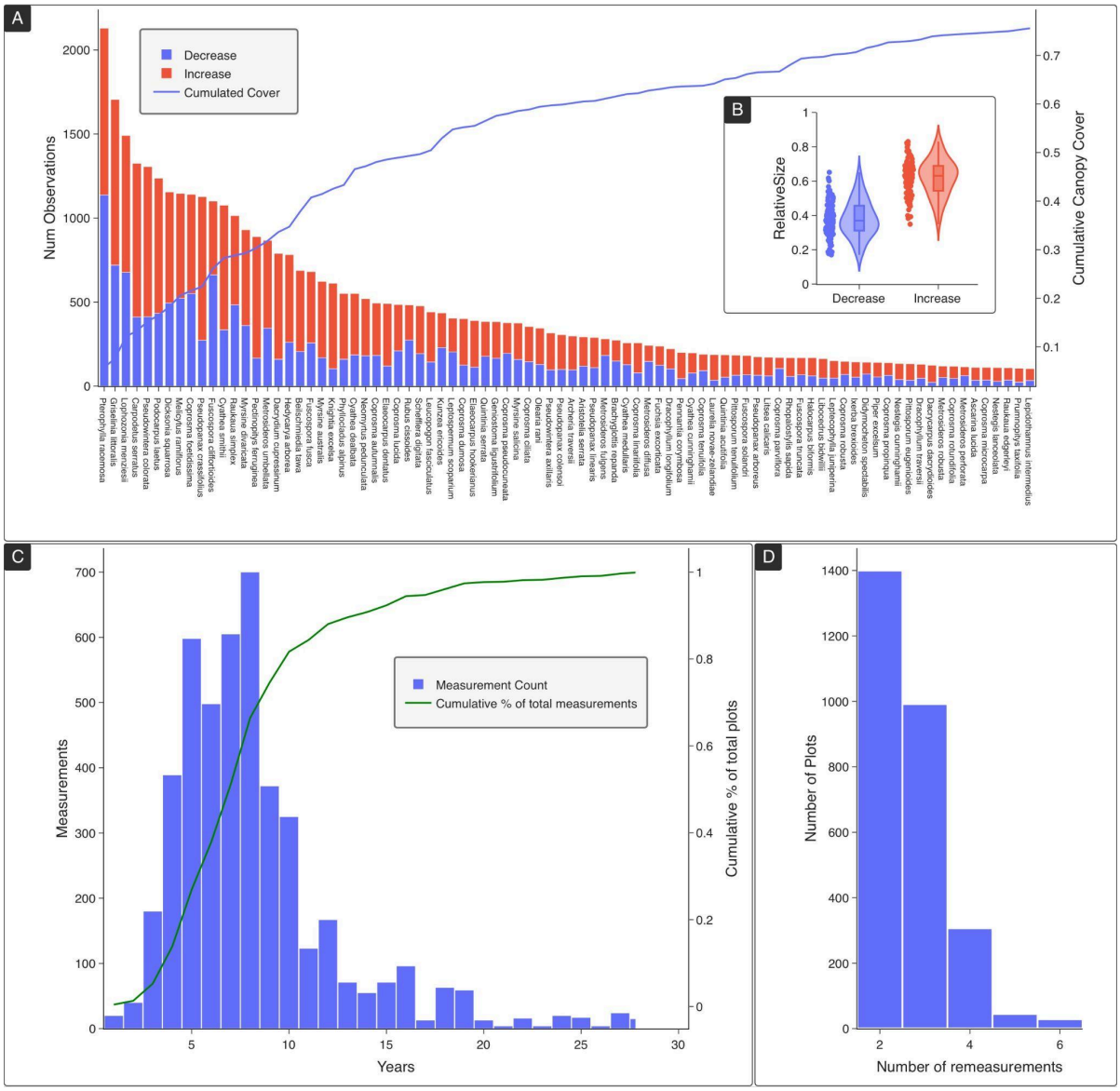


***Figure C1**: Data statistics for the Abundance and DBH dataset containing 86 species with sufficient data and covering 75.59% of the forest canopy. A: Number of observations by species and their cumulative canopy cover, ordered by the number of observations. B: The distribution of the classes shows a slight class imbalance. C: Number of measurements by time between them. Each measurement is a plot that has been surveyed twice, with a certain number of years between measurements. D: The average number of plot remeasurements. Most plots have only been measured twice, yielding a single observation for the occurring species.*

CC2. Variable Sets

The full set of predictor variables consisted of 37 mostly climatic and edaphic variables, with 3 being biotic presence layers for rats, possums and deer. As many correlated variables would make explanations more difficult, we clustered variables by their correlation (**Fig. C2** A) and kept one representative from each cluster. This approach has an advantage over Principal Component Analysis as an ordination technique by keeping the variables separate. While a PCA axis will contain many variables with a decreasing degree of importance (**Fig. C3**), the clustering method will use easily interpretable variables. The result is a reduced set of variables showing a much lower correlation (**Fig. C2** B) than the full set.

To make a more objective choice of representative variable in each cluster, we calculated each predictor variable's mutual information (or cross-entropy) value (Kullback 1959). Mutual information (MI) quantifies the dependency between the continuous environmental variables and binary abundance increase or decrease target variable, providing a measure of how much information about the target is gained through the environment. Mathematically, MI is defined as the difference (i.e. the Kullback-Leibler divergence) between the product of the marginal distributions of an (environmental) variable $p(x)$ with the binary target variable $p(y)$ and their joint distribution $p(x, y)$. If x and y are independent $p(x, y) = p(x)p(y)$ making their Kullback-Leibler divergence zero. Thus, low MI values indicate environmental variables that are statistically independent of an abundance decrease or increase. For each cluster, we aimed to use the variable with the highest MI value but also considered how common this variable was in the literature (**Table C1**). MI naturally has no upper limit, as it is defined by the entropy of the variables. For readability, we scaled the MI values for each variable to sum up to 100. Since each species had its own MI values due to different biological responses to environmental drivers (**Fig. C2** C), we used the average across all species to determine a single MI value per environmental variable.

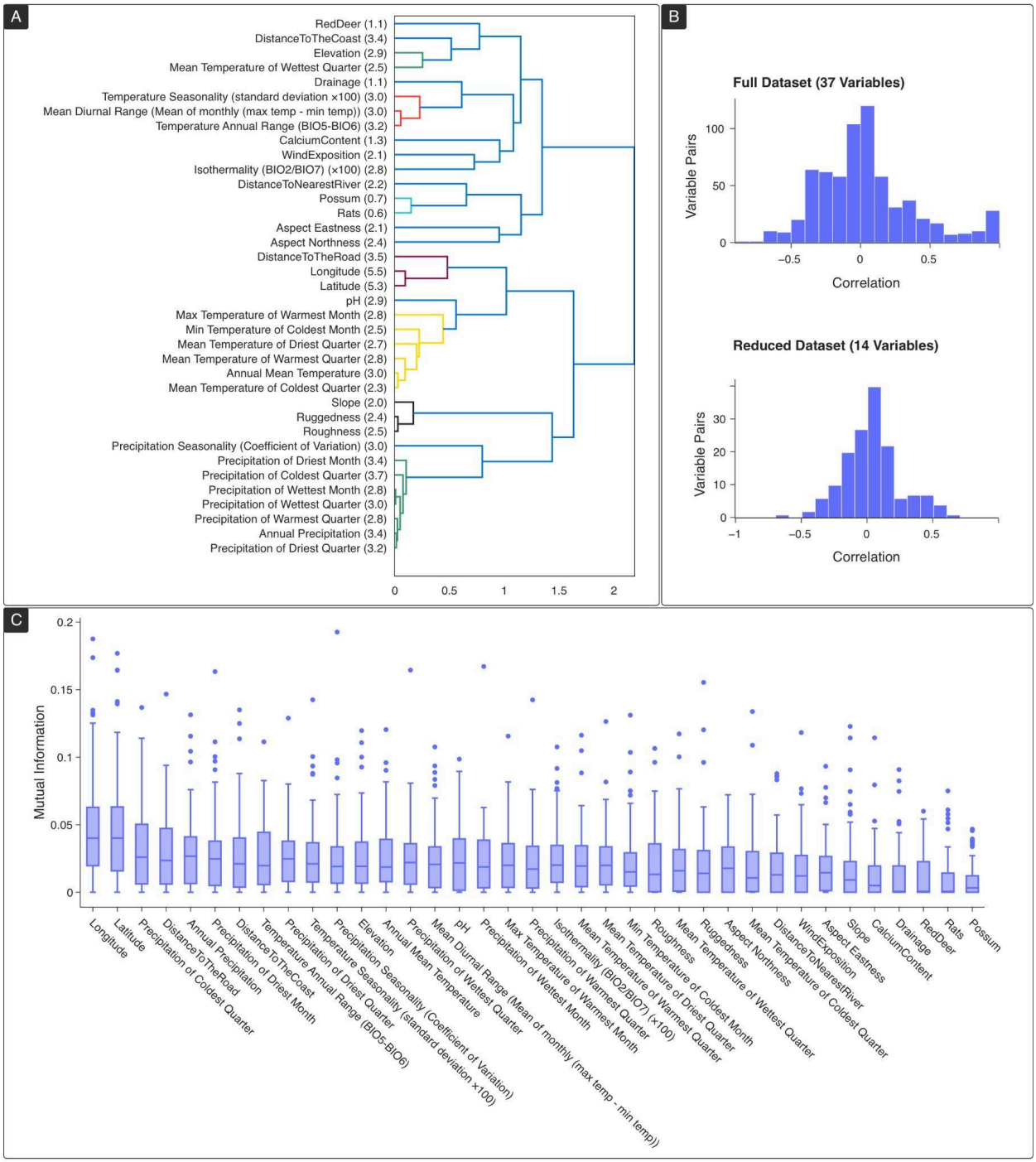

A
RedDeer (1.1)
DistanceToTheCoast (3.4)
Elevation (2.9)
Mean Temperature of Wettest Quarter (2.5)
Drainage (1.1)
Temperature Seasonality (standard deviation ×100) (3.0)
Mean Diurnal Range (Mean of monthly (max temp - min temp)) (3.0)
Temperature Annual Range (BIO5-BIO6) (3.2)
CalciumContent (1.3)
WindExposition (2.1)
Isothermality (BIO2/BIO7) (×100) (2.8)
DistanceToNearestRiver (2.2)
Possum (0.7)
Rats (0.6)
Aspect Eastness (2.1)
Aspect Northness (2.4)
DistanceToTheRoad (3.5)
Longitude (5.5)
Latitude (5.3)
pH (2.9)
Max Temperature of Warmest Month (2.8)
Min Temperature of Coldest Month (2.5)
Mean Temperature of Driest Quarter (2.7)
Mean Temperature of Warmest Quarter (2.8)
Annual Mean Temperature (3.0)
Mean Temperature of Coldest Quarter (2.3)
Slope (2.0)
Ruggedness (2.4)
Roughness (2.5)
Precipitation Seasonality (Coefficient of Variation) (3.0)
Precipitation of Driest Month (3.4)
Precipitation of Coldest Quarter (3.7)
Precipitation of Wettest Month (2.8)
Precipitation of Wettest Quarter (3.0)
Precipitation of Warmest Quarter (2.8)
Annual Precipitation (3.4)
Precipitation of Driest Quarter (3.2)
0
0.5
1
1.5
2
B
Full Dataset (37 Variables)
Variable Pairs
100
50
0
−0.5
0
0.5
Correlation
Reduced Dataset (14 Variables)
Variable Pairs
30
20
10
0
−1
−0.5
0
0.5
Correlation
C
Mutual Information
0.2
0.15
0.1
0.05
0
Longitude
Latitude
Precipitation of Coldest Quarter
DistanceToTheRoad
Annual Precipitation
Precipitation of Driest Month
DistanceToTheCoast
Temperature Annual Range (BIO5-BIO6)
Precipitation of Driest Quarter
Temperature Seasonality (standard deviation ×100)
Precipitation Seasonality (Coefficient of Variation)
Elevation
Annual Mean Temperature
Precipitation of Wettest Quarter
Mean Diurnal Range (Mean of monthly (max temp - min temp))
pH
Precipitation of Wettest Month
Max Temperature of Warmest Month
Precipitation of Warmest Quarter
Isothermality (BIO2/BIO7) (×100)
Mean Temperature of Warmest Quarter
Min Temperature of Coldest Month
Mean Temperature of Driest Quarter
Roughness
Mean Temperature of Coldest Month
Ruggedness
Aspect Northness
Mean Temperature of Wettest Quarter
DistanceToNearestRiver
WindExposition
Mean Temperature of Coldest Quarter
Aspect Eastness
Slope
CalciumContent
Drainage
RedDeer
Rats
Possum

***Figure C2**: Dimensionality reduction used to generate the Reduced Dataset. A: Result of the hierarchical clustering procedure with distance metric set to the absolute value ofthe correlation between values and Ward's linkage. Clusters below 0.5 are highlighted in different colours. The number behind each variable is the mean mutual information value. For readability, it is normalised such that all values sum up to 100. B: Histogram of pair-wise correlations between the variables in the Full and Reduced datasets, respectively. Showing a reduction of highly correlated variables. C: Mutual information of the variable and the training label (increase/decrease) across all species. Lower numbers indicate lower dependence of the target labels on the variable.*

Cluster	Variable	MI Value	Comment
1	*Possum*	0.7	Uninformative, most of New Zealand has Possums
	Rats	0.6	Uninformative, most of New Zealand has Rats
2	**DistanceToNearestRiver**	2.2	
3	**Aspect Eastness**	2.1	
4	**Aspect Northness**	2.4	
5	**Elevation**	2.9	Highest ecological relevance
	Mean Temperature of Wettest Quarter	2.5	Closely correlated to precipitation cluster (#17)
6	*DistanceToTheCoast*	3.4	Unspecific, correlates with elevation (R^2 > 0.6)
7	**RedDeer**	1.1	Included since it is of ecological interest
8	**Temperature Annual Range (BIO5-BIO6)**	3.2	Max MI in cluster and clear interpretation
	Mean Diurnal Range (Mean of monthly (max temp - min temp))	3.0	
	Temperature Seasonality	3.0	

	(standard deviation ×100)		
9	*Drainage*	1.1	Excluded low MI
10	**WindExposition**	2.1	
11	**Isothermality (BIO2/BIO7) (×100)**	2.8	
12	*CalciumContent*	1.3	Excluded low MI (and categorical)
13	**Latitude**	5.3	More informative than longitude for climate.
	Longitude	5.5	Correlates with latitude in New Zealand ($R^2 > 0.9$)
	DistanceToTheRoad	3.5	
14	**Annual Mean Temperature**	3.0	Highest MI in cluster
	Max Temperature of Warmest Month	2.8	
	Min Temperature of Coldest Month	2.5	
	Mean Temperature of Driest Quarter	2.7	
	Mean Temperature of Warmest Quarter	2.8	
	Mean Temperature of Coldest Quarter	2.3	
15	**pH**	2.9	
16	**Slope**	2.0	Easier to interpret than ruggedness/roughness
	Ruggedness	2.4	
	Roughness	2.5	
17	**Annual Precipitation**	3.4	Easiest to interpret in cluster; High MI
	Precipitation of Wettest Month	2.8	
	Precipitation of Driest Month	3.3	

	Precipitation of Wettest Quarter	3.0	
	Precipitation of Driest Quarter	3.2	
	Precipitation of Warmest Quarter	2.4	
	Precipitation of Coldest Quarter	3.7	
18	**Precipitation Seasonality (Coefficient of Variation)**	3.0	

***Table C1**: List of variables included in the Reduced dataset. Lists the 18 clusters from Figure S2 along with their mutual information values (normalized so that they sum up to 100). From each cluster, one (in some cases none) variable is included, and the reason for including and excluding is given in the "Comment" column. The result is a dataset of 14 variables that are weakly correlated and of ecological relevance.*

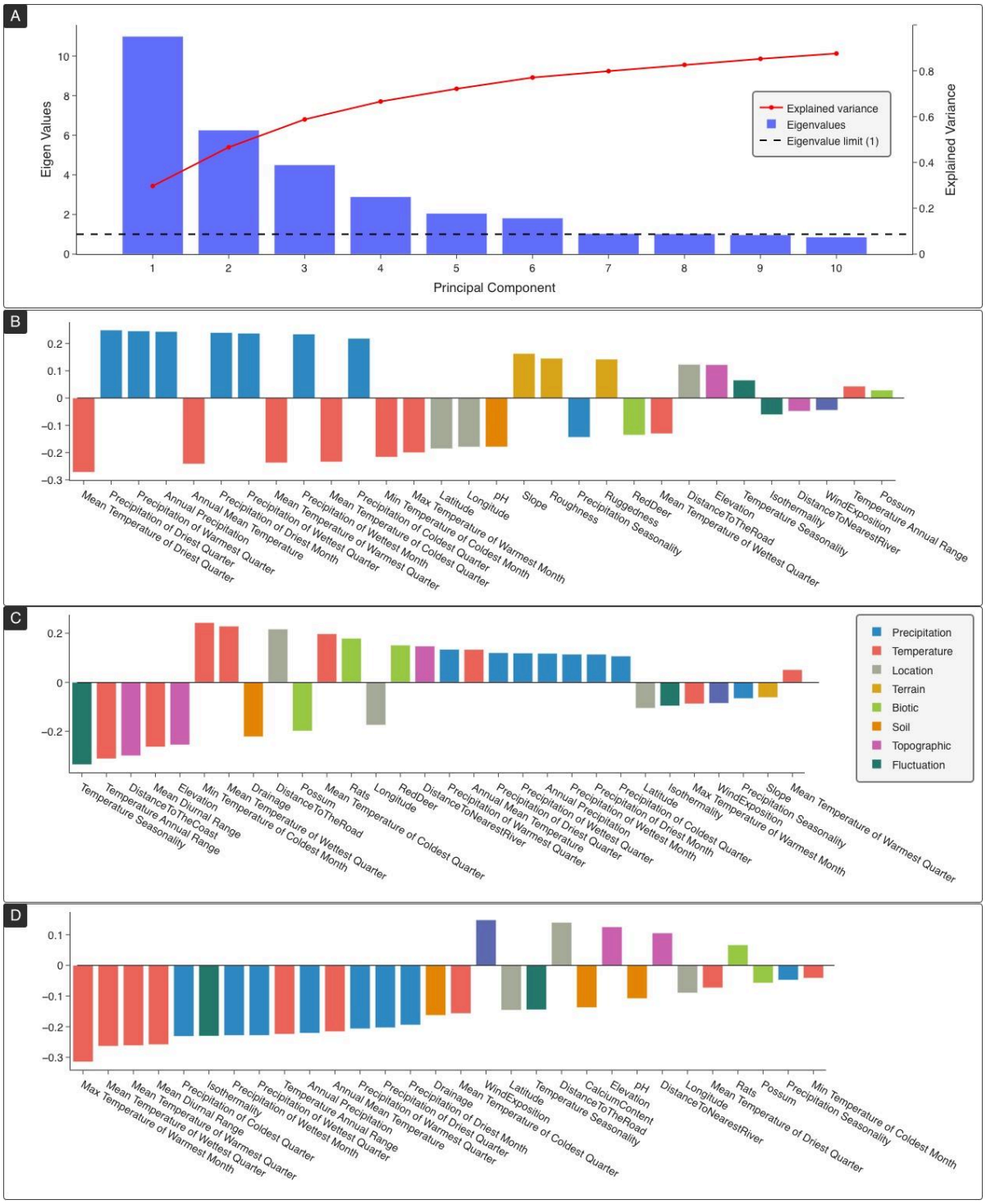

A
Eigen Values
Explained Variance
Principal Component
Explained variance
Eigenvalues
Eigenvalue limit (1)
B
Mean Temperature of Driest Quarter
Precipitation of Driest Quarter
Precipitation of Warmest Quarter
Annual Precipitation
Annual Mean Temperature
Precipitation of Driest Month
Precipitation of Wettest Quarter
Mean Temperature of Wettest Quarter
Precipitation of Wettest Month
Precipitation of Coldest Quarter
Min Temperature of Coldest Month
Max Temperature of Warmest Month
Latitude
Longitude
pH
Slope
Roughness
Precipitation Seasonality
Ruggedness
RedDeer
Mean Temperature of Wettest Quarter
DistanceToTheRoad
Elevation
Temperature Seasonality
Isothermality
DistanceToNearestRiver
WindExposition
Temperature Annual Range
Possum
C
Precipitation
Temperature
Location
Terrain
Biotic
Soil
Topographic
Fluctuation
Temperature Seasonality
Temperature Annual Range
DistanceToTheCoast
Mean Diurnal Range
Elevation
Min Temperature of Coldest Month
Mean Temperature of Wettest Quarter
Drainage
DistanceToTheRoad
Possum
Mean Temperature of Coldest Quarter
Rats
Longitude
RedDeer
DistanceToNearestRiver
Precipitation of Warmest Quarter
Annual Mean Temperature
Precipitation of Driest Quarter
Annual Precipitation
Precipitation of Wettest Quarter
Precipitation of Driest Month
Latitude
Isothermality
Max Temperature of Warmest Month
WindExposition
Precipitation Seasonality
Slope
Mean Temperature of Warmest Quarter
D
Max Temperature of Warmest Month
Mean Temperature of Wettest Quarter
Mean Diurnal Range
Mean Temperature of Warmest Quarter
Precipitation of Coldest Quarter
Isothermality
Precipitation of Wettest Month
Precipitation of Wettest Quarter
Temperature Annual Range
Annual Precipitation
Annual Mean Temperature
Precipitation of Warmest Quarter
Precipitation of Driest Quarter
Drainage
Mean Temperature of Driest Month
WindExposition
Latitude
Mean Temperature of Coldest Quarter
Temperature Seasonality
DistanceToTheRoad
CalciumContent
Elevation
pH
Longitude
DistanceToNearestRiver
Rats
Mean Temperature of Driest Quarter
Possum
Precipitation Seasonality
Min Temperature of Coldest Month

***Figure C3**: Principal components of the Full dataset. A: Blue bars are eigenvalues, and the red line indicates the cumulative explained variance by all PCs up to this number (secondary y-axis). A dashed line indicates the Kaiser rule threshold of λ=1 for relevant principal components. B-D: Loadings on the first three principal components. For overview, only the first 20 variables are displayed. Variables are color-coded by category (legend in panel C). Absolute y-axis values are for comparison only and indicate the loading onto the principal component.*

CC3. Noise filtering

The noise filtering algorithm is a k-nearest neighbour classifier with two modifications:

1. We set a maximum distance αR from a point to its nearest neighbours, where R is defined as the average distance to the K-th neighbour. This allowed us to identify outliers in feature space (i.e. the environmental attributes of a plot) and explicitly keep them in the dataset while removing labelling outliers as we don't have information on whether feature outliers are mislabeled or not (**Fig. C4** (3)).
2. We used the distance to the neighbours to derive a continuous number $\epsilon_i \in [0; 1]$ that describes how likely a point is (**Fig. C4** (4-6)) to be mislabeled. This allowed the removal of a fixed percentage of the most noisy data from the dataset. Distance is defined as $dist(i, k) = ||x_i - x_k||_1$ the sum of differences of all environmental variables (L1 norm).

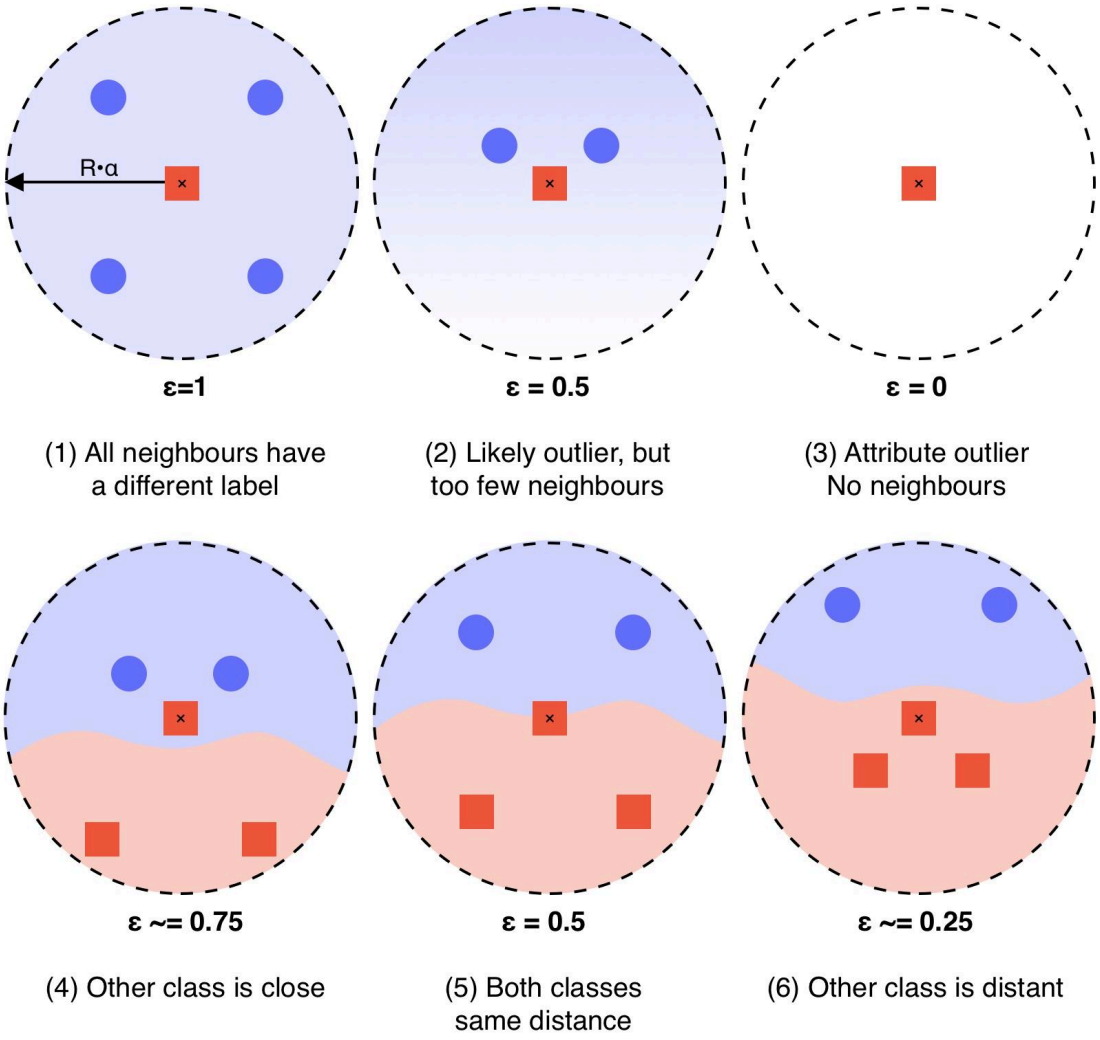


***Figure C4**: Examples of noise score assignment using our modified nearest neighbour noise detection for K=4. The point with a black cross in the centre is the one receiving the noise score, indicated under the circle. The circle represents the maximum distance to its neighbours: αR. The noise score is 0 (not mislabeled) and 1 (likely mislabeled). (1, top left) All neighbours have a different label. This point is, therefore, likely mislabeled. (2) Point has only K/2 neighbours; this limits the maximum noise score to 0.5, and since all neighbours have a different label, the maximum noise score of 0.5 is assigned. (3) Feature outlier that has no neighbours and this can't be considered mislabeled. (4-6) Closeness of a point to members of the other class modulates how likely it will be considered noise. The shade indicates a hypothetic class decision boundary.*

The exact procedure employs the following steps:

1. Set R to be the average distance to the K-th neighbour across all instances in the dataset.
2. For each x_i, get the K nearest neighbours $NN(x_i)$.
3. Filter out the neighbours that are farther than αR away.

   $NNR(x_i) = \{x_j \in NN(x_i) | \, dist(i,j) \leq \alpha \cdot R\}$ On average, NNR and NN will contain the same points, as R is the average distance to the K-th neighbour.
4. Remove points with the same label to yield the set of different label neighbours:

   $DLN(x_i) = \{x_j \in NNR(x_i) | \, y_i \neq y_j\}$
5. Set $\epsilon_i = 0$ if DLN_i is empty. Continue to step 2 with the next point.
6. For each, $x_j \in NNR(x_i)$ assign an influence score $I(x_j) = 1 - \frac{dist(i,j)}{\alpha R}$. Influence diminishes the closer the points are to the αR limit.
7. Normalise the sum of influence scores:

$$\bar{p}_j = \frac{|NNR(x_i)|}{K} \cdot \frac{I(x_j)}{\sum_n I(x_n)}$$

8. The noise score is equal to the sum of normalised influence scores. $\epsilon_i = \sum_{p_j \in DLN_i} \bar{p}_j$
9. Continue in step 2 with the next point.

Step 7/8 ensures that the sum of all influences (i.e. the noise score ϵ_i) sums up to $\frac{|NNR(x_i)|}{K}$ which is 1 only if the point has all of its neighbours within the αR limit. Points with fewer neighbours (i.e. outliers in environmental variables are prevented from reaching a high ϵ_i and are unlikely to be

excluded (see **Fig. C4**). This ensures that plots located in unusual environments (e.g. high elevation) are retained.

To determine the optimal hyperparameters, we compared how well the unlearnable set (as determined by Random Forest) matches the points the noise detection algorithm removed using the $F_{0.5}$ score for different values K, α and the percentage of data removed (**Fig. C5**). The F.05 score penalises false positives (excluding a valid point) stronger than false negatives (missing a noisy point) and is a typical measure for labelling noise identification tasks (Brodley and Friedl 1999). The result suggested an optimal cutoff of ~11% of data at $K = 20$, $\alpha = 1.5$ and the use of the L1 norm for distance calculation. The algorithm is insensitive towards a choice of K and α. As long as $\alpha \geq 1.5$ the difference for any choice of K and α produces $F_{0.5}$ scores between 0.62 and 0.67 (**Fig. C5** A).

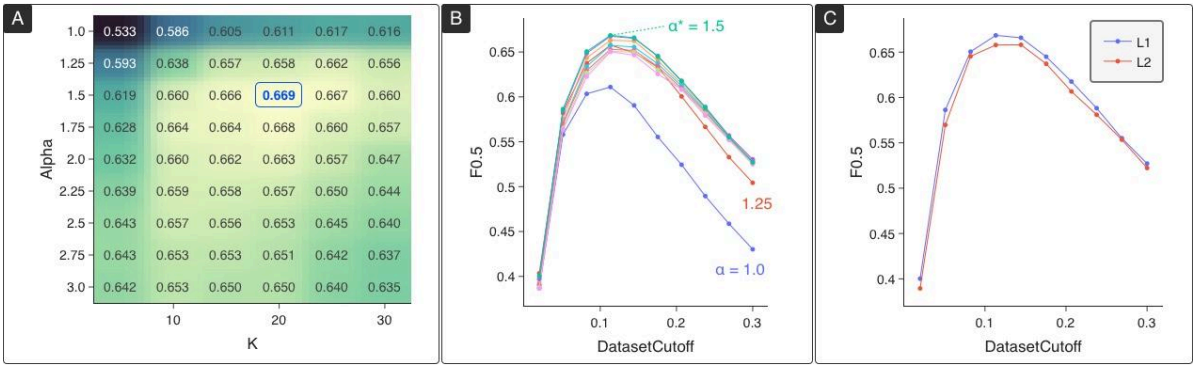


***Figure C5**: Finding optimal noise detection hyperparameters for random forest using the F0.5 score that penalises false positives (excluding a valid point) stronger than false negatives (missing a noisy point). A: Values of F0.5 score over alpha and K values with the optimal value highlighted at K* = 20 and Alpha* = 1.5. B: Performance for K* = 20 over the cutoff of data. The optimal F0.5 score is at 11.3% cutoff at Alpha* = 1.5. C: Comparison of the influence of using L1 vs L2 distance norm during noise detection at K* and Alpha*. L1 shows slightly improved performance.*

C1.4. Model training

We employed and compared four popular classification machine learning models used in Ecology (Pichler and Hartig 2023) from the Scikit Python package (Buitinck et al. 2013):

- Kernel **S**upport **V**ector **M**achine with **W**eighted regularisation (SVMW**,** (Chang and Lin 2011)): SVMs learn a decision boundary that separates two classes, maximising the distance between the boundary and the training points. Errors made on the minority class were penalised stronger (balanced class weight setting). Radial basis functions were used as kernels.

- **R**andom **F**orests (RF**,** (Breiman 2001)): Random Forests learn to classify data by constructing many decision trees during training. Each tree is built from a random subset of the training data. The final decision is based on the majority vote of all trees.
- **G**eneralised **L**inear **M**odels (GLM): Logistic regression (binomial family with a logit link, no random effects) without interaction terms. To prevent overfitting and class imbalance problems a regularisation constant parameter C was used and, as with SVMW, the minority class was more strongly penalised.
- **A**rtificial **N**eural **N**etwork (ANN1**,** (Bishop 2006)): A neural network is a composite function of environmental variables made up of layers of non-linear activation functions (nodes) and their weighted sums. Since species had as few as 100 training points and up to 37 predictor variables, networks with more than one hidden layer were infeasible.

A grid search (SciKit's GridSearchCV) determined hyperparameters and training errors, i.e., by trying all combinations of hyperparameters with nested cross-validation over the values listed in **Table C2**. First, the data was split into four stratified training T_i and test D_i sets. T_i was subdivided into five stratified folds to determine optimal hyperparameters and score for the model. The best hyperparameters were then used to train M_i on the entire training set T_i. D_i was then used to determine the test score S_i of M_i. This resulted in four models and test scores.

As models trained on each fold differed and yielded binary predictions, we averaged the four binary outputs of all models for prediction, resulting in a discrete prediction of 0, 0.25, 0.5, 0.75 or 1.

Model	**Parameter**	**Grid search values**
kSVM	Regularization C	0.001, 0.01, 0.1, 0.5, 1, 2, 5, 10, 100, 1000, 10000
	Kernel size Gamma	0.001, 0.01, 0.1, 0.5, 1, 2, 5, 10, 100, 1000, 10000, "scale", "auto"
RF	Maximum Depth of Trees	4, 5, 6, 7, 8, 9, 10

	Number of Trees	50, 100, 200, 300, 400, 500
	Min number of samples to split an internal node	2,5,10
GLM	Regularization C	1, 10^2, 10^3, 10^4, 5 * 10^4, 10^5, 5 * 10^5,10^6
ANN1	Size of hidden layer in % of input nodes	5%, 10%, 15%, 25%, 50%, 75%
	Activation function	Tanh, ReLu
	L2 Regularization term alpha	0.0001, 0.001, 0.01, 0.1
	Learning Rate	constant, invscaling, adaptive
	Learning Rate Initial Value	0.001, 0.01, 0.1

***Table C2**: Values of hyperparameters that were compared during hyperparameter tuning for each classifier.*

C1.5. Similarity masking

To compute similarity, we defined the distance of each grid cell i and its environmental conditions x_i to the environmental conditions at

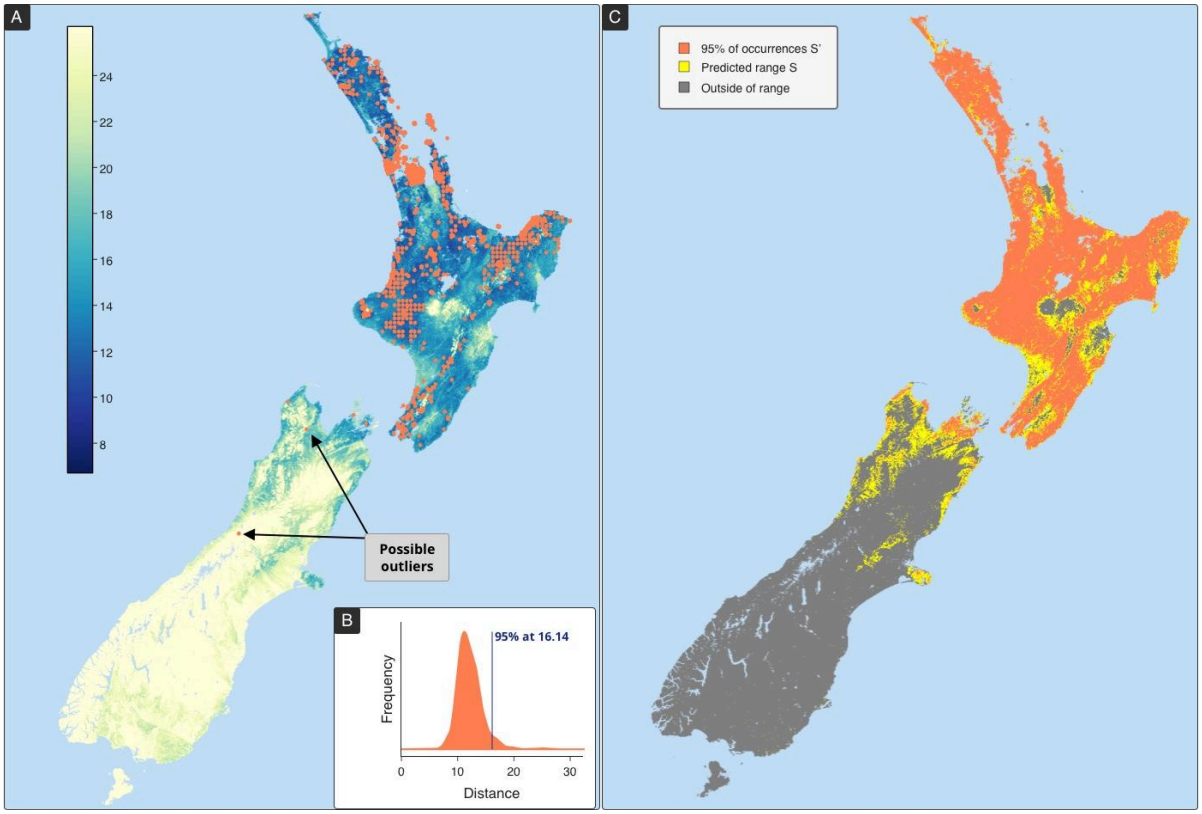


***Figure C6**: Visualisation of the similarity surface method for Geniostoma ligustrifolium, a North Island shrub. A: Distance D of average climatic and topographic conditions to the occurrence set. Coral dots are plots where the species has been observed. Darker colours are areas of higher similarity or shorter distances. Possible outliers are marked to visualise the need for the 95% cutoff. (For contrast, distances above 25 have been set to 25) B: Distribution of distances with 95% percentile marked (S'). Since the distance is an average across all years and climatic variables fluctuate, the mean is not very close to zero. C: The final similarity mask with the 95% percentile (S') in orange and the additional area gained by upscaling S to S' in yellow. Grey areas are excluded from prediction.*

C1.6. Difficulty score

Each survey plot got assigned a difficulty score, that allowed us to evaluate which parts of the dataset were readily learned by the model. We defined a difficulty for a model and point $dif_k \in [0, N]$ as the number of times it gets misclassified when trained on N randomised subsets of the data. High difficulty indicated points that a classifier could not learn, regardless of the training dataset. The data was split N=10 times into four randomised and stratified sets of test/training splits and N*4 models trained to determine the difficulty:

1. For each species and classifier, initiate the difficulty: $dif_k = 0$
2. Split the dataset using randomised, stratified 4-fold cross-validation, giving four training and test data sets (D_i, T_i). The points T_i are randomly chosen but satisfy: $X = \bigcup_i T_i$ and $\emptyset = T_i \cap T_j$ (Each point is assigned to exactly one T_i)
3. Train and validate a classifier for each (D_i, T_i).
4. If a point in T_i was incorrectly classified, increase the difficulty $dif_k = dif_k + 1$. Each point is classified exactly once, and difficulty can't increase by more than one point in each iteration.
5. Repeat steps 2-4 N times.

This procedure assigned a difficulty of 0 - N to each point. For clarity we categorised the difficulties as trivial (0), learnable (1 to (N-1)), or unlearnable (N).

To assess whether the difficulty score was related to specific climatic conditions or particular species, we first plotted the mean and 75% interval of difficulty scores of the training data for all species (**Fig. C7** A). The species are sorted by mean difficulty and show only insignificant differences in average difficulty. This is particularly apparent when looking at the 75% interval of all points (shaded area) that remained mostly unchanged for all species except for very few species on the far right, likely owed to a stronger class imbalance for these species.

Similarly, the average correlation between the difficulty of the training points (i.e. a site surveyed twice) with the environmental predictor variables at this site is very close to zero for all predictor variables, as well as the year difference between remeasurements of a site (**Fig. C7** B). The 75% interval of all species (boxes in **Fig. C7** B) contains correlations only between -0.1 and 0.1. In conclusion, there seems to be no indication of correlations between predictor variables and difficulties, except for single outliers that were correlated up to 0.2 - 0.3.

The only prominent correlation we found for the random forest classifier was between the degree of class imbalance for a species and the mean difficulty of its training set (**Fig. C7** C). This was likely owed to models finding trivial solutions (predicting the majority class) for imbalanced species. However, the average difficulty trend dropped from ~4.5 to ~3 on a 0-10 scale and, given the wide distributions of difficulty per species (**Fig. C7** A) might be of little practical impact.

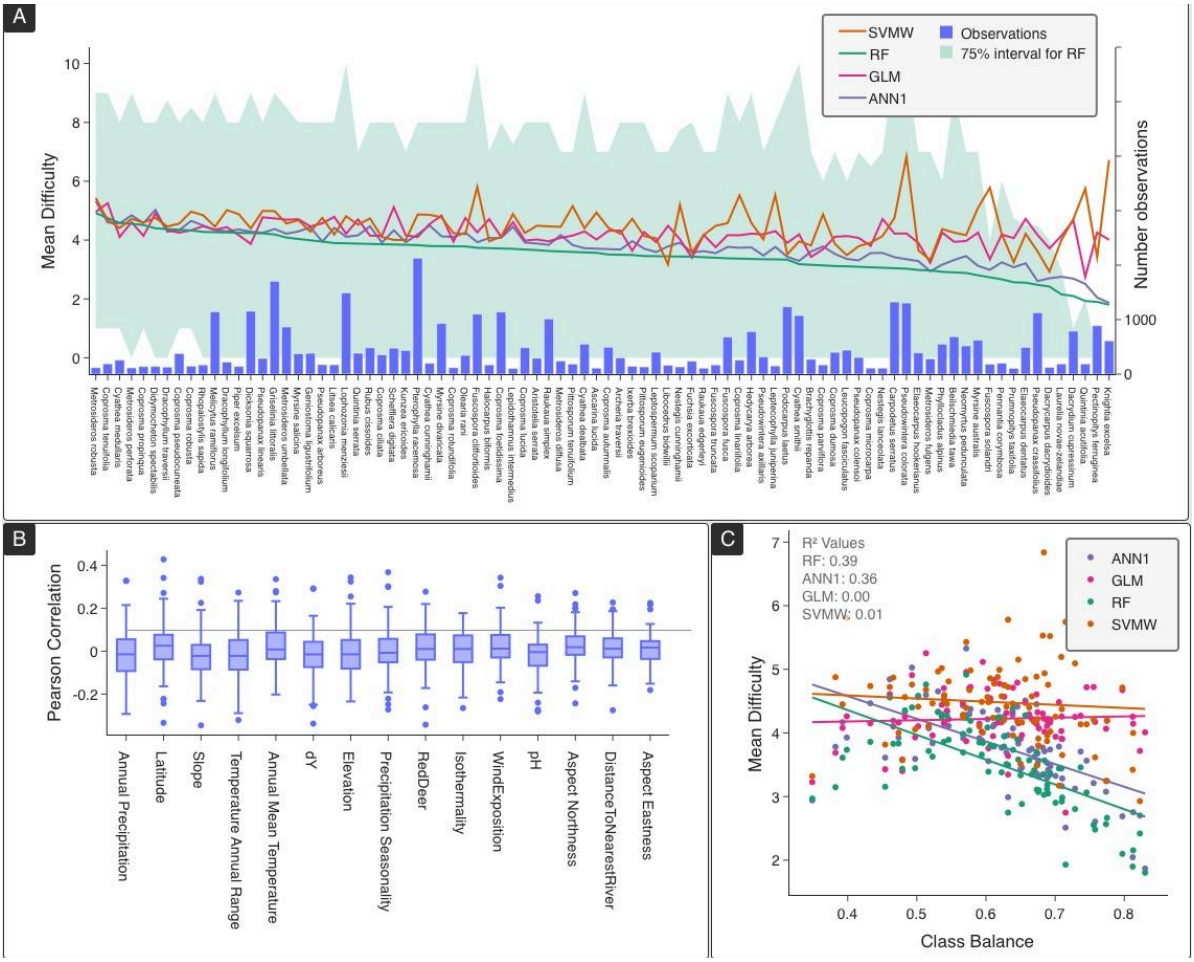


***Figure C7**: Relation of Difficulty score to species and predictive variables. A. Average difficulty by species ordered by mean difficulty for the Random Forest classifier. Means of other classifiers shown as lines. Bars indicate the number of observations for this species (secondary Y axis). B. Pearson correlation of Random Forests's numeric difficulty with variables from the "Reduced" set of variables. Each point in the box plot represents a species. dY variable is the number of years between measurements. C: Correlation of mean difficulty with class imbalance (ratio of "Increase" points vs all points).*

C1.7. Regression To The Mean

Regression to the mean is a statistical phenomenon in which repeated measurements on the same subject/location show a negative correlation between the change in the measured quantity and its initial value, often due to stochasticity (Mazalla and Diekmann 2022). This stochastic effect can mask

true statistical relationships between variables. For example, if we were to draw twice from a random distribution, and the first measurement happened to be unusually low, the second measurement would very likely be closer to the mean and result in a larger difference between the two. Analysing multiple such draws, we would find a negative correlation between the first draw and the difference between the first and second draw (change score). To account for this stochastic effect, models inferring change scores should therefore incorporate the initial draw as a predictive variable (Mazalla and Diekmann 2022).

For each plot, we use the abundance values at two time points a_0, a_1 and a change score $\Delta_a = a_1 - a_0$. ATI binarises the change score to a class label $cl(a_1, a_0)$, which is "Increase" if $a_0 < a_1$ or "Decrease" otherwise (See Section 6.3.1). The solution by (Mazalla and Diekmann 2022) suggest to add a_0 to the set of predictive variables to avoid the RTM effect. However, in the binary case, a_0 and a_1 are never both 0, as this would allow arbitrary plot to be added to the training set. Therefore, including a_0 as a predictive variable would indicate to the model that the label is always "Increase", as we can't decrease from 0 and $a_1 > 0$, thus artificially inflating the model performance. To avoid this, we included the average abundance $a_{Avg} = \frac{1}{2}(a_1 + a_0)$ instead, which is always larger than 0 and does not indicate the class label. Adding this variable as a predictive variable substantially increases the model scores (**Fig. C12** A). However, the abundance is not generally known when using ATI models for prediction. This limits the inclusion of the abundance and the increased model performance to inference use cases, where a model is trained to analyse, for instance, the feature importance values or linear coefficients (See section 6.3.8).

Since we can't eliminate the effect of RTM when using ATI for prediction, we assessed the strength of this effect by evaluating the correlation of a_{Avg} and the class label $cl(a_1, a_0)$ and compared this to the correlation of a_{Avg} and the change score $\Delta_a = a_1 - a_0$, which estimates RTM if ATI predicted abundance differences rather than a binary class. To calculate the correlation between a_{Avg} and the $cl(a_1, a_0)$ we used the Point-biserial correlation coefficient (Glass 1996), which is equivalent to the Pearson correlation, with one dichotomous variable.

For the binary classification case, the strength of RTM was low, with only 25% of species exhibiting statistically significant relationships (**Fig. C8**B), and these relationships explained on average only 1% of variation (**Fig. C8** A). However, the correlation for the continuous change score was on average six times higher, with over 70% of species being affected by RTM. This suggests that transitioning from a regression to a binary classification problem significantly reduces the RTM effect.

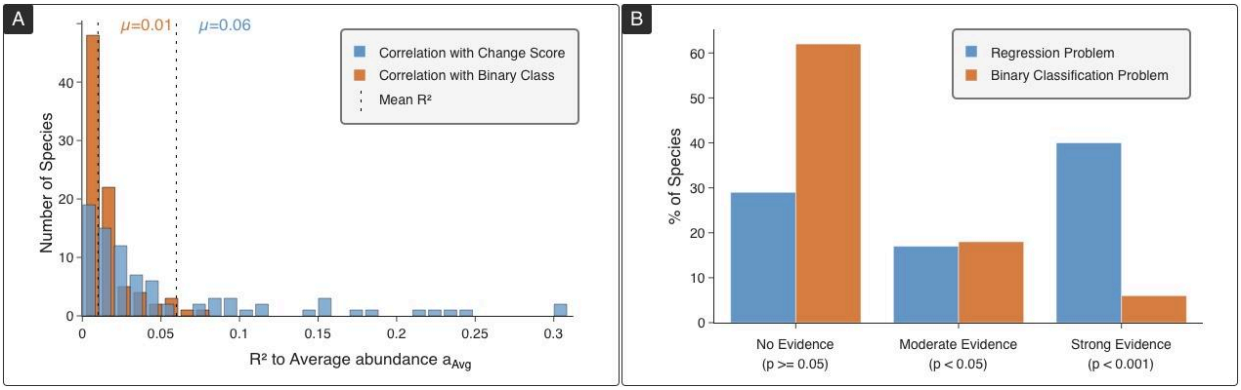


***Figure C8**: Analysis of the susceptibility of the regression to the mean (RTM) effect following (Mazalla and Diekmann 2022). Each data point consists of an abundance measurement at two time points a_1, a_0. RTM strength is assessed by correlating the species average abundance $a_{Avg} = \frac{1}{2}(a_1 + a_0)$ with the binary class label (i.e. increase or decrease in abundance, as implemented in this study in orange) or the continuous change score $\Delta_a = a_1 - a_0$ (i.e. abundance difference). (A) Histogram of the correlation R^2 for the binary and continuous case. (B) Bar plot of p-values for the same evaluation indicating whether a correlation, and thus the RTM effect, exists.*

C1.8. Binarisation of data and regression

Based on environmental variables, ATI learns to distinguish between areas of abundance increase and abundance decrease in a classification problem. ATI does not learn the absolute change in abundance, and thus, areas with different abundance changes are assigned the same label. We analysed the distribution of absolute abundance changes to assess the uncertainty associated with binary predictions.

First, we examined the change in abundance $\Delta a(i, s)$ across observations i for all species s. To make the distributions comparable across species, we standardised Δa by subtracting the mean and dividing by the standard deviation, yielding a $\widetilde{\Delta a}(i, s) = \frac{\Delta a(i,s) - \mu_s}{\sigma_s}$. A kernel density estimation was done on $\widetilde{\Delta a}(i, s)$ to derive a continuous density distribution of the standardised change in number of individuals for each species $\widetilde{p}(s)$ (**Fig. C9**A, grey lines). We averaged across all species (**Fig. C9**A, blue line) and approximated a Gaussian distribution (**Fig. C9**A, red line). The change in the number of individuals showed a nearly Gaussian shape with heavier tails for all species.

Additionally, we computed the Kullback-Leibler divergence (KLD) (Kullback 1959) of $\widetilde{p}(s)$ to a Gaussian distribution of the same mean and variance, as well as a uniform distribution (**Fig. C9**B). KLD is a measure of how similar two distributions are. The KLD to a Gaussian distribution was substantially lower than to a uniform distribution.

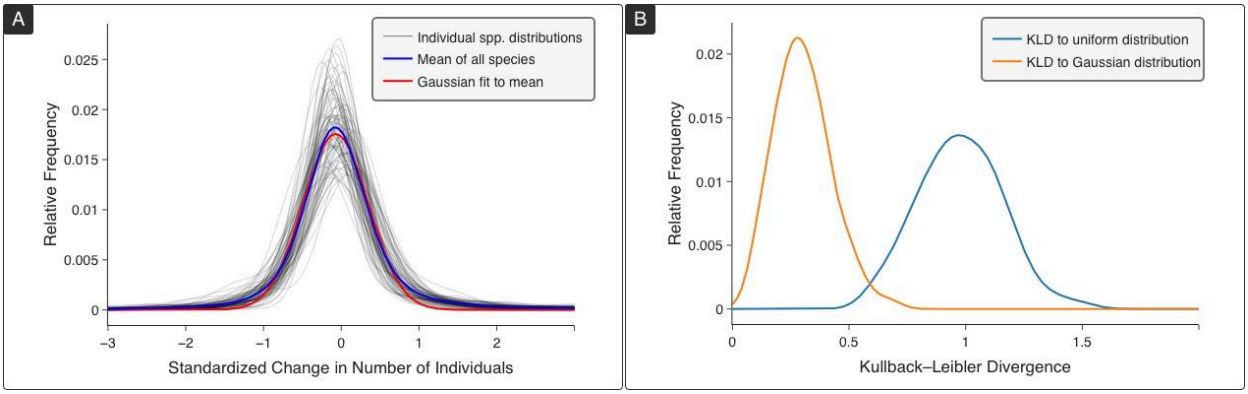


***Figure C9**: Analysis of the distributions of change in number of individuals across all observation pairs in the training data. (A) Change in abundance across all species standardised to zero mean and unit variance ($\widetilde{p}(s)$, grey lines), average for all species (blue line) and a Gaussian fit to the average (red line). The average changes in abundance are close to Gaussian but with heavier tails. (B) Distribution of Kullback-Leibler divergences of species abundance changes $\widetilde{p}(s)$ to a uniform distribution (blue line) and a Gaussian distribution (orange line). Changes in abundance $\widetilde{p}(s)$ resemble a Gaussian distribution more closely than a uniform distribution.*

Collectively, the Gaussian distribution suggests that extreme shifts in abundance are less frequent than more moderate changes and implies a more predictable dynamic for species movement. In contrast, a uniform distribution of abundance changes would render any magnitude of change equally probable, leading to greater uncertainty and unexpected outcomes in observed shifts. Therefore, the observed normal distribution indicates that species tend to exhibit range shifts at a predictable, species-specific rate, driven by biological responses and environmental interactions.

ATI's binary predictions could therefore be extended into a Bayesian framework with Gaussian priors, allowing for the quantification of uncertainty in species-specific shifts and potentially refining predictions of future range dynamics.

C2. Evidence for Data Errors

Irregularities and errors are present in ecological data and should be excluded. In this work, we are concerned with labelling errors (e.g. a site receives an "increased" target label, where it should be "decreased"). Suppose for example, a species increases in abundance in a set of nearby sites except for one where it decreases. In that case, we need to ask whether this is due to human error in collecting, measuring, digitising, and curating forest inventory data, or whether it occurred due to natural stochasticity, the influence of latent variables, rare climatic events, or biotic interactions. The former case warrants excluding the training point from our training set (i.e., treating it as noise or labelling error); the latter case calls for better algorithms or predictor variables to capture additional mechanisms.

To our knowledge, the question of reliability in forest inventory data has only been rarely addressed. Two studies estimated these errors from 5.9% (Scott and Hallam 2003) to 21% (Verheyen et al. 2018) of species richness. This is unsurprising, as forests constantly change, and previously gathered data cannot be resurveyed to assess its accuracy. Here, we gathered evidence for different types of errors to confirm the presence of labelling noise in our dataset, estimate its lower bound, and justify our noise-removal procedure.

C2.1. Rapid shifts in community composition

We compared two surveys of the same plot using the Jaccard index to assess how quickly the community has turned over in our dataset. The Jaccard index measures the similarity of two sets of species, with 1 indicating the same species being present in both sets and 0 indicating no shared species (**Fig. C10**). For this study, we utilised a dataset where each adult plant with a measurable diameter at breast height is tagged and measured (Hurst 2022). The turnover rate, as expected, is, on average, slow (**Fig. C10**A). However, there were outliers in the data where almost every woody species was replaced within five years. We found that ***2.7% of our dataset*** consisted of stark outliers with a Jaccard index below 0.35. The reasons may be undocumented surveying methods, errors or forests recovering from catastrophic events (e.g. a drought or cyclone). An example of human error is evident in the Orongorongo forest, surveyed in 1994, 1995, and 2006 (**Fig. S10**A, left-most box). Together with the data provider, we investigated this particular issue for the four plots with a Jaccard index of 0.33-0.17 and discovered that the 1995 survey only examined tree ferns, ignoring all woody species, a fact mentioned in an internal note that was not available to us initially. Errors like these could generate dozens of erroneous and contradictory target labels. In our case, the 1994-1995 comparison would generate a “decrease” label for all woody species (since they “disappeared” from the record) and then an increased label for 1995-2006. Only the climatic variables would experience a slight change over the 11-year period, leading to two nearly contradictory sets of labels. This legitimates our model-agnostic approach to label noise removal.

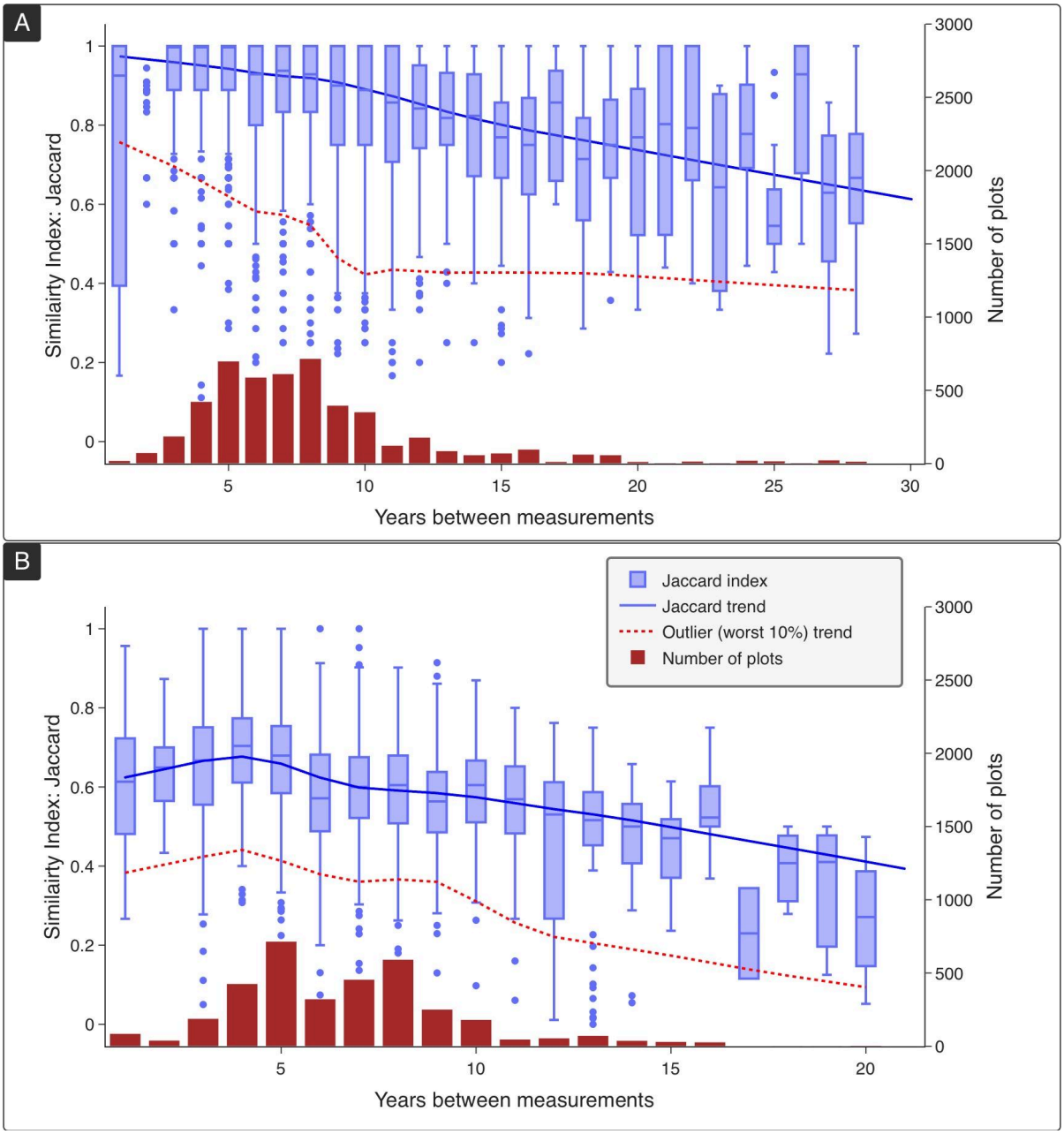

A
Similairty Index: Jaccard
Number of plots
Years between measurements
B
Jaccard index
Jaccard trend
Outlier (worst 10%) trend
Number of plots
Similairty Index: Jaccard
Number of plots
Years between measurements

***Figure C10**: Jaccard similarity between plot surveys by the time between surveys. High values indicate similar species composition. A: For a dataset of tagged woody plants. B: For the RECCE dataset that measures a much wider range of species (also non-woody) in height and cover tiers. Trendlines are rolling averages over a 15(A) and 10 (B) year window, respectively.*

The Jaccard similarity is worse when using the RECCE method (Hurst 2022) of surveying. In this method, all species are recorded (seedlings, saplings and non-woody species). The average similarity after 1-5 years is far lower than in the stems method, likely due to the difficulty of detecting small plants and seedlings. Here, outliers with nearly complete species turnover are also present. It should be noted that all surveyed plots are located in forests that are neither commercially exploited nor subject to experiments. In conclusion, these numbers and examples indicate the presence of some errors, and we hope to sensitise researchers working on forest inventory data to consider its reliability.

C2.2. Measurement goals impact plot surveys

Our dataset consisted of five plots, each measured twice in the same year as part of different projects with varying goals.

The species composition, as measured by the Jaccard index, was close but not identical (1, 1, 0.9, 0.75, 0.6, and 0.33). Shockingly, the remeasurement of the worst matching plot omitted 4 out of 6 recorded species, recording their abundance as 0 (**Table C3**). The reason might be because the first measurement was taken by the New Zealand Biodiversity Monitoring System (Public Land), which explicitly records all species, while the second one was done by the “New Zealand Indigenous

Carbon Monitoring System" and likely excluded the shrub species, as they contribute less to woody biomass than trees. This illustrates another source of error in forest inventory data.

Species	Counts Project 1	Counts Project 2
Coprosma propinqua	121	
Discaria toumatou	17	
Euonymus europaeus	1	
Griselinia littoralis	3	2
Kunzea ericoides	8	8
Veronica salicifolia	1	

***Table C3**: Two measurements of the same plot in 2012 as part of different projects. Project 1 measured biodiversity, and Project 2 measured carbon. As a result, we suspect that shrubs were excluded.*

C2.3. Misidentification of species of the same genus

New Zealand's flora includes 58 species of the Coprosma genus (Rubiaceae family), which, even for experienced botanists, can be challenging to distinguish. To find evidence for misclassification of this type, we analysed plot survey pairs and looked for instances where the first survey contained a Coprosma species A but the second survey contained a congeneric species B instead, which presumably might be due to the surveying botanists identifying the same plant as species A in one year and as species B in another year. We found that these congeneric swaps, on average, occurred in 3.68% of surveys. Misclassifications like these would lead to the introduction of labelling noise and erroneous data, as species A would be labelled as "decrease" while species B would be labelled as

“increase”. The former data point may be mislabeled, and the latter may be fictitious, as species B might not be present in this plot. Moreover, both A and B might be misclassified, which is entirely undetectable in retrospect. The 3.68% misclassification rate, therefore, should be seen as a lower bound for misclassification errors. A detailed evaluation by species is shown in **Table C4**.

Species present in the first survey	**Species present in the second survey**	**Plots**
Coprosma "small-leaved"	*C. "small-leaved" (50.0%)*	2
	C. propinqua (25.0%)	1
	C. foetidissima (25.0%)	1
Coprosma arborea	*C. arborea (87.5%)*	28
	C. lucida (3.1%)	1
Coprosma areolata	*C. areolata (84.7%)*	61
	C. autumnalis (1.4%)	1
Coprosma colensoi	*C. colensoi (63.4%)*	45
	C. lucida (1.4%)	1
	C. tenuifolia (1.4%)	1
	C. rugosa (1.4%)	1
	C. rotundifolia (1.4%)	1
	C. pseudociliata (1.4%)	1
	C. parviflora (1.4%)	1
	C. foetidissima (1.4%)	1
	C. dumosa (1.4%)	1
	C. ciliata (1.4%)	1
Coprosma cuneata	*C. cuneata (66.7%)*	10
	C. pseudocuneata (13.3%)	2
	C. colensoi (6.7%)	1

Coprosma lucida	*C. lucida (71.9%)*	348
	C. autumnalis (1.7%)	8
Coprosma parviflora	*C. parviflora (45.7%)*	96
	C. dumosa (2.9%)	6
	C. ciliata (1.4%)	3
	C. foetidissima (1.4%)	3
	C. lucida (1.4%)	3
	C. rugosa (1.0%)	2
	C. microcarpa (1.0%)	2
	C. autumnalis (1.0%)	2
Coprosma pseudociliata	*C. pseudociliata (93.0%)*	40
	C. dumosa (4.7%)	2
Coprosma rhamnoides	*C. rhamnoides (51.1%)*	24
	C. propinqua (2.1%)	1
	C. parviflora (2.1%)	1
	C. lucida (2.1%)	1
	C. foetidissima (2.1%)	1
	C. ciliata (2.1%)	1
	C. autumnalis (2.1%)	1
Coprosma rigida	*C. rigida (95.8%)*	23
	C. rhamnoides (4.2%)	1
Coprosma robusta	*C. robusta (71.2%)*	94
	C. autumnalis (3.8%)	5
Coprosma rotundifolia	*C. rotundifolia (91.7%)*	99
	C. propinqua (0.9%)	1
Coprosma rugosa	*C. rugosa (45.2%)*	14
	C. lucida (6.5%)	2

	C. foetidissima (3.2%)	1
Coprosma tenuicaulis	*C. tenuicaulis (9.1%)*	2
	C. rhamnoides (4.5%)	1
	C. autumnalis (4.5%)	1
Coprosma tenuifolia	*C. tenuifolia (83.0%)*	146
	C. autumnalis (1.1%)	2
	C. dumosa (1.1%)	2
Cyathea cunninghamii	*C. cunninghamii (89.8%)*	132
	C. smithii (2.0%)	3
Cyathea medullaris	*C. medullaris (89.6%)*	190
	C. cunninghamii (1.4%)	3
Freycinetia baueriana	*F. baueriana (22.2%)*	4
	F. banksii (11.1%)	2
Hoheria glabrata	*H. glabrata (78.4%)*	80
	H. lyallii (1.0%)	1
Metrosideros robusta	*M. robusta (84.8%)*	95
	M. perforata (1.8%)	2
Olearia arborescens	*O. arborescens (67.7%)*	21
	O. ilicifolia (3.2%)	1
	O. lacunosa (3.2%)	1
Podocarpus totara	*P. totara (83.6%)*	56
	P. laetus (1.5%)	1
Pseudopanax arboreus	*P. arboreus (79.8%)*	130
	P. colensoi (1.2%)	2
Veronica parviflora	*V. parviflora (63.6%)*	7
	V. leiophylla (9.1%)	1
Total species confusion weighed by plots		**3.68%**

***Table C4**: Results of the analysis of two measurements of the same plot where a species of a genus is "replaced" by another species of the same genus. For example, in the last row, "Veronica parviflora" was detected in the first survey of a plot (first column). In 63.6% of the results, it was detected in the second survey of this plot (some years later). But in 9.1% of the cases V. leiophylla was recorded while V. parviflora disappeared (second column). This indicates possible misclassification. The remaining 27.3% are cases where neither V. parviflora nor any other Veronica species was present in the second survey. Note that Coprosma "small-leaved" was excluded from the final dataset and kept here as an illustration of the classification difficulty of the Coprosma genus.*

C2.4. Conclusion

While only an experiment can reveal the percentage of errors in forest inventory data, our findings indicate that errors do exist mainly for three reasons:

- Intransparent method documentation
- Varying goals in capturing the data (e.g. carbon capture vs biodiversity) that lead to incompleteness
- Confusion of congeneric or anatomically similar species

We estimated lower bounds of 2.70 % and 3.68 % of suspicious data using different methods, which are likely to be additive. Many other error sources remain undiscovered. For example, data collection in the New Zealand Forest Inventory dataset relies on handwritten sheets containing 6-letter species codes; a source of error might be as trivial as bad handwriting. Taken together, we conclude that, at a minimum, approximately 5% of our forest inventory data is likely to be corrupt.

C3. Supplementary Results

C3.1. Training performance on subsets of data

Using the difficulty categories (Trivial, Learnable and Unlearnable, Section C1.6), we individually tracked the classification accuracy in each subset of the data (**Fig. C11**). The learnable category showed the largest increase in accuracy, ruling out the removal of unlearnable instances as the single cause of score improvement. The accuracy of unlearnable instances, too, improved since, for example, removing one of two contradicting (and thus unlearnable) instances would make the remaining instances more likely to follow a general trend and therefore become learnable.

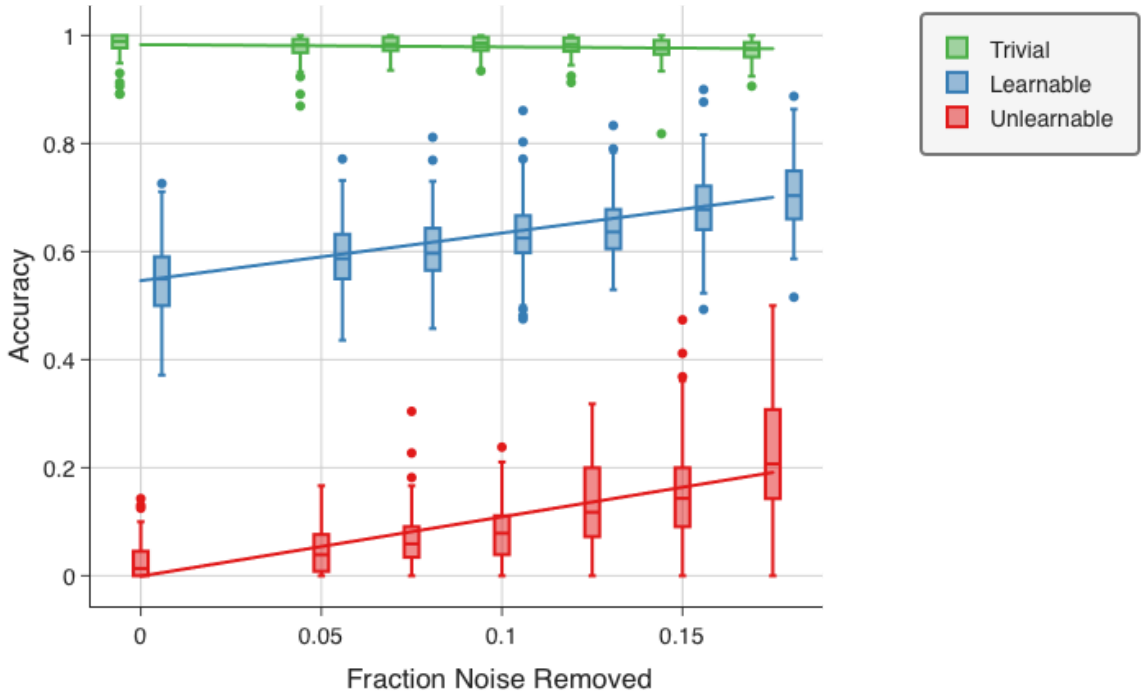


***Figure C11**: Prediction accuracy of the dataset split by difficulty categories of the random forest classifier. Accuracy is the ratio of correctly classified instances to the total number of training instances.*

C3.2. An optimal noise removal rate is 12-15%

We evaluated the AUC score for four machine learning models (Section 6.3.4) trained on three different variable sets: Full (39 variables), Explain (14 variables) and Explain + Abundance (15 variables) (Section 6.3.2) at different levels of noise filtering (Section 6.3.3) (**Fig. C12** A). The Explain+Abundance dataset was used to offset the Regression To The Mean effect (Mazalla and Diekmann 2022), and it adds the number of individuals as an additional variable to the Explain dataset (Section S4.7). The random forest (RF) classifier with all variables performed best, with other classifiers 5-10% behind. All other classifiers showed comparable performance at noise reduction rates below ~10%. Above 10% the GLM classifier was outperformed by the non-linear ANN1 and SVMW.

We assessed the collective canopy cover and number of sufficiently accurately classified (AUC > 0.7, Section 6.3.4) species (**Fig. C12**B and C). A noise reduction of less than 15% prevented the classifiers from learning well. Removing more than 15%, on the other hand, caused rarer species to fall below the 100-observation limit, making 15% the optimum. Notably, SVMW covered a higher canopy percentage than GLM, despite having a lower average score in a high-noise setting, indicating an advantage of complexity when classifying more widespread species.

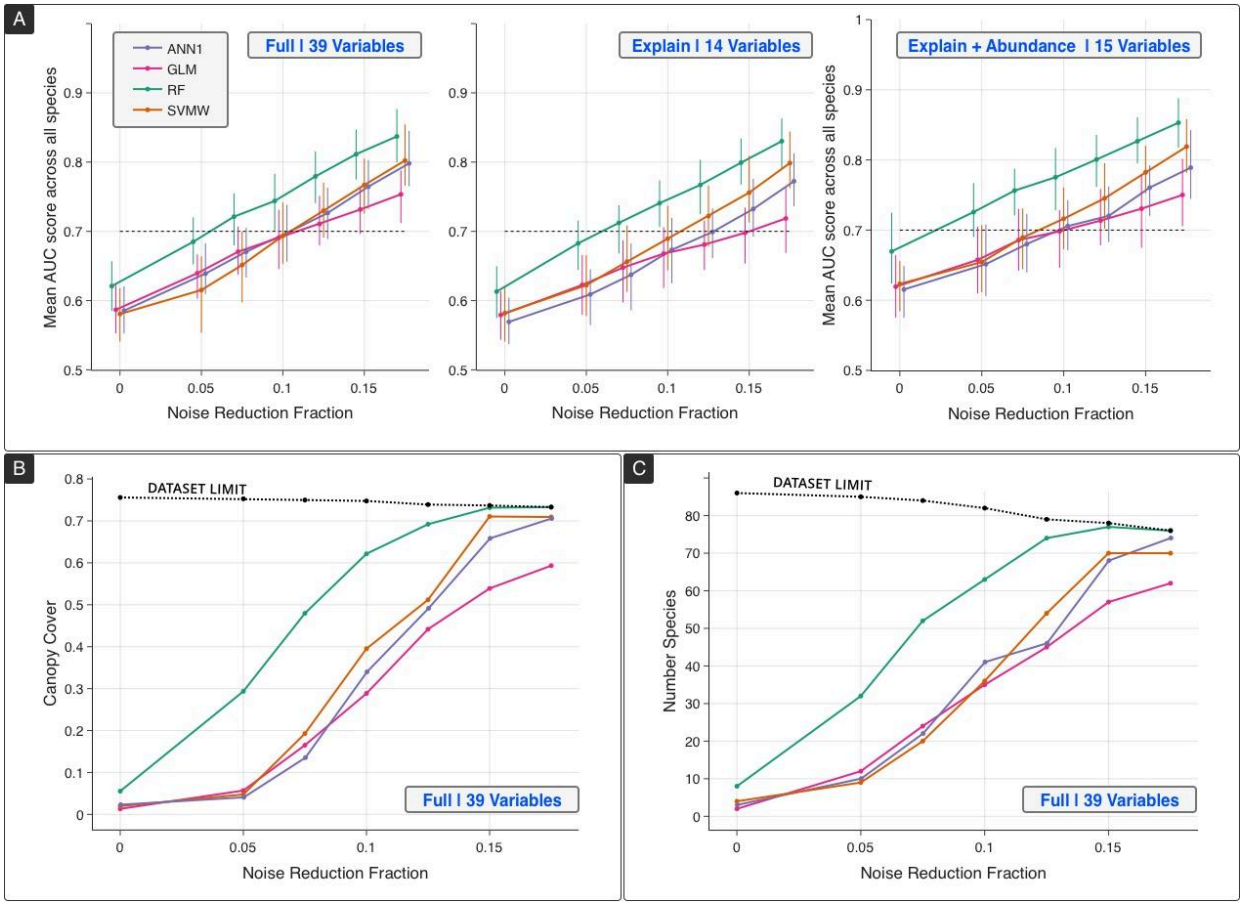


***Figure C12**: Classifier performance on different sets of variables using the Abundance and DBH Dataset. A: Mean AUC scores over three variable sets. B and C: Cumulative canopy cover and number of species of all species classified with an AUC score above 0.7 over the fraction of noise removed. A single legend is used for all panels.*

Species	Abundance Only	Abundance and DBH	Cover in %
Quintinia acutifolia	0.9493	0.9389	0.88
Brachyglottis repanda	0.8959	0.9253	0.46
Fuscospora solandri	0.9105	0.8918	0.79
Fuscospora truncata		0.8917	1.26
Fuchsia excorticata	0.8951	0.89	0.29
Ixerba brexioides		0.882	0.31
Laurelia novae-zelandiae		0.88	0.43
Metrosideros fulgens	0.7803	0.8771	0.44
Coprosma rotundifolia		0.866	0.14
Coprosma parviflora	0.9117	0.8652	0.07
Pterophylla racemosa	0.8103	0.8622	5.78
Pittosporum tenuifolium		0.8622	0.27
Fuscospora cliffortioides	0.8329	0.8598	3.72
Leptospermum scoparium	0.8336	0.8595	1.83
Coprosma foetidissima	0.8553	0.8594	0.98
Coprosma autumnalis	0.8124	0.8589	0.88
Fuscospora fusca	0.9021	0.8565	2.86
Pseudowintera axillaris	0.813	0.8532	0.26
Raukaua simplex	0.8638	0.8497	0.51
Coprosma lucida	0.8815	0.8471	0.31
Aristotelia serrata	0.8303	0.8467	0.34
Coprosma ciliata	0.7996	0.8461	0.28
Pittosporum eugenioides		0.8421	0.14
Leucopogon fasciculatus	0.801	0.8413	0.8
Kunzea ericoides	0.8086	0.8381	2.46
Neomyrtus pedunculata	0.8818	0.8346	0.6
Metrosideros diffusa	0.7513	0.8303	0.57

Beilschmiedia tawa	0.8301	0.8289	3.15
Myrsine salicina	0.8336	0.8283	0.58
Olearia rani	0.8464	0.8263	0.59
Coprosma dumosa	0.8145	0.8262	0.44
Nestegis cunninghamii		0.8257	0.11
Carpodetus serratus	0.8085	0.8233	1.14
Podocarpus laetus	0.8722	0.8229	1.23
Pseudowintera colorata	0.8001	0.8226	1.99
Quintinia serrata	0.8444	0.8218	1.04
Cyathea cunninghamii	0.7742	0.8154	0.09
Knightia excelsa	0.7922	0.8131	1.07
Rubus cissoides	0.7516	0.8107	0.41
Pennantia corymbosa	0.8263	0.808	0.17
Cyathea dealbata	0.8349	0.8079	3.26
Geniostoma ligustrifolium	0.8051	0.8068	1.04
Archeria traversii	0.7879	0.8048	0.31
Phyllocladus alpinus	0.7679	0.7986	0.79
Coprosma robusta	0.7408	0.7944	0.17
Coprosma pseudocuneata	0.7193	0.7941	0.42
Rhopalostylis sapida		0.7881	1.4
Piper excelsum	0.7713	0.7861	0.48
Lophozonia menziesii	0.7593	0.7858	4.54
Dracophyllum longifolium	0.8115	0.7846	0.37
Schefflera digitata	0.8121	0.7845	0.37
Pseudopanax crassifolius	0.7689	0.7811	0.85
Pseudopanax colensoi	0.6873	0.78	0.17
Myrsine australis	0.7838	0.7795	0.72
Coprosma tenuifolia	0.6793	0.7792	0.08
Didymocheton spectabilis		0.7774	0.88
Coprosma linariifolia	0.8054	0.7759	0.16
Myrsine divaricata	0.7469	0.7753	0.49
Cyathea smithii	0.7478	0.7748	2.17

Hedycarya arborea	0.7632	0.7734	1.09
Cyathea medullaris	0.7566	0.7727	0.52
Dicksonia squarrosa	0.7447	0.7704	1.82
Pseudopanax linearis	0.6522	0.7699	0.1
Pseudopanax arboreus	0.7872	0.7695	0.38
Griselinia littoralis	0.7886	0.7691	1.81
Dracophyllum traversii		0.7676	0.35
Coprosma propinqua		0.7667	0.69
Elaeocarpus hookerianus	0.6832	0.76	0.28
Melicytus ramiflorus	0.7914	0.7554	2.27
Metrosideros umbellata	0.7993	0.751	1.42
Metrosideros robusta		0.7496	0.24
Dacrydium cupressinum	0.8346	0.7464	1.82
Litsea calicaris		0.7416	0.1
Leptecophylla juniperina		0.7411	0.47
Libocedrus bidwillii		0.7408	0.11
Pectinopitys ferruginea	0.7275	0.7395	1.1
Halocarpus biformis		0.7258	0.24
Elaeocarpus dentatus	0.7509	0.6947	0.53

***Table C5**: Individual AUC scores for the random forest model on the Abundance Only dataset (at 10% label noise reduction) and Abundance and DBH dataset (at 15% reduction). The total cover of each species is given in the right-most column. Since data-deficient species are not included, the cover column sums up to ~73% of forest cover and the Abundance Only dataset contains fewer species. The table is sorted by Abundance and DBH score. (Scores below below 0.7 are included due to rounding precision)*

C3.3. Noise removal is necessary for accurate predictions

A subset of ~15% of points was consistently misclassified (unlearnable) by classifiers, regardless of the chosen training data (**Fig. S13**B), resulting in poor model performance before noise removal

(**Fig. C12**). The remaining points, however, could be learned even by a linear model (average AUC test score of 0.83; **Fig. C13**A). There was a strong pairwise agreement among all four classifiers on which points are "Learnable" (**Fig. C13**C, blue boxes). This indicates that abundance shifts are driven by a general trend (i.e., ~85% of the data) that can be easily captured by simple models (such as logistic regression) and an unexplained residual. This could not be explained by species, environmental variables or time between plot surveys (**Fig. C7**).

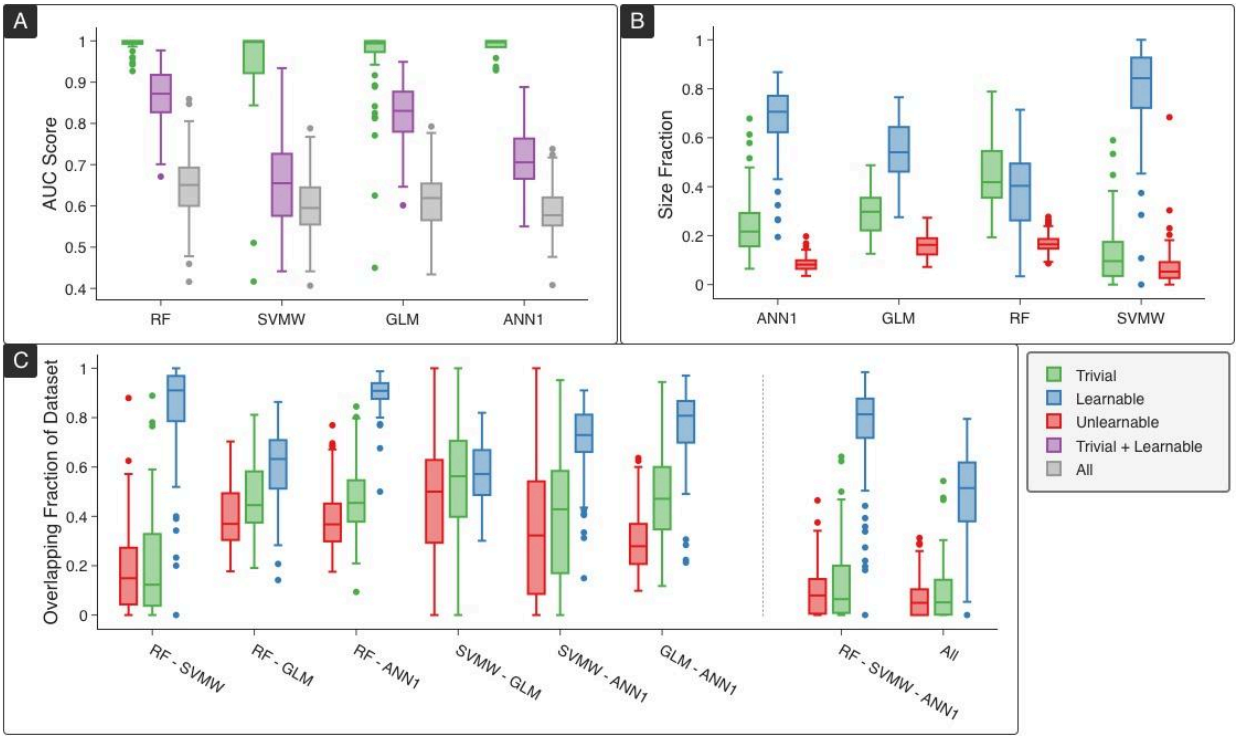


***Figure C13**: Learnability of the dataset. Each point in the box plots is a species. Acronyms describe the different models (Section C1.4). (A) Models trained on trivial, trivial + learnable or full (sub) data sets (see Section 6.3.8). (B) Fraction of trivial, learnable and unlearnable data points. (C) Similarity of difficulty labels between pairs of classifiers (left) and all (non-linear) classifiers (right).*

C3.4. Synthetic Species Experiment

We tested our method on three synthetic species that were generated to shift their abundance to areas of higher elevation, latitude or annual precipitation gradient, respectively. The synthetic data was generated using the following procedure:

1. We estimated the distribution of plot locations in the original dataset using kernel density estimation and sampled 2000 random plot locations from it. (Publication of original plot locations was not permitted by New Zealand's Vegetation Survey NVS, (Wiser et al. 2001))
2. Each plot received two hypothetical observations for the years 1990 and 2019, resulting in a total of 4,000 observations.
3. We determined the mean and standard deviation of elevation, latitude, and annual precipitation (μ_V, σ_V), where the index V denotes the respective variable. The distribution of variables V across all observations are depicted as a solid black in **Fig. C14**.
4. For each environmental variable, we generated two Gaussian sampling distributions describing the species' elevational, latitudinal, and precipitation preferences for the two observation years 1990 and 2019: ${N_V}^{1990}(\mu_V - \frac{1}{2}s_V,\ 0.2 \cdot \sigma_V)$ and ${N_V}^{2019}\ (\mu_V + \frac{1}{2}s_V,\ 0.2 \cdot \sigma_V)$. The amount by which the species shifted, denoted by s_V was chosen to match trends observed globally: $s_E = 31.45m$, $s_L = 40km$ and $s_P = 90mm$. This approximately matches the range shifts for latitude and elevation of 11.8km/decade and 9m/decade in (Rubenstein et al. 2023) and the rate of climate change for precipitation in New Zealand of -22m/decade (unpublished data). Dashed lines in **Fig. C14** denote the distributions describing the species' preferences.

5. We then drew a set of 1000 plot observations using these two Gaussians to determine the plots where the species was present. For each species, this yielded 2000 observation pairs (P_i^{1990}, P_i^{2019}) with $P_i^y = 1$ if plot i was among the 1000 selected plots for year y or 0 else (solid lines **Fig. C14**). This step ensured that the presence distributions also followed the distribution of the plots (black lines **Fig. C14**).
6. Abundance values were assigned based on the values of the observation pairs. If $(P_i^{1990}, P_i^{2019}) = (0, 1)$ the abundance was chosen randomly but satisfies $A_i^{2019} > A_i^{1990} > 0$ and anlogously if $(P_i^{1990}, P_i^{2019}) = (1, 0)$ the abundance was set to $0 < A_i^{2019} < A_i^{1990}$. Where $P_i^{1990} = P_i^{2019}$ abundance did not need to be assigned, as our method can only use changes in abundance, and thus these observations would be ignored for model training, unless tree diameter measurements were available (see Section 6.3.1 for a description of the method).

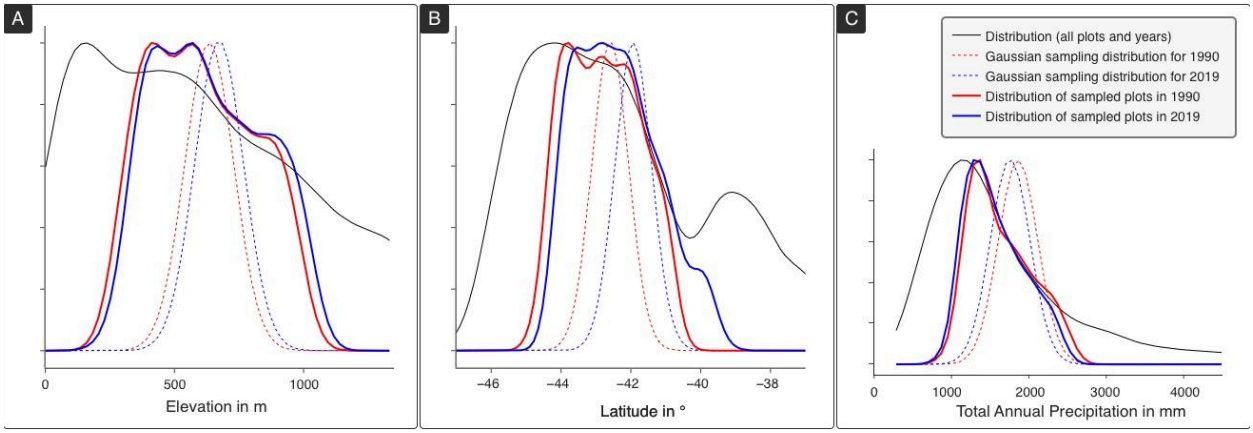


***Figure C14**: Synthetic species generation for a hypothetical species shifting abundance towards higher elevation (A), latitude (B) or lower precipitation (C). The Gaussian sampling distributions for the years 2000 and 2019 (dashed lines) are determined using the mean and standard deviation of the distribution of all plots (black line). Their offset simulates a species abundance shift along the gradient of this variable. The distributions of the 1000 sampled plots are displayed as solid lines. They can be seen as the elevational, latitudinal, or precipitation distribution in the years 1990 and 2019, with an abundance relocation towards higher values occurring during this time period.*

As the areas of abundance for the synthetic species are separated by elevation or precipitation, this task is almost perfectly solved by a linear model (AUC score of 0.85, 0.86 and 0.99 for the elevation, precipitation, and latitude species, respectively) without the need for noise filtering. The resulting ATI surface (**Fig. C15** A - C) is strongly correlated with the respective environmental variable (**Fig. C15** D - F), and thus, the areas of abundance increase coincide with montane regions and New Zealand's rainy west coast, respectively. Elevation is also strongly correlated with annual temperature (**Fig. C16**A), similar to the different precipitation values (**Fig. C16**B), leading to high correlations with variables not directly used in the generation of the synthetic species' range shifts. This result contrasts the simplicity of predicting range shifts for species that are governed by a single variable to much more complex conditions found in a forest and suggests that focusing on a single variable, such as precipitation, elevation, or temperature, is likely not sufficient for accurate prediction of real-world scenarios.

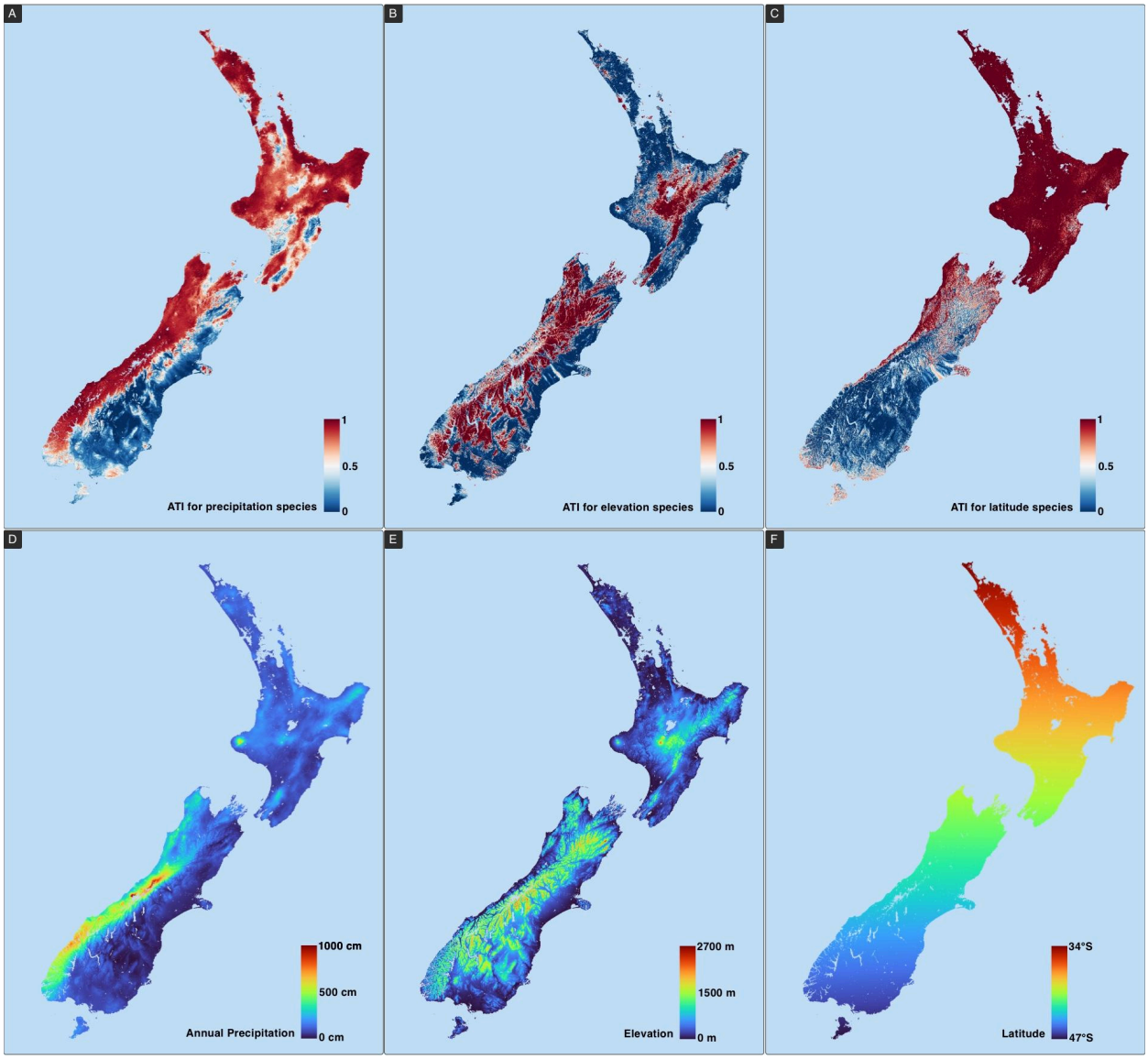


***Figure C15**: ATI predictions for the synthetic species with an abundance gradient towards higher precipitation (A) or elevation (B), or latitude (C). As well as the average precipitation, elevation and latitude (D-F) in the study area and time period.*

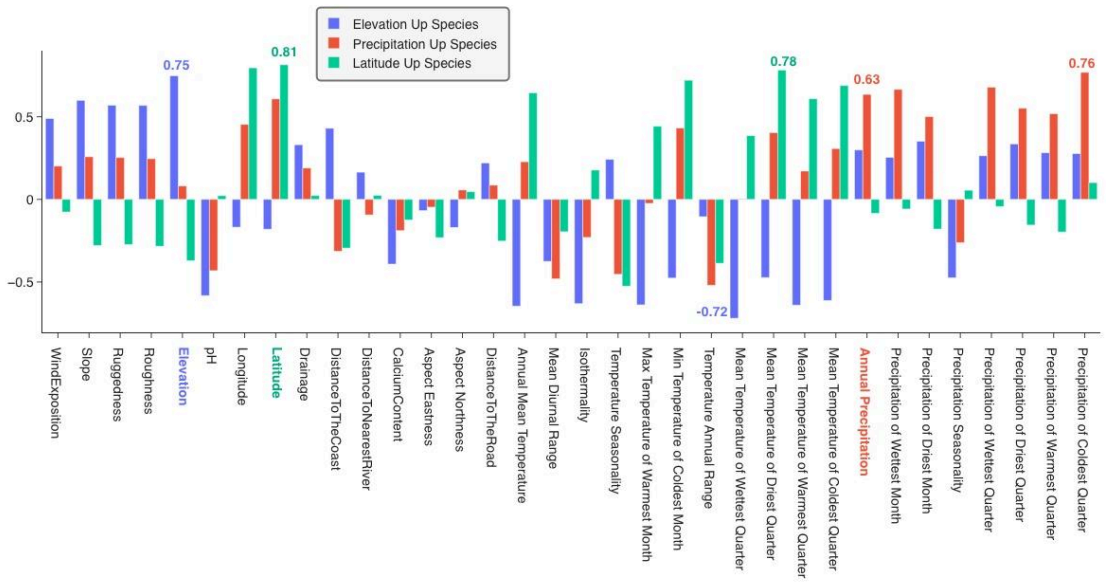


***Figure C16**: Correlation of predicted ATI values for the three synthetic species with the environmental predictor variables. The highest correlation values, as would be expected, occur with the variables used to generate the synthetic species themselves.*

C3.5. Statistical Significance Testing for the Abundance Gradient

Statistical significance testing of abundance gradients (**Fig. 3**) involved comparing the average conditions under which each of the 77 studied species increased or decreased in abundance. Since these conditions can't generally be assumed to be normally distributed, we used a Mann-Whitney U test (Mann and Whitney 1947), which provided a test statistic and a p-value (**Table C6**).

Metric	U statistic	p-value
DistanceToNearestRiver	3025	0.828354
Aspect Eastness	3147	0.510753

Aspect Northness	4032	**0.000115**
Elevation	2076	**0.001333**
Latitude	3328	0.189615
Annual Precipitation	2706	0.351184
Slope	1975	**0.000352**
pH	3308	0.215180
Annual Mean Temperature	3624	**0.017250**
WindExposition	2436	0.056397
Isothermality	3742	**0.004989**
RedDeer	3502	0.052322
Temperature Annual Range	2403	**0.042642**
Precipitation Seasonality	3180	0.437210

***Table C6**: Test statistics for statistical significance testing of abundance gradients in Fig. 3. Values with p < 0.05 highlighted in bold.*

C4. References

Bishop, C. M. (2006). *Pattern Recognition and Machine Learning (Information Science and Statistics)*. Springer-Verlag. https://dl.acm.org/doi/10.5555/1162264

Breiman, L. (2001). Random Forests. *Machine Learning*, *45*(1), 5–32. https://doi.org/10.1023/A:1010933404324

Brodley, C. E., & Friedl, M. A. (1999). Identifying Mislabeled Training Data. *Journal of Artificial*

Intelligence Research, *11*, 131–167. https://doi.org/10.1613/jair.606

Buitinck, L., Louppe, G., Blondel, M., Pedregosa, F., Mueller, A., Grisel, O., Niculae, V., Prettenhofer, P., Gramfort, A., Grobler, J., Layton, R., VanderPlas, J., Joly, A., Holt, B., & Varoquaux, G. (2013). API design for machine learning software: experiences from the scikit-learn project. *ECML PKDD Workshop: Languages for Data Mining and Machine Learning*, 108–122.

Chang, C.-C., & Lin, C.-J. (2011). LIBSVM: A library for support vector machines. *ACM Transactions on Intelligent Systems and Technology*, *2*(3), 1–27. https://doi.org/10.1145/1961189.1961199

Glass, G. V. (1996). *Statistical methods in education and psychology* (K. D. Hopkins (ed.); 3rd ed). Allyn and Bacon. https://archive.org/details/statisticalmetho00glas

Hurst, J. M. (2022a). *A permanent plot method for monitoring indigenous forests - field manual*. Manaaki Whenua Press. https://doi.org/10.7931/DA3M-GE93

Hurst, J. M. (2022b). *The Recce method for describing New Zealand vegetation - field manual*. Manaaki Whenua Press. https://doi.org/10.7931/P48H-ZB65

Kullback, S. (1959). *Information Theory and Statistics*. Wiley. https://play.google.com/store/books/details?id=XeRQAAAAMAAJ

Mazalla, L., & Diekmann, M. (2022). Regression to the mean in vegetation science. *Journal of Vegetation Science: Official Organ of the International Association for Vegetation Science*, *33*(2), e13117. https://doi.org/10.1111/jvs.13117

Pichler, M., & Hartig, F. (2023). Machine learning and deep learning—A review for ecologists. *Methods in Ecology and Evolution / British Ecological Society*, *14*(4), 994–1016. https://doi.org/10.1111/2041-210x.14061

Rubenstein, M. A., Weiskopf, S. R., Bertrand, R., Carter, S. L., Comte, L., Eaton, M. J., Johnson, C. G., Lenoir, J., Lynch, A. J., Miller, B. W., Morelli, T. L., Rodriguez, M. A., Terando, A., & Thompson, L. M. (2023). Climate change and the global redistribution of biodiversity: substantial variation in

empirical support for expected range shifts. *Environmental Evidence*, *12*(1), 1–21. https://doi.org/10.1186/s13750-023-00296-0

Scott, W. A., & Hallam, C. J. (2003). Assessing species misidentification rates through quality assurance of vegetation monitoring. *Plant Ecology*, *165*(1), 101–115. https://doi.org/10.1023/a:1021441331839

Verheyen, K., Bažány, M., Chećko, E., Chudomelová, M., Closset-Kopp, D., Czortek, P., Decocq, G., De Frenne, P., De Keersmaeker, L., Enríquez García, C., Fabšičová, M., Grytnes, J.-A., Hederová, L., Hédl, R., Heinken, T., Schei, F. H., Horváth, S., Jaroszewicz, B., Jermakowicz, E., … Baeten, L. (2018). Observer and relocation errors matter in resurveys of historical vegetation plots. *Journal of Vegetation Science: Official Organ of the International Association for Vegetation Science*, *29*(5), 812–823. https://doi.org/10.1111/jvs.12673

Wiser, S. K., Bellingham, P. J., & Burrows, L. E. (2001). Managing biodiversity information: development of New Zealand's National Vegetation Survey databank. *New Zealand Journal of Ecology*, *25*(2).